646

FERMILAB TEVATRON PROPOSAL

Search for the ν_τ and Study of ν_e and $\bar{\nu}_e$ Interactions

H.H. Bingham and G. Yost
Univ. of California, Berkeley

C. Baltay, M. Bregman, R. Fine, H. French, M. Hibbs,
J. Okamitsu, G. Ormazabal, and R.D. Schaffer
Columbia University

D. Bogert, J. Schmidt, W. Smart, and L. Voyvodic
Fermilab

R. Cence, F. Harris, M. Jones, S. Parker, M. Peters,
V. Peterson, and V. Stenger
Univ. of Hawaii

P. Jacques, M. Kalelkar, R. Plano, and R. Stamer
Rutgers University

E.B. Brucker and E.L. Koller
Stevens Institute of Technology

Scientific Spokesman - C. Baltay, Columbia University.

Outline of Proposal

(Appendix to follow.)

Summary of Proposal

1. Detector - The Fermilab 15 foot Bubble chamber filled with heavy neon (60 to 65% atomic neon + hydrogen)

2. Beam - A new beam dump neutrino beam with the beam dump located 200 to 250 meters from the bubble chamber.

3. Running Time - 2×10^{18} protons in dump at Tevatron energies (800 to 1000 GeV). This could be packaged as 100,000 pictures with 2×10^{13} protons per pulse or 200,000 pictures with 1×10^{13} protons per pulse.

Summary of Event Rates Expected

For 2×10^{18} 1000 GeV protons interacting in the dump at 200 meters from the 15' BC filled with heavy neon, we expect the following nos. of events:

$\nu_\mu + Ne \rightarrow \mu^- + \ldots$	6000
$\bar{\nu}_\mu + Ne \rightarrow \mu^+ + \ldots$	2400
$\nu_e + Ne \rightarrow e^- + \ldots$	4000
$\bar{\nu}_e + Ne \rightarrow e^+ + \ldots$	1600
$\nu_\tau + Ne \rightarrow \tau^- + \ldots$	850
$\bar{\nu}_\tau + Ne \rightarrow \tau^+ + \ldots$	350
$\nu + Ne \rightarrow$ all hadrons	4800
$\overset{(-)}{\nu}_e + e^- \rightarrow \overset{(-)}{\nu}_e + e^-$	5
events with visible τ decays	75

Summary of Physics Goals

1. Search for the ν_τ

   a) Events with visible inflight $\tau^\pm$ decays

   $\overset{(-)}{\nu}_\tau$ + neon → $\tau^\pm$ + hadrons

   ↳ visible inflight decay

   ∿ 75 events with visible decays expected

   b) Via events with unusual kinematics using ∿ 1200 ν_τ and $\bar{\nu}_\tau$ interactions in the bubble chamber

   c) Rough measurement of the $\tau^\pm$ lifetime

   d) Search for ν_τ decays (in case the ν_τ has a finite mass)

2. Study of ν_e and $\bar{\nu}_e$ Interactions

   a) Neutral current/charged current ratio for ν_e + $\bar{\nu}_e$

   b) Study of $\overset{(-)}{\nu}_e + e^- \rightarrow \overset{(-)}{\nu}_e + e^-$

   c) Search for electron type heavy leptons $E^\pm$

   ν_e + neon → $E^\pm$ + hadrons

   d) Universality tests in charged current interactions

3. Study of charm and F $\bar{F}$ production in beam dump with ∿10,000 "prompt neutrino" events.

4. Search for new, unexpected phenomena.

I. Introduction and Physics Motivation.

One of the most important development of the last few years has been the discovery of a new heavy lepton , the $\tau^{\pm}$, by Perl [1] et al. at SLAC. The following question then arises naturally: is the τ a member of a new family, associated with a new distinct neutrino, the tau-neutrino ν_{τ}, or does it couple preferentially to one of the already known neutrinos. From the characteristics of tau pair production in $e^{+}e^{-}$ collisions it can be inferred [2] that the τ^{-} does not couple strongly to the $\bar{\nu}_{\mu}$ or the $\bar{\nu}_{e}$. From neutrino scattering data in the Fermilab 15 foot bubble chamber [3] we know that the $\tau^{\pm}$ does not couple strongly to the ν_{μ}, since the process ν_{μ} + Neon → $\tau^{\pm}$ + hadrons was not observed. The possibility however that the τ^{-} couples strongly to the ν_{e} still remains.

It is therefore of some inportance to experimentally verify the existence of the ν_{τ} and show that it is distinct from the ν_{e}. This is the main goal of the experiment we are proposing. The verification of the existence of the ν_{τ} would consist of showing the existence of a neutral penetrating particle (produced in a beam dump and penetrating ~ 75 meters of steel) that interacts in the bubble chamber and produces a $\tau^{\pm}$ and other hadrons, but no additional direct $\mu^{\pm}$ or $e^{\pm}$. The ability of the heavy neon chamber to detect the presence or absence of a $\mu^{\pm}$ or an $e^{\pm}$ is by now well recognized. The $\tau^{\pm}$ would be detected by actually observing its decay inflight, i.e. a short charged track that decays either into a visible $e^{\pm}$ or $\mu^{\pm}$ or one or more visible charged hadrons. This is made possible by the fine grain visibility of the interaction vertex in the bubble chamber (examples of decays of charmed particles with track lengths before decay of 0.5 to 2 cm have been observed in the 15 foot chamber) and the high energies available at the Tevatron. Typical ν_{τ} energies will be ~ 100 BeV, producing typically 50 BeV taus, with time dilation factors of $\gamma \sim 30$. The lifetime of the τ is expected to be ~ 3×10^{-13} sec giving a mean decay length of 0.3 cm! Thus a sizeable fraction of the taus would travel longer than 0.5 cm and thus be observable in the 15 foot chamber with its present optics. Improved optics, as discussed in section V, would improve things further. We expect a sample of 75 events with a visible $\tau^{\pm}$ decay. With such a sample a crude measurement of the τ lifetime should be possible, which is an important measurement in its own right. As will be discussed in section III, backgrounds due to hadron interactions or charm decays are expected to be less then one event (in any case charmed particles are made by neutrinos predominantly by the charged current interactions, and thus would be accompanied by a $\mu^{\pm}$ or $e^{\pm}$, while τ decays would not be accompanied by other μ's or e's in the event).

Confirmation that the observed short decaying tracks are taus would come from the consistency with the expected lifetime and consistency with the decay modes and branching ratios measured for the τ in e^+e^- interactions. Additional evidence, although circumstantial, for the presence of ν_τ interactions would come from the distinctive kinematics of events where the $\tau^{\pm}$ decays into $\mu^{\pm}\nu\bar{\nu}$ and $e^{\pm}\nu\bar{\nu}$. The study of the hadrons accompanying the τ in ν_τ interactions (i.e. strange particle content, multiplicity, etc.) would also be possible in the bubble chamber and would be of some interest.

Another interesting possibility is the search of ν_τ decays. If the ν_τ mass were not zero but as large as a few MeV, then it might be unstable. A probable decay mode would be $\nu_\tau \to e^+ + e^- + \nu_e$, observable in the neon chamber as an unassociated energetic e^+e^- pair. We know from our previous work on $\nu_\mu + e^- \to \nu_\mu + e^-$ scattering that the background of unassociated e^+e^- pairs is very small, so that a sensitive search should be possible.

It should also be possible in this experiment to show that the ν_τ is distinct from the ν_e since we expect a ν_e flux from charm decays in the dump which is about an order of magnitude larger then the ν_τ flux. Thus if the τ coupled to the ν_e full strength, we should see a large signal of τ's produced by ν_e

$$\nu_e + \text{Neon} \to \tau + \ldots$$

We should be able to set a limit on the $\nu_e - \tau$ coupling, similar to the limit we set on the $\nu_\mu - \tau$ coupling in our previous wideband ν_μ experiment [3].

Just as the best source of high energy ν_μ are π and K meson decays, the best source of a ν_τ beam are the decays of the yet to be discoverd (but sure to exist) F mesons produced by the primary protons in the beam dump.

$$p + \text{dump} \to F + \bar{F} + \ldots$$
$$F \to \tau + \nu_\tau(1), \qquad \tau \to \nu_\tau(2) + \ldots$$

Each F decay will give two ν_τ, a softer one directly from the decay, $\nu_\tau(1)$, and a more energetic one, $\nu_\tau(2)$, from the decay of the τ. Both of these ν_τ are of interest in this experiment. Both the F and the τ lifetimes are expected to be short enough that the particles will decay before they are absorbed in the dump (thus producing "prompt neutrinos"). The background of ν_μ and $\bar{\nu}_\mu$ from π and K decays will be greatly suppressed since π's and K's will typically be absorbed in the dump before they decay. The main background, a roughly equal flux of ν_μ, $\bar{\nu}_\mu$, ν_e, and $\bar{\nu}_e$, will be due to decays of charmed particles produced in the dump (these however will be useful in other aspects of the experiment).

To obtain a useful flux of tau neutrinos, the beam dump must be moved closer to the detectors then the present 1400 m from neutrino target to the 15 foot chamber. The ν_τ flux should increase like (not quite, but almost) one over the distance squared. We are therefore proposing a new beam dump located 200 to 250 meters from the 15 foot chamber in the neutrino area. A possible lay out is shown in Fig. 1. The dump would be located $\sim$ 100 meters upstream of the end of the existing earth berm. This location would also be very advantageous to the other neutrino detectors in the neutrino area interested in beam dump experiments. The main technical problem of having the dump so close to the detectors is that there is no longer enough room for a full range passive shield to stop muons up to 1000 BeV by energy loss. We believe however that we have a design for a magnetized iron shield, consisting of 75m of iron of which the first 25 m is magnetized to 20 kgauss, that will reduce the μ flux through the bubble chamber to below the tolerable level of $\sim$ 100 μ's per pulse. This design is discussed in detail in the Appendix to this proposal.

Since the detection of short tracks is of central importance in this experiment it is worth considering improving the optics of the 15 foot chamber. At the present the bubble size is $\sim$ 500 μ in space, and is essentially due to the size of the diffraction pattern on the film due to the f 17 lenses used. We believe that the bubble size on film can be reduced by a factor of 3 by going to f 5.6 lenses. This would improve the resolution near the vertex from the present 150 μ in space by a factor of 2 or 3, which would obviously be a great advantage. The proposed improvements in the optics is discussed in detail in section IV of this proposal.

The second aim of the proposed experiment is the study of ν_e and $\bar{\nu}_e$ interactions. The electron neutrino fluxes from charm decays in a beam dump beam with the dump 200 meters from the detector are comparable to the fluxes that can be obtained in a ν_e beam using K^o_L decays. The expected sample of $\sim$ 4000 charged current and $\sim$ 1600 neutral current ν_e and $\bar{\nu}_e$ interactions in the neon bubble chamber with good electron and hadron detection make such a study quite interesting. Some of the topics that we foresee to be of interest are:

a) Measurement of the neutral current to charged current ratio for inclusive ν_e and $\bar{\nu}_e$ interactions. No decent measurement of this fundamentally important ratio has been done before. Since ν_e induced neutral current events can not be distinguished experimentally from ν_μ induced neutral current events, the number of $(\nu_e + \bar{\nu}_e)$ induced N.C. events will be obtained by taking the total number of neutral current events and subtracting the number of $(\nu_\mu + \bar{\nu}_\mu)$ induced N.C. events (which can be deduced from the known N.C./C.C. ratios for ν_μ and $\bar{\nu}_\mu$ multiplied by the number of ν_μ and $\bar{\nu}_\mu$ charged current events (events with μ^- and μ^+, respectively) measured in the experiment). Events induced by ν_τ interaction will lead to a small but not negligible correction here since a large fraction of the charged current ν_τ interactions will look like neutral current events. However, the τ branching ratios are measured well enough in e^+e^- experiments to allow us to make this small correction.

b) A crude measurement of the cross section for the very rare processes $\overset{(-)}{\nu}_e + e^- \rightarrow \overset{(-)}{\nu}_e + e^-$. These cross sections are very small and we expect only 5 such events. This would allow a rough measurement of this cross section, which is however of some value since these processes are of fundamental importance and there exists no measurement of their cross sections at high energies.

c) Search for heavy leptons E with the quantum numbers of the $e^\pm$ via the processes $\overset{(-)}{\nu}_e$ + Neon $\rightarrow$ E + ..., similar to the search we have done for muon type heavy leptons in the wideband ν_μ experiment [3].

d) Tests of universality in the charged current ν_e and $\bar{\nu}_e$ interactions by comparing x,y, etc. distributions, strange particle content and other features of the hadrons, in this sizeable $\overset{(-)}{\nu}_e$ sample with those in $\overset{(-)}{\nu}_\mu$ interactions.

Another topic that may be of some interest is the study of the production of charm (D mesons, and hopefully F mesons) by protons in the beam dump with the sizeable sample of $\sim$ 10,000 prompt neutrino interactions in the bubble chamber. For this purpose we might want to do some short runs with different proton beam energies and different incident proton beam angles.

An additional non-negligible reason for doing this experiment is that something new and unexpected could show up. This is always an important consideration when entering a new energy domain, as with the Tevatron. Because of the closeness of the dump to the detector and the increased energies available at the Tevatron, this experiment represents a two order of magnitude increase in sensitivity over previous experiments ($\sim$10,000 prompt neutrino interactions compared to 61 in BEBC in the CERN beam dump experiments).

The ν_τ physics discussed is especially appropriate, if not unique, at the Tevatron. Colliding beam machines (e^+e^-, p p, $\bar{p}$ p) are unlikely to shed any light on these questions, and the higher energy of the Tevatron in this particular case is a very large advantage over lower energy fixed target accelerators since the factor of $\sim$ 2 in energy comes in cubed or to the fourth power in the relative merits of this experiment (inclusive F production increases, the ν_τ production angles shrink and thus a larger fraction of the ν_τ hit the detector, the ν_τ interaction cross section increase with energy, and the τ decay lengths increase due to the larger γ's of the τ's).

It is likely that the large electronic counter neutrino detectors at Fermilab will also participate in beam dump neutrino running. We believe that the 15 foot bubble chamber with a heavy neon fill complements these detectors. While the electronic detectors will have much larger event rates, the chamber has some unique features as a neutrino detector. The observation of events with a visible τ decay without additional $e^\pm$ or $\mu^\pm$ will greatly strengthen the case for the verification of the existence of the ν_τ. The rough measurement of the τ lifetime will not be possible in other detectors. And the ability of the chamber to identify electrons in a complicated final state, as is necessary in the study of inelastic ν_e and $\bar{\nu}_e$ interactions, is unique to the neon chamber. In addition, the ability to see details of hadrons and detect strange particles and study final state effective mass distributions may turn out to be important. We therefore believe that the neon chamber should play an important role in beam dump neutrino experiments at the Tevatron.

II. Calculation of Neutrino Fluxes and Event Rates.

Our estimates of the event rates in this experiment are based on an extrapolation from the measured number of prompt neutrino induced events in the CERN bubble chamber BEBC filled with heavy neon in two beam dump runs at the CERN SPS. It is now generally accepted that the dominant source of these prompt neutrinos is charm decays (D, $\bar{D}$, etc.) in the beam dump. We use the sum of the 1977 run (3.5×10^{17} protons) and the 1979 full density dump run (8.0×10^{17} protons) with a total of 1.15×10^{18} 400 GeV protons in the dump at the CERN SPS. The distance from the dump to BEBC was 820 meters in both runs. The numbers of events observed [4)] in these runs with $E_{vis} > 10$ GeV were as follows:

Event Type	Total Seen	From π, K Decay	From Prompt ν
Charged current (Sum of ν_μ, $\bar{\nu}_\mu$, ν_e, $\bar{\nu}_e$)	148	87	61
Neutral current	33	16	17

The total number of charged current events from prompt ν, N (prompt CC), that we expect at the Tevatron with 1000 GeV protons and a beam dump to bubble chamber distance of 200 meters is (the fiducial mass in the 15 foot is similar to BEBC) :

NC (prompt CC) = 61 x R(protons) x R(D prod) x R(Ω) x R($\sigma\nu$)

where R(protons) is the ratio of the total nos. of protons incident on the dump.

R(D prod) is the increase in inclusive D production from 400 to 1000 GeV.

R(Ω) is the increase in the solid angle subtended by the detector.

R($\sigma\nu$) is the increase in event rate due to the larger interaction cross section for the higher energy neutrinos at the Tevatron.

We would expect the inclusive charm production to increase linearly with incident proton energy. We use the estimate from the Bourquin & Gaillard [5] model of charm production, which predicts a factor of 2.1 increase from 400 to 1000 GeV.

R (D prod) = 2.1

The other two factors might be expected to be $R(\Omega) = (1000/400)^2 \times (820/200)^2 = 6.25 \times 16.8 = 105$, where the first factor is due to the fact that the neutrinos are emitted at smaller angles at the Tevatron, and the second factor is due to the smaller dump to detector distance; and $R(\sigma\nu) = (1000/400) = 2.5$ if the average ν energy scales with incident proton energy.

To make a more careful astimate of these last two factors we have written a Monte Carlo program to calculate ν fluxes from the beam dump. We generate D and F mesons in the dump, let then decay via the modes $D \to K\mu\nu$, $D \to Ke\nu$, $F \to \tau + \nu_\tau$ followed by $\tau \to \nu_\tau + e + \nu_e$, and propagate the ν's to the detector. The calculation is very straight forward; the only uncertainty is the x_F and p_T distribution of the D and F production. To check the sensitivity on the details of charm production, we have used three fairly different models; a) the Bourquin-Gaillard model, b) assuming that D's are made with the same x_F and p_T distribution as π's and K's, and c) using the best fit to charm production by Wachsmuth et al., $(1 - x_F)^N e^{-bp_T}$, with N = 3 and b = 2 (we also varied N and b).

We found that the ratios $R(\Omega)$ and $R(\sigma\nu)$ needed for extrapolating from the CERN SPS to the Tevatron are quite insensitive to these charm production models, and are therefore fairly reliable. We obtain from these calculations

$$R(\Omega) = 3.8 \times 11 = 42$$

where again the first factor is due to the increased energy and the second to the smaller dump to detector distance, and

$$R(\sigma\nu) = 1.2.$$

Our best estimate for the number of prompt neutrino induced charged current events (sum of ν_μ, $\bar{\nu}_\mu$, ν_e, and $\bar{\nu}_e$) is then

$$N \text{ (prompt CC)} = 61 \times \frac{2.0 \times 10^{18}}{1.15 \times 10^{18}} \times 2.1 \times 42 \times 1.2 = 11{,}000$$

This is almost a factor of 200 improvement over the CERN BEBC beam dump experiment.

The expected numbers of events of the various categories are listed in Table I. We have assumed equal fluxes of the four kinds of neutrinos as is expected from D and $\bar{D}$ decays. We have also used the numbers of events from π and K decays in BEBC and extrpolated them to our case, noting that the π and K decay background relative to the prompt neutrinos are smaller at higher energies because the π and K's are less likely to decay before they are absorbed.

We estimate the ν_τ flux from the prompt neutrino flux extrapolated from BEBC, and the ratio

$$\frac{\nu_\tau \text{ flux}}{\text{prompt } \nu \text{ flux}} = \frac{\text{F production}}{\text{D production}} \times \frac{2 \times \text{B.R. } (F \to \tau + \nu_\tau)}{\text{B.R. } (D \to e + \ldots) + \text{B.R. } (D \to \mu \ldots)}$$

The prompt ν flux is the sum of ν_μ and ν_e, so we use the sum of the μ and e D branching ratios in the denominator. The factor of 2 in the numerator is there because we get two ν_τ for each F decay. The F branching ratio has been estimated theoretically to be

$$\text{B.R. } (F \to \tau + \nu_\tau) = 0.03$$

and the D semileptonic branching ratios have been measured to be $\sim$ 8%. The F to D production ratio is analogous to the K to π ratio, since both the F and the K require an additional s $\bar{s}$ loop relative to D or π production. However the F is close to the D in mass while the K is much heavier then the π, so we expect the F to D ratio to be larger then the K to π ratio, which is 0.10 to 0.15. We therefore take the F to D production ratio to be 0.3, which is not likely to be wrong by more then a factor of two either way. We thus have

$$\frac{\nu_\tau \text{ flux}}{\text{prompt } \nu \text{ flux}} = 0.3 \times \frac{2 \times .03}{(.08 + .08)} = 0.11$$

and we expect the sum of ν_τ and $\bar{\nu}_\tau$ interactions to be

$$\nu_\tau + \bar{\nu}_\tau \text{ interactions} = (0.11) \times 11{,}000 \text{ prompt } \nu \text{ interactions} = 1200 \text{ events.}$$

This leads to the number of ν_τ and $\bar{\nu}_\tau$ interactions shown in Table I, assuming that at these high energies the ν_τ and $\bar{\nu}_\tau$ have the same interaction cross sections as the ν_μ and $\bar{\nu}_\mu$.

As a consistency check on the extrapolation of the prompt neutrino event rate from BEBC data, we have calculated the neutrino fluxes from charm decay in the beam dump using the Monte Carlo program discussed above, and the measured charm production cross section of 17 μbarns at 400 GeV, using either the Bourquin-Gaillard x_F and p_t charm distributions or $(1 - x_F)^3 e^{-2p_T}$. We get numbers of events which are consistent with those of Table I. We have also compared with calculations by S. Mori and J.K. Walker, Fermilab TM 953, and find good agreement.

The energy spectra for the various kinds of neutrinos from the beam dump, as calculated by the Monte Carlo program discussed above, are shown in Fig. 2. Again we find good agreement with the calculation by S. Mori and J.K. Walker.

III. Discussion of the Data Analysis - Efficiencies, Backgrounds etc.

1. Search for the ν_τ.

a) Events with visible inflight τ decays .

The lifetime of the τ is expected to be 3×10^{-13} sec, assuming that it has the same strength of weak interactions as the muon. For time dilation factors of $\gamma \sim 30$ for the taus available at the Tevatron the lifetime in the lab is $\sim 10^{-11}$ sec, or a mean decay length of 0.3 cm. We have in the past observed visible charmed particle decays in the 15 foot chamber with decay lengths between 0.5 cm and 2 cm. We can thus expect to see a non-negligible fraction of the τ decays.

We have written a Monte Carlo program to calculate the efficiency of observing τ decays. We start with the ν_τ spectrum calculated for F decays in the beam dump. Both ν_τ and $\bar{\nu}_\tau$ are then allowed to interact in the neon, and the momenta and angles of the $\tau^\pm$ produced are calculated assuming that the ν_τ and $\bar{\nu}_\tau$ have the same interaction cross sections and x and y distributions as the ν_μ and $\bar{\nu}_\mu$. The energy distribution of the 1200 interacting tau neutrinos is shown in Fig. 3, and the momentum distribution of the $\tau^\pm$ produced in these events is shown in Fig. 4. The τ's are then allowed to decay randomly with a lifetime of 3×10^{-13} sec. The distribution in the τ decay length for these 1200 events is shown in Fig. 5. The curve in Fig. 6 shows the fraction of the $\tau^\pm$ decays beyond a distance ℓ from the ν_τ interaction vertex. We find that

19% of the τ decays (230 events) occur at decay distances greater than 0.5 cm. Unfortunately not all of these decays will be detectable, partly because of the small decay angles in the lab. We expect that the detection efficiency will be different for the different τ decay modes. Table II lists the various τ decay modes, the measured branching ratios [2] for these modes and thus the numbers we expect for them. We now discuss the efficiencies for the different decay modes in turn:

i) Decays into a single charged prong.

If the decay angle in the lab (i.e. the angle between the τ and the single charged decay product) is too small the decay will be hard to detect even if the τ track is 0.5 cm or longer. For a decay product with a momentum p_{cm} in the τ center of mass, and making the approximation that $\beta \sim 1$ for the decay product, the lab momenta of the decay product are

$$p_{\parallel} = \gamma\, p_{cm}\, (1 + \cos\theta^*)$$

$$p_{\perp} = p_{cm} \sin\theta^*$$

where θ^* is the center of mass decay angle and $\gamma = E/m$. The lab angle θ_{lab} then is

$$\theta_{lab} \approx \frac{p_{\perp}}{p_{\parallel}} = \frac{1}{\gamma}\, \frac{\sin\theta^*}{1 + \cos\theta^*}$$

Fig. 7 shows θ_{lab} vs. $\cos\theta^*$ for a 50 GeV $\tau \rightarrow e + \nu + \bar{\nu}$ decay (this also applies for other decay products since p_{cm} approximately cancels out). We believe from past experience with the 15 foot chamber that a lab decay angle of 5° or larger is clearly detectable. We see from Fig. 7 that only backward decays with $\cos\theta^*$ between -0.7 and -1.0, or about 15% of the decays, will give lab angles larger then 5°. Thus the fraction ε of the single charged prong decays with both decay length over 0.5 cm and decay angle over 5° is

$$\varepsilon \sim 0.19 \times 0.15 \sim 3\%$$

(we can multiply the two probabilities since they are independent).

This is for a typical τ momentum of 50 GeV/c (see Fig. 4). We feel that the efficiency for other momenta should be similar since the decay length goes like γ, the decay angle like $1/\gamma$, and in some sense the efficiency depends on their product which is independent of γ.

In fact, one could discuss the detection efficiency in terms of a distance of closesst approach δ of the decay prong to the ν interaction vertex,

$$\delta \sim d\, \theta_{lab}$$

where d is the decay length. The mean decay length is $d \sim \beta \gamma \tau_o c$, so

$$\delta \sim \beta \gamma \tau_o c \times \frac{1}{\gamma} \frac{\sin \theta^*}{1 + \cos \theta^*} \sim \tau_o c \beta \frac{\sin \theta^*}{1 + \cos \theta}$$

which is independent of the τ momentum once $\beta \simeq 1$.

Our resolution at the present in the 15 foot chamber with heavy neon is 150 μ. With the improved optics, with the bubble size reduced by a factor of 3, we expect this resolution to improve by at least a factor of 2 (we are here concerned about the local resolution in the vicinity of the vertex. Many effects such as uncertainties in the optical constants that affect the resolution relevant when measuring the momentum of a long high energy muon, for example, are irrelevant here). We therefore believe that we can detect a decay where the decay product misses the vertex by more then 500 μ. This checks with our previous visibility criteria of decay length > 0.5 cm, $\theta_{lab} > 5^o$.

To obtain a more quantitative estimate of the efficiency, we use the Monte Carlo program mentioned above in which $\tau^{\pm}$ are generated in tau neutrino interactions. The $\tau^{\pm}$ are then allowed to decay via $\tau^{\pm} \to e^{\pm} \nu_e \overset{(-)}{\nu}_e$, assuming that the decay in the τ center of mass is like μ decay (ρ value = 0.75, etc.). The $e^{\pm}$ are then transformed into the lab and the distance of closest approach to the ν interaction vertex for each event is calculated. The number of decays in which the closest approach is larger then some value δ is plotted vs. δ in Fig. 8. We see that 3% have a closest approach larger then 500 μ, which is in agreement with the 3% efficiency from the qualitative discussion above.

We further reduce this estimate of the efficiency to take into account losses due to obscuration by other tracks etc. to 2½ %.

ii) Efficiency for τ decays into 3 or more charged prongs. We believe that decays into 3 charged prongs are much easier to detect then decays with a single charged prong. This is partly due to the fact that out of 3 charged tracks at least one is more likely to be backwards in the center of mass and therefore leave at a larger angle in the lab, and partly because we have other handles such as change of ionization bubble density and track width when a single track decays into 3 tracks. Our estimate of the detection efficiency is thus the 19% that have decay length over 0.5 cm, reduced by losses due to obscuration due to other tracks, etc. to 15%.

Using these efficiencies and the numbers of τ decays in Table II we expect to be able to detect 75 visible inflight τ decays.

b) We now discuss the backgrounds to the sample of 75 visible τ decays. We have considered backgrounds due to strange and charmed particle decays and the close in secondary interactions of charged hadrons produced in the ν interactions. The main discrimination against all of these backgrounds comes from the observation that the τ is the leading particle in the ν_τ interactions and therefore will be very energetic (see Fig. 4). Furthermore the low energy τ are unlikely to have long decay paths and are thus less likely to be visible decays. In Fig. 9 we show the distribution in the momentum of the τ's with decay path longer then 0.5 cm. On the other hand hadrons produced in neutrino interactions tend to have relatively low energies. Fig. 10 shows the distribution in the momentum of hadrons produced in the wide-band ν_μ experiment in the 15 foot BC. From these two figures we see that essentially all of the visible τ decays will have momenta above 20 GeV while less then a few percent of the hadrons are above 20 GeV/c. We therefore will make a cut on the total energy visible in the τ decays around 20 GeV, with every little loss in the number of visible decays. An estimate of the remaining backgrounds is the following:

i) Strange particle decays. We expect about 500 $K^\pm$ produced in the 4800 neutral current (ν_μ, $\bar{\nu}_\mu$, ν_e, and $\bar{\nu}_e$) interactions in the experiment. The probability of a $K^\pm$ decaying between 0.5 and 2.0 cm of the vertex (with an average γ of 4 or so) is

$$P = \frac{1.5}{\beta\gamma\tau_o c} = \frac{1.5}{4 \times 371} = 10^{-3}$$

or a total of 0.5 events. The 20 BeV cut will reduce this by at least a factor of 20 (using the K^o momentum distributions from the wideband ν runs) so that the remaining background of 0.025 events is negligible.

ii) We expect 10% charm production, half of which is charged, in the 13000 charged current ($\nu_\mu + \bar{\nu}_\mu + \nu_e + \bar{\nu}_e$) interactions in the experiment (see Table I) or a total of $\sim$650 charged charmed particles. We estimate that less then 10% of these, or < 65 events, will be above 20 BeV/c. The mean decay path of these particles is $\lambda = \beta\gamma\tau_o c = 15 \times 5 \times 10^{-13} \times 3 \times 10^{10} \simeq 0.23$ cm using 5×10^{-13} sec for the lifetime and an average γ of 15 (since we are now duscussing only those above 20 BeV/c). The fraction that will have a decay path longer then 0.5 cm is $e^{-(0.5/0.23)}$ $\sim$1/10, so we expect to see < 6½ visible charm decays. However we recall that charm particles in neutrino interactions are made only via the charged currents (we know that associated charm production in neutral current events is very small) so that these few visible charm decays will have a $\mu^{\pm}$ or an $e^{\pm}$ with them in the event, while the τ decays will not have another charged lepton in the event. Since the μ and e detection efficiency in the heavy neon chamber is very good, visible charm decays will not be a background to the τ decays.

iii) Close in hadron interactions. With a charged hadron multiplicity of 5, the 4800 neutral current events will have $\sim$ 25000 charged hadrons in them. With an interaction length of 125 cm in the heavy neon, the number of charged hadrons interacting between 0.5 and 2.0 cm will be

$$25000 \times \frac{1.5}{125} = 300 \text{ interactions.}$$

We use the measured momentum distribution of the charged hadrons in (see Fig. 10a) E-546 (since the neutrino energies in the quad-triplet beam used in E-546 is similar to the ν energies we expect from the prompt neutrino events in this experiment) to estimate that less then 4% of the hadrons will be above 20 BeV/c. Furthermore the total charge from $\tau^{\pm}$ decays must be ±1, while our experience in heavy neon indicates that less then half of the secondary interactions have a net charge of ±1 ($\pi^+ p$ and $\pi^- p$ have 2 and 0, and there are also recoil stubs). A final cut could be that $\phi > 120^o$, where ϕ is the azimuthal angle around the ν direction between the p_T of the decaying track and the p_T of the vector sum of the other hadrons in the event. This is essentially no loss to the τ signal since the τ will be on the opposite side of the hadrons, while only 10% of the energetic hadrons are on the other side of the rest of the hadrons (see Fig 10b) We thus have a remaining background of

$$300 \times 0.04 \times 0.5 \times 0.1 = 0.6$$

or less then one event in the sample of 75 visible τ decays.

c) Search for the ν_τ using event kinematics. Tau neutrino interactions in which the tau decays purely leptonically, $\tau^\pm \to (\mu^\pm \text{ or } e^\pm) + \nu + \bar{\nu}$ will look like ν_μ or ν_e induced charged current events in that they have a single charged lepton in the final state. Albright, Shrock, and Smith [6] have pointed out however that the kinematics of the ν_τ induced events will be different from the others since the observed lepton carries only part of the τ energy, causing a shift down in the x_{vis} distribution and a shift upward in the y_{vis} distribution. Furthermore a relatively large amount of momentum is carried off by the two neutrinos which appears as a large p_T missing in the ν_τ events, and this missing momentum, coming from the τ decay, tends to be in the opposite direction from the p_T of the hadrons, or peaking near 180° in $\Delta\phi$ (m,H) where $\Delta\phi$ (m,H) is the azimuthal angle between p_T missing and p_T of the hadrons. The expected distributions from Albright et al. [6] are shown in Figs. 11 and 12. The background charged current events also have an apparent missing momentum due to undetected neutral hadrons and measurement errors, but for these events $\Delta\phi$ (m,H) is small. The selection criteria for ν_τ interactions is thus

$$\Delta\phi\ (m,H) > 120^\circ$$
$$p_{T\ miss} \gtrsim 1\ \text{BeV/c or so.}$$

We expect 440 tau neutrino events with purely leptonic tau decay in a background of 13000 charged current mu or electron neutrino events. We find from a sample of charged current events measured in the 15 foot neon chamber in E-546 that $\sim$10% of the events have $\Delta\phi$ (m,H) > 120° (Fig. 13); thus this cut can be expected to reduce the background to 1300 events. Fig. 14 shows the effect of the $p_{T\ miss}$ cut [8]: a factor of 5 reduction from this cut shouldgive us a sample in which the background and the ν_τ signal is comparable. The x and y distributions then can be expected to show a significant effect (as in Fig. 15).

d) Search for ν_τ interactions using hadronic decays of the produced tau. Since the taus are very energetic (see Fig. 4) the hadrons from decays like $\tau \to \nu_\tau$ + hadrons will tend to carry a lot of energy. We remarked earlier that the hadrons in the usual neutrino interactions tend not to be very energetic (see Fig. 10). Thus these ν_τ events will look very unusual. In particular the branching ratios for $\tau \to A_1 + \nu_\tau$ and $\tau \to \rho + \nu_\tau$ have been measured to be 11% and 22% respectively, so we expect 130 A_1's and 260 ρ's from τ decays in this experiment. For example, half of the A_1's will decay into three pions, so the A_1 mass can be reconstructed. A signal of 65 A_1's with 10, 20, or 30 GeV of energy should be very striking. Since the τ branching ratio into A_1 has been measured, this may well be the best way to obtain the total number of ν_τ interactions.

e) A rough measurement of the τ lifetime, as we discussed above, is of some interest, and we know of no other experiment that is likely to be able to do such a measurement. With 75 visible τ decays a fit to the decay length distribution will give a measurement of the lifetime. The precision of the measurement will most likely be limited by the uncertainty in the detection efficiency as a function of decay length. It would be a great help in this measure if a $\tau \to A_1 + \nu_\tau$ signal were seen, as discussed above, and would yield information on the size and momentum distribution of the parent sample. Otherwise we would have to depend on the beam Monte Carlo for the τ momentum distribution.

f) Search for ν_τ decays. If the ν_τ had a non-zero mass it might be unstable. A likely decay mode [7] would be $\nu_\tau \to e^+ + e^- + \nu_e$. The signal for such a decay in the bubble chamber would be a very energetic e^+e^- pair at a very small angle with the ν beam direction, and unassociated with other events in the chamber. We know that the heavy neon chamber has a very good efficiency for detecting such pairs. The backgrounds to such a signal are very small and can be estimated from the data of the wideband ν_μ run of E53a measuring the cross section for $\nu_\mu + e \to \nu_\mu + e$ scattering. In a total of 106,000 charged current interactions a total of 22 unassociated e^+e^- pairs with energy over 2 GeV were seen, 8 of which were at a small enough angle to be consistent with ν_τ decay (keeping in mind the experimental limit from SLAC on the ν_τ mass of $m_{\nu\tau} < 250$ MeV). We thus expect a background of $\sim$ 1 event in this experiment with 13000 charged current interactions. We should thus be able to see a signal of even a small number of decays, or set an upper limit $n_{dec} < 5$ events if the ν_τ is stable.

To get a feeling for our sensitivity, we start from the total flux of $N_\nu = 5 \times 10^{13}$ tau neutrinos traversing the chamber in the whole run with 2×10^{18} protons on target. The average path of the ν_τ in the chamber is $\ell = 2$ m, and the distance from the beam dump to the chamber is $L = 200$ m. The no. of decays then is

$$n_{dec} = N_\nu \; e^{-L/\lambda} \; (1 - e^{-\ell/\lambda})$$

where λ is the mean decay length of the ν_τ.

i) Long lifetime limit. In this case the number of decays depends on $e^{-\ell/\lambda}$, and $e^{-L/\lambda} \sim 1$. Thus

$$(1 - e^{-\ell/\lambda}) \cong \ell/\lambda = \frac{n_{dec}}{N_\nu}$$

$$\frac{2\ \text{m}}{\lambda} < \frac{5}{5 \times 10^{13}} = 10^{-13}$$

$$\lambda > 2 \times 10^{13} \text{ meters.}$$

To convert this to a limit on the ν_τ lifetime $\tau(\nu_\tau)$, we need the average ν_τ energy, which is ~ 75 GeV, and the mass of the ν_τ, which has to be above 1 MeV for this decay to occur, and is experimentally known to be less then 250 MeV.

Thus

$$\lambda = \beta \gamma \; \tau(\nu_\tau) \; c = \frac{E_\nu}{m_\nu} \; \tau(\nu_\tau) \; C$$

$$\tau(\nu_\tau) = \frac{m_\nu}{E_\nu} \; \frac{\lambda}{c} > \frac{m_\nu}{75} \; \frac{2 \times 10^{13}}{3 \times 10^{8}} \; .$$

With no observed decay signal we can thus set the limits

$$\begin{aligned} \tau(\nu_\tau) &> 1000 \times m_\nu \text{ (in GeV) sec} \\ &> 1 \text{ sec for } m_\nu = 1 \text{ MeV} \\ &> 250 \text{ sec for } m_\nu = 250 \text{ MeV.} \end{aligned}$$

ii) Short lifetime limit. In this case the number of decays in the chamber are limited by the decay of the ν_τ sample before they reach the detector. If no signal is observed, the limit of $n_{dec} \leq 5$ events gives a limit on λ of

$$5 \geq 5 \times 10^{13} \; e^{-200/\lambda} \; (1 - e^{-2/\lambda})$$

or $\lambda \leq 7$ meters.

This gives limits on $\tau(\nu_\tau)$ of

$$\begin{aligned} \tau(\nu_\tau) &\leq 3 \times 10^{-10} \times m_\nu \text{(in GeV) sec} \\ &\leq 3 \times 10^{-13} \text{ sec for } m_\nu = 1 \text{ MeV} \\ &\leq 0.75 \times 10^{-10} \text{ sec for } m_\nu = 250 \text{ MeV.} \end{aligned}$$

Thus if no decay signal is observed, we should be able to conclude, using the existing ν_τ mass limits, that the ν_τ lifetime is less then 0.75×10^{-10} sec or longer then 1 sec. Conversely, if the ν_τ has a lifetime between these values we should be able to observe their decays.

2. Study of ν_e and $\bar{\nu}_e$ Interactions.

a) Measurement of the neutral current to charged current ratio for $\overset{(-)}{\nu}_e$ and $\overset{(-)}{\nu}_\tau$ inclusive interactions. The $\overset{(-)}{\nu}_e$ or $\overset{(-)}{\nu}_\tau$ induced N.C. events can not be distinguished experimentally from the ν_μ induced N.C. events so we have to take the total number of N.C. events and subtract the ν_μ and $\bar{\nu}_\mu$ induced N.C. events

$$\text{N.C. } (\overset{(-)}{\nu}_e + \overset{(-)}{\nu}_\tau) = \text{total N.C.} - \text{N.C}(\nu_\mu + \bar{\nu}_\mu)$$

We use the total number of ν_μ and $\bar{\nu}_\mu$ charged current events that will be measured in the experiment (see Table I) and the known NC/CC ratios (we use here 0.30 and 0.38 for ν_μ and $\bar{\nu}_\mu$ respectively) to obtain

$$\text{N.C. } (\overset{(-)}{\nu}_e + \overset{(-)}{\nu}_\tau) = 5550 - (6000 \times .3 + 2400 \times .38)$$
$$= 2850 \pm 100$$

(We have added the $\sim$ 750 charged current ν_τ events that will look like N.C. events to the 4800 real N.C. events listed in Table I).

A correction will have to be made for ν_τ induced events that look like N.C. events. Suppose we see a signal of 65 events with an $A_1 \to \pi^\pm \pi^+ \pi^-$ from τ decay. From this we infer the total number of ν_τ interactions to be $65 \times 2 \times 1/(.11 \pm .03) = 1200 \pm 400$ (without the A_1 signal we will have to use the estimate of the total ν_τ rate from the visible τ decays or the analysis using the Albright, Shrock, Smith kinematic selections). Using the branching ratio for $\tau \to \nu_\tau$ + hadrons we expect that of the 1200 charged current ν_τ interactions 750 ± 280 will look like N.C. events. We then obtain

$$\text{N.C. } (\overset{(-)}{\nu}_e + \overset{(-)}{\nu}_\mu) = (2850 \pm 100) - (750 \pm 280)$$
$$= 2100 \pm 300$$

Thus a 15 to 20% measurement seems feasible.

b) Observation of and a rough measurement of the cross section for the processes $\overset{(-)}{\nu}_e + e^- \rightarrow \overset{(-)}{\nu}_e + e^-$. Figure 16 shows the cross sections for these processes expected in the Weinberg-Salam model. Using $\sin^2\theta = 0.23$ we expect 5 events for the sum of the ν_e and $\bar{\nu}_e$ induced processes. These events can not be distinguished experimentally from the process $\overset{(-)}{\nu}_\mu + e \rightarrow \overset{(-)}{\nu}_\mu + e$. However, the cross sections for the ν_μ induced process has been measured and is a factor of 6 smaller then the ν_e induced process is expected to be. We thus expect a "background" of ~ 1 event of the type $\overset{(-)}{\nu}_\mu + e \rightarrow \overset{(-)}{\nu}_\mu + e$ in addition to the 5 events induced by $\overset{(-)}{\nu}_e$, and the subtraction can be made in a straigth forward way by using the total number of ν_μ and $\bar{\nu}_\mu$ charged current events measured in the experiment. We do not expect the process $\nu_\tau + e^- \rightarrow \nu_\tau + e^-$ to be a significant background. To obtain cross sections we can use the total number of ν_e and $\bar{\nu}_e$ charged current events observed, which should be a very reliable normalization in the heavy neon chamber.

IV. Improved Optics for the 15 foot chamber.

At the present the resolution in the 15 foot chamber has been limited by bubble size of 8 μ diameter on film, which with an average demagnification of 60 represents an effective bubble size of 500 μ in space. The chamber conditions with heavy neon can easily be arranged to produce bubbles a factor of 3 or 4 smaller then this. The limitation comes from the size of the diffraction pattern on the film due to the F17 lenses used. The angular full width of the diffraction pattern is

$$\theta = \frac{\lambda}{a}$$

where $\lambda \sim 5000$ A, and a is the lens aperture. The size of the diffraction pattern on the film is

$$d = f\,\theta = \frac{f\lambda}{a}$$

where f is the focal length of the lens. At the present f/a = 17, the F stop of the lens, giving

$$d = 17 \times 5000\ \text{A} = 8\tfrac{1}{2}\ \mu$$

which is the apparent bubble size on film. If the lenses were changed to F 5.6, and the chamber run with smaller bubbles, the effective bubble size could be reduced by a factor of 3. The grain size of the Kodak Microfile film presently used is about 3 μ. Tests would have to be made to see wether sufficent contrast can be achieved with 3 μ image size on this (or some other) film.

One consequence of going to an F 5.6 lens is that the depth of field is reduced to about ± 50 cm and the entire volume of the chamber will not be in focus. The proposal is therefore to keep the existing lenses in the usual three camera ports on the 15 foot to get pictures as we are used to now. The chamber has three additional ports with cameras. These could be changed to the F 5.6 lenses, focusing each one for a different depth, so with the ± 50 cm depth of field of each lens the entire fiducial volume can be covered, so that any given event can be seen by at least one high resolution camera.

Another alternate approach is possible. A new lens could be used with F 17 aperture but a longer focal length then the existing lenses to reduce the demagnification to about 20 from the present 60. The same 8½ μ bubble size on film then would correspond to a 170 μ bubble size in space. BEBC is going to use this approach, and they have actually tested such a lens in a recent run. They have obtained beautiful pictures with a measured bubble size that corresponds to 200 μ in space. The depth of field was measured to be ± 50 cm, so again 3 lenses would have to be used focused at different depths. With 70 mm wide film and demagnification of 20 the field of view is limited to 140 cm sideways; with a spherical volume however this is not a very large loss in the number of events visible. CERN has actually obtained an estimate from Zeiss for designing and making such lenses. The estimate some years ago was $ 40,000 to design and $ 25,000 to make a set of three lenses. Inflation is probably not negligible and CERN is now asking for a new estimate. Since the 15 foot chamber camera ports are exact copies of those at BEBC, we might conceivably join forces with CERN and share the design costs.

The detection of short tracks is likely to be important in the coming years, considering the short lifetimes of the τ, charmed particles, and possibly the particles with b and t quarks. A factor of two or three improvement in the resolution is then quite important and well worth the modest costs of the new lenses required. The improvement in optics will benefit other users of the 15 foot chamber as well.

V. Analysis Effort required for the Experiment.

The main effort in the analysis of this experiment is scanning the 100,000 or 200,000 pictures involved and the measurement of ∿ 20,000 events, assuming that we measure all events of all categories that occur in the film. From past experience with the 15 foot chamber we estimate that a scanner can scan 100 frames or measure 10 events in a nominal 8 hour shift. This means a total effort of 4000 scanner shifts. For the combined groups in this collaboration this represents about a one year effort, which is a very reasonable time scale for the analysis of such an experiment. The computer time necessary to analyze the measurements is now available to these groups and therefore does not represent a problem.

TABLE I

Numbers of events expected in the 15 foot chamber filled with heavy neon, with 2 x 10^{18} 1000 GeV protons in the beam dump, located 200 meters from the chamber

Event type	Prompt	From π, K decay	Total
$\nu_\mu + N_e \to \mu^- + \ldots$	4000	2000	6000
$\bar{\nu}_\mu + N_e \to \mu^+ + \ldots$	1600	800	2400
$\nu_e + N_e \to e^- + \ldots$	4000		4000
$\bar{\nu}_e + N_e \to e^+ + \ldots$	1600		1600
Neutral current	3900	900	4800
$\nu_\tau + N_e \to \tau^- + \ldots$	850		850 } 1200
$\bar{\nu}_\tau + N_e \to \tau^+ + \ldots$	350		350 }

TABLE II

Numbers of visible τ Decays expected for the various τ Decay Modes (sum of τ^+ and τ^-)

Decay Mode	Branching Ratio	Events expected	Efficiency for Visible decays	No. of Visible Decays
$\tau^{\pm} \to e^{\pm} + \nu_\tau + \overset{(-)}{\nu}$	.18	215	2½%	5
$\tau^{\pm} \to \mu^{\pm} + \nu_\tau + \overset{(-)}{\nu}_\mu$	.18	215	2½%	5
$\tau^{\pm} \to$ (1 charged hadron) + ν_τ + (neutral)	.33	400	2½%	10
$\tau^{\pm} \to$ (3 charged hadrons) + ν_τ + (neutrals)	.31	370	15%	55
Totals		1200		75

REFERENCES

1) M.L. Perl et al., Phys. Rev. Letters 35, 1489

2) For a recent review, see G. Feldman and M. Perl, Physics Reports 33C, 268 (1977), and G. Feldman, Proceedings of the XIXth International Conference on Particle Physics, Tokyo (1978).

3) A.M. Cnops et al., Phys. Rev. Letters 40, 145 (1978).

4) D.C. Cundy et al., private communication, April 1980 at CERN.

5) M. Bourquin and J.M. Gaillard, CERN Preprint.

6) C.H. Albright, R. Shrock, and J. Smith, Phys. Rev. D20, 2177 (1979).

7) Chris Quigg, Discussion at Argonne, Oct. 1979.

8) Luc Pape, CERN, private communication.

GENERAL LAYOUT OF THE BEAM DUMP NEUTRINO BEAM

IN THE NEUTRINO AREA

(Not to Scale)

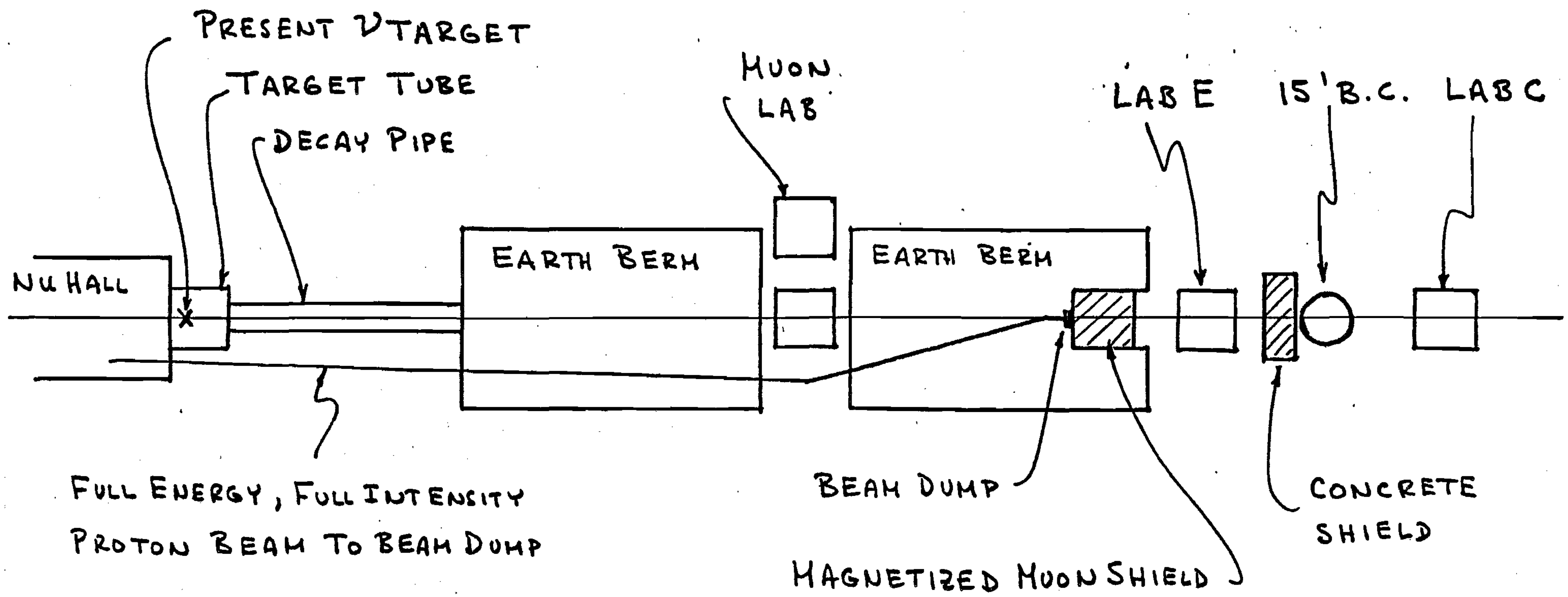

FIG. 1a

LAYOUT OF THE MUON SHIELD

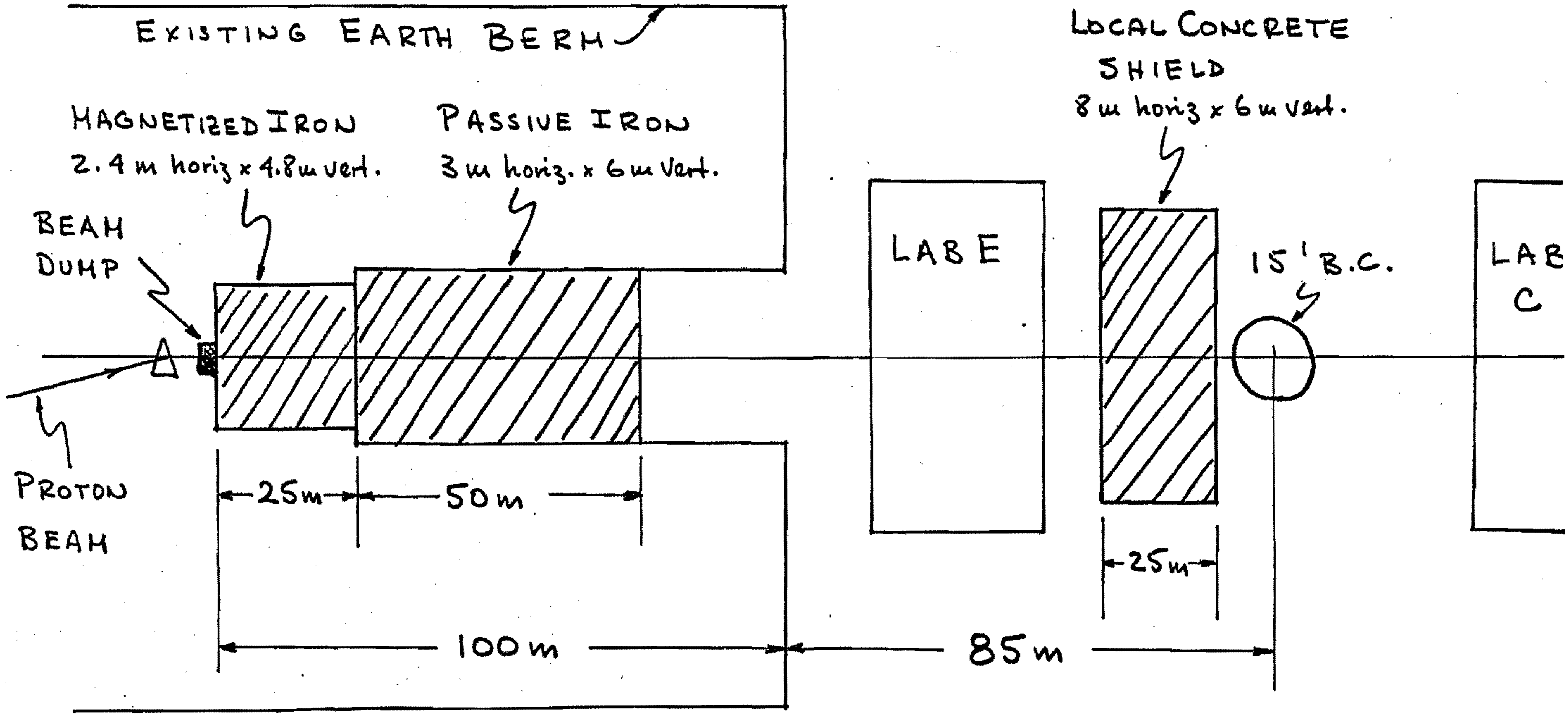

FIG 1b

SCHEMATIC OF THE MAGNETIZED SHIELD

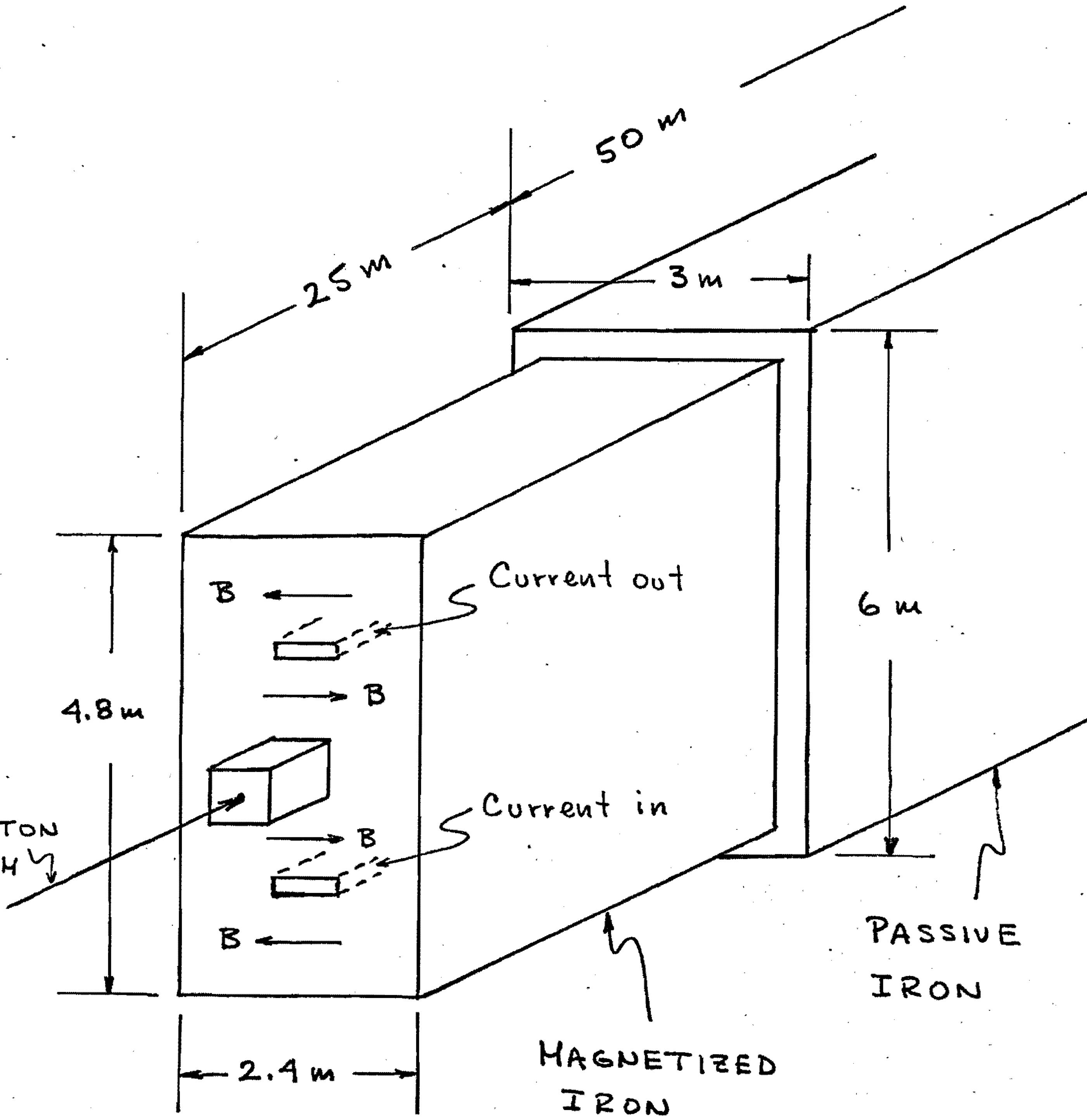

FIG. 1C

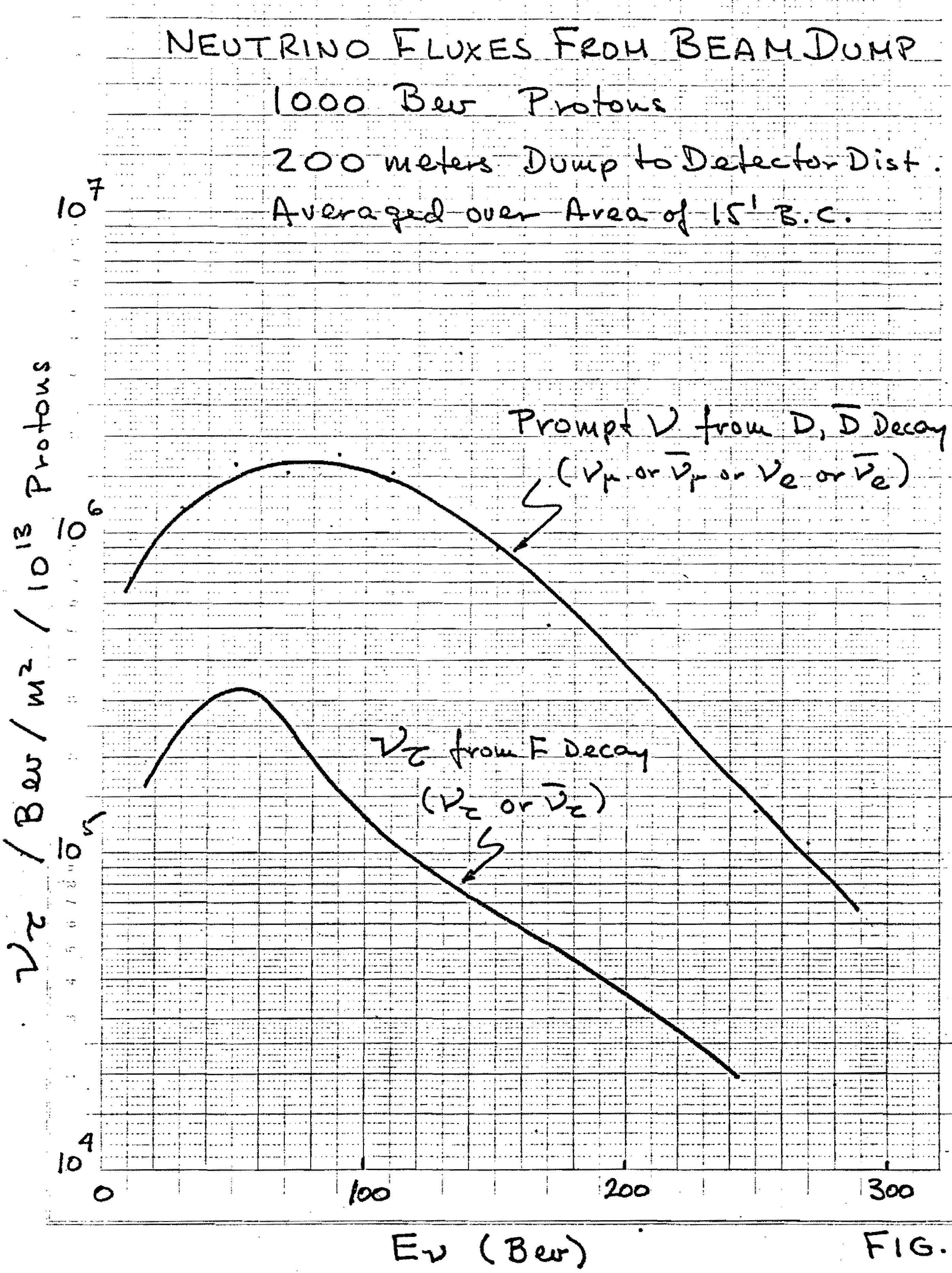

NEUTRINO FLUXES FROM BEAM DUMP
1000 Bev Protons
200 meters Dump to Detector Dist.
Averaged over Area of 15' B.C.
10^7
10^6
10^5
10^4
ν_τ / Bev / m² / 10^{13} Protons
Prompt ν from D, D̄ Decay
(ν_μ or $\bar{\nu}_\mu$ or ν_e or $\bar{\nu}_e$)
ν_τ from F Decay
(ν_τ or $\bar{\nu}_\tau$)
0
100
200
300
Eν (Bev)

FIG. 2

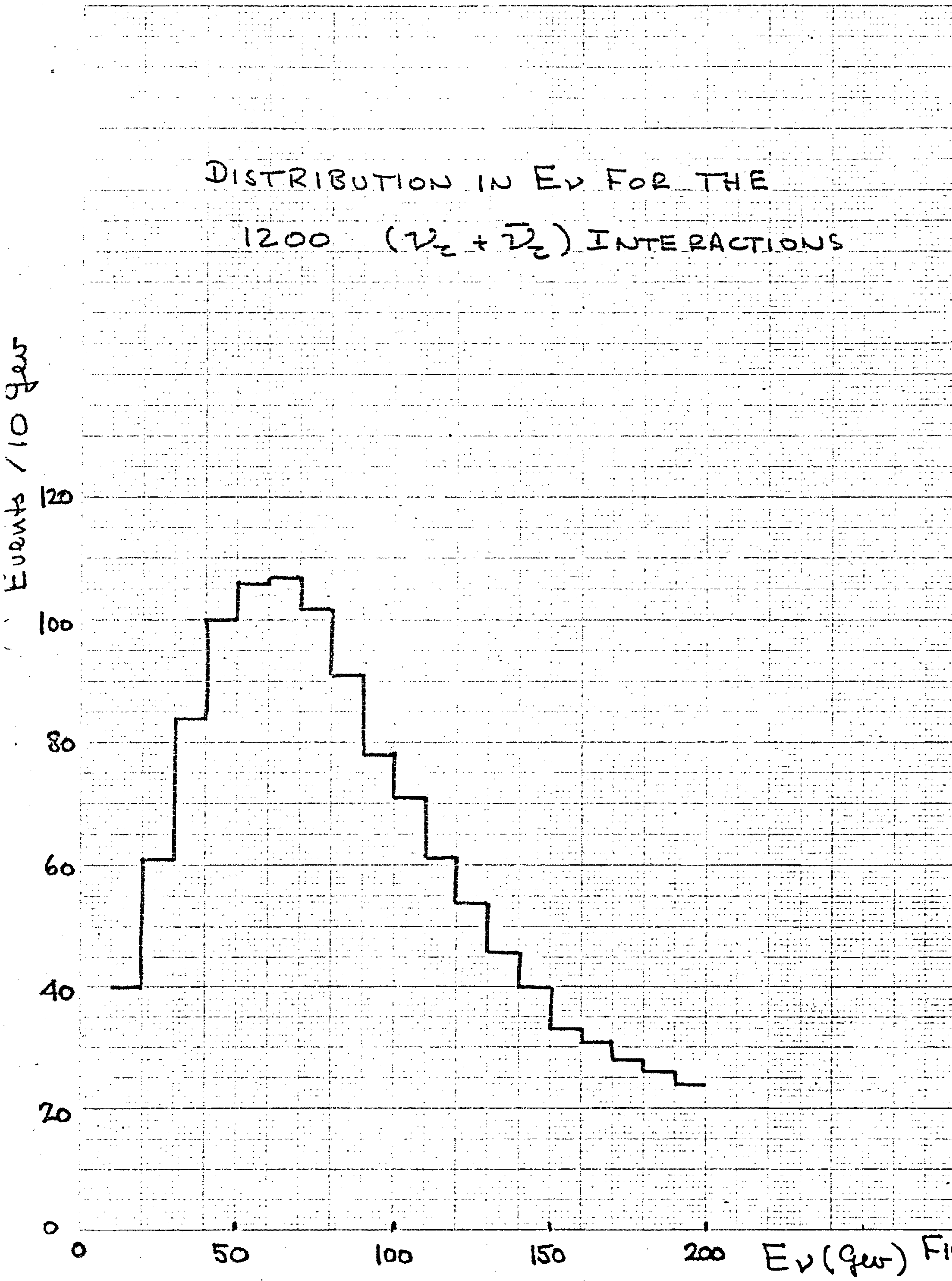

DISTRIBUTION IN Eν FOR THE
1200 (ν_τ + ν̄_τ) INTERACTIONS
Events / 10 GeV
0
20
40
60
80
100
120
0
50
100
150
200
Eν (GeV)

FIG. 3

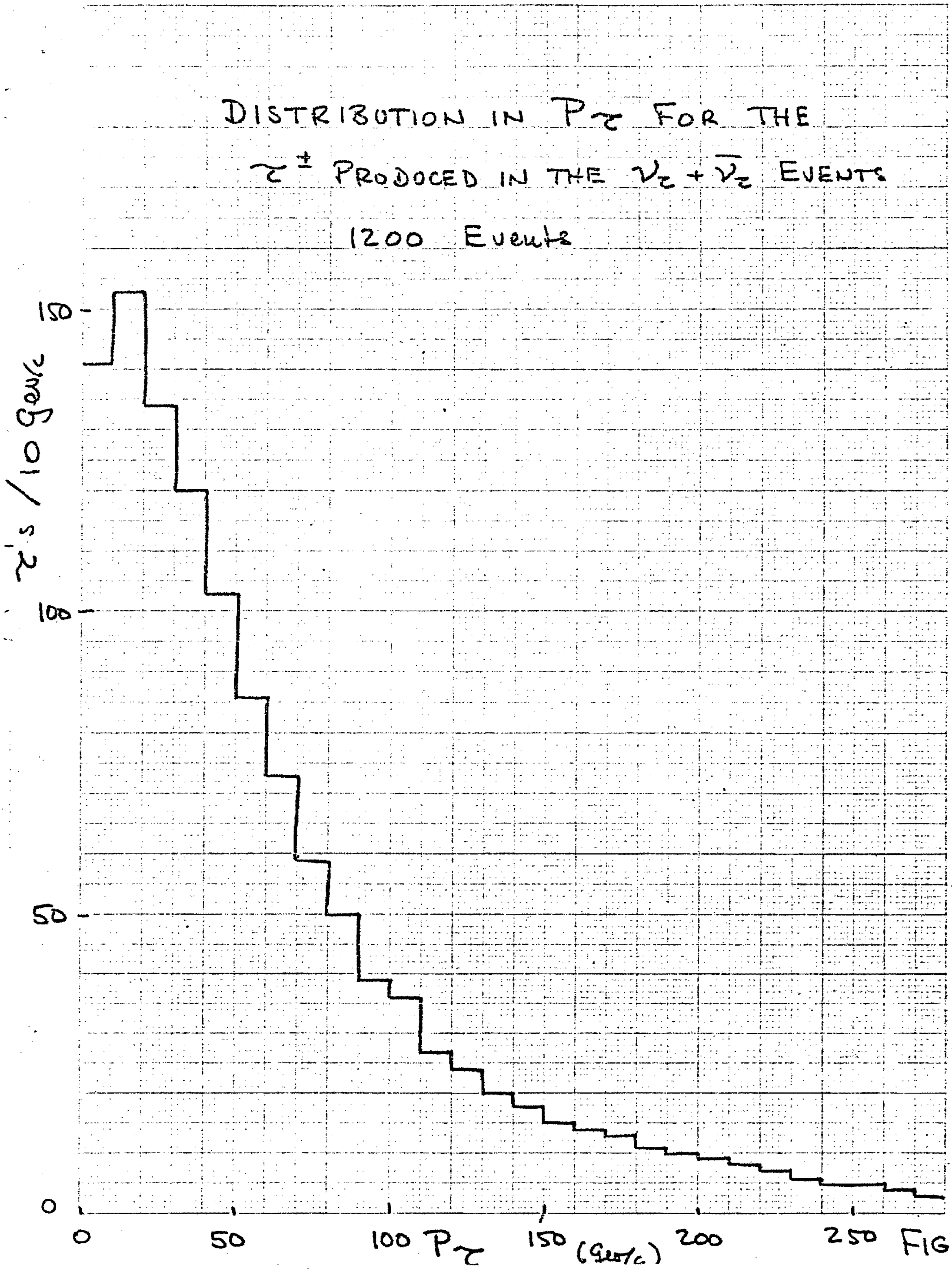

DISTRIBUTION IN P_τ FOR THE
$\tau^\pm$ PRODUCED IN THE $\nu_\tau + \bar{\nu}_\tau$ EVENTS
1200 Events
τ's / 10 GeV/c
150
100
50
0
0
50
100 P_τ
150 (GeV/c)
200
250

FIG. 4

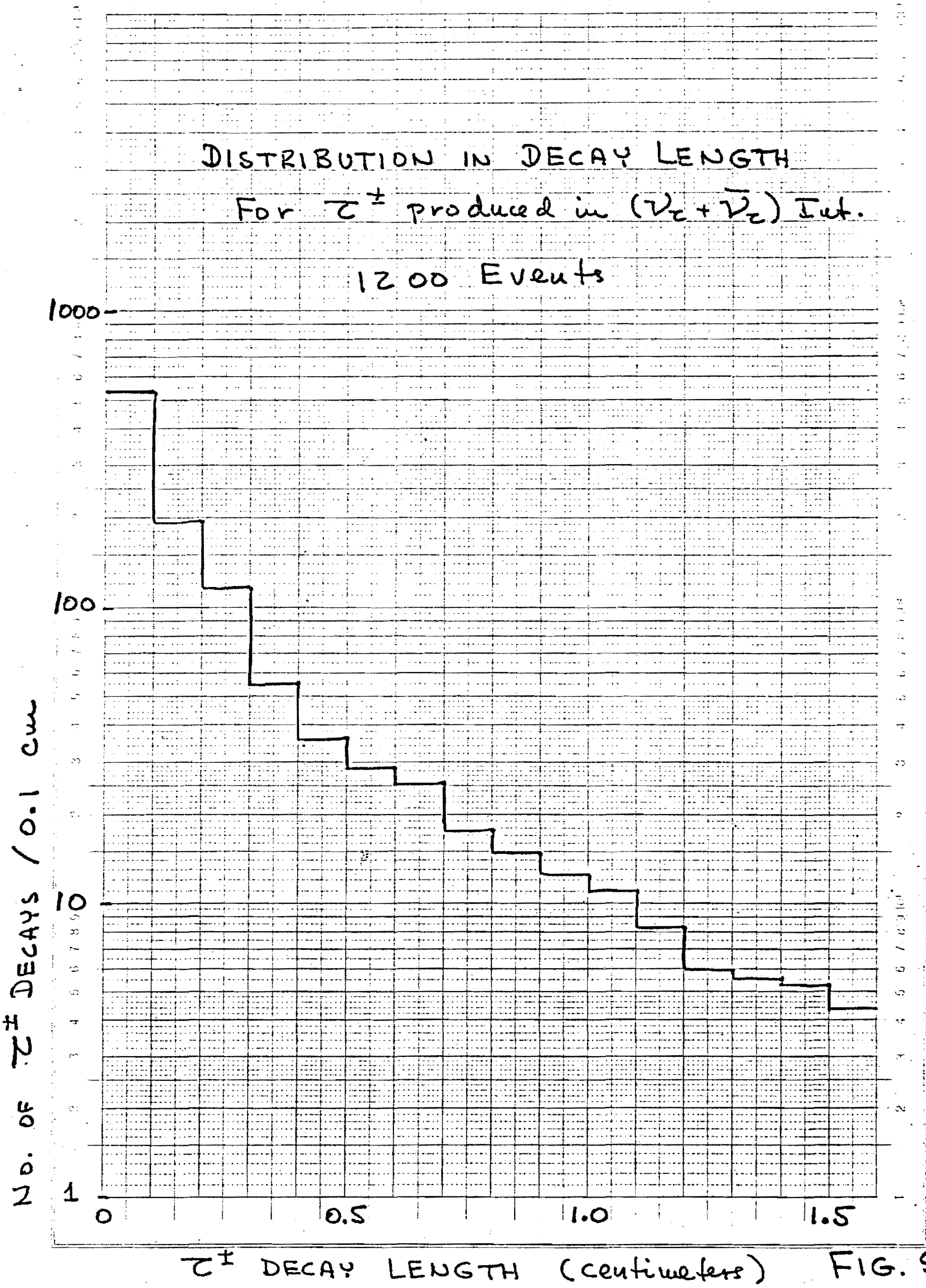

DISTRIBUTION IN DECAY LENGTH
For τ± produced in (ν_τ + ν̄_τ) Int.
1200 Events
1000
100
10
1
0
0.5
1.0
1.5
No. OF τ± DECAYS / 0.1 cm
τ± DECAY LENGTH (centimeters)

FIG. 5

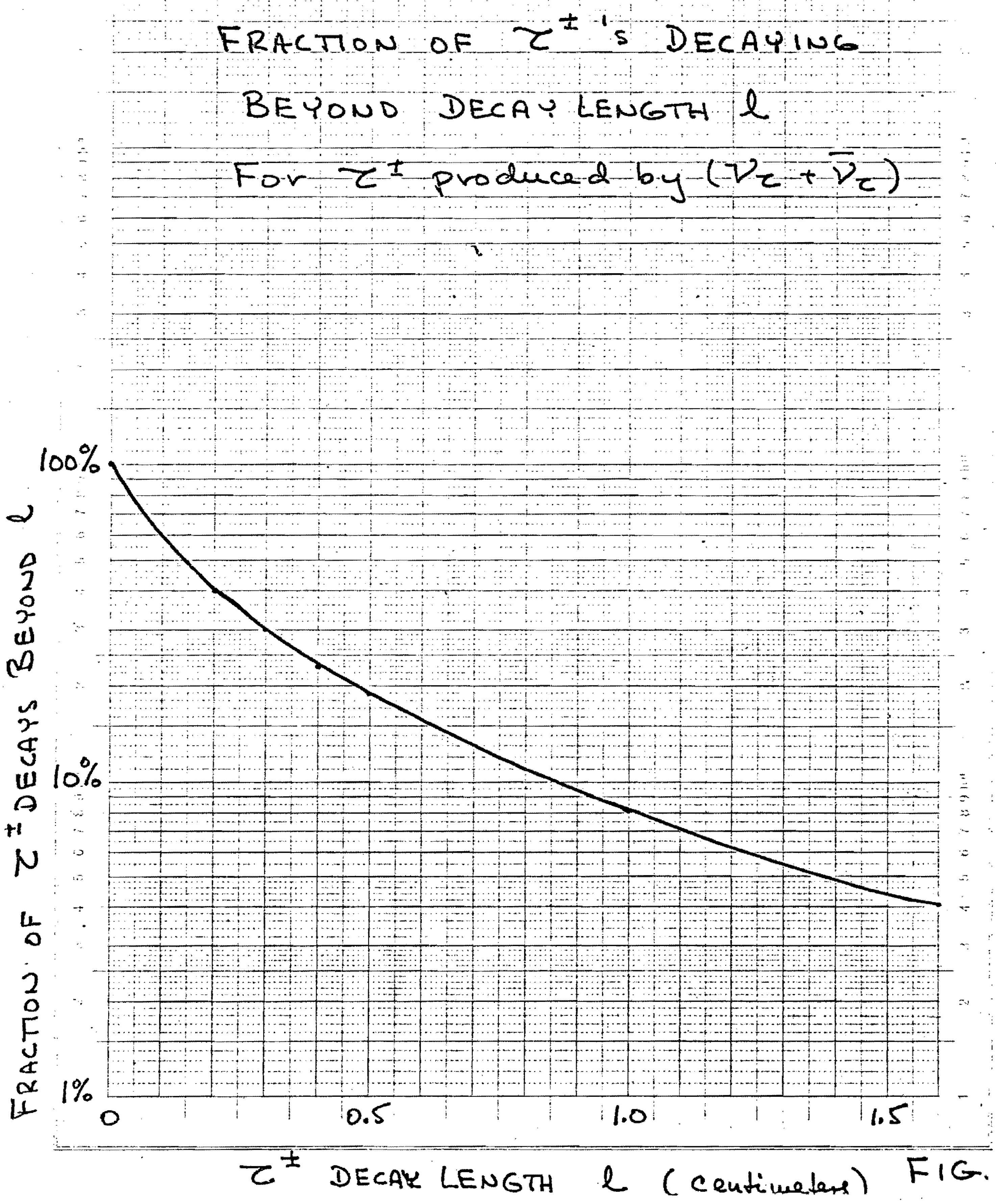

FRACTION OF τ±'s DECAYING
BEYOND DECAY LENGTH ℓ
For τ± produced by ($\nu_\tau + \bar{\nu}_\tau$)
100%
10%
1%
FRACTION OF τ± DECAYS BEYOND ℓ
0
0.5
1.0
1.5
τ± DECAY LENGTH ℓ (centimeters)

FIG. 6

50 BeV/c $\tau^- \rightarrow e^- + \nu_\tau + \bar{\nu}_e$ Decay Kinematics

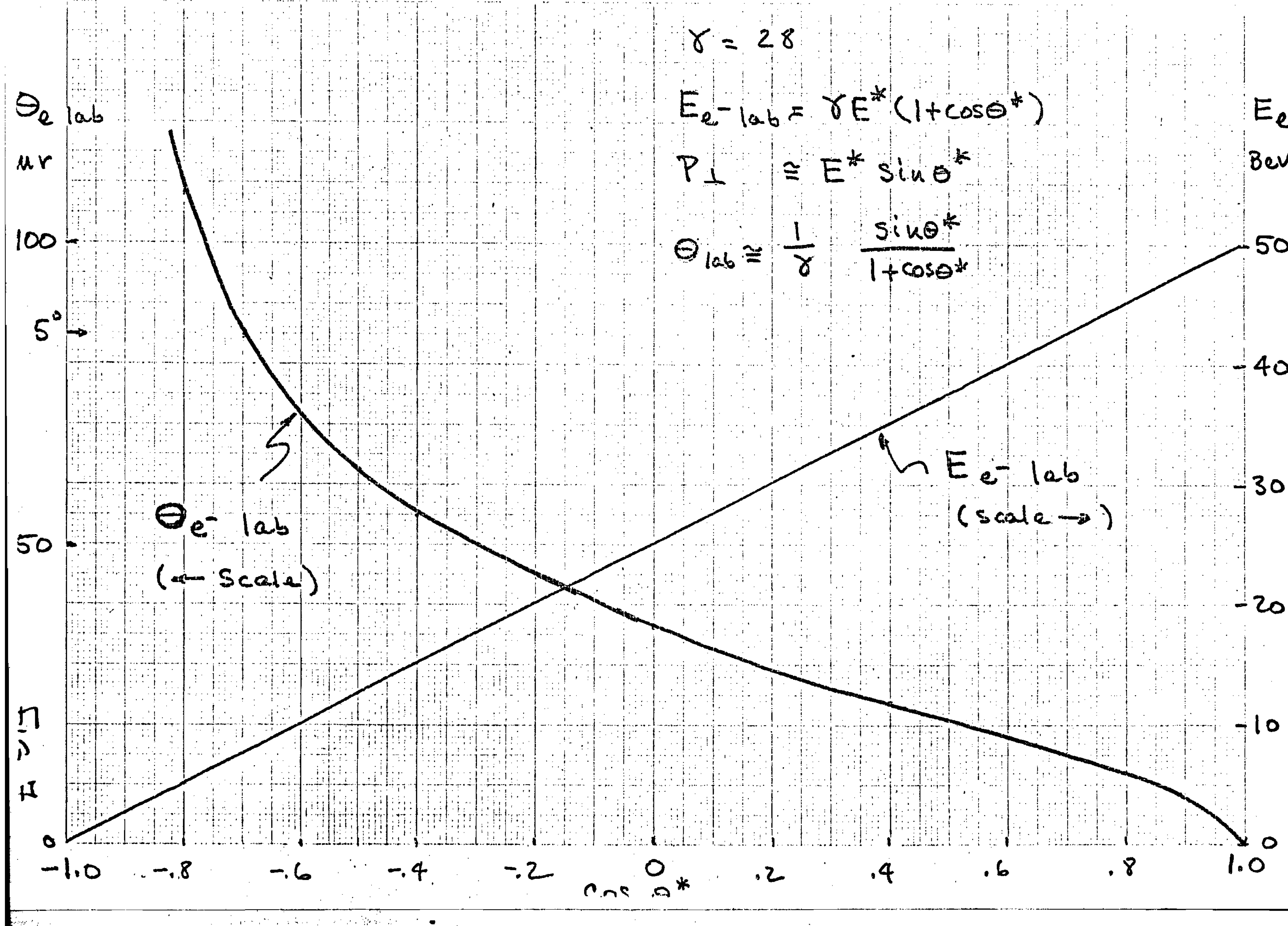

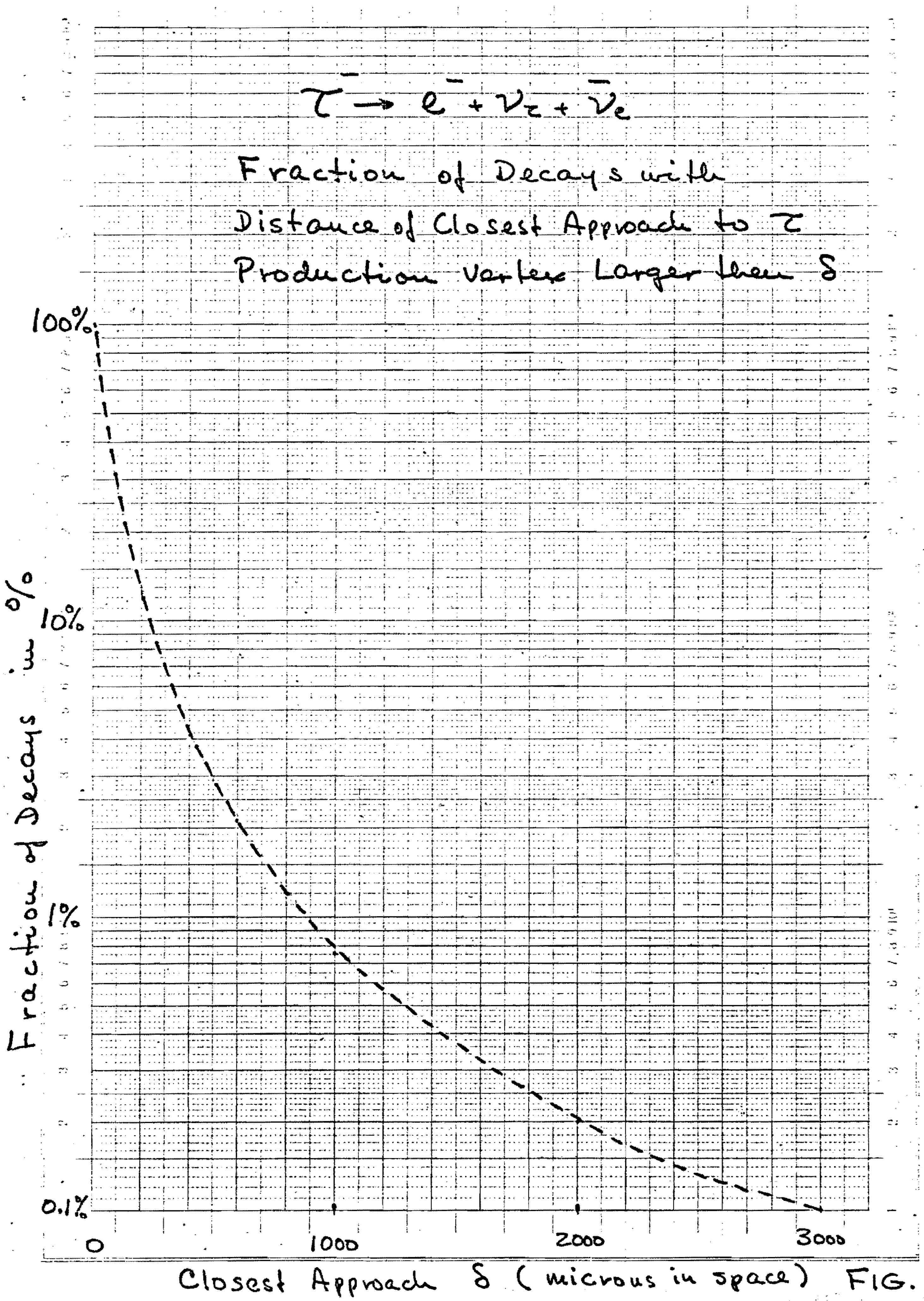

τ⁻ → e⁻ + ν_τ + ν̄_e
Fraction of Decays with
Distance of Closest Approach to τ
Production Vertex Larger than δ
100%
10%
1%
0.1%
Fraction of Decays in %
0
1000
2000
3000
Closest Approach δ (microns in space)

FIG. 8

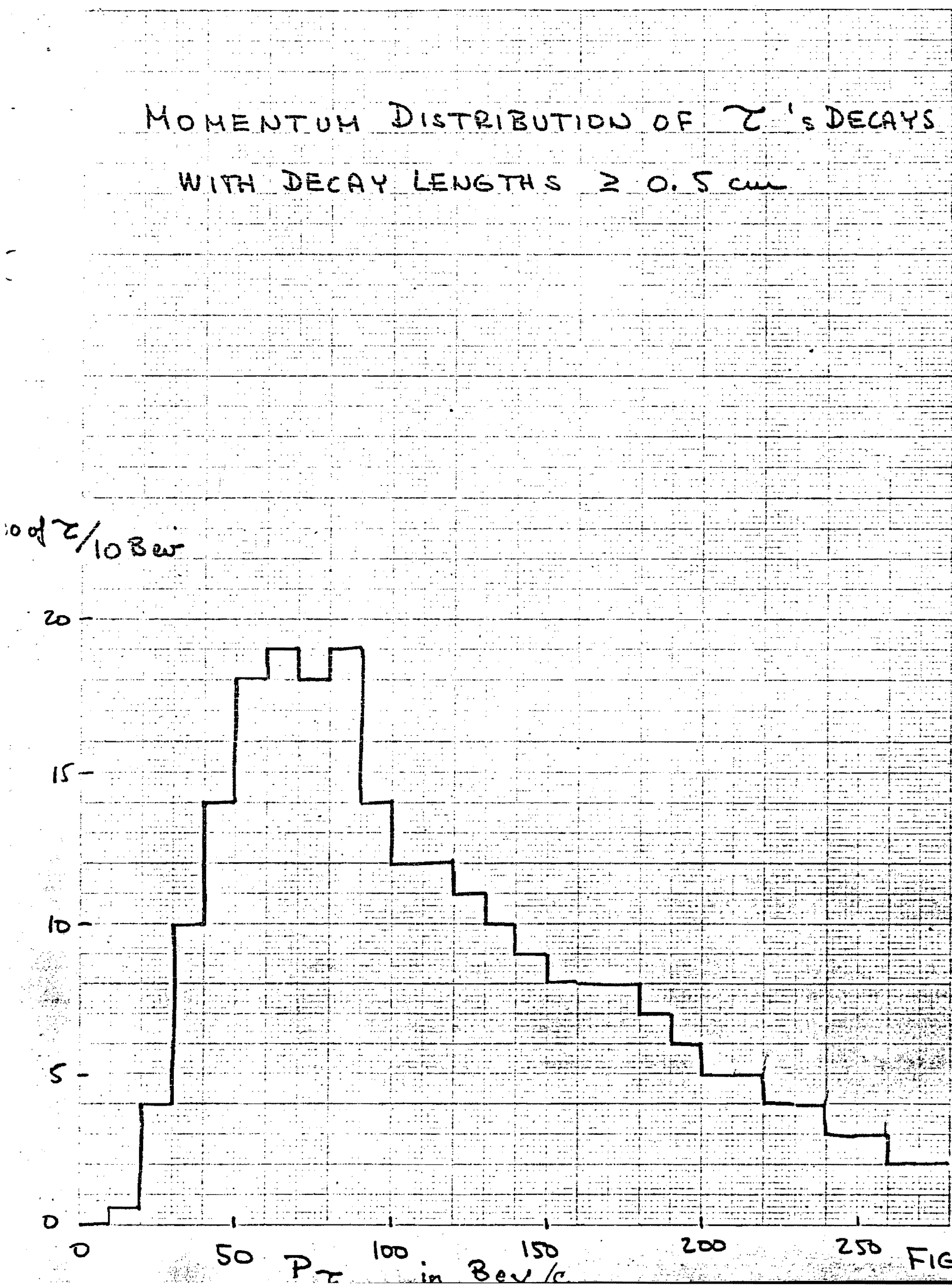

MOMENTUM DISTRIBUTION OF τ's DECAYS
WITH DECAY LENGTHS ≥ 0.5 cm
No of τ/10 Bev
20
15
10
5
0
0
50
100
150
200
250
Pτ in Bev/c

FIG. 9

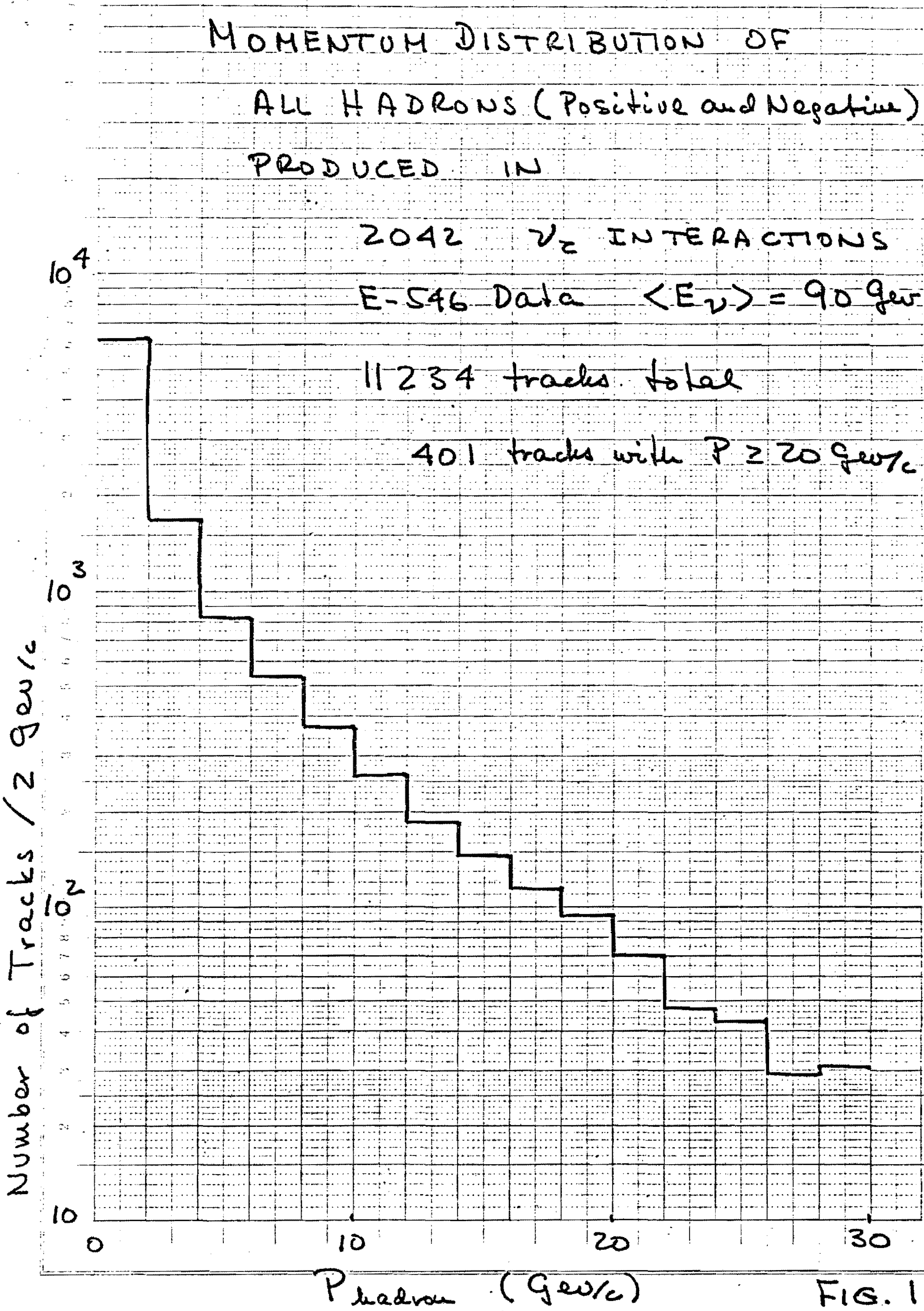

MOMENTUM DISTRIBUTION OF
ALL HADRONS (Positive and Negative)
PRODUCED IN
2042 ν_e INTERACTIONS
E-546 Data $\langle E_\nu \rangle$ = 90 GeV
11234 tracks total
401 tracks with P ≥ 20 GeV/c
10^4
10^3
10^2
10
0
10
20
30
Number of Tracks / 2 GeV/c
P hadron (GeV/c)

FIG. 10a

2042 ν_μ INTERACTIONS IN 15' NEON BC

E-546 Data, $\langle E_\nu \rangle = 90$ GeV

ϕ DISTRIBUTION OF ALL HADRONS WITH $P \geq 20$ GeV/c

401 Tracks total

40 Tracks with $\phi \geq 120°$

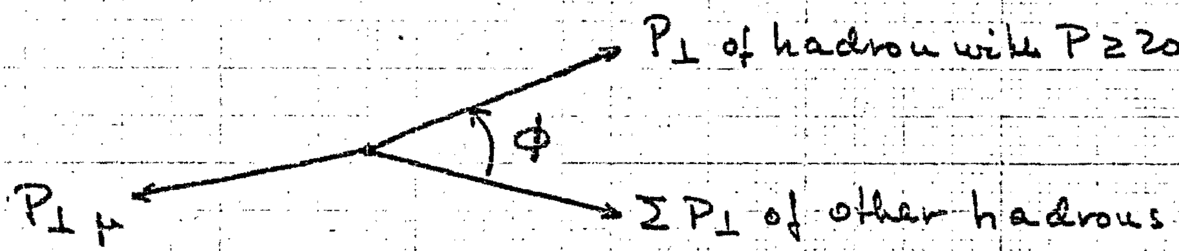

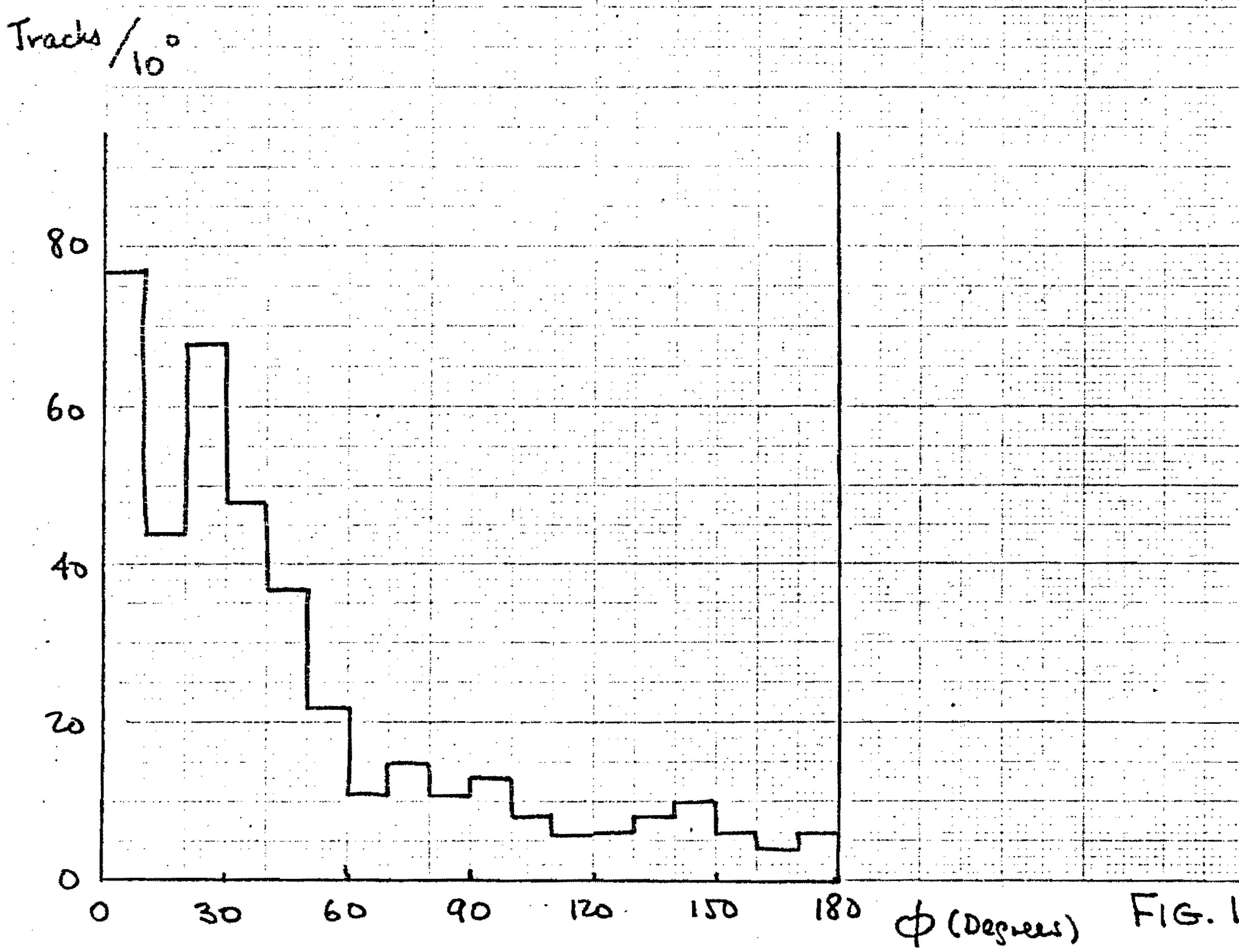

FIG. 10b

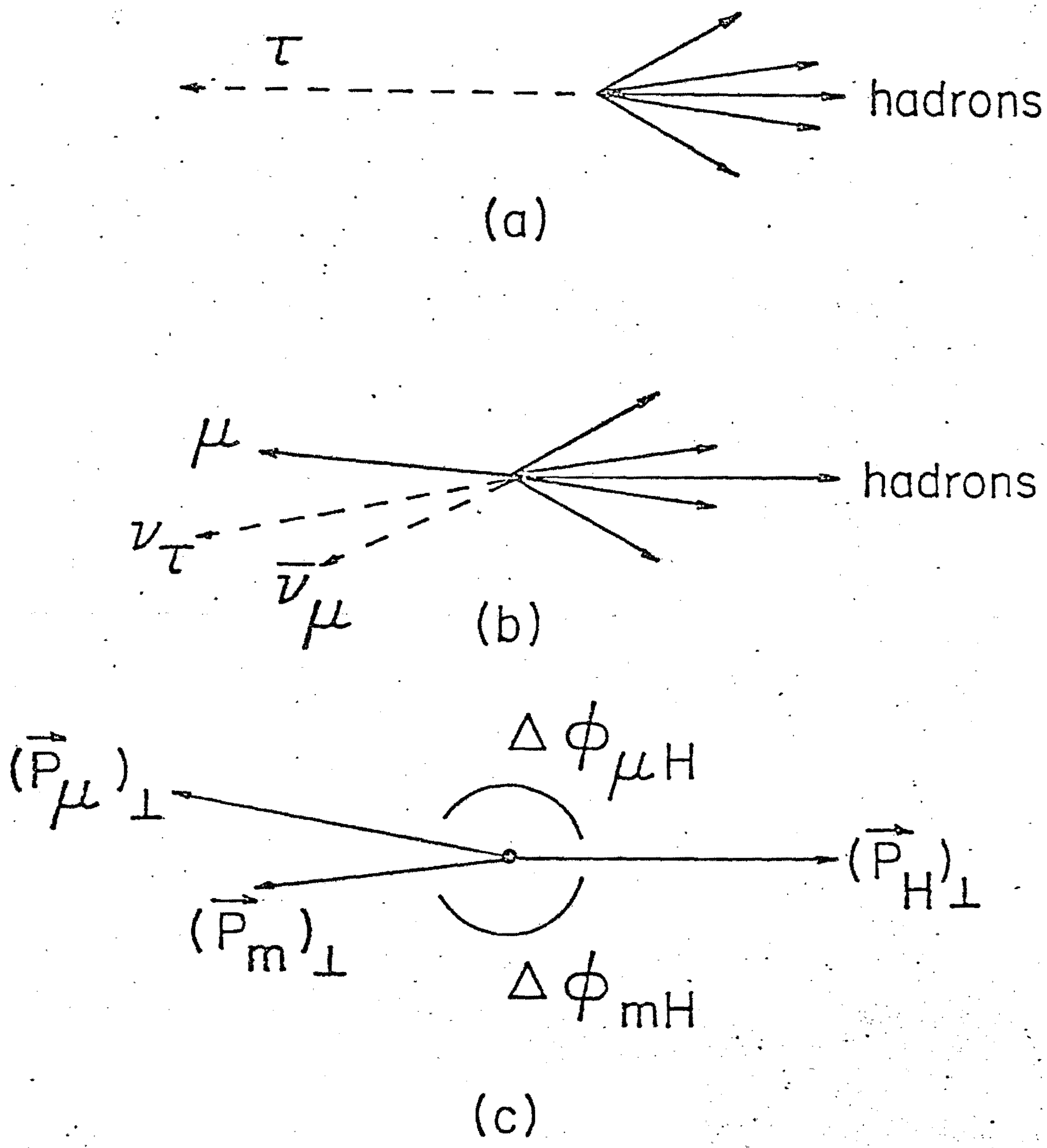

Figure 11

Kinematics of $\tau \rightarrow \mu + \nu + \bar{\nu}$ Decays in $\nu_\tau + N \rightarrow \tau$ + hadrons (H)

From Albright, Shrock, & Smith

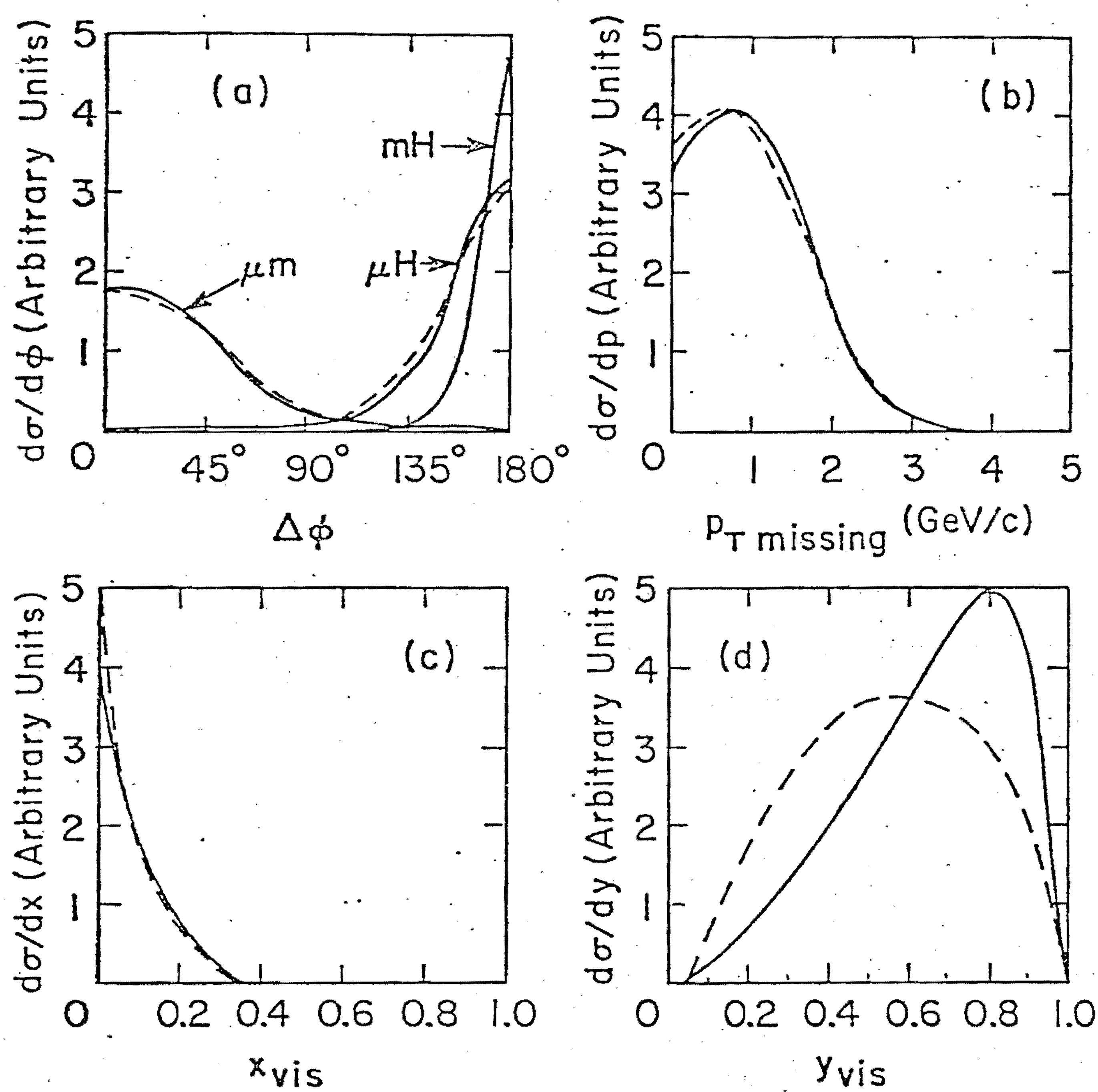

Figure 12

KINEMATICS OF τ DECAYS

$\nu_\tau + N \to \tau + \text{hadrons (H)}$

$\tau \to \mu + \nu + \bar{\nu}$

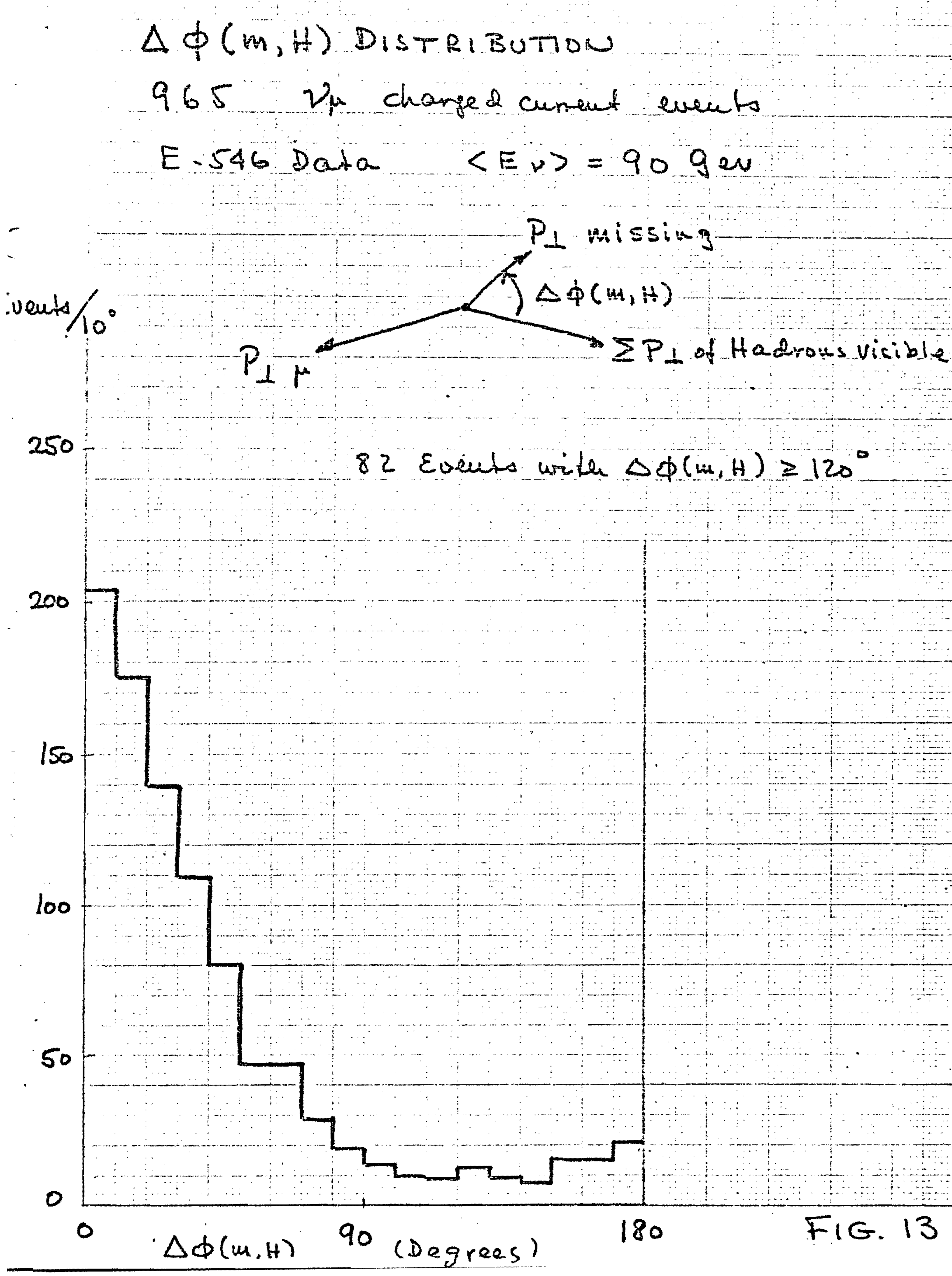

Δφ(m,H) DISTRIBUTION
965 ν_μ charged current events
E-546 Data ⟨Eν⟩ = 90 Gev
P⊥ missing
Δφ(m,H)
ΣP⊥ of Hadrons vicible
P⊥ μ
Events/10°
82 Events with Δφ(m,H) ≥ 120°
250
200
150
100
50
0
0
90
180
Δφ(m,H) (Degrees)

FIG. 13

DISTRIBUTION IN MISSING TRANSVERSE MOM. P_t miss

For ν_μ charged current events

BEBC Narrow Band Run in Neon $\langle E_\nu \rangle \sim 100$ GeV

SELECTING 838 EVENTS WITH $\Delta\phi(m,\mu) \leq 90°$

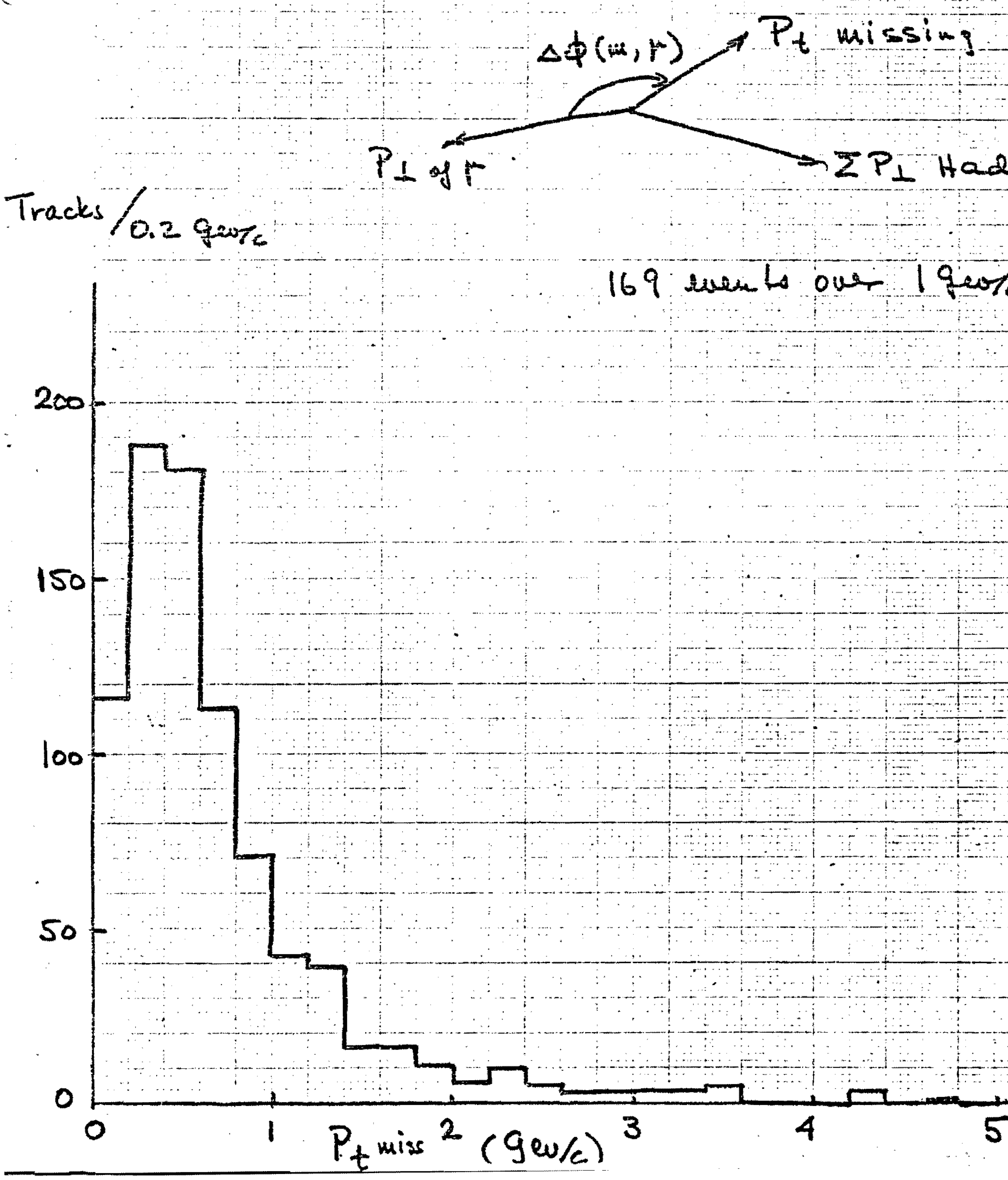

FIG. 14

EXPECTED y_{vis} DISTRIBUTIONS

AFTER CUTS TO OBTAIN EQUAL NOS. of ν_τ and $(\nu_\mu + \nu_e)$ Background events

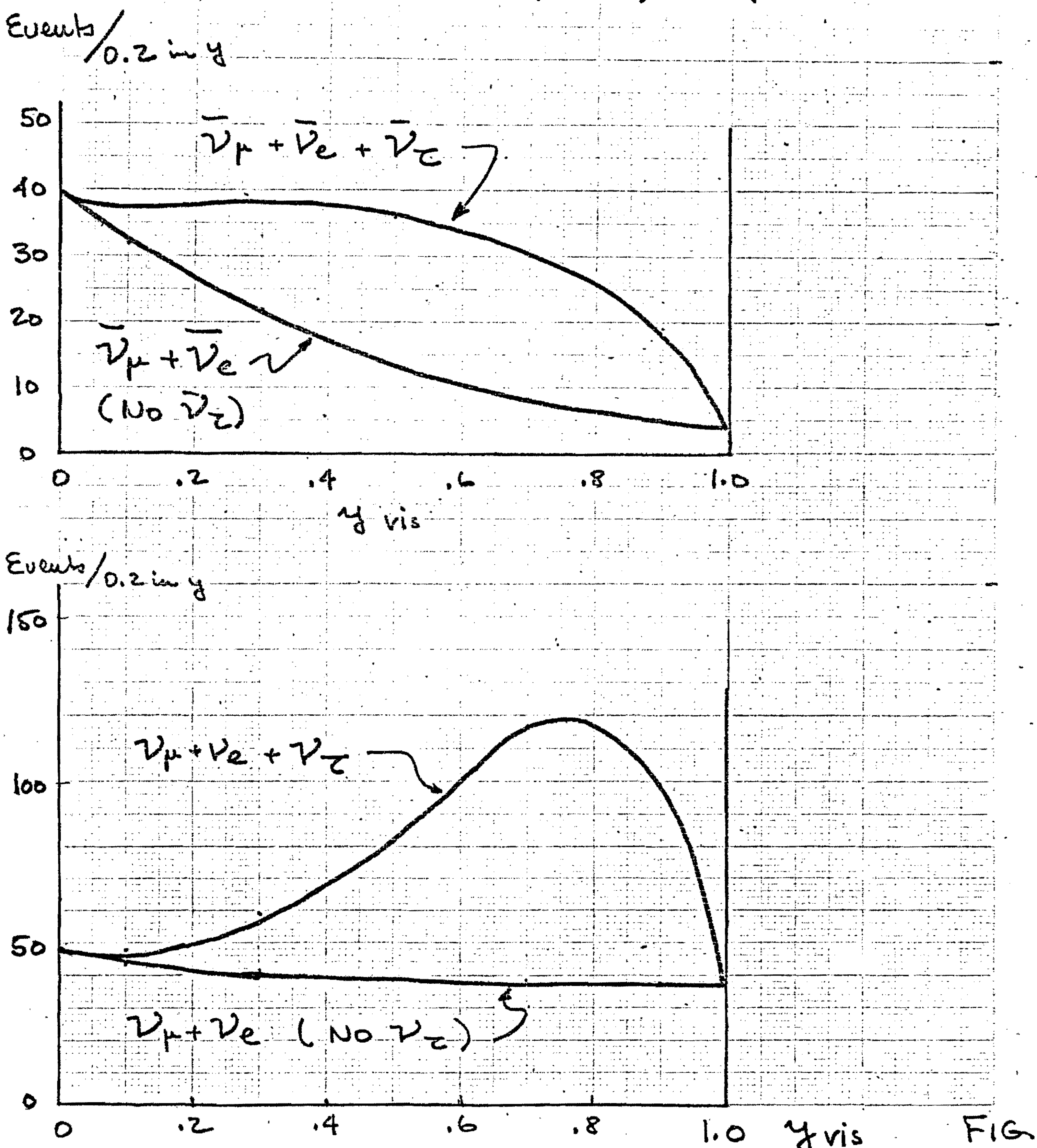

FIG 15

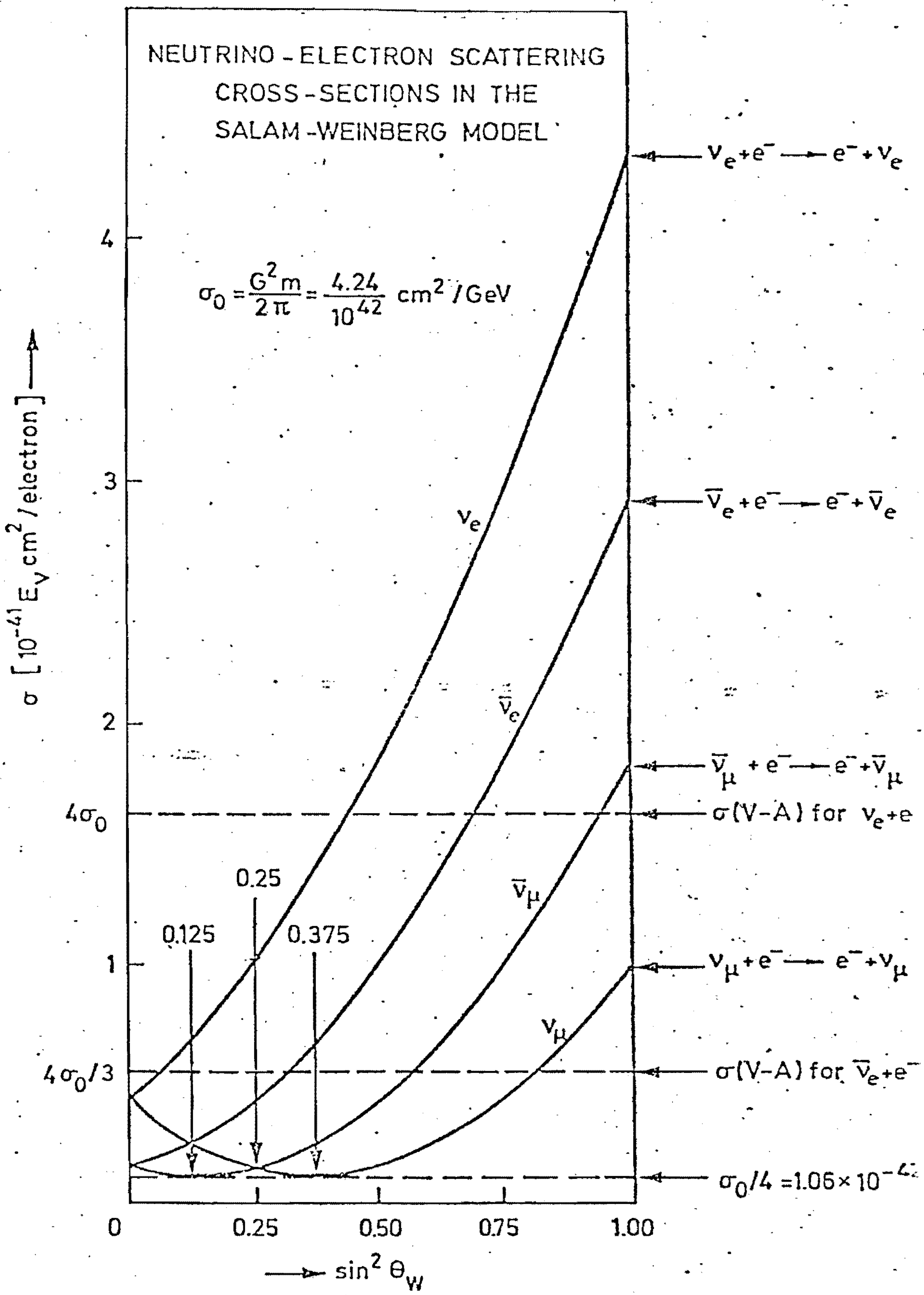
NEUTRINO - ELECTRON SCATTERING CROSS-SECTIONS IN THE SALAM-WEINBERG MODEL
$\sigma_0 = \frac{G^2 m}{2\pi} = \frac{4.24}{10^{42}}$ cm^2/GeV
σ [$10^{-41} E_\nu$ cm^2/electron]
4
3
2
1
$4\sigma_0$
$4\sigma_0/3$
ν_e
$\bar{\nu}_e$
$\bar{\nu}_\mu$
ν_μ
0.125
0.25
0.375
0
0.25
0.50
0.75
1.00
$\sin^2\theta_W$
$\nu_e + e^- \rightarrow e^- + \nu_e$
$\bar{\nu}_e + e^- \rightarrow e^- + \bar{\nu}_e$
$\bar{\nu}_\mu + e^- \rightarrow e^- + \bar{\nu}_\mu$
σ(V-A) for $\nu_e + e$
$\nu_\mu + e^- \rightarrow e^- + \nu_\mu$
σ(V-A) for $\bar{\nu}_e + e^-$
$\sigma_0/4 = 1.06 \times 10^{-42}$

FIG. 16

646

Ch. Baltay
CERN, Geneva
8 May 1980

RECEIVED
MAY 12 1980
DIRECTOR'S OFFICE
FERMILAB

APPENDIX

to the Tevatron Proposal:

Search for the ν_τ and Study of ν_e and $\bar{\nu}_e$ Interactions

The Beam Dump Neutrino Beam and the Muon Shield

A. Introduction and Summary.

The preceeding proposal outlined an experimental search for the ν_τ and a study of ν_e and $\bar{\nu}_e$ interactions using the 15 foot Bubble chamber and a new beam dump neutrino beam in the neutrino area. The proposed location of the beam dump is about 200 meters upstream of the 15' B.C., as shown in Fig. A1. The neutrino flux calculations, discussed in section II of the main proposal, indicate more then an order of magnitude higher flux of ν_τ's and ν_e's for this beam dump location compared to a dump located at the present hadron dump in enclosure 100, which is $\sim$ 1000 meters from the 15' B.C. This increase in flux is quite important for this experiment, as can be seen from Table II of the proposal.

The main problem of having the beam dump this close to the bubble chamber is the background of muons coming out of the dump. In section C of this appendix a magnetized muon shield is described which we believe will reduce the muon flux through the chamber to a tolerable level by ranging out the low energy muons, which is the bulk of the flux, and magnetically deflecting the high energy muons. A careful calculation of this muon background, described in section D, predicts tens of muons per pulse in the chamber, while we believe that we could analyze pictures whith up to 100 muons per pulse. The bakcgrounds from scraping in the proton beam transport to the dump can be kept to a tolarable level, as discussed in section E, estimating from the measured limits on the proton beam scraping ($< 4 \times 10^{-6}$) that have been achieved in the recent beam dump experiments at the CERN SPS. The radiation levels due to the negative muons that are deflected up by the magnetized shield are tolerable, as discussed in section F. In section G the materiel and power requirements of the magnetized shield are estimated. The costs of the coils to magnetize the iron ($\sim$ \$ 50,000) and the power required for operation ($\sim$ 35 kilowatts) seem quite modest. The shield requires $\sim$ 2000 tons magnetizable iron and an additional 7000 tons of passive iron. Based on discussions with people in the neutrino lab we assume that this iron can come from existing sources such as the Argonne ZGS magnets and iron stockpiled in the neutrino lab for purposes of improving the shield, and thus no actual cash outlays are required.

B. General Location and Lay out of the Beam.

The proposed beam dump would be located 100 meters upstream of the present end of the earth berm. The full intensity full energy proton beam to the dump in this location presents no problem. One possible solution suggested by Ray Stefanski is shown in Fig. A2. The beam originates in enclosure G-2, passes through Nu-hall a few feet east of the proton beam to the existing neutrino target, is bent some more to the east in enclosure 100, and is bent back toward the dump near the Wonder Building. The protons approach the dump at an angle of $\sim$ 30 mrad. A final bending magnet just in front of the dump bends the protons towards the detectors. This magnet can be used to vary the angle of the proton beam incident on the dump so that prompt neutrino production can be studied from 0 to 30 mrad in the stationary detectors.

The dump should be as dense a material as possible. For practical reasons copper might be a good material. A block 50 cm by 50 cm transverse to the beam and 100 cm long should be sufficient since it would be followed immediately by the solid iron muon shield. The proton beam can be blown up to a few cm in diameter to reduce local heating, so that the full proton intensity can be incident on the dump. The dump will probably have to be water cooled; this is a detail to be worked out with the neutrino department.

C. The Magnetized Muon Shield.

The major problem associated with moving the beam dump so close to the bubble chamber is that there is no room for a full range shield to stop muons by energy loss. The muon shield will therefore have to be magnetized to deflect the higher energy muons away from the detector. The magnetic configuration we have chosen is a solid iron dipole with the field horizontal, as shown in Fig. A1c. Thus the muons from the dump are bent in the vertical plane, with the μ^+ bent down into the ground and the μ^- bent up onto the sky. The skyshine, or flux of negative muons, is at a tolerable level from the radiation safety point of view, as discussed in more detail in section F of this appendix. Figures A3a to d show ray traces of muons of various momenta through the shield. The magnetized iron part is 25 m long, followed by a drift space of 160 m to the plane of the bubble chamber. With a field of 20 kilogauss, which is near saturation of good magnet steel (such as the Argonne ZGS iron) the magnet gives a perpendicular momentum kick of Δp = 15 GeV/c. Thus even 1000 GeV/c muons get a deflection of 15 mrad and thus miss the center of the chamber by $\sim 2\frac{1}{2}$ meters, as shown in Fig. A3d.

One important design consideration has to do with the fact that any magnet must have a return leg where the field reverses direction. With a field strong enough to deflect 1000 GeV/c muons away from the detector, some low energy muons will be bent into the return leg, where they will be bent back toward the detector. This focusing effect at low energies is shown in Fig. A3a for 70 GeV/c muons. One solution to this problem is to make the good field region wider; but this is expensive and only moves the problem to lower momenta, but does not eliminate it. We must therefore have enough iron in the muon shield to range out the low energy muons that get into the return leg. For this reason we follow the magnetized iron by 50 meters of passive iron so that muons up to $\sim$140 GeV/c are ranged out. The width of 2.4 meters of the good magnetic field was then chosen so that muons over 140 GeV/c are not bent back toward the detector by the return leg (see Figs. A3b and A3c). Another advantage of having this much passive shielding is that by ranging out muons up to 140 GeV/c the number of muons we have to worry about are reduced by almost two orders of magnitude (see Fig. A5).

We thus end up with magnetized iron 2.4 m wide in the non-bend plane and 4.8 m tall vertically in the bend plane, including the two return legs which are 1.2 m each. The passive iron, 3 m horizontally by 6 m vertically, extends out slightly beyond the magnetized iron in order to stop muons that emergy nearly tangent to the magnetized iron on the side, as the + 90 mr ray almost does on Fig. A3a.

The ray traces of Fig. A3 show the central 0 mr muons and the muons at the limiting angles which correspond to a perpendicular muon momentum of $p_\perp \sim 6$ GeV/c beyond which there should be less then one muon for 10^{13} protons in the dump (see Fig. A6). The ray traces also take the energy loss of the muons in the iron into account. A study of many such ray tracs covering the entire kinematic range allowed for muons produced by 1000 GeV protons in the dump indicate that at the present level of discussion, i.e. considering only magnetic deflection and energy loss, the geometry and field strength of this design are sufficient to either range out or deflect away all muons produced in the dump down to a level well below one muon in the chamber for 10^{13} protons in the dump. However there are additional effects such as multiple scattering and inelastic muon interactions in the iron of the shield that tend to scatter muons back toward the detector. We have studied these problems carefully using Monte Carlo programs tracing muons through the shield taking all of these effects into account. These calculations and their results are discussed in the next section.

D. Calculation of the Muon Background in the 15' B.C.

The background muon fluxes through the 15 foot bubble chamber were estimated using a set of Monte Carlo programs. These programs generated muons leaving the dump from 0 to 1000 GeV/c in momentum and 0 to 10 GeV/c in transverse monetum. The muons were then stepped through the magnetized iron, the passive iron, and then to the detector plane, taking typically 10 steps in each region. In each step the magnetic deflection, if any, and the energy loss were taken into account. In each step the muon was allowed to undergo an inelastic interaction, and the final state muon, with a reduced energy and a changed angle was followed the rest of the way. In addition to the above, the probability of multiple scattering into the chamber was accumulated. The effect of the magnetic field of the 15 foot chamber was taken into account in the drift space before the chamber. The μ^+'s, which are bent down, are propagated through earth below and beyond the iron shield all the way to the chamber, taking energy loss, inelastic, and multiple scattering into account. The μ^-'s, which are bent up, were propagated through air beyong the iron shield. The energy losses used in the calculations were 1.8 GeV/meter in iron and 0.4 GeV/meter in earth, which are the values deduced from the performance of the existing 500 GeV muon shield [1)]. One technical problem that required a great deal of thought was the problem of getting sufficient statistics. We start with $\gtrsim 10^9$ muons out of the dump and want to end up with less then 100 in the chamber. This problem was overcome partly by careful and efficient programming and partly by the use of the CERN CDC 7600 computer.

We now discuss some of the more important aspects of this calculation in more detail.

1. Muon fluxes out of the Dump.

We have taken the muon fluxes out of the dump to be the sum of the prompt single muon production measured in many experiments at Fermilab and the the muons expected from π and K decays in the dump. A collection of all of the available measurements [2)] on the prompt μ/π ratio, shown in Fig. A4, is fit quite well by the expression

$$\mu^+/\pi^+(\text{prompt}) = (1.0 \times 10^{-4})\ (1 - x_F)^3$$

independent of $p_\perp$, where $x_F = p_{\mu or \pi} / p_{prot}$.
To this muon flux we added the muons from π and K decay in the dump, as calculated by our Monte Carlo program using the Sanford Wang meson production formula and an effective 30 cm absorbtion length in the dump. At small x and $p_\perp$ the muons from π and K decays are about twice the prompt muon flux, but fall to below the prompt muon flux at large x and $p_\perp$, consistent with the backgrounds observed in the experiments measuring the μ/π ratios.

The resulting muon flux is shown plotted vs. the momentum p and the transverse momentum $p_\perp$ of the muon in Figs. A5 and A6, respectively. These figures show the number of muons produced by 10^{13} protons at 1000 Gev in the dump. We see that there is non-negligible numbers of muons out to beyond 900 GeV/c in p_μ. In $p_\perp$ the flux falls to less then one muon per pulse of 10^{13} protons beyond $p_\perp \simeq$ 6 GeV/c. We expected a total of 3.6×10^{13} π^+ and 6.3×10^9 μ^+ to be produced in the dump by 10^{13} protons. Of these μ^+, most are below 140 GeV/c and will be ranged out by the 75 m of iron and the 25 m of concrete in the muon shield. We expect 1.8×10^8 μ^+ above 140 GeV/c that penetrate the shield and have to be deflected by the magnetic field.

2. Multiple and Molière Scattering.

The geometry and the field strength of the muon shield as discussed above are sufficient to sweep the muons away from the bubble chamber to a level of well below one muon in the chamber per 10^{13} protons in the dump. However we must consider the scattering of the muons in the material of the shield which tend to deflect muons back toward the chamber. To get a feeling for the order of magnitude of the problem due to multiple scattering, we estimate the scattering in 75 m of iron

$$\Theta_{rms} = \frac{15\ \text{MeV/c}}{p} \sqrt{t/x_o} = \frac{15\ \text{MeV/c}}{p} \sqrt{75/.018} = \frac{970\ \text{MeV/c}}{p}$$

We can talk of this as a deviation in $p_\perp$:

$$\Delta p_{\perp rms} = p\ \Theta_{rms} = 0.97\ \text{GeV/c}$$

This has to be compared to the transverse momentum kick of Δp = 15 GeV/c from the magnet. Thus the typical muon has to scatter by more then 15 standard deviations to get into the chamber, which is negligible. Even the worst case of a muon produced with $p_\perp$ = = - 6 GeV/c ends up with a $p_\perp$ = 9 GeV/c after the magnet, and has a negligible probability of scattering back in.

We have also considered the non-gaussian tail of the scattering distribution, usually called the Molière scattering tail, shown in Fig. A7. The Molière scattering theory was developed around 1950 for low energy particles; its much quoted experimental verification by A.O. Hansen et al., whose results are shown in Fig. A7, scatterd 15.7 MeV electrons on 19 and 37 milligrams/cm^2 gold foils. One has to take some care in applying this formula to 100 GeV muons in many meters of iron. Specifically, the leading term of the asymptotic form of the Molière formula [4)] for the single scattering tail is

$$p(\Theta) = \frac{2\pi N t\ e^4\ Z^2}{E^2\ \Theta^4}$$

where N is the no. of atoms/cm^3, t is the thickness traversed, and Z is the nuclear charge. One recognizes this as the Rutherford scattering formula with the mall angle approximation $\sin^4(\Theta/2) \rightarrow 1/16\ \Theta^4$, which is as it should be since the Molière tail is due to single elastic scatters off the nuclear charge Z. To get a feeling of the angles, or more relevantly the momentum transfers, involved in our case we have calculated the scattering distribution, both the Gaussian and Molière tail, for the scattering of 280 BeV/c muons in 2.3 meters of iron. We plot the distribution vs. $p_{\perp}$ of the scattering in Fig. A8. We calculate for 280 BeV/c muons in 2.3 m of iron because there is some useful experimental data from a test run of the European Muon Collaboration (EMC) at the CERN SPS on the inelastic scattering of an accumulated total of 10^{12} incident 280 GeV/c muons in a 2.3 m iorn target, where they measured the number of scattered muons as a function of $p_{\perp}$. Their result [5] is also shown on Fig. A8 for comparison. The number of muons from elastic scattering was negligible in this measurement compared to the number of inelastic scatters at the values of $p_{\perp}$ plotted.

From Fig. A8 we see that at these energies the Gaussian multiple scattering extends nearly up to 1 GeV/c in $p_{\perp}$, and the Molière single scattering tail is dominant above 1 GeV/c. We also see that the blind use of the Molière formula predicts scattering an order of magnitude larger then the measuremnts of Gabathuler et al. We realize of course that we should not have used the formula with Z^2 in the coefficient, since we no longer have single elastic scatters off the iron nucleus at momentum transfers of 2 or 3 GeV/c. Thus Z^2 should be replaced by Z x (1^2) multiplied by the nucleon form factors which for elastic scattering drop off like $1/q^8$. We see then that the Molière tail,,calculated correctly for this energy range, is completely negligible compared to the inelastic muon scattering.

We have therefore used the sum of the Gaussian multiple scattering distribution and the inelastic muon scattering to treat the muon scattering in the shield in our calculations. Using the Monte Carlo program discussed above we find that the effects of multiple scattering are not very large - the number of muons scattered into the chamber remains in the vicinity of one muon per 10^{13} protons in the dump. This result is not surprising in view of the fact that the rms multiple scattering in 75 m of iron is $\sim$1 GeV/c in $p_{\perp}$ compared to the $\Delta p_{\perp} \sim$15 GeV/c deflection of the magnet. The effects of inelastic muon scattering are somewhat more serious and will be discussed in the next section.

3. Inelastic Muon Scattering.

Inelastic muon scattering has been extensively studied experimentally at both Fermilab and the the CERN SPS and is now sufficiently well understood for the purposes of our calculation. In the Monte Carlo program used to propagate the muons through the shield, the muon is allowed to scatter inelastically in each slice of sthe material (typically a few meters thick each). Both the energy and angle of the scattered muon are changed randomly according to the scattering cross-section given by the formula

$$\frac{d\sigma}{dq^2\, d\nu} = \frac{2\pi\alpha^2}{q^4}\,\frac{1}{E^2}\left[\left(2EE' - \frac{q^2}{2}\right) W_2(q^2,\nu) + (q^2 - 2m_\mu^2)\, W_1(q^2,\nu)\right]$$

where E and E' are the energies of the incident and scatterd muon, respectively, and q^2 and ν are the usual inelastic scattering variables, $q^2 = 2EE'(1 - \cos\theta)$ and $\nu = E - E'$, and θ is the scattering angle. For the form factos W_2 and W_1 we used a recent parametrization[6)] by Tom Kirk, which included scale breaking effects etc. (i.e. the latest experimental information). The scattered muon was then propagated through the remainder of the shield, earth, etc. including further energy loss and multiple scattering.

To check the absolute normalization and general correctness of this program (i.e. that we not forget a 4π or $\hbar/c$ etc.) we used the same program to calculate the inelastic scattering of 280 GeV/c muons in 2.3 meters of iron, and compared with the experimental data of Gabathuler et al. from the CERN SPS. The experimental data were taken with a q^2 cut around 3 GeV/c^2 and requiring visible hadron energy over 40 GeV or so. We made the same cuts for this comparison, which is shown in Fig. A9. The agreement at low $p_\perp$ is very good, while our program is somewhat higher then the data at the higher values of $p_\perp$. The discrepancy may be due to the slightly different cuts in q^2 and ν which we do not know precisely for the data. In any case we feel safe since the program if anything overestimates the scattering probability.

When all of the effects discussed so far are included in the calculation i.e. the μ^+ fluxes from the dump, the magnetic deflection, energy loss, multiple scattering and inelastic muon scattering, we find the following :

a) There is a large flux (thousands) of very soft (a few GeV) muons emerging from the shield. These can be eliminated by a local shield just in front of the 15 foot chamber (see Fig. A1). This shield can not be iron because of the fringe field of the chamber; a concrete shield 25 m thick would stop muons up to 10 GeV/c, which is sufficient to eliminate the soft muon flux. This local shield will not itself produce new soft muons since there are very few energetic muons hitting it (the energetic muons are bent away from the chamber and this local shield). There is sufficient room for such a local concrete shield immediately in front of the chamber and no problems are foreseen in installing it.

b) The calculation predicts a flux of $\sim$ 30 muons hitting the 15 foot chamber with enough energy to penetrate the local concrete shield. In previous experiments with the 15 foot chamber we have analyzed pictures with one or two dozen background muons in the chamber. We feel that the pictures would be analyzable with up to 100 straight through muons. The muon background from the 200 m beam dump therefore appears to be quite tolarable.

One can understand why inelastic scattering does not have a larger effect by looking at Fig. A9. Most of the scatters change the $p_\perp$ of the muon by less then 1 or 2 GeV/c. But the original muon has typically 15 GeV/c of $p_\perp$ away from the chamber due to the magnetized iron and thus a change of 1 or 2 GeV/c is not sufficient to deflect it into the chamber. Large $p_\perp$ scatters on the other hand are very rare. There are $\sim 10^4$ scatters beyond a $p_\perp$ of 6 GeV out of 10^{12} incident muons for the experiment shown on Fig. A9, or a probability of 10^{-8} per muon. With $\sim 2 \times 10^8$ muons traversing the chield this is not a problem.

4. Effects of the Chamber Field.

We have also considered the possibility that the fringe field of the bubble chamber magnet might bend soft muons into the chamber. We have put the fringe field of the chamber into some versions of the Monte Carlo program used to calculate the muon background fluxes and find that there is no significant increase in the muon background. We can understand this result qualitatively by thinking about the geometry of the chamber fringe field, sketched in Fig. A10. The main component of the chamber field is vertical, so that the field region where muons would be bent toward the chamber is mainly on the sides of the chamber. However the magnetized muon shield bends the muons vertically so that most of the muon flux is above and below the chamber, where the field is mostly in the vertical direction so that the muons are deflected side ways and not toward the chamber.

E. Backgrounds from Proton Beam Scraping.

The proton beam from Nuhall to the beam dump is shown in Fig. A2. If there is any scraping of this beam along the way, i.e. some small fraction of the protons interact in the vacuum pipe walls or magnet pole tips, π and K mesons are produced which can then decay and produce background neutrinos or muons. The experience at CERN in the 1979 beam dump run was that with some care the scraping can be kept at a very low level. Careful measurements using radiation monitors indicated that the scraping was less then 4×10^{-6} of the proton beam intensity [7]. At this level the neutrino background from this source is completely negligible.

However in the beam we are proposing at the Tevatron we do have to worry about the muon background in the bubble chamber from beam scraping, since the more energetic muons from this source can penetrate the earth shielding and reach the detectors. The most troublesome place for scraping along the proton beam line would be the large horizontal bend near the wonder building where the protons are bent back toward the beam dump. There must be a point along this bend where the proton beam aims directly at the chamber. This bend is about 500 m from the chamber, and there is about 340 m of earth between this bend and the chamber so that muons up to $\sim$ 140 BeV/c are stopped by energy loss. To estimate the size of the muon background from scraping at this bend we used the Monte Carlo program described in the previous section. For this calculation we made the assumption that the sraped proton interacts in some solid material, and thus the mesons that are produced will also interact in the material and the muons came from their decay before being absorbed i.e. one gets the same muon spectrum as in the beam dump. The number and momentum spectrum of the muons that would hit the 15 foot chamber 500 m away are shown in Fig. A11. The three curves correspond to the cases where the scraping protons are aimed directly at the chamber (0 mr curve), or are aimed at 10 and 20 mr from the chamber. From the first curve we expect 1.4 x 10^8 muons with p > 140 GeV/c that can penetrate the earth berm for 10^{13} protons scraping at 0 mr, i.e. aimed at the chamber. If the total scraping around the bend is kept to 10^{-6}, and 10% of the scraped protons are aimed within a few milliradians of the chamber (the total bend is about 50 mrad) we expect a background of the order of 10 μ's hitting the B.C. However this number could increase if the pions produced by the scraped protons were not absorbed immediately but had some longer decay path. This latter possibility can be eliminated by placing lead shielding in the appropriate places along the beam.

A much safer solution to the scraping problem would be to incline the beam vertically during this large bend by about 20 mr, and then bend it back down to the dump. In this way there would be no point along the proton beam line where the beam points toward the detectors to within 20 mrad. Looking at the spectrum of muons with the protons aimed 20 mr away from the detector, the curve labelled 20 mr on Fig. A11, we see that the number of muons above 140 GeV/c that could penetrate the earth berm and reach the detectors is negligible. Discussions with Ray Stefanski indicate that there is no great difficulty in arranging the beam to have such a vertical incline at the large horizontal bend.

Another problem we have considered is scraping along the last leg of the proton beam line after the large horizontal bend, as the beam approaches the dump. At this leg the protons are at 30 mr with respect to the line toward the chamber so that muons from this scraping would not go into the chamber. However this halo of muons around the proton beam which would be one ot two meters in diameter would hit the face of the muon shield and some of them might be deflected by the magnetized iron into the chamber. This is not a serious probem for two reasons :

a) These muons would have to penetrate $\sim$230 m of earth and the 75 m of the iron shield, and thus only those with p $\gtrsim$ 230 GeV could reach the chamber. From Fig. A11 we see that the number of μ's with p > 230 GeV is $\sim 2 \times 10^7$ for 10^{13} scraped protons, or about 20 μ's for a scraping of 10^{-6} of the beam, which is not a very large number.

b) The bending in the magnetized iron is in the vertical direction, so that the muon halo hitting the shield would be bent up or down, but would continue at $\sim$ 30 mrad in the horizontal plane, and would thus miss the chamber, which is another 180 meters down the line, by more then 5 meters.

F. Skyshine Muon Fluxes.

The magnetic field in the magnetized muon shield has been arranged to be in the horizontal direction partly to reduce the radiation safety problems due to the muons which are deflected by the magnet. The μ^+ are bent into the ground and are not a problem. The μ^- are bent up into the sky; we have calculated the flux of these muons (the skyshine) in the Monte Carlo program used to trace the muons through the shield. The muon fluxes at an altitude of 100 meters directly above the beam center-line are shown in Fig. A12 as a function of the horizontal distance from the dump. We find that the maximum flux is $\sim 6 \times 10^5$ μ's/m^2 for 10^{13} protons at a distance of 1000 m from the dump. With a 60 sec cycle time this corresponds to

$$\text{Max } \mu^- \text{ flux} = 1 \ \mu \ / \ cm^2 \ / \ sec$$

This flux is within an order of magnitude of the cosmic ray flux of all particles, and should thus be not a problem.

G. Materiel and Power Requirements for the Magnetized Shield.

The muon shield consists of 2.4 m x 4.8 m x 25 m or 2300 tons of magnetized steel and 3 m x 6 m x 50 m or 7000 of passive iron shield. The iron for the magnetized part could be part of the Argone ZGS magnet iron which used to run up to 22.5 kgauss so we should have no trouble running it at 20 kgauss in the muon shield. The iron for the passive part could come from the available iron stock piled in the neutrino lab, so that no new iron needs to be purchased (and thus no money has to be spent) for this shield.

To get a feeling for what is involved in magnetizing the shield we present one possible design; a more optimum one may well be found by the engineers when the time comes.

We assume a permeability of 1000 for the iron so we need 20 oersteds to produce 20 kgauss. In the size we are discussing this requires 16,000 ampere turns. We assume we can put a current of 200 amps/cm^2 through the copper conductor without water cooling, so we need a coil of 80 cm^2 crossectional area. The length of the conductor has to be 25 m + 25 m + + 10 m for ends or 60 m total, so we need 60 m x 80 cm^2 = 0.48 m^3 of copper, or 10,000 lbs of copper. At \$5 a lb (?) this is \$50,000.

The resistance of the coil, if we make it 16 turns with 1000 amps (5 cm^2 crossectional area) each is

$$R = \frac{L}{A} = 1.8 \times 10^{-6} \times \frac{6000 \times 16}{5} = 3.5 \times 10^{-2} \text{ ohms.}$$

The voltage required is

$$V = iR = 1000 \times 3.5 \times 10^{-2} = 35 \text{ volts}$$

with a power consumption of

$$P = V\,i = 35 \text{ kilowatts.}$$

Thus neither the cost of the coils nor the power consumption seem to be excessive.

The local shield in front of the 15 foot chamber, 8 m wide by 6 m high by 25 m long, can be stacked concrete blocks in the clear space immediately in front of the chamber. The concrete blocks are available at the lab; in fact Dennis Therriot remarked that he has been looking for a place to store some concrete blocks, and the parking lot in front of the chamber is as good a place as any.

REFERENCES (Appendix)

1. Report of the neutrino area subgroup, 1977 Fermilab Summerstudy

2. J.L. Ritchie et al., Phys. Rev. Lett. 44, 230 (1980).
J.G. Branson et al., Phys. Rev. Lett. 38, 457 (1977).
L.B. Leipuner et al., Phys. Rev. Lett. 35, 1613 (1975)
and Phys. Rev. Lett. 36, 1007 (1976).
D. Buchholz et al., Phys. Rev. Lett. 36, 932 (1976).
K.W.B. Merritt et al., in Proceedings of the 1978 Vanderbilt Conference.

3. A.O. Hanson et al., Phys. Rev. 84, 634 (1951).

4. See for example the review article on multiple scattering by R.D. Birkhoff in Volume 34 of the Handbuch der Physik.

5. E. Gabathuler, private communication.

6. T. Kirk, private communication.

7. H. Wachsmuth, in the Proceedings of the Photon and Lepton Conference held in August 1979 at Fermilab.

GENERAL LAYOUT OF THE BEAM DUMP NEUTRINO BEAM

IN THE NEUTRINO AREA

(Not to Scale)

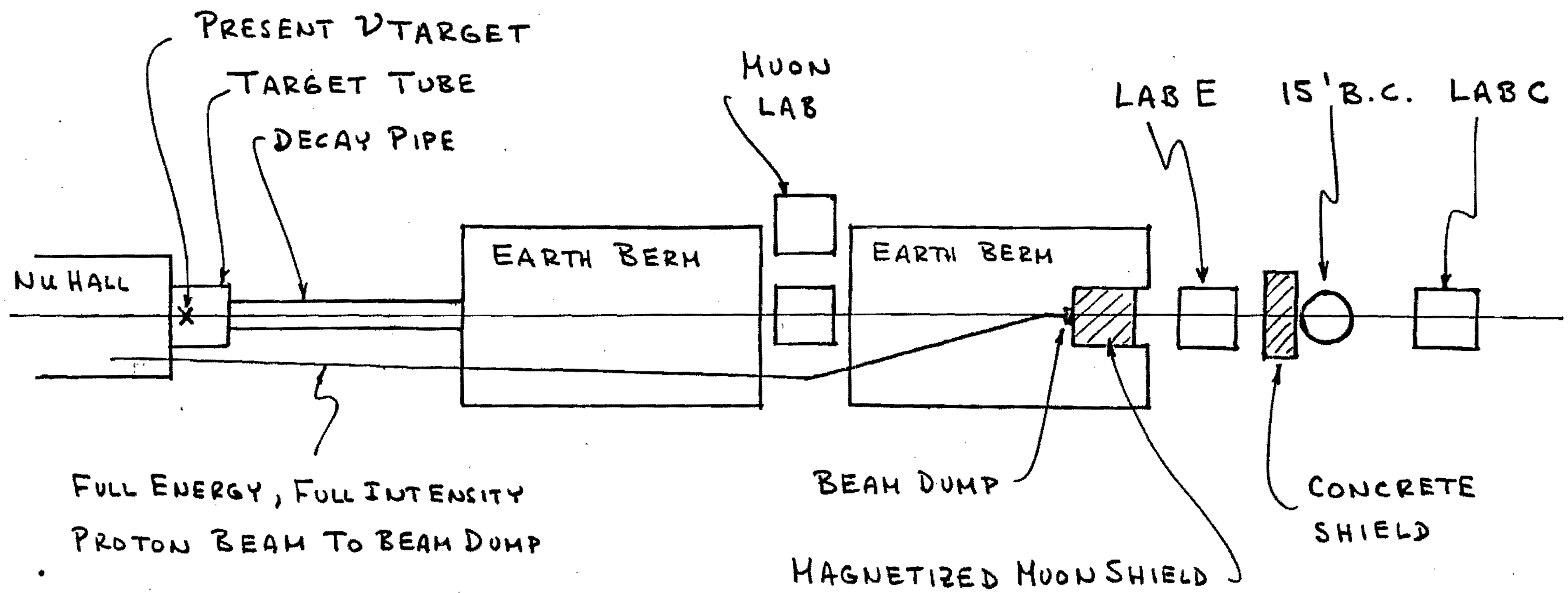

FIG A1a

LAYOUT OF THE MUON SHIELD

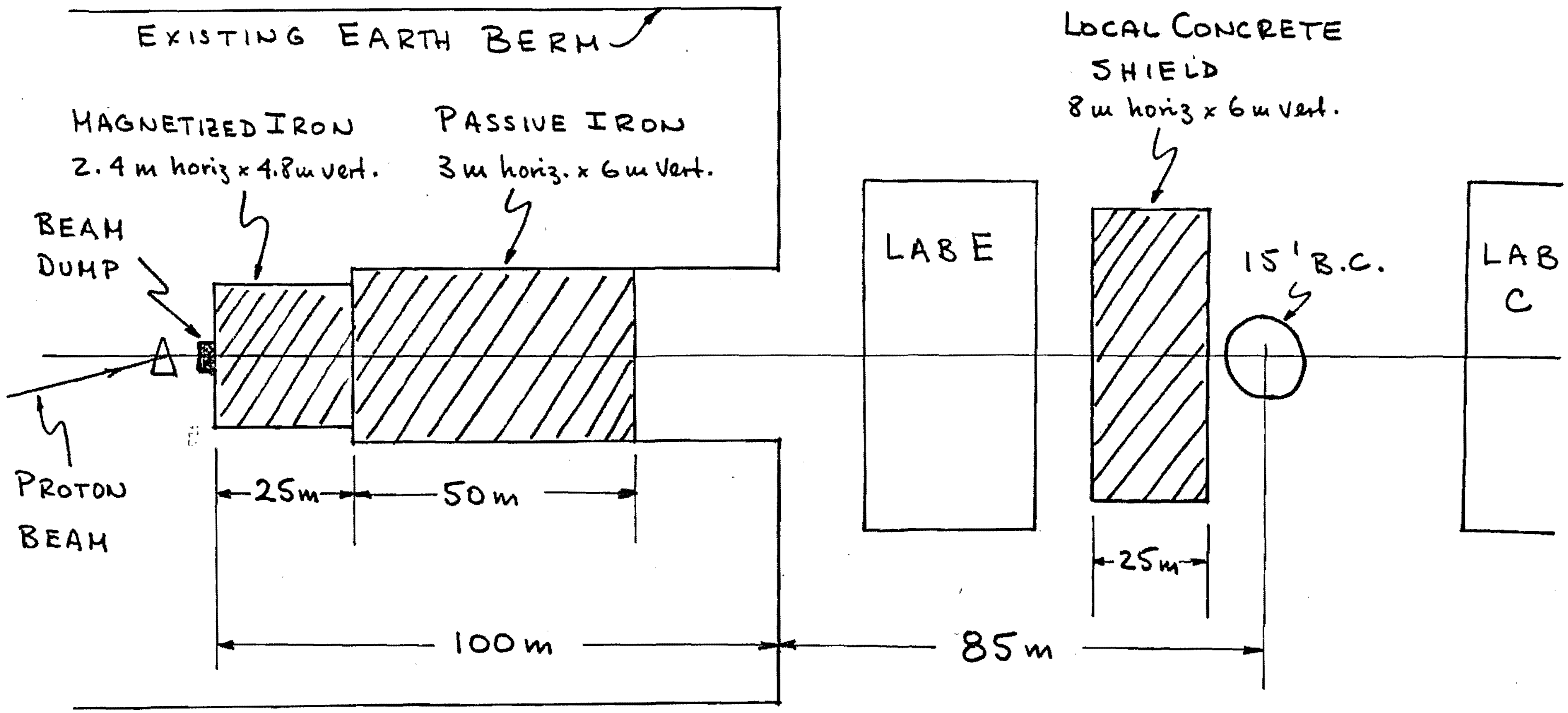

FIG A1b

SCHEMATIC OF THE MAGNETIZED SHIELD

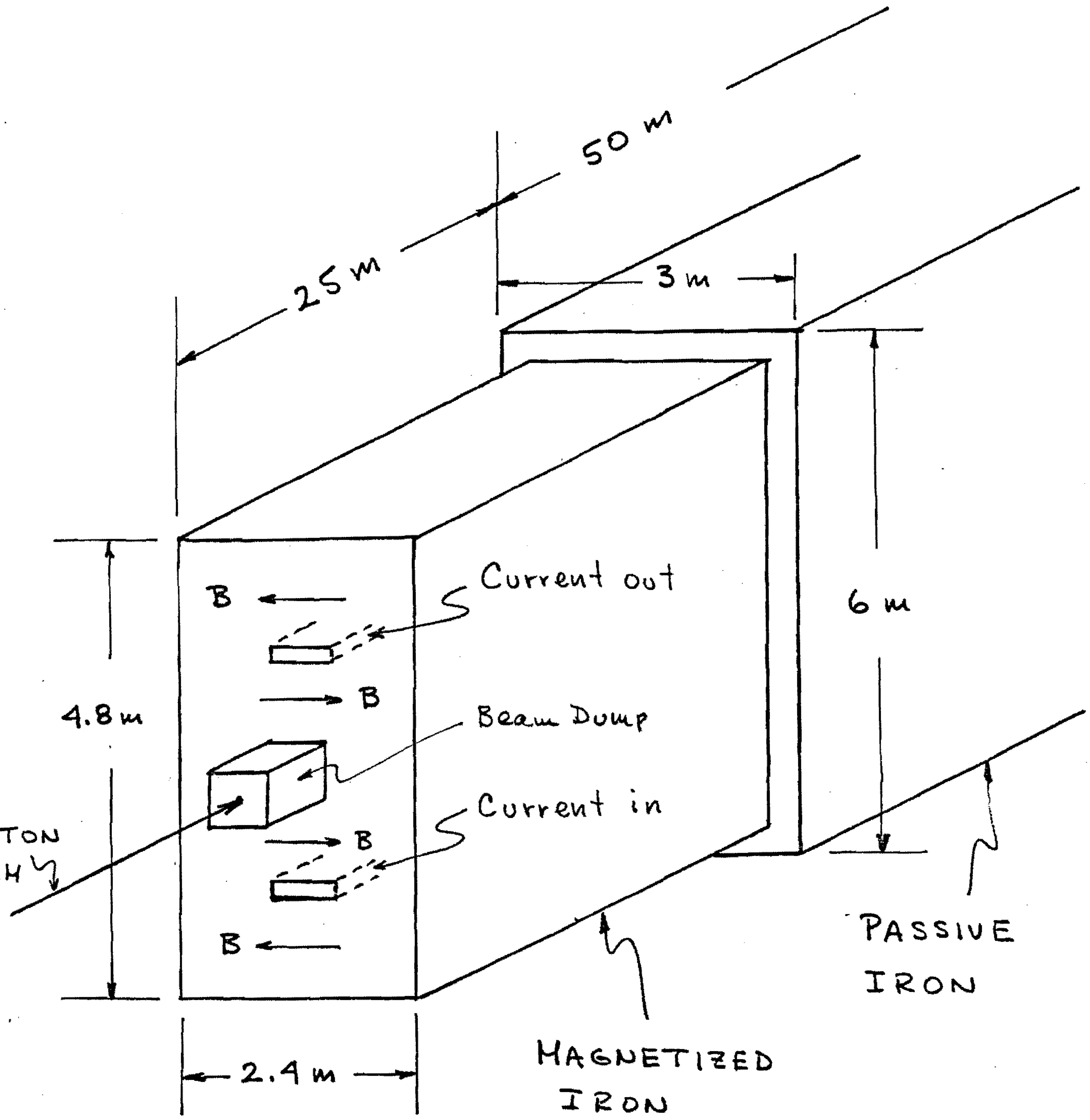

FIG A1c

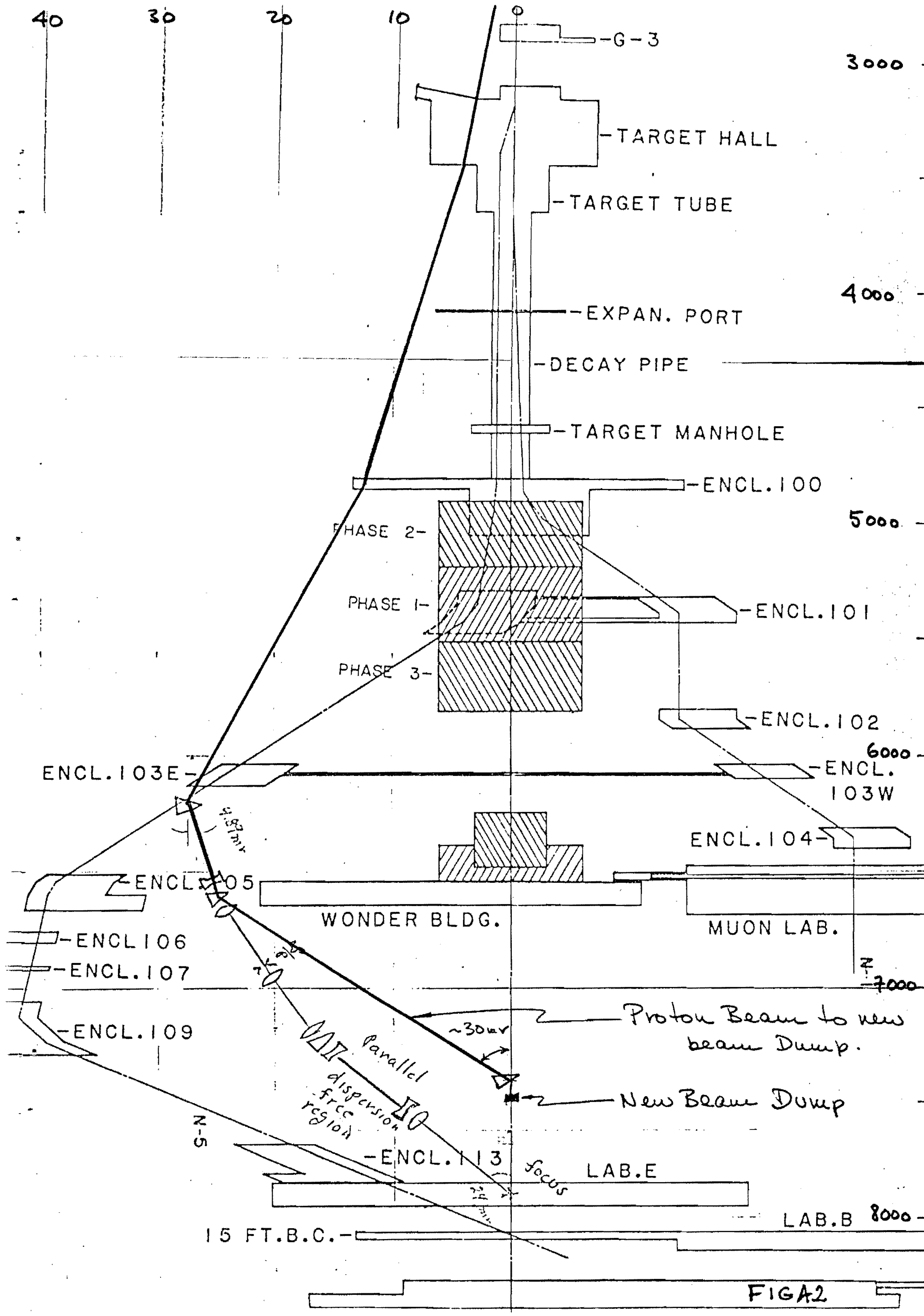
40
30
20
10
0
G-3
3000
TARGET HALL
TARGET TUBE
4000
EXPAN. PORT
DECAY PIPE
TARGET MANHOLE
ENCL.100
5000
PHASE 2
PHASE 1
PHASE 3
ENCL.101
ENCL.102
6000
ENCL.103E
ENCL.103W
ENCL.104
ENCL.105
WONDER BLDG.
MUON LAB.
ENCL.106
ENCL.107
7000
ENCL.109
~30mr
Proton Beam to new beam Dump.
Parallel dispersion free region
New Beam Dump
N-5
ENCL.113
focus
LAB.E
LAB.B
8000
15 FT.B.C.

FIG A2

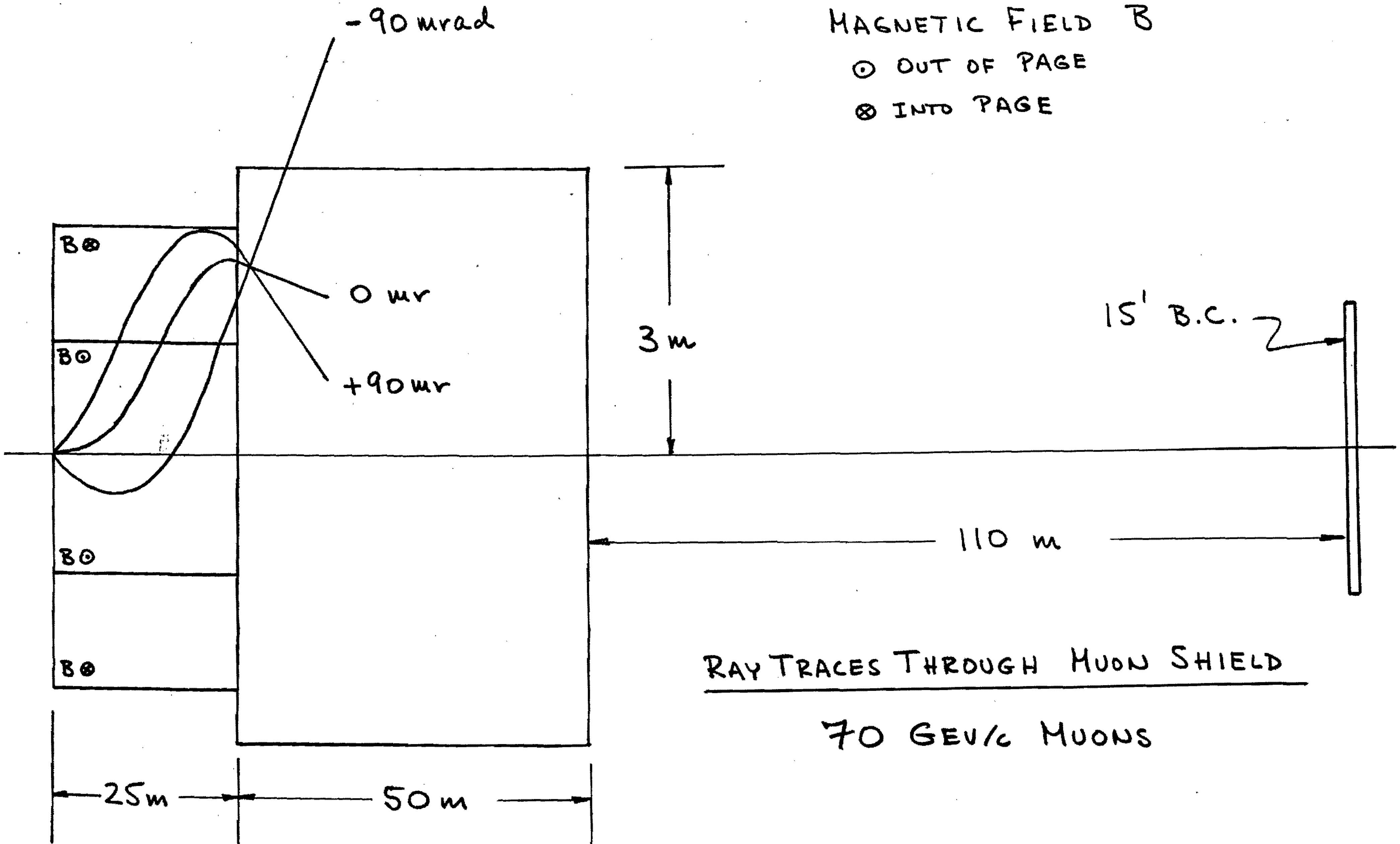

RAY TRACES THROUGH MUON SHIELD

70 GEV/c MUONS

FIG. A3 a

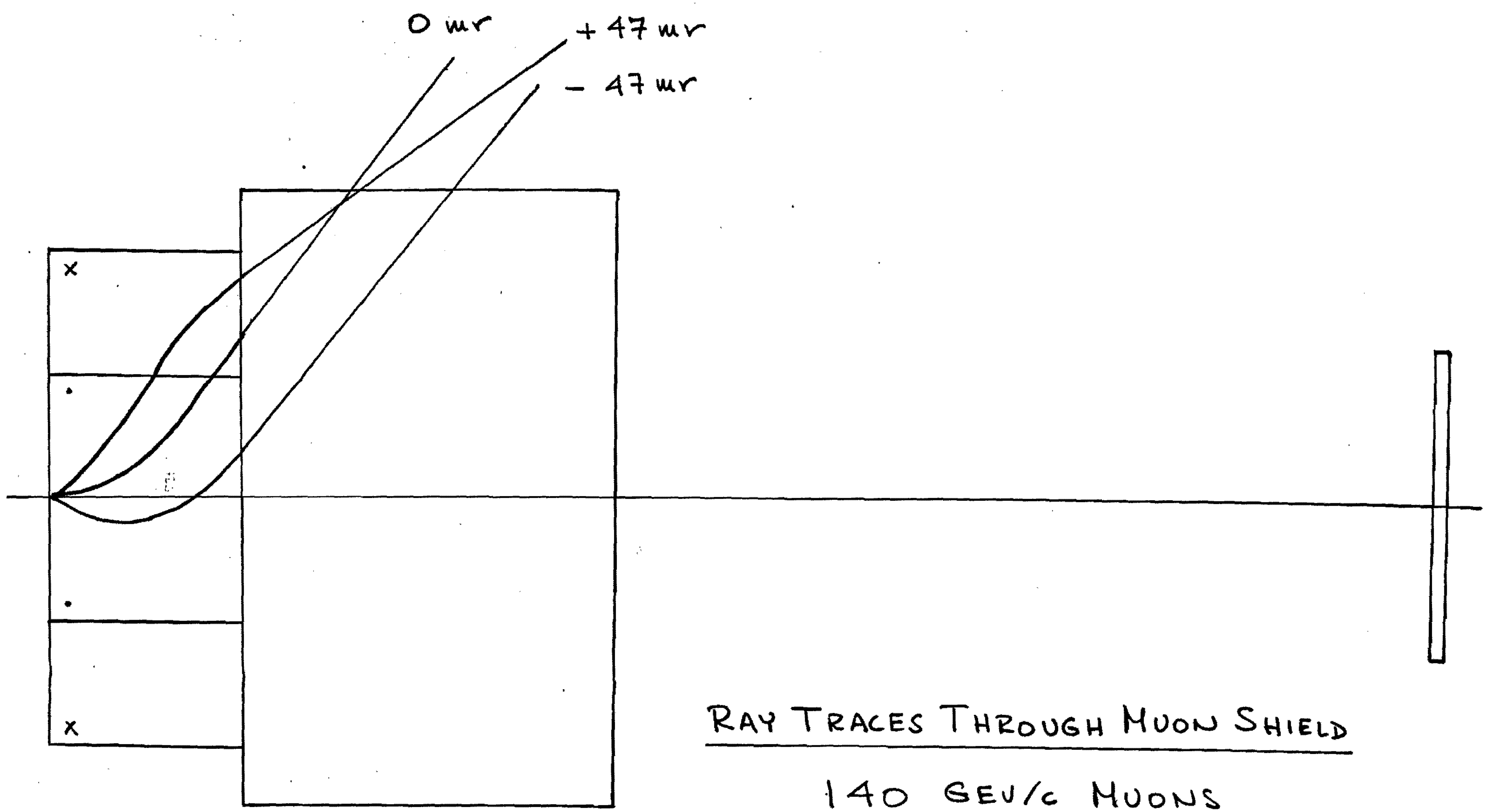

RAY TRACES THROUGH MUON SHIELD

140 GEV/c MUONS

FIG. A 3 b

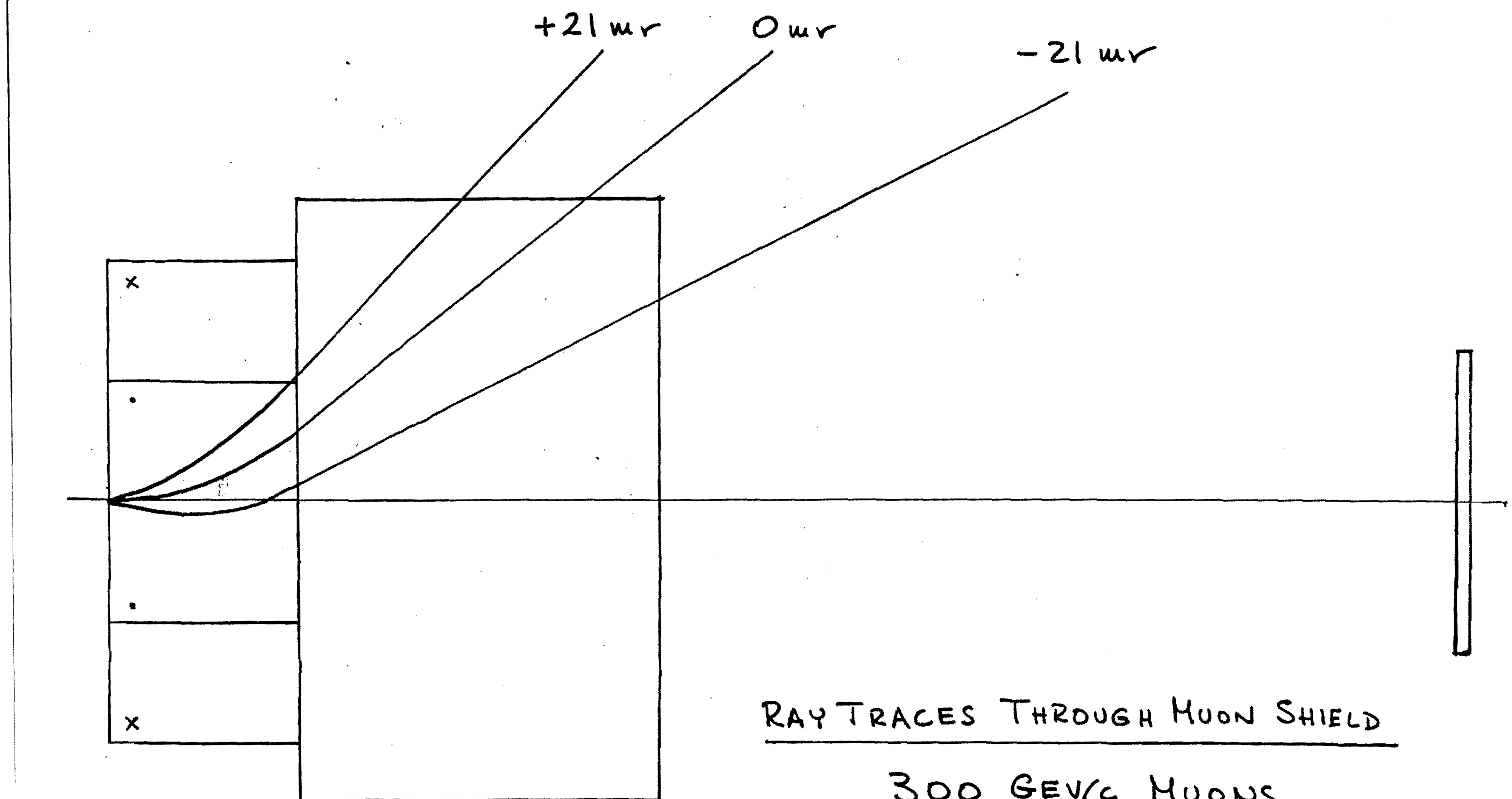

RAY TRACES THROUGH MUON SHIELD

300 GeV/c MUONS

FIG. A 3c

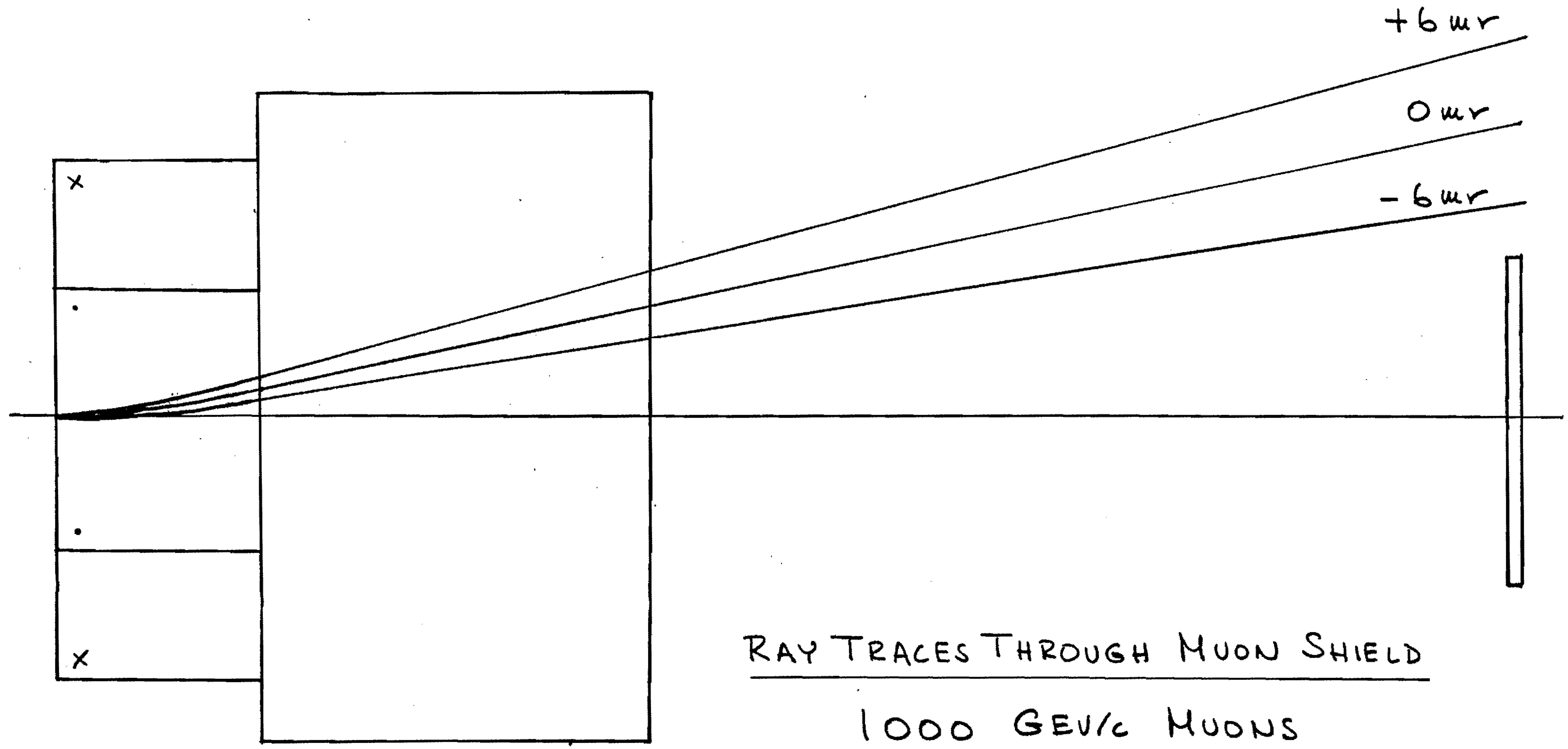

RAY TRACES THROUGH MUON SHIELD

1000 GEV/c MUONS

FIG A 3 d

$$\frac{\mu}{\pi} = (1.0 \times 10^{-4})(1 - X_F)^3$$

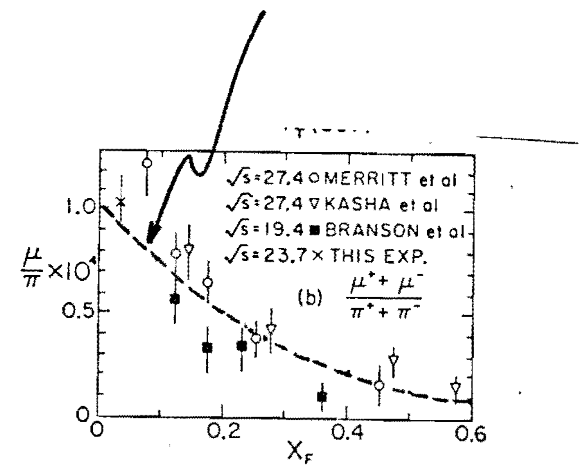

FIG. A4

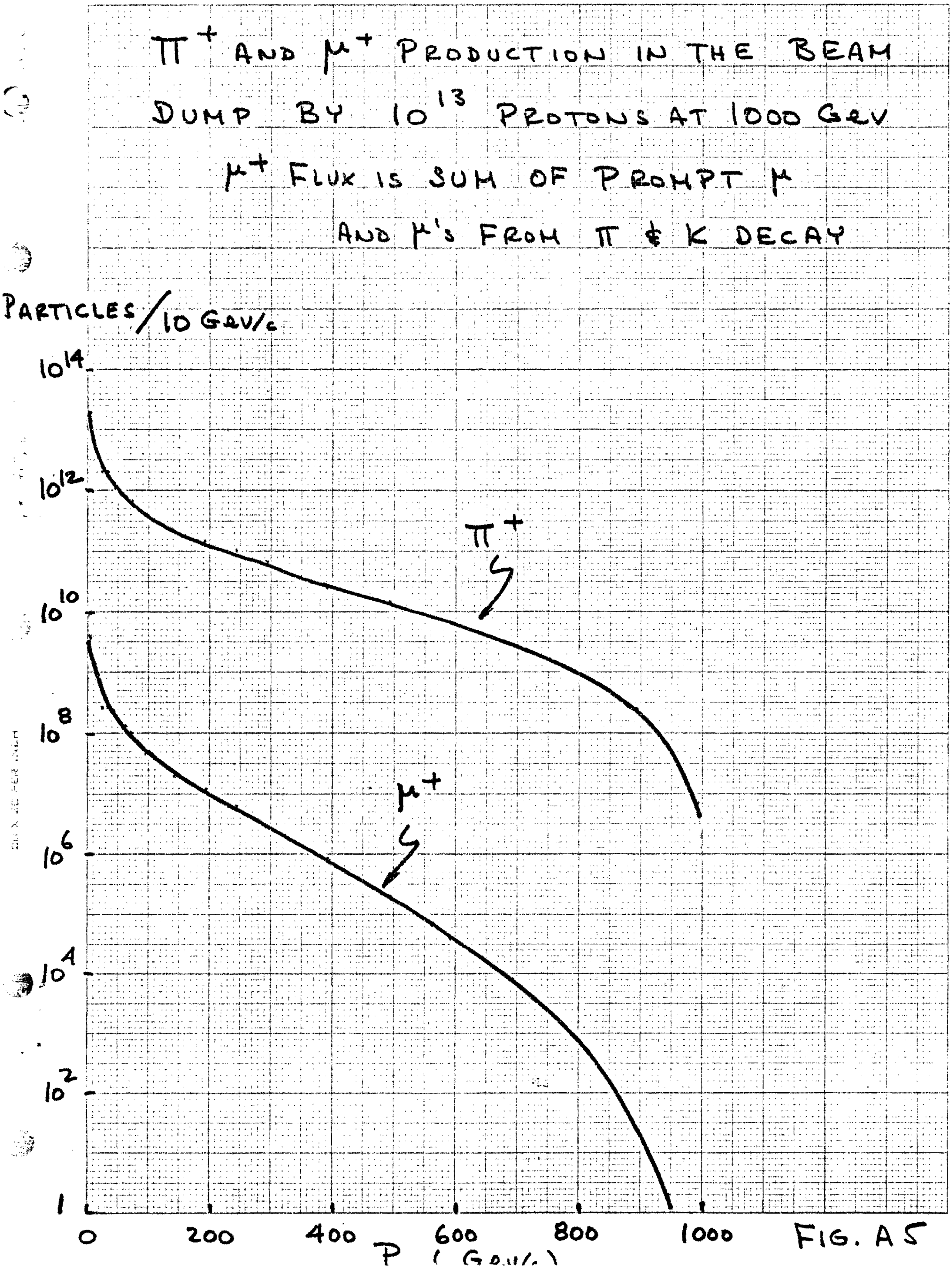

π+ AND μ+ PRODUCTION IN THE BEAM DUMP BY 10^13 PROTONS AT 1000 GeV
μ+ FLUX IS SUM OF PROMPT μ AND μ'S FROM π & K DECAY
PARTICLES/10 GeV/c
10^14
10^12
10^10
10^8
10^6
10^4
10^2
1
π+
μ+
0
200
400
600
800
1000
P (GeV/c)

FIG. A5

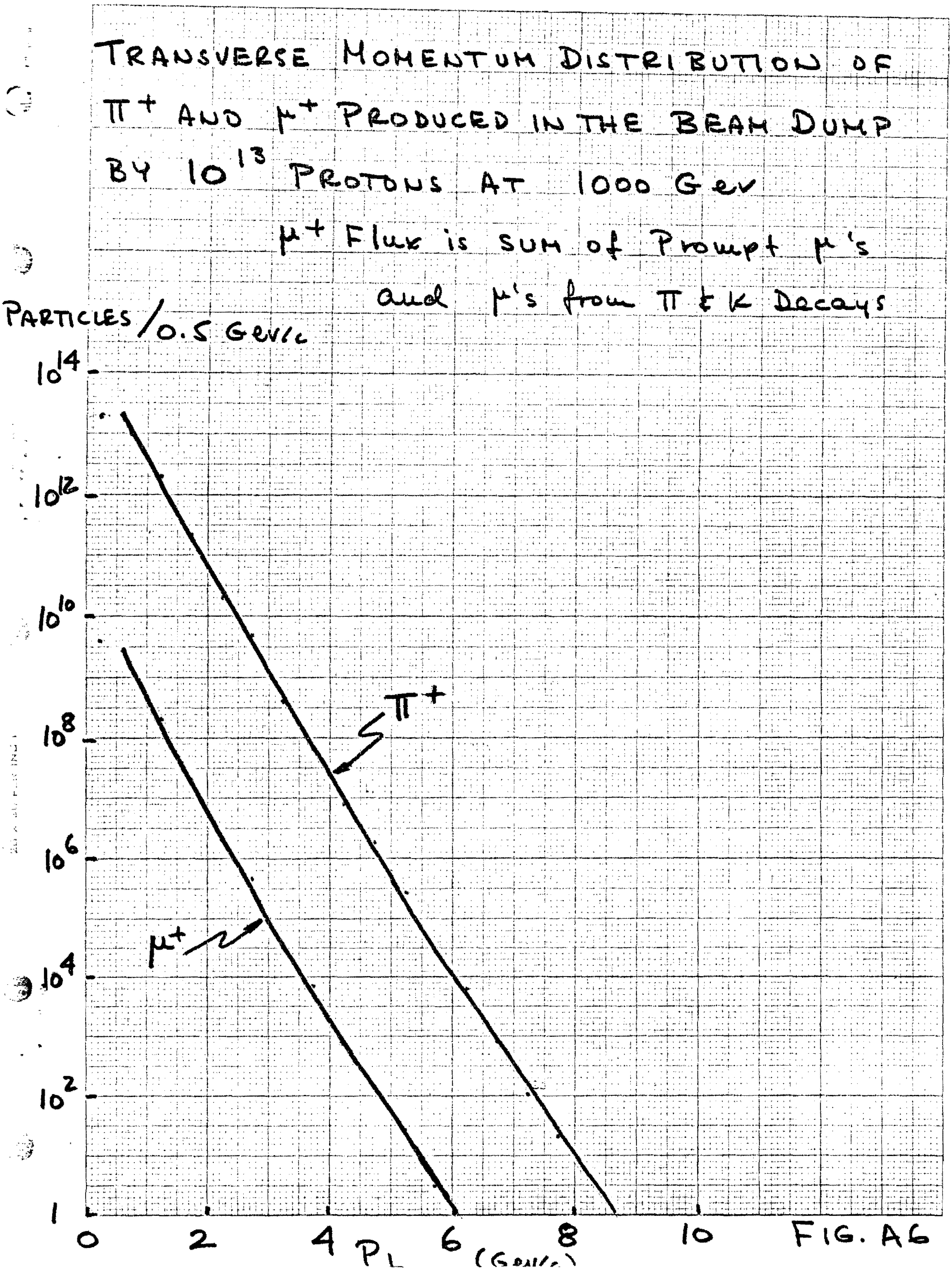

TRANSVERSE MOMENTUM DISTRIBUTION OF
π+ AND μ+ PRODUCED IN THE BEAM DUMP
BY 10^13 PROTONS AT 1000 GeV
μ+ Flux is sum of Prompt μ's
and μ's from π & K Decays
PARTICLES/0.5 GeV/c
10^14
10^12
10^10
10^8
10^6
10^4
10^2
1
π+
μ+
0
2
4
6
8
10
PL

FIG. A6

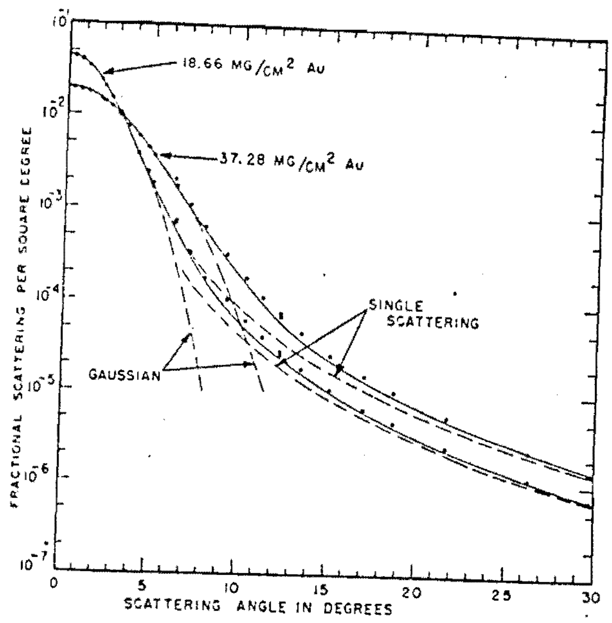

FIG. 3. Angular distribution of electrons from thick and thin gold foils from 0° to 30°. The solid line represents the theory of Molière extrapolated through the region where his small and large angle approximations give different values. The dotted lines at small angles represent the continuation of the gaussians of Fig. 1. At larger angles, the dotted line represents the single scattering contribution.

FIG. A 7

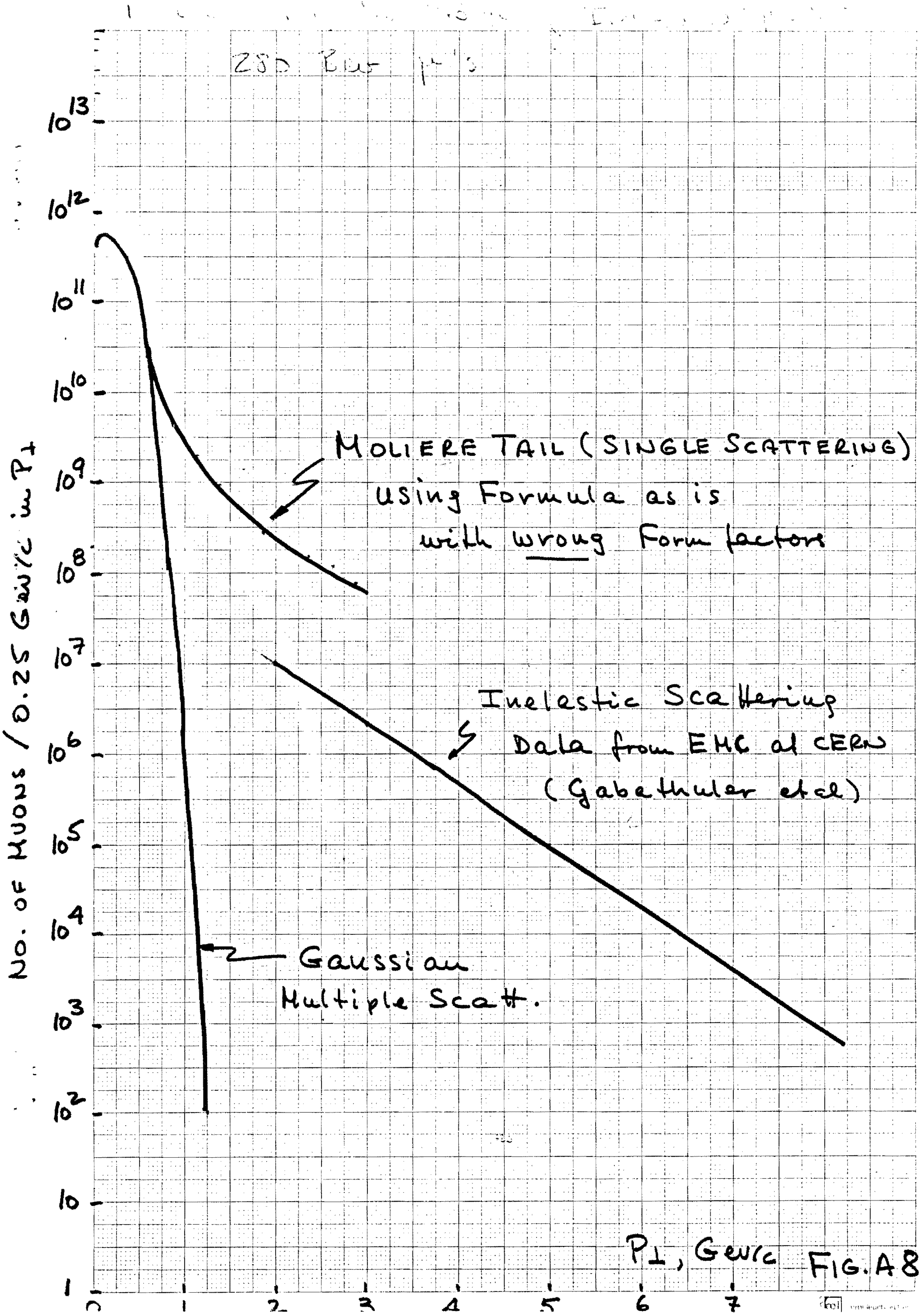

No. of Muons / 0.25 GeV/c in P⊥
10^13
10^12
10^11
10^10
10^9
10^8
10^7
10^6
10^5
10^4
10^3
10^2
10
1
0
1
2
3
4
5
6
7
P⊥, GeV/c
Moliere Tail (Single Scattering)
using Formula as is
with wrong Form factor
Inelastic Scattering
Data from EMC at CERN
(Gabathuler et al)
Gaussian
Multiple Scatt.

FIG. A8

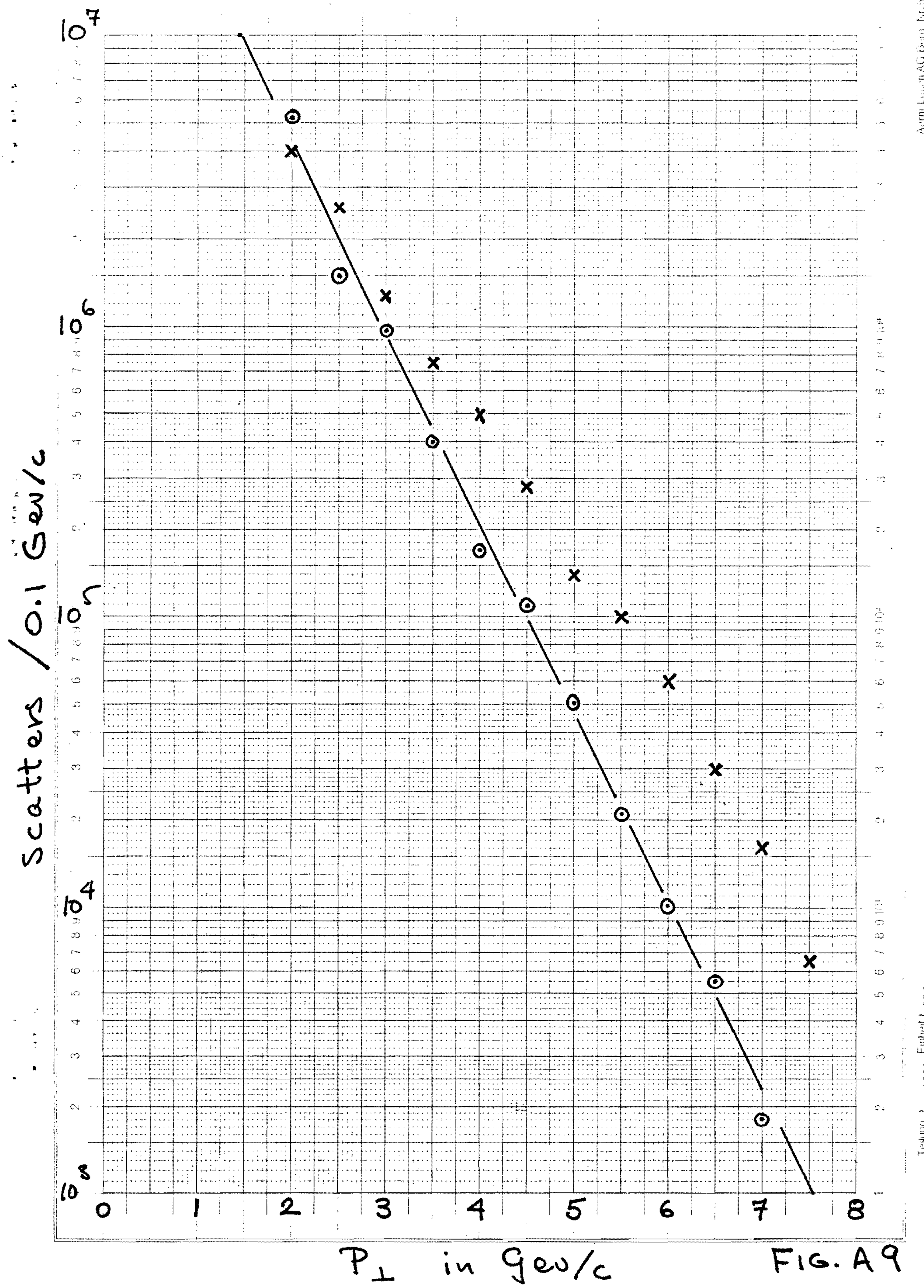

FIG. A9

EFFECT OF 15' B.C. FRINGE FIELD

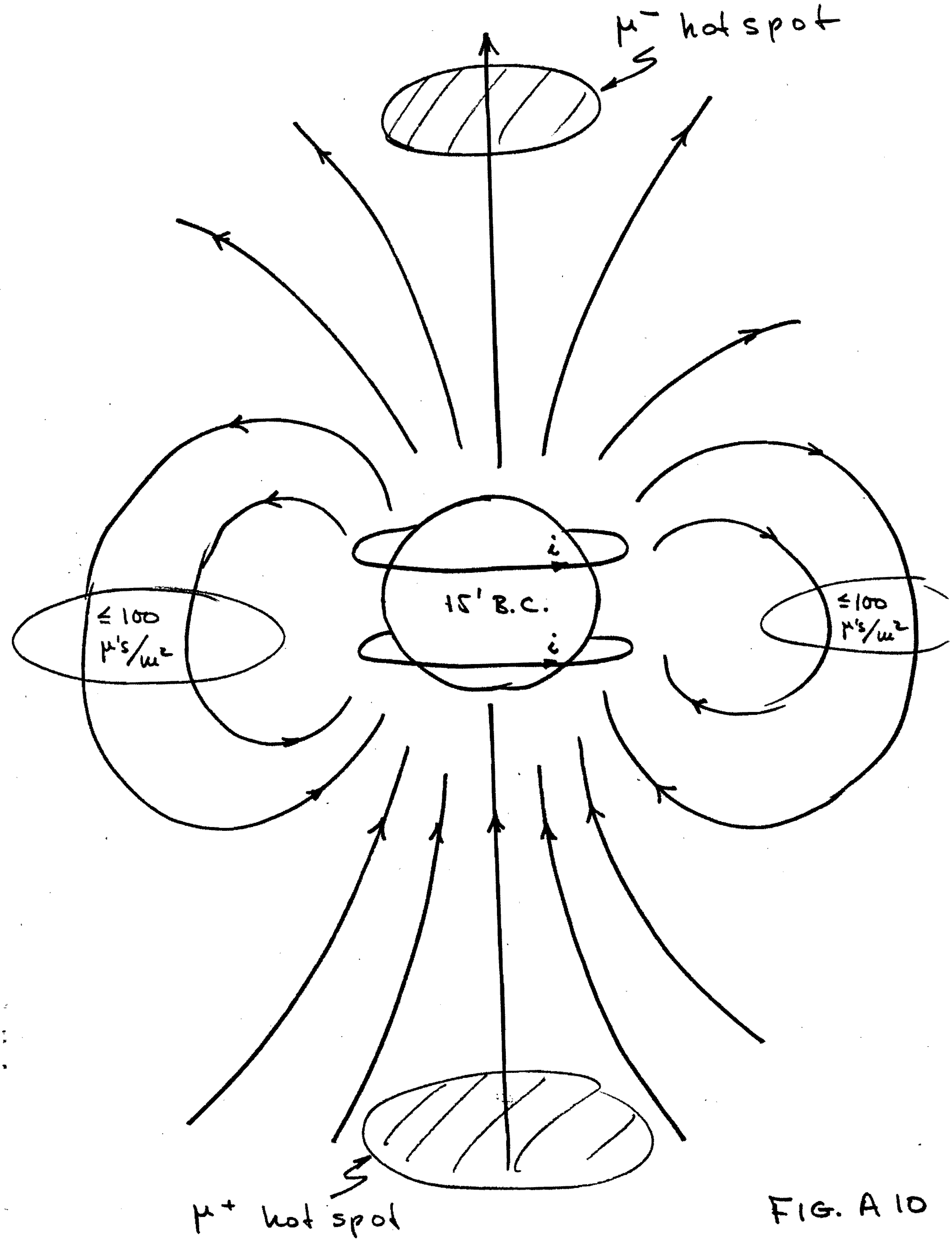

FIG. A 10

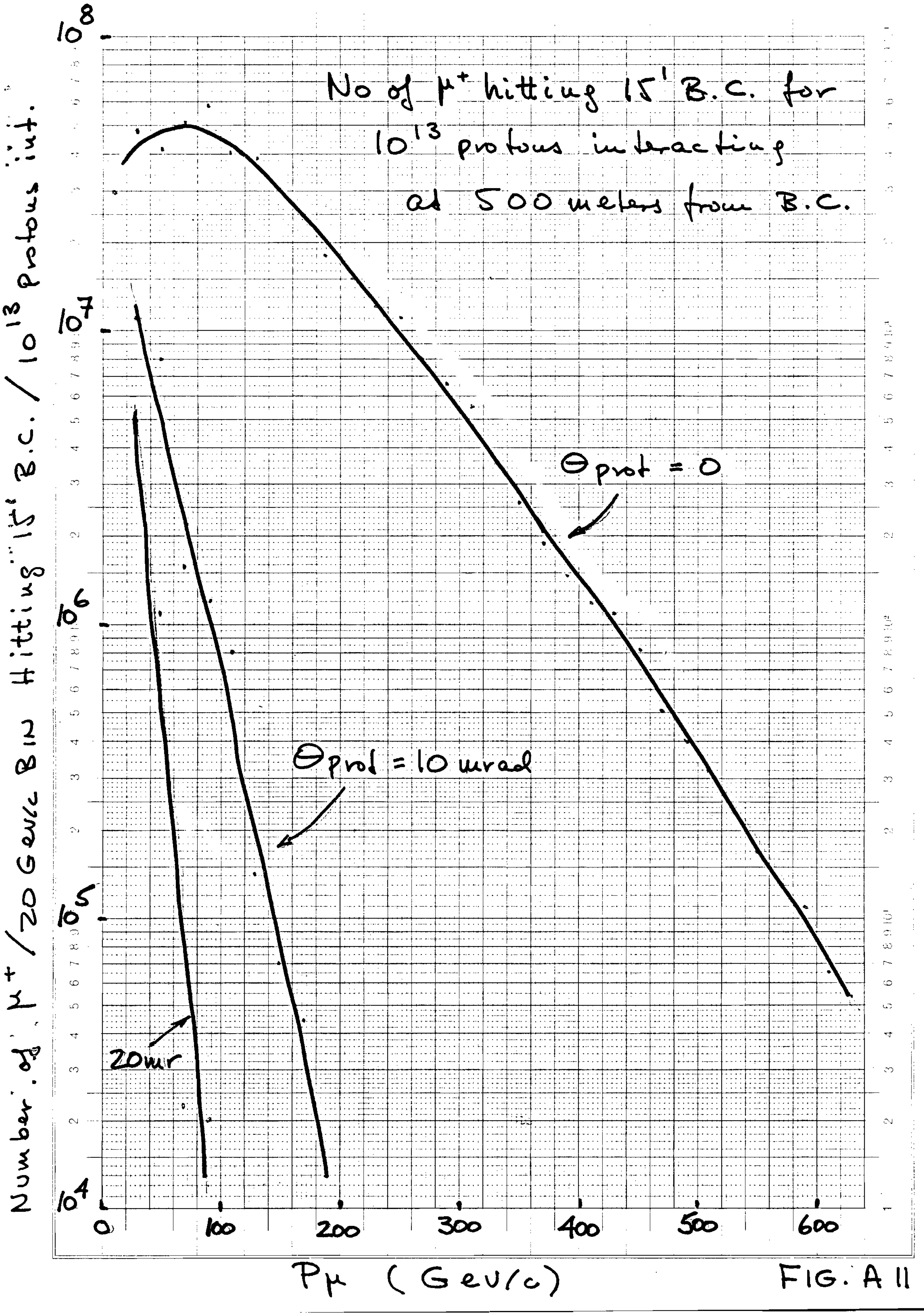

No of μ+ hitting 15' B.C. for
10^13 protons interacting
at 500 meters from B.C.
Number of μ+ / 20 GeV/c BIN hitting 15' B.C. / 10^13 protons int.
10^8
10^7
10^6
10^5
10^4
θprot = 0
θprod = 10 mrad
20mr
0
100
200
300
400
500
600
Pμ (GeV/c)

FIG. A11

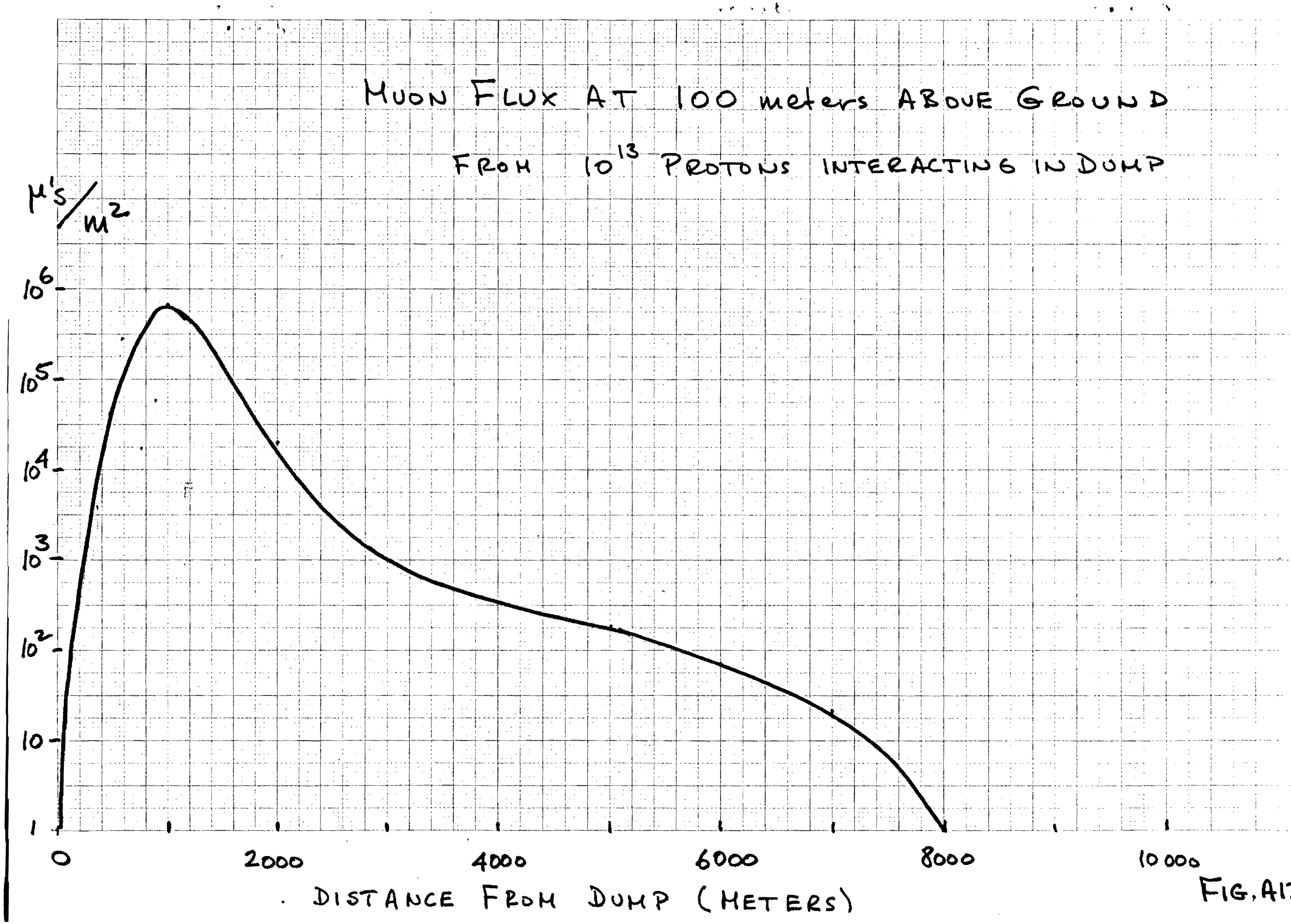

MUON FLUX AT 100 meters ABOVE GROUND
FROM 10^13 PROTONS INTERACTING IN DUMP
μ's/m²
10^6
10^5
10^4
10^3
10^2
10
1
0
2000
4000
6000
8000
10 000
DISTANCE FROM DUMP (METERS)

FIG. A12

646 22 Sept '86

ν_τ event rate

C.T. Murphy - presentation

J. Morfin, J. Schneps - real work

Kitegaki, Bugg, Peters, Bjorken, - valuable
Childress, ... suggestions

Outline

1. Intro / abstract
2. Morfin / (Malensek) M.C.
3. Factors to multiply Morfin
   - most > 1, one < 1

Introduction / Abstract

Source of ν_τ

$$F^\pm \rightarrow \nu_\tau^F \, \tau^\pm \quad \hookrightarrow \nu_\tau^\tau + X \Big\} \; 2 \; \nu_\tau\text{'s}$$

Morfin M.C:

1. Use E613 (Fermilab beam dump) raw data for $\nu_{\mu,e}$ prompt @400GeV + $f(x_F, P_\perp)$ model which $\approx$ fits data to scale to Tohoku & 15'ch
   - W target, E613, Tohoku, 15' (avoid A-dependence issue)
   - acceptances similar ($x_F \gtrsim 0.3$)
2. M.C. handles credibly and automatically non-linear (i.e., not just "scale factors") such as:
   - Kinematic differences between $F \rightarrow \nu_\tau^F \, \tau \hookrightarrow \nu_\tau^\tau$ and $D \rightarrow \nu_{e,\mu} X$

- kinematic differences between
  $\sqrt{s} = 400$ GeV (E613)
  $\sqrt{s} = 900$ GeV (including $\sigma_\nu \sim \sqrt{s}$) (E646/636)
- detector acceptance differences

3. Important linear scale factors assumed by Morfin:

   a. $BR(F \to \tau \nu_\tau) = 2\%$

   b. $$\frac{\sigma_{pN}(F^\pm)}{\sigma_{pN}(D^\pm_0)} = 10\%$$

   c. $$\frac{\sigma_{F,D}(1\,TeV)}{\sigma_{F,D}(.4\,TeV)} = 2.0$$ Bourquin-Gaillard scaling

"current wisdom"

3. <u>Results</u> (for detectors at 90 m & 190 m and 2×10^{18} protons)

ν_τ interactions = **104 events**

Same for 15' + Tohoku

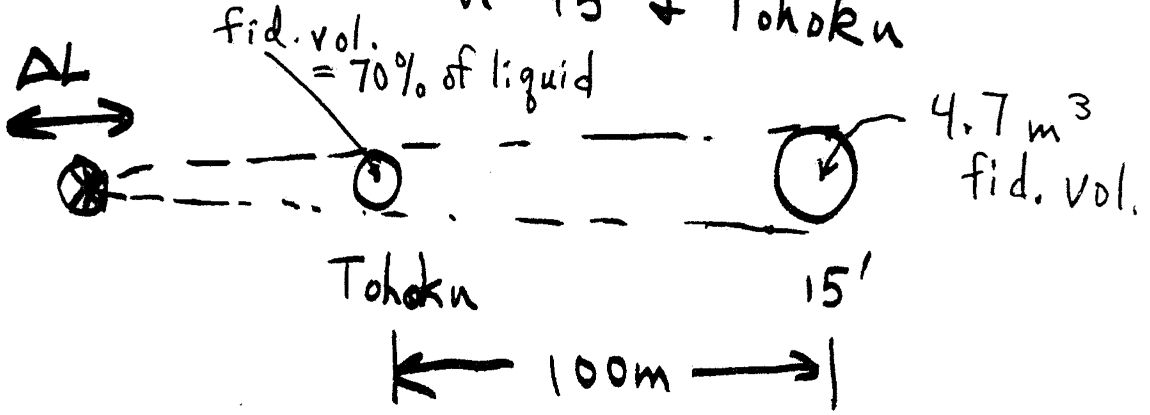

Correction factors to Morfin

effect	Factor
BR ($F \to \tau \nu_\tau$): 2% → 3% (see Schneps)	1.5
F/D : 0.10 → 0.12 (see Schneps)	1.2
$D \to \tau \nu_\tau$, BR = 0.043% (omitted)	1.08
$P+N \to K^{\pm}_{0} + N \to F$ (omitted)	1.1
$\tau \to \nu_\tau \rho \pi$ (")	1.04
$\tau \to \nu_\tau X$ polarized: $1 + \cos\theta$	> 1
Energy: 1 TeV (MC) → 0.9 (real?)	0.8
Subtot	> 1.8

	15' BC	Tohoku
ΔL = 15 m	1.14	1.27
Density freon: 1.2 → 1.4	—	1.17
Total	> 2.0	> 2.6

Details of Morfin M.C.

(FN - 434 , enclosed)

1. E613 appropriate as basis?
   - W target (avoid A dependence
   - measures prompt ν_μ
   - similar acceptance ($x_F \gtrsim 0.3$)
   - agrees with other beam dump results:

	Expt.	σ/nucleon A^1	$A^{0.75}$
400GeV	E613	16 μb	57 ± 3
	BEBC	19 ± 5	52 ± 13
	CDHS	20	
200GeV	ACCMOR	25 ± 4 ± 11	

   - why not use LEBC $pp \to D/\bar{D}$
     - mostly near $x_F = 0$
     - how do A dependence?

$$\sigma_A = K \sigma_H A^\alpha$$

↑ ? (K)

$$\alpha = f(x_F, P_\perp)$$

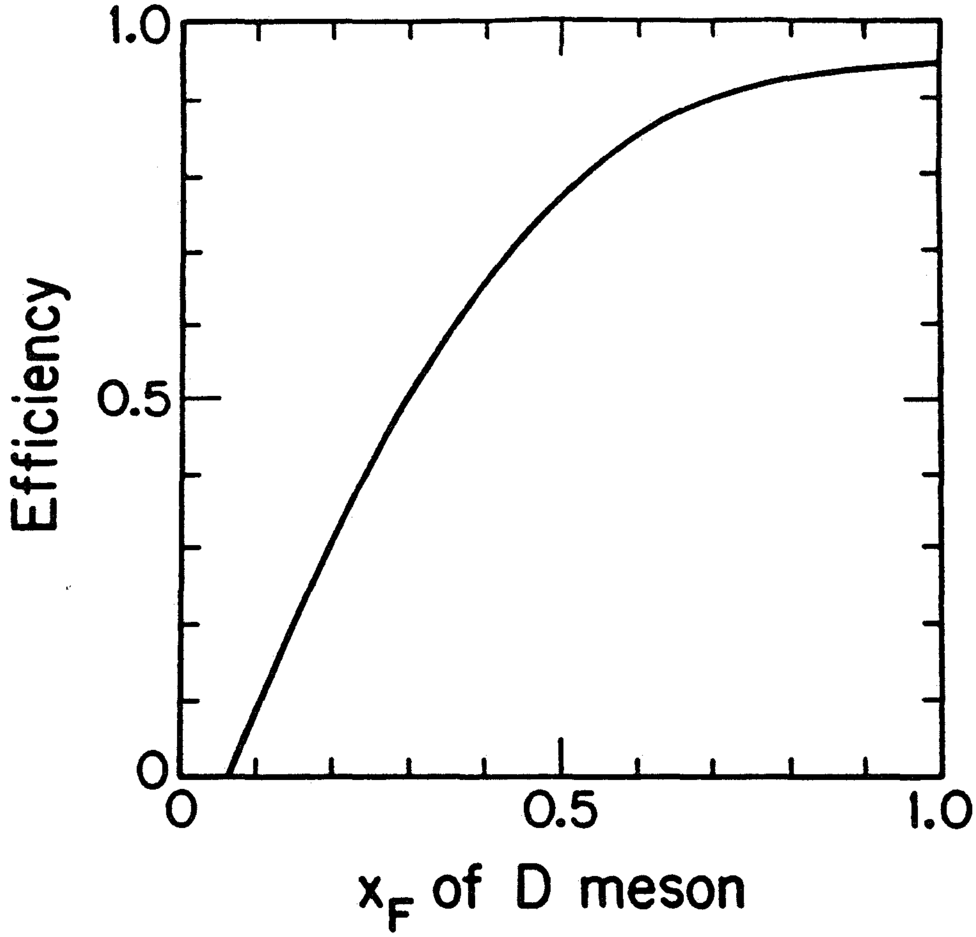

E613 acceptance

Fig. 3

Morfin: M.C. vs. E613 data

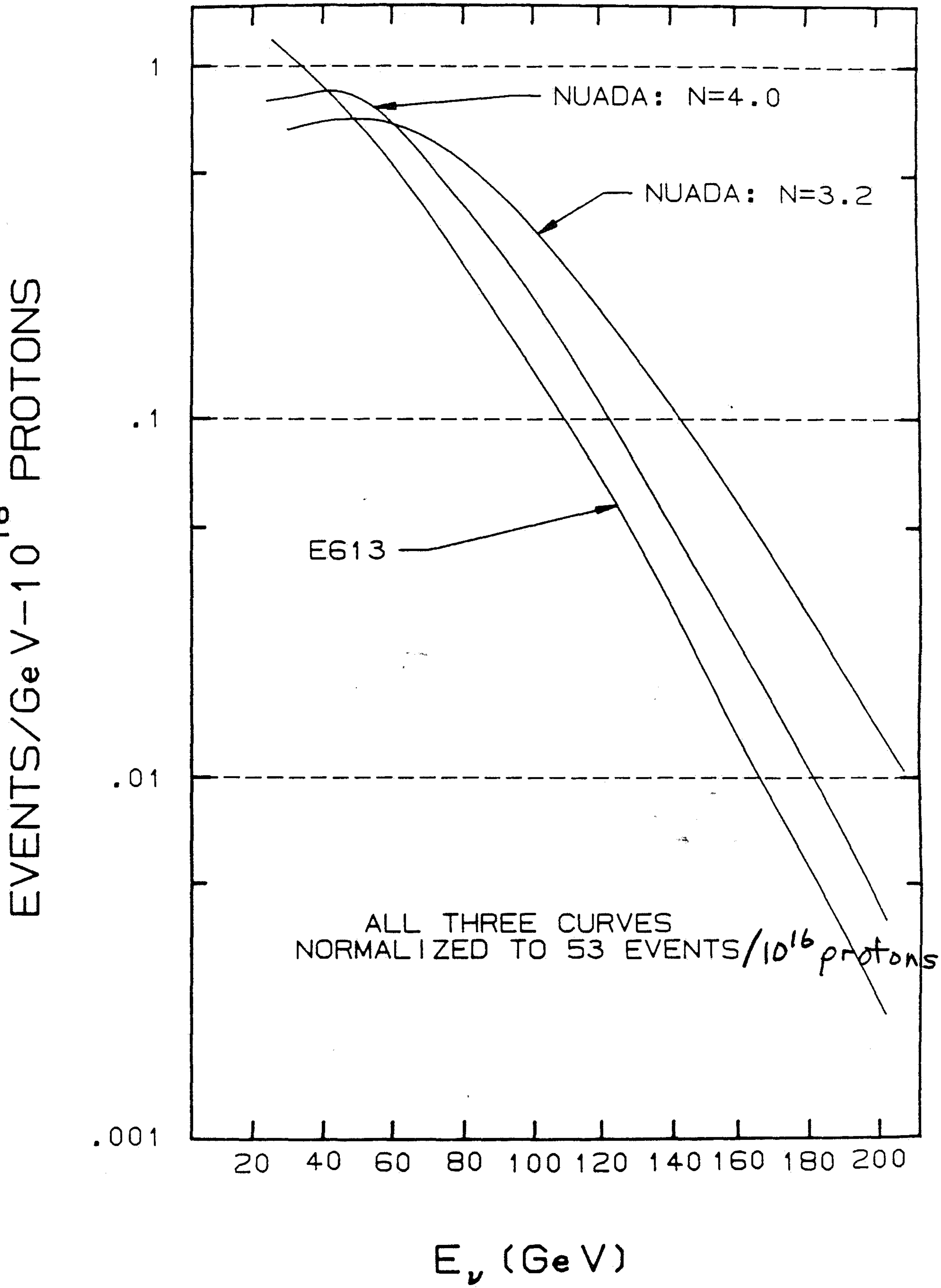

simple minded check

$$\frac{\nu_\tau}{\nu_e} = \frac{F}{D} \, \frac{BR(F^\pm \to \tau^\pm \nu_\tau^F)}{BR(D^\pm_0 \to e X)} \; 2.0 \times A$$

$= .02$ with Morfin assumption.

M.C. yields

$$\frac{\nu_\tau}{\nu_e} = .0144$$

Differences understood:

a) only 67% of $\tau \to \nu_\tau^\tau$ modes contribute $[.02 \to .0167]$

b) ν_τ^F soft, $\sigma_\nu \sim E$

Fig. 5 (Morfin)

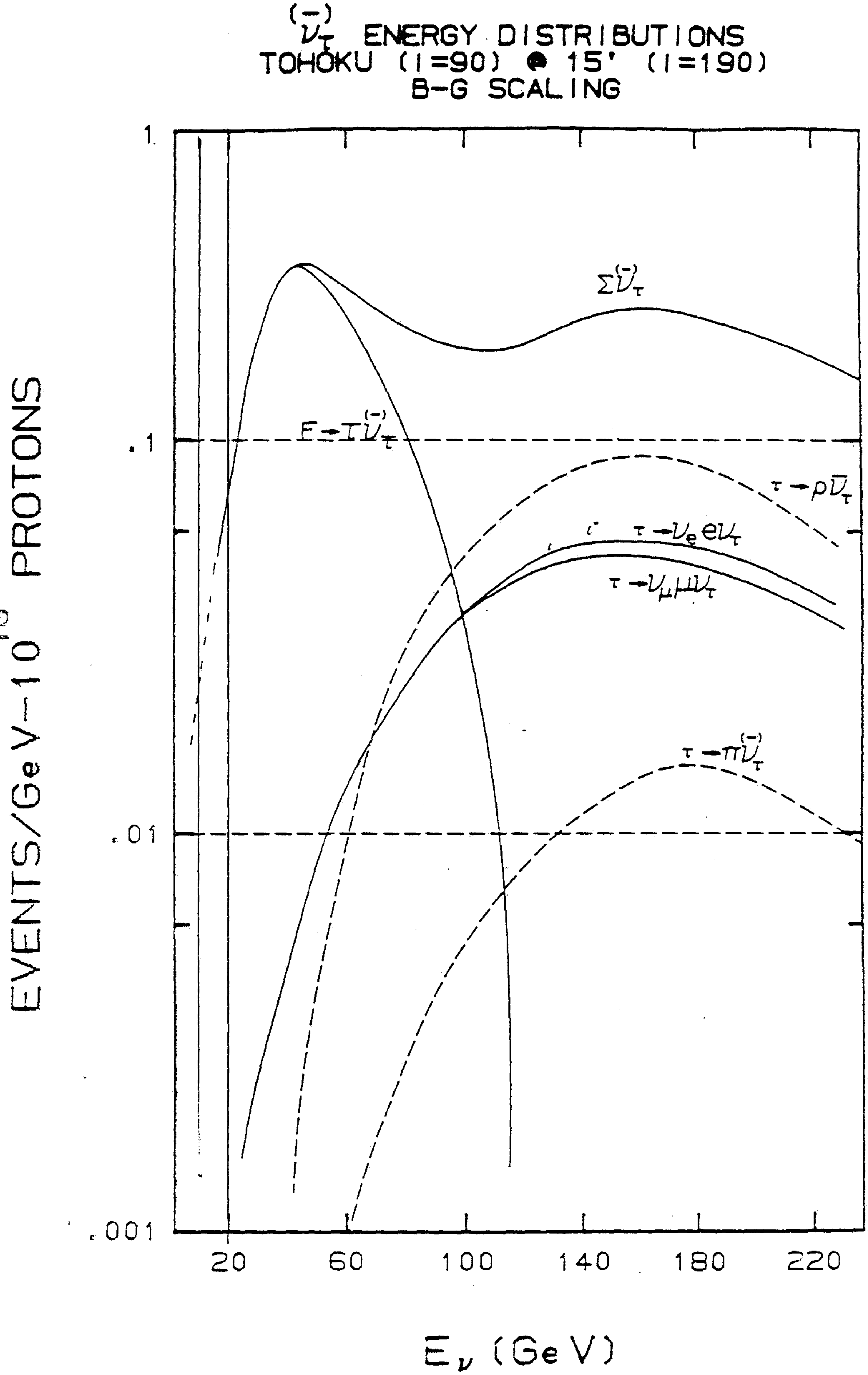

$\overset{(-)}{\nu}_\tau$ ENERGY DISTRIBUTIONS
TOHOKU (l=90) @ 15' (l=190)
B-G SCALING
EVENTS/GeV-10^{19} PROTONS
1
.1
.01
.001
20
60
100
140
180
220
E_ν (GeV)
$\Sigma \overset{(-)}{\nu}_\tau$
$F \to \tau \overset{(-)}{\nu}_\tau$
$\tau \to \rho \bar{\nu}_\tau$
$\tau \to \nu_e e \nu_\tau$
$\tau \to \nu_\mu \mu \nu_\tau$
$\tau \to \pi \overset{(-)}{\nu}_\tau$

Fig. 6 (Morfin)

NUTRINO EVENT ENERGY DISTRIBUTIONS
TOHOKU (ℓ=90) 15' (ℓ=190)
B-G SCALING

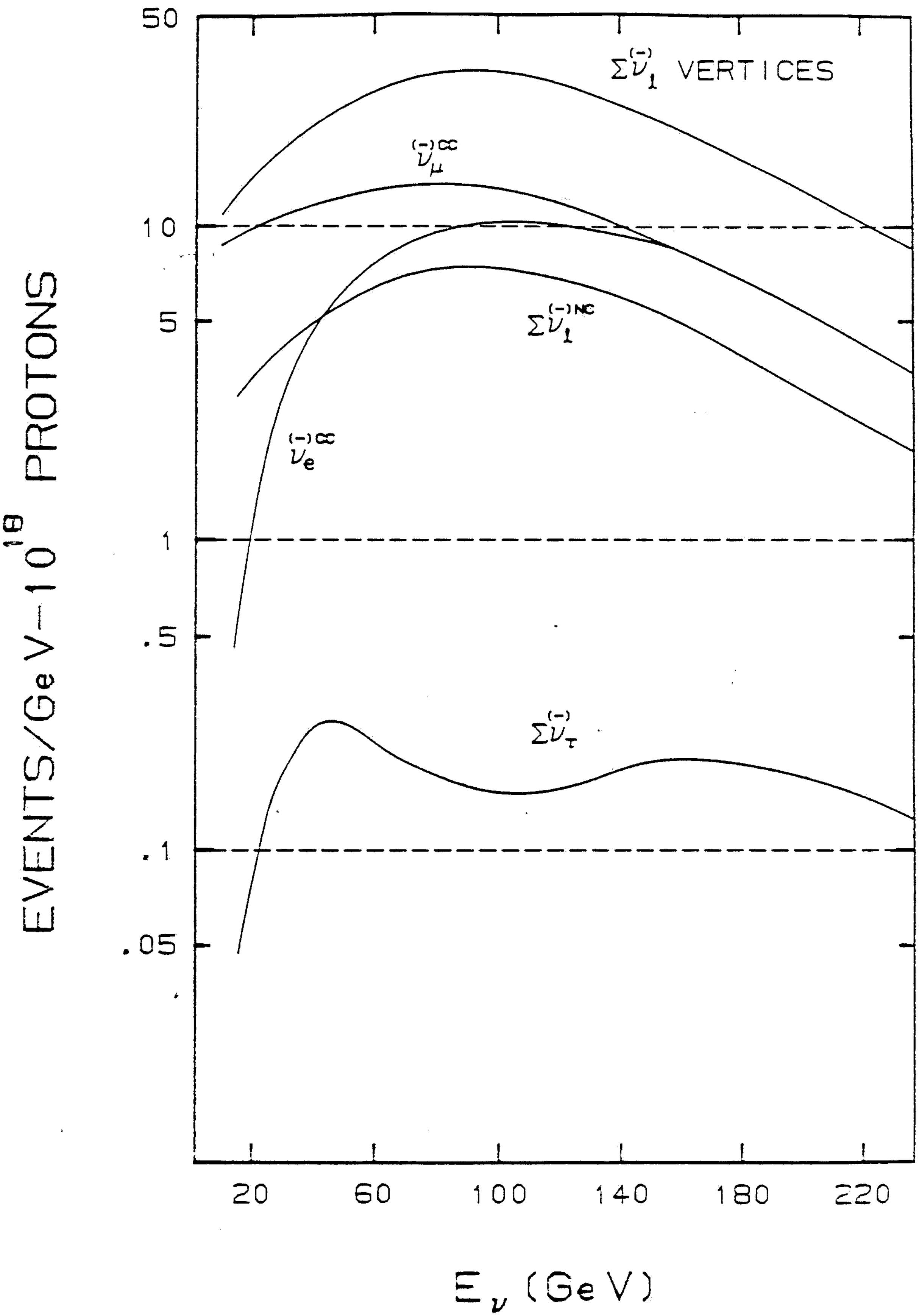

LEBC NA27

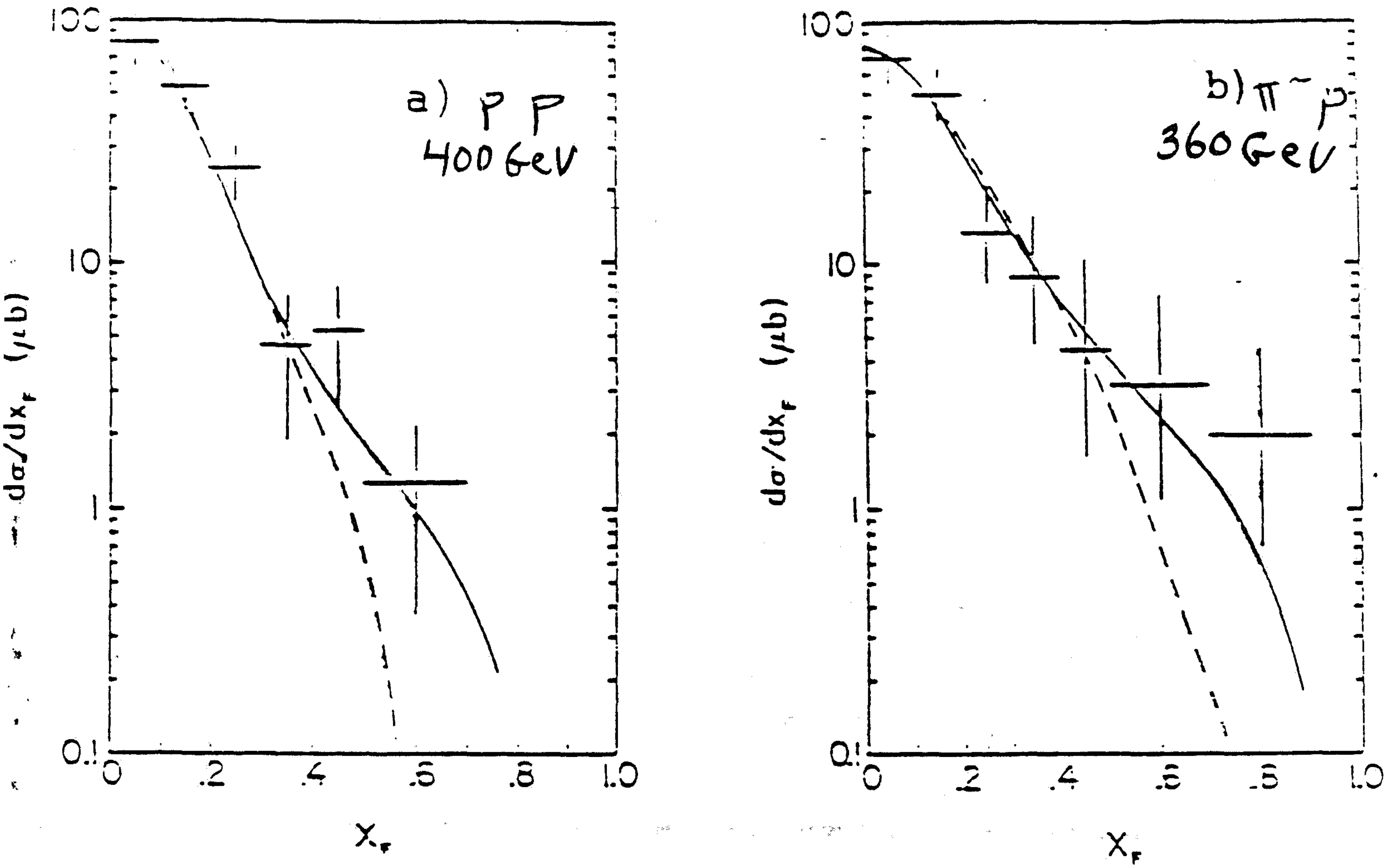

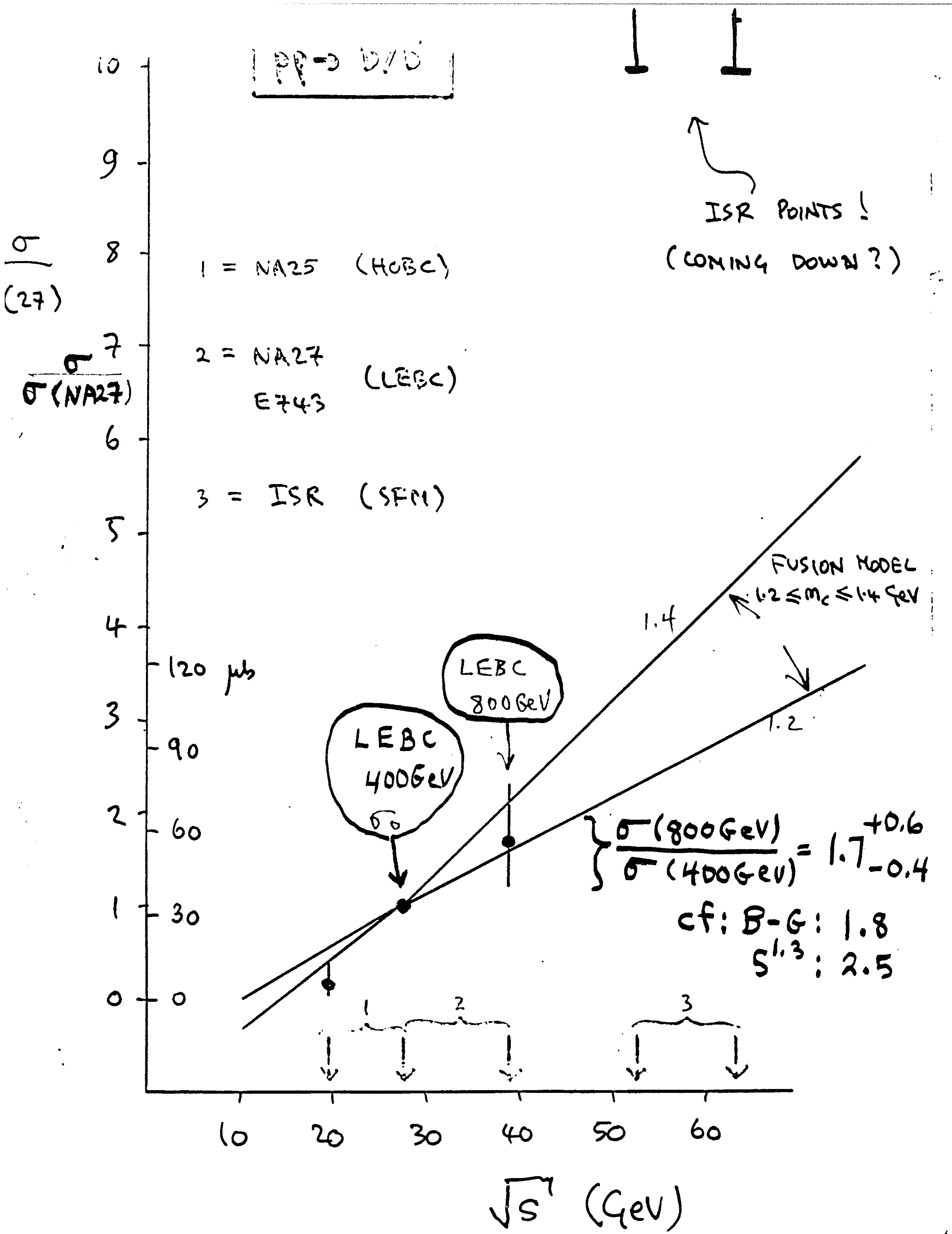

pp → D/D̄
ISR POINTS !
(COMING DOWN ?)
1 = NA25 (HOBC)
2 = NA27 / E743 (LEBC)
3 = ISR (SFM)
σ / σ(27)
σ / σ(NA27)
120 μb
90
60
30
0
FUSION MODEL
1.2 ≤ m_c ≤ 1.4 GeV
1.4
1.2
LEBC 800GeV
LEBC 400GeV
σ₀
$\frac{\sigma(800GeV)}{\sigma(400GeV)} = 1.7^{+0.6}_{-0.4}$
cf: B-G: 1.8
$s^{1.3}$: 2.5
√s (GeV)

BR ($F^{\pm} \to \tau^{\pm} \nu$) (see Schneps- encl.)

τ_F was $\sim 2.5 - 3 \times 10^{-13}$ sec

Now: E691: $(4.0^{+1.2}_{-0.8} \pm 0.6) \times 10^{-13}$, improving

NA32 (ACCMOR) : $(3.8 \pm 1.0) \times 10^{-13}$

Theory:

R.M. Schindler.

$$\Gamma_{M \to \ell \nu_\ell} = \left(\frac{G_F^2}{8\pi}\right) f_M^2 M_\ell^2 M_M \left[1 - \left(\frac{M_\ell}{M_M}\right)^2\right]^2 |V q_1 q_2|^2$$

	f_F(GeV)	Br($F^{\pm} \to \tau^{\pm} \nu$)
$f_F = f_K$	0.157	1.8%
	0.168	2.0%
potential model	0.210	3.1%
	0.250	4.4%
$f_F = f_D$ upper limit	0.340	8.2%

Non-observation of $F^{\pm}$ in $\pi^- N$, pN collisions

1. Only published upper limit:

   NA27 (LEBC) $\pi^- p$ @ 360 GeV

   $$\sigma_F \cdot BR(F^{\pm} \to K^{\pm} X) \leq 650 \text{ nb}$$

   $$\Rightarrow \frac{\sigma_F}{\sigma_D} < 13\% \quad \underline{\underline{\text{if}}} \quad BR = \frac{1}{3}$$

2. ACCMOR (NA32) sees F only in $K^- N$ interactions

   $$\frac{\sigma_{K^- N \to F}}{\sigma_{\pi^- N \to F}} > 10$$

   - early ACCMOR (NA11) did not separate K^- & π^- beam
   - NA11 did not separate int. + decay vertices

3. E623 (MPS)

Berkeley '86

ACCMOR, NA32 (active target)

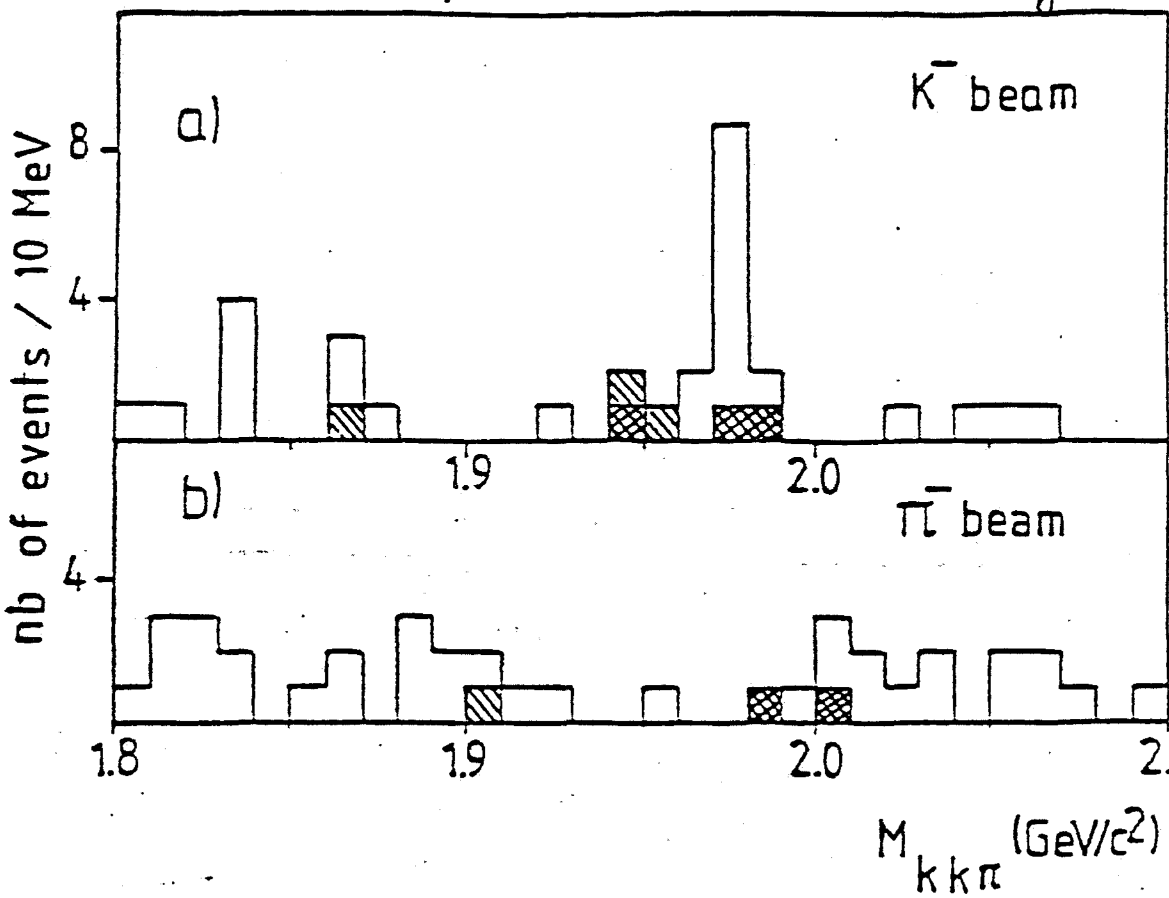

- active target allows cut:
  decay vertex separated from interaction vertex
- unbiased trigger

$$\frac{\sigma_{x_F>0}(\pi^- N \to D)}{\sigma_{x_F>0}(K^- N \to D)} = 0.9 \pm 0.2$$

NA32 ACCMOR '86

Using the NA11 acceptance curve, the ratio is also 0.9.

Separating the sample into $D^0/\bar{D}^0$ and D^+/D^- we obtain

$$\frac{\sigma_{x_F>0}(\pi^- N \to D^0/\bar{D}^0)}{\sigma_{x_F>0}(K^- N \to D^0/\bar{D}^0)} = \boxed{1.3 \pm 0.4}$$

and

$$\frac{\sigma_{x_F>0}(\pi^- N \to D^\pm)}{\sigma_{x_F>0}(K^- N \to D^\pm)} = \boxed{0.6 \pm 0.2}$$

Figure 3 shows the invariant mass distribution for the $KK\pi$ mass combinatior for the π^- and K^- incident beam separately. A clear F peak at a mass : 1975 MeV/c^2 appears in the K^- data. No equivalent structure is observed in the π data. The background level in the two distributions scales as the number of π^- ar K^- interactions, i.e. 2.5 and 3 events for K^- and π^- interactions respectively in th mass region 1.95 to 2.0 GeV/c^2. A few events marked in the figure are considere ambiguous with a $D \to K\pi\pi$ or a $\Lambda_c \to Kp\pi$ interpretation. This occurs in the case of K/π or a K/p ambiguity in the particle identification when simultaneously the $K\pi$ mass or the $Kp\pi$ mass is compatible with the D or the Λ_c mass. We obtain an upp limit

$$\frac{\sigma_{x_F>0}(\pi^- N \to F^\pm)}{\sigma_{x_F>0}(K^- N \to F^\pm)} < 0.1 \text{ at } 90\% \text{ C.L.}$$

Since the K^- beam favours F production, we separate the F^- and F^+ to stuc the effect of the incident s quark. Of the events in the mass range 1.95 : 2.0 GeV/c^2, 8 are F^- and 6 events are F^+. Figure 4 shows their x_F distribution: th F^- events indicate a harder x_F distribution than the F^+, an average x_F of 0.45 for F and 0.16 for F^+ including the ambiguous events. Figure 4a shows for comparison th

4-K trigger

pc → φφX ; 400 GeV/c : $D^{\pm}$ but no F? $D_s^{\pm}$

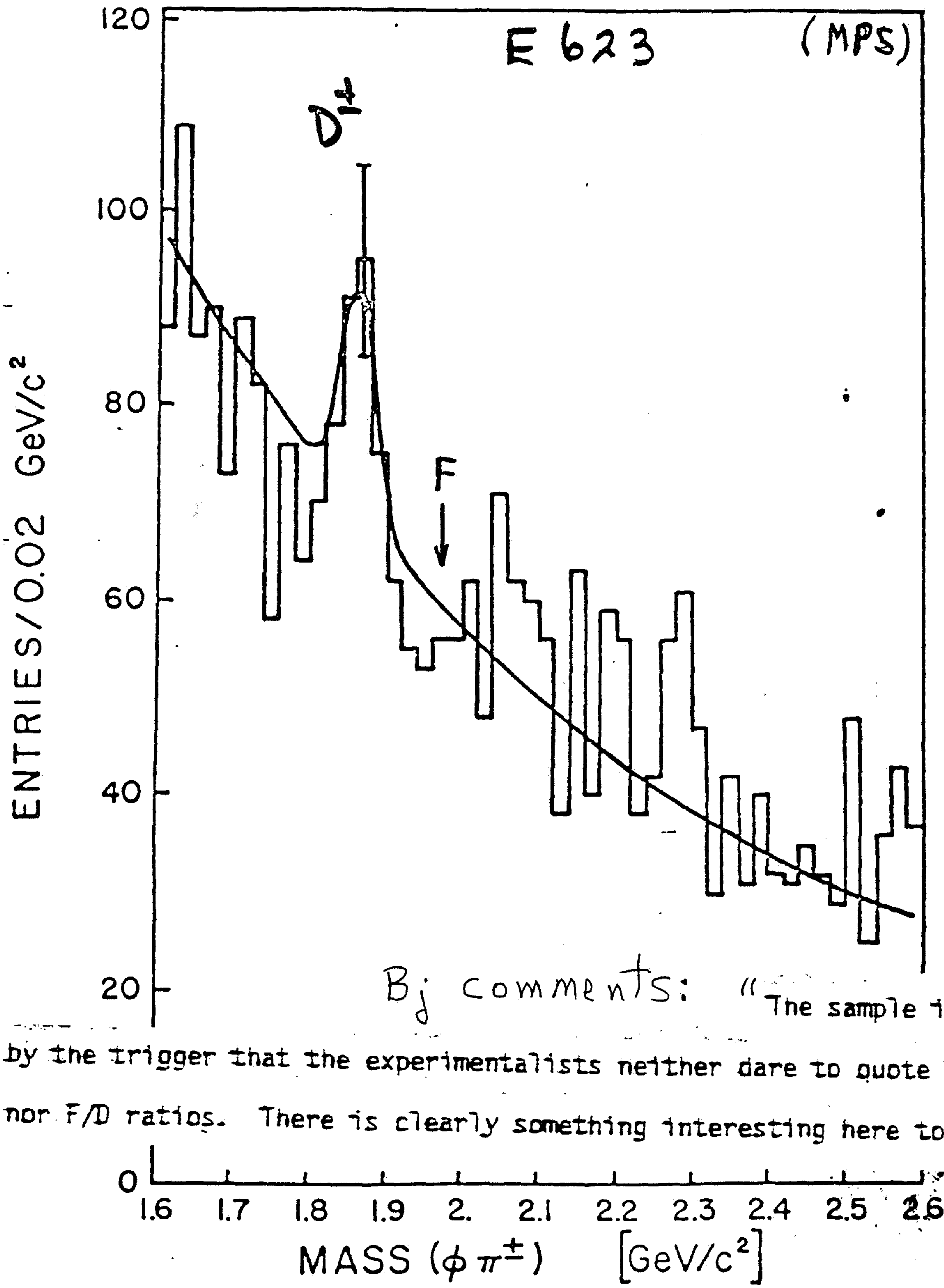

Bj comments: "The sample is so badly biased by the trigger that the experimentalists neither dare to quote D cross sections nor F/D ratios. There is clearly something interesting here to pursue further."

Why choose $\frac{F}{D} = 0.12$ as best guess?

① 3 experiments:

$$e^+e^- \to \frac{F}{D} \to \phi\pi$$

$$\gamma p \to \left\{ \begin{matrix} F \\ D \end{matrix} \right\} \to \phi\pi$$

$$B \to F\,X, \quad F \to \phi\pi$$

with a little help from theory: $BR(F \to \phi\pi) = 4.6\%$

all support the conventional theory that c-quarks turn into F's 15% of the time. Why should quarks behave differently in hadroproduction?

[see details in Schneps memo]

② But let us respect the upper limit from LEBC ($\pi^- p$ @ 360 GeV) of $\frac{\sigma_F}{\sigma_D} < 13\%$ $(x_F > 0)$

$\Rightarrow$ somewhat arbitrarily, set $\frac{F}{D} = 0.12$

(Morfin)

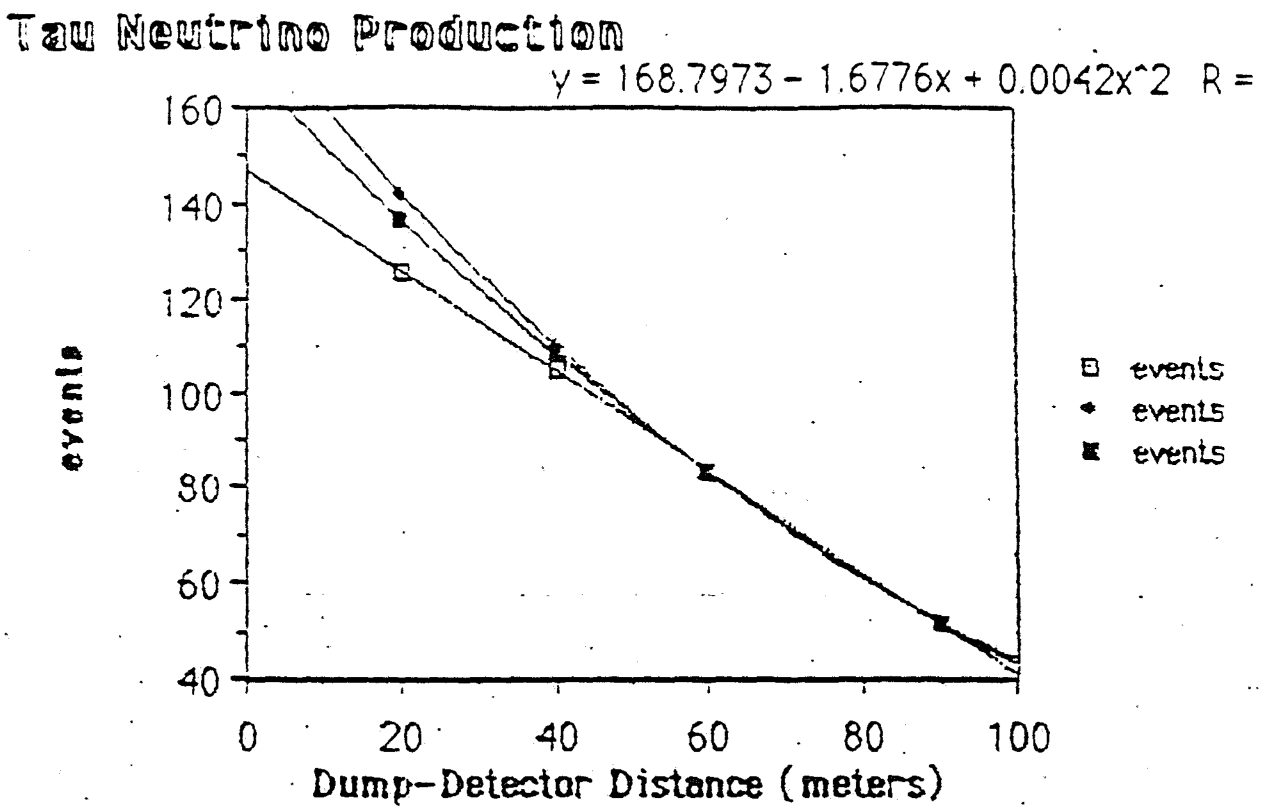

Tau Neutrino Production
y = 168.7973 - 1.6776x + 0.0042x^2 R =
160
140
120
100
80
60
40
0
20
40
60
80
100
events
Dump-Detector Distance (meters)
events
events
events

V2P copy

TUFTS UNIVERSITY

TO: Mike Peters

FROM: Jack Schneps

DATE: September 9, 1986

SUBJECT: F/D Ratio and $F \rightarrow \tau\nu_\tau$ Branching Ratio

What follows is a review of the $F \rightarrow \tau\nu_\tau$ branching ratio and the F/D hadroproduction ratio using the latest information I was able to get my hands on (with much help from Austin Napier). I hope it may be useful for the E646 proposal.

$F \rightarrow \tau\nu_\tau$ Branching Ratio

The nominal value used for the branching ratio $F \rightarrow \tau\nu_\tau$ in estimating production from a beam dump has been 2%.

We review the calculations of this branching ratio using the latest information available on relevant parameters, e.g. the F lifetime and mass and pseudoscalar coupling constants.

To calculate this we begin with the formula for the decay rate of a meson $M \equiv q_1\bar{q}_2$ into a lepton ℓ and an ℓ-neutrino as given, for example, in the Berkeley transparencies of R.M. Schindler.

$$\Gamma_{M \rightarrow \ell\nu_\ell} = \left(\frac{G_F^2}{8\pi}\right) f_M^2 \, M_\ell^2 \, M_M \left[1 - \left(\frac{M_\ell}{M_M}\right)^2\right]^2 |Vq_1q_2|^2$$

G_F here means $G_F/(\hbar c)^3 = 1.166 \times 10^{-5}$ GeV^{-2}

With masses given in GeV and Γ in GeV the pseudoscalar coupling constant f_M will also be in GeV. To obtain Γ(GeV) from $\Gamma(\text{sec}^{-1})$ note $\Gamma(\text{GeV}) = \hbar\,\Gamma(\text{sec}^{-1})$ where $\hbar = 6.582 \times 10^{-25}$ GeV sec.

For $\pi^+ \rightarrow \mu^+\nu_\mu$ using the pion lifetime and $|Vud|^2 = 0.9483$ one obtains $f_\pi = 0.132$ GeV.

For $K^+ \rightarrow \mu^+\nu_\mu$ using the kaon lifetime and branching ratio into $\mu^+\nu_\mu$ and $|Vus|^2 = 0.0506$ one obtains $f_K = 0.157$ GeV.

For the D, Schindler gives an upper limit for f_D, namely $f_D < 0.340$ GeV. He also points out that theory suggests $f_D < f_F$ and that potential and bag models estimate $f_D \sim 0.15$ GeV and potential models estimate $f_F \sim 0.21$ GeV.

To calculate $Br(F^+ \to \tau^+\nu_\tau)$ we determine $\Gamma_{F^+ \to \tau^+\nu_\tau}$ from the above formula for several values of f_F; and Γ_{F^+}, the total decay rate, from experimental lifetime measurements. In our judgement, the most reliable F lifetime measurement is the recent result from Fermilab experiment E691 (Tagged Photon Beam) based on $F \to \phi\pi$ decays. The latest result (Sept. 86) is $\tau_F = 0.42$ psec.,[2] consistent with the result presented at Berkeley,[3]

$$\tau_F = (0.40 \pm {}^{.12}_{.08} \pm 0.06)_{ps}$$

$$\text{Thus } \Gamma_{F^+} = 2.38 \times 10^{12}\ s^{-1} = 1.57 \times 10^{-12}\ \text{GeV}$$

From the formula we obtain $\Gamma_{F^+ \to \tau^+\nu_\tau} = 1.12 \times 10^{-12} f_F^2$ GeV

$$\text{Thus } Br(F \to \tau\nu_\tau) = \frac{\Gamma_{F^+ \to \tau^+\nu_t}}{\Gamma_{F^+}} = 0.71 f_F^2 \text{ (with } f_F \text{ in GeV)}$$

The results for several values of f_F are as follows:

	f_F(GeV)	$Br(F^+ \to \tau^+\nu_\tau)$
$f_F = f_K$	0.157	1.8%
	0.168	2.0%
potential model	0.210	3.1%
	0.250	4.4%
$f_F = f_D$ upper limit	0.340	8.2%

The conclusion is that, based on present knowledge, the branching ratio is somewhere in the range 1.8 to 8.2%. The nominal 2% used for the beam dump event rate estimates is conservative and near the minimum value. A best estimate would be more like 3-4%. The main reason for the previous choice of 2% was probably the use of earlier, less reliable, measurements of the F lifetime (in the range $(0.25\text{–}0.30) \times 10^{-12}$ sec).

We also point out the following branching ratios for $D^+ \to \tau^+\nu_\tau$.

	f_D(GeV)	$Br(D^+ \to \tau^+\nu_\tau)$
potential and bag models	0.150	0.043%
f_D upper limit	0.340	0.22%

If, for example f_D = .15GeV, f_F = .21 GeV and the D to F ratio is ~ 10 we would expect an additional 15% ν_τ events coming from D's.

$$\frac{.043\%}{3.1\%} \times 10 = 0.14$$

F/D Hadroproduction

The F/D hadroproduction ratio in non-strange beams is very poorly known. The best estimate one can make probably comes from observation of $\phi\pi$ decay modes of D and F in the CERN experiments NA11 and NA32 which used beams in the 100-200 GeV range.

NA11 results can be found in the report NIKHEF -H/85-5.[4] In tables with details of the events 20 are listed which were detected with an inclusive ϕ-trigger and have a non-strange (π or p) beam particle. Of these 4 are consistent with an F mass and 5 with a D mass. This suggests

$$\frac{\sigma_{F^\pm}\ BR(F \to \phi\pi)}{\sigma_{D^\pm}\ BR(D \to \phi\pi)} = 0.8$$

On the other hand Daum in a talk on NA32 at Fermilab (5/19/86)[5] presented a mass plot for ϕ-trigger events associated with π^- beam particles. Three events are consistent with an F mass and 15 with a D mass, however, the three events are barely above background so that the most one can say is

$$\frac{\sigma_{F^\pm}\ BR(F \to \phi\pi)}{\sigma_{D^\pm}\ BR(D \to \phi\pi)} < 0.2.$$

Superceded by Berkeley paper

The branching ratio of the D into $\phi\pi$ has been found to be 1.0%.[6] For the F we use 4.6% (to be explained shortly).

Then NA11 suggests $\frac{\sigma_{F^\pm}}{\sigma_{D^\pm}} \sim \frac{0.8}{4.6} \sim 0.2$

Whereas NA32 suggests $\frac{\sigma_{F^\pm}}{\sigma_{D^\pm}} < \frac{0.2}{4.6} \sim 0.05.$ } Superceded by Berkeley

The LEBC-EHS collaboration[7] (Plano et. al.) reported a limit $\frac{\sigma_{F^\pm}}{\sigma_{D^\pm}} < 0.13$ in 1985 from 360 GeV π^-p interactions.

Berkeley paper sees no $F \to KK\pi$ nor $D \to KK\pi$ in π^-N interactions, above background

But sees good $F \to \pi KK$ in K^-N interactions

Several points should be made here:

1. None of the previous results are inconsistent with F/D being about 10%.

2. These experiments may be biased toward finding leading charm, which would not be surprising in searches for the decays of very short-lived particles. Since the F's from non-strange beams are centrally produced the σ_F/σ_D ratios given above may be underestimated.

3. Let us give a crude estimate of the F/D ratio. We know that each time one charmed particle is made another is made. If a leading D is produced the second charmed particle (neglecting baryons) is F or D. If charmed quark fragmentation is similar to that of the u-quark, then about 15% of the second charmed particles will be F's and F/D will be ~8%. If the $c\bar{c}$ pairs are centrally produced then F/D should be ~18%. Thus F/D should be somewhere in the range 8-18% if our understanding of these things is at all reasonable.

4. There is plenty of evidence that in u-quark hadronization the probability of picking up an s-quark from the sea is $f_s \sim 15\%$. What evidence is there that this is also the case for c-quark hadronization? We combine a bit of theory with three different experimental results.

   a) The main theoretical result we use is the calculation by Fakirov & Stech[8] of the F decay rate into $\phi\pi$, $\Gamma_{F \to \phi\pi} = 11 \times 10^{10}$ sec^{-1}. Combining this with $\Gamma_F = 2.4 \times 10^{12}$ sec^{-1} given earlier, we obtain $BR(F \to \phi\pi) = 4.6\%$.

   b) Derrick et. al.[9] have measured the ratio

   $$\frac{\sigma_F \, BR(F \to \phi\pi)}{\sigma_D} = 0.0059 \pm 0.0020 \text{ in } e^+e^- \text{ collisions at 29 GeV at PEP.}$$

   We can interpret this as $\dfrac{\sigma_F}{\sigma_D} = \dfrac{.0059}{BR(F \to \phi\pi)}$. Using $BR(F \to \phi\pi) = 0.046$ gives $\dfrac{\sigma_F}{\sigma_D} = .13$ or $\dfrac{\sigma_F}{\sigma_F + \sigma_D} = .12$, consistent with 15%.

   c) E691[3] has measured the ratio of $F \to \phi\pi$ to $D \to \phi\pi$ in photoproduction. The result is:

   $$\frac{\sigma_{F^+} \, BR(F^+ \to \phi\pi^+)}{\sigma_{D^+} \, BR(D^+ \to \phi\pi^+)} = 2.4 \, {}^{+1.3}_{-0.9} .$$

   Using 4.6% and 1.0% for the branching ratios $\dfrac{\sigma_{F^+}}{\sigma_{D^+}} = .52$. Now $\dfrac{\sigma_{F^+}}{\sigma_{F^+} + \sigma_D} = \dfrac{\sigma_{F^+}}{\sigma_{F^+} + \sigma_{D^+} + \sigma_{D^\circ}}$.

If we assume D^* photoproduction is three times that of D and use the known branching ratio for D^{*+} and $D^{*°}$ we find $\sigma_{D^+} = 0.24\sigma_D$ and $\sigma_{D^\circ} = 0.74\sigma_D = 2.85\sigma_{D^+}$.

Thus

$$\frac{\sigma_{F^+}}{\sigma_{F^+} + \sigma_D} = \frac{\sigma_{F^+}}{\sigma_{F^+} + 3.24\sigma_{D^+}} = \frac{\sigma_{F^+}/\sigma_{D^+}}{\sigma_{F^+}/\sigma_{D^+} + 3.24} = \frac{.52}{.52 + 3.24} = 0.14$$

again consistent with 15%.

d) Finally we consider a result from CLEO[10] on the decay of the B-Meson to F, followed by $F \to \phi\pi$. They find the product $BR(B \to FX) \cdot BR(F \to \phi\pi) = 0.0038 \pm .0010$. Using $BR(F \to \phi\pi) = .046$ gives $BR(B \to FX) = 0.083$. Suzuki[11] has shown that if $f_s = 0.15-0.17$ in charm hadronization than $BR(B \to FX) = 0.09$, in agreement with our result.

The conclusion is that three different kinds of experiments - e^+e^- production of charm, photoproduction of charm, and B-Meson decay into charm - combined with a fairly reliable theoretical estimate of the $F \to \phi\pi$ branching ratio support the reasonable hypothesis that c-quarks turn into F-Mesons 15% of the time. It would be unbelievable that they change their behavior when hadro-produced. Thus the F/D ratio in the beam dump experiment can be taken with great confidence to lie in the range 8-18% as indicated earlier. The fact that this has not yet been clearly seen is simply due to the fact that the hadron experiments have not yet been sensitive enough. This will be corrected when E769 observes F-mesons in large numbers directly produced from hadron beams and when E646 observes the ν_τ's from their decay in the 15-foot bubble chamber.

I would also point out, as others have done, that the presence of kaons among the secondary particles from primary proton interactions would produce an enhancement in the overall F/D ratio in the beam dump. A crude estimate I have made suggests this would be 20-30%. Perhaps others have done more precise calculations.

Summarizing, I would say that the previous estimates of ν_τ event rates were too conservative. We gain a factor of perhaps 1.5 from better estimates of $F \to \tau\nu_\tau$; a factor of 1.15 from $D \to \tau\nu_\tau$; a more reasonable F/D ratio might be 12-13%, giving us a factor of ~1.2; secondary kaons may also give us a gain of aobut 1.2. Putting all of these together suggests that the event rate should be more than twice the earlier estimates.

1. New Results on Charm Decay from the Mark III at SPEAR, R.M. Schindler, Berkeley Conference (July 1986).
2. Private Communication.

3. Early Results on Charm Photoproduction, Fermilab TPS Collaboration, Berkeley Conference (July 1986).
4. Observation of Hadronically Produced Charmed F-Mesons, ACCMOR Collaboration, NIKHEF-H/85-5.
5. Hadroproduction and Decay of Charm, D. Daum talk at Fermilab, 5/19/86.
6. BR($D^+ \to \phi\pi$) = 0.97± 0.27 ± 0.14%, P.R.L. 55, 150 (1985).
7. A Search for F Production.... PL 156B, 444 (1985).
8. D. Fakirov and B. Stech, Nuc. Phys. B133, 315 (1978).
9. M. Derrick et. al., P.R.L. 54, 2568 (1985).
10. Haas et. al., Observation of the Decay $B \to FX$, CLNS-86/727, CLEO-86-4.
11. M. Suzuki, Phys. Rev. D31, 1158 (1985).

W. Bugg
9/22/86

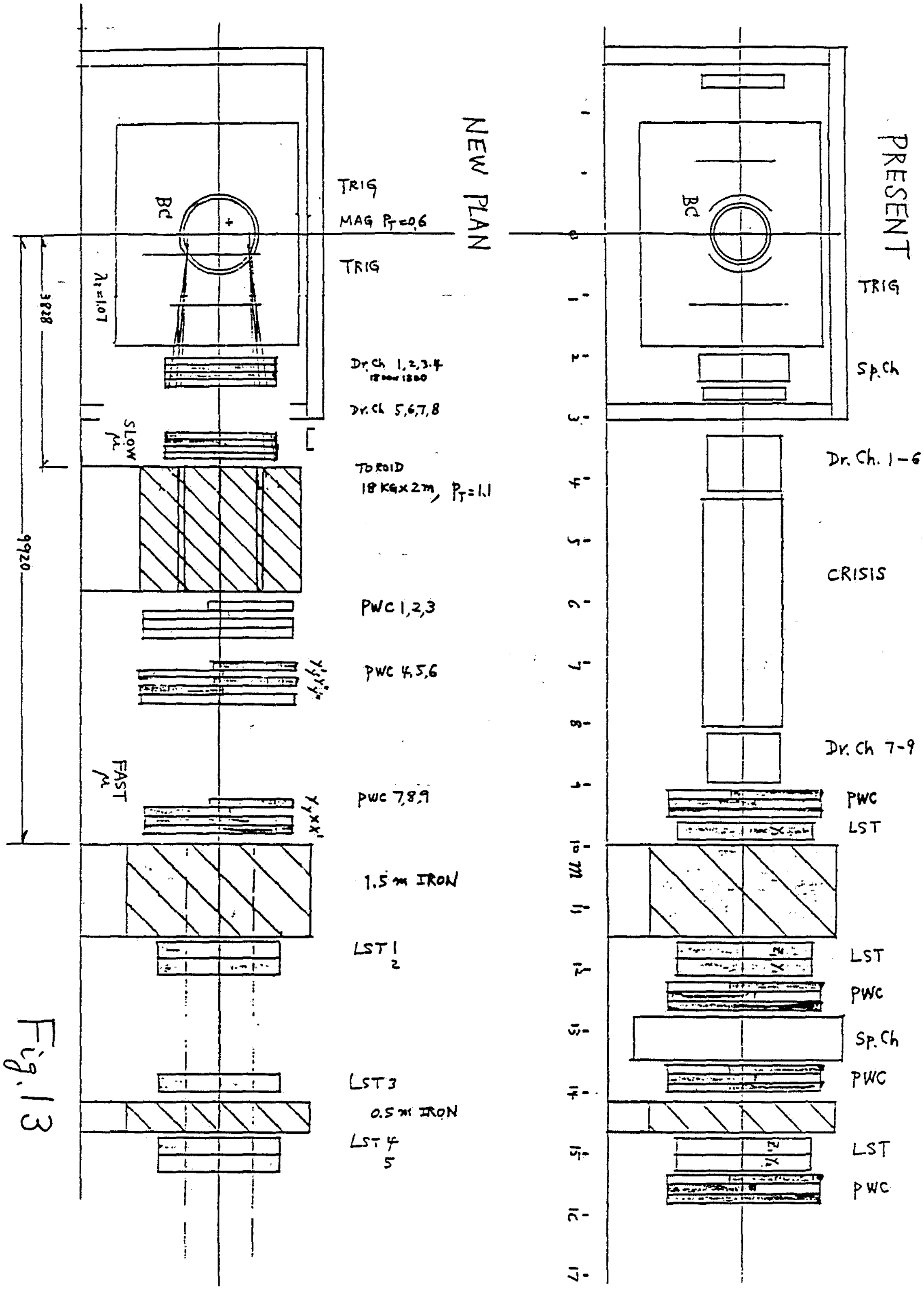

Fig. 13

Improvements for E-745

I. Bubble Chamber

A) Larger Bubble Chamber Body

B) Widened Magnet Gap

II. Counter System

A) Improved Interaction Trigger

B) Improved Muon acceptance
  1. Toroid
  2. Drift Chambers

III Improved Optics

A) Normal Optics

B) Holograms

C) Holographic Reconstruction

Bubble Chamber Body

(mfc: Ishikawajima Heavy Industry)

	Old	New
Depth :	1.0 m.	1.4 m.
Max. Diameter :	0.83 m.	1.12 m.
Fiducial Volume :	340 ℓ.	700 ℓ.

to be shipped Sept. 25, 1986

—·—

Magnet

	old	new
Gap in Magnet iron	0.60 m.	1.70 m.
Coil Gap	0.60 m.	1.00 m.
Magnetic Field	28 Kg.	18 Kg.

—·—

Fig. 14

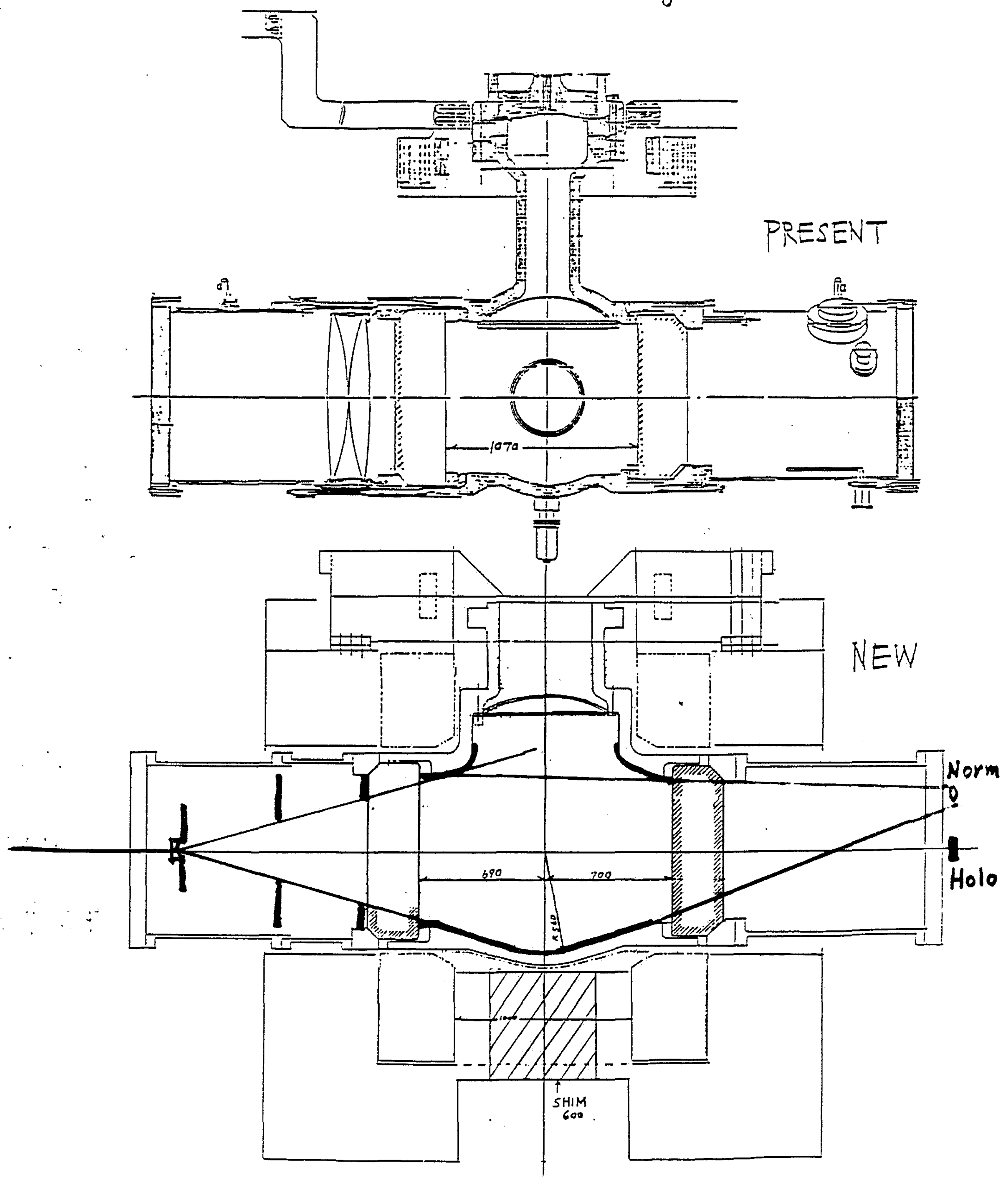

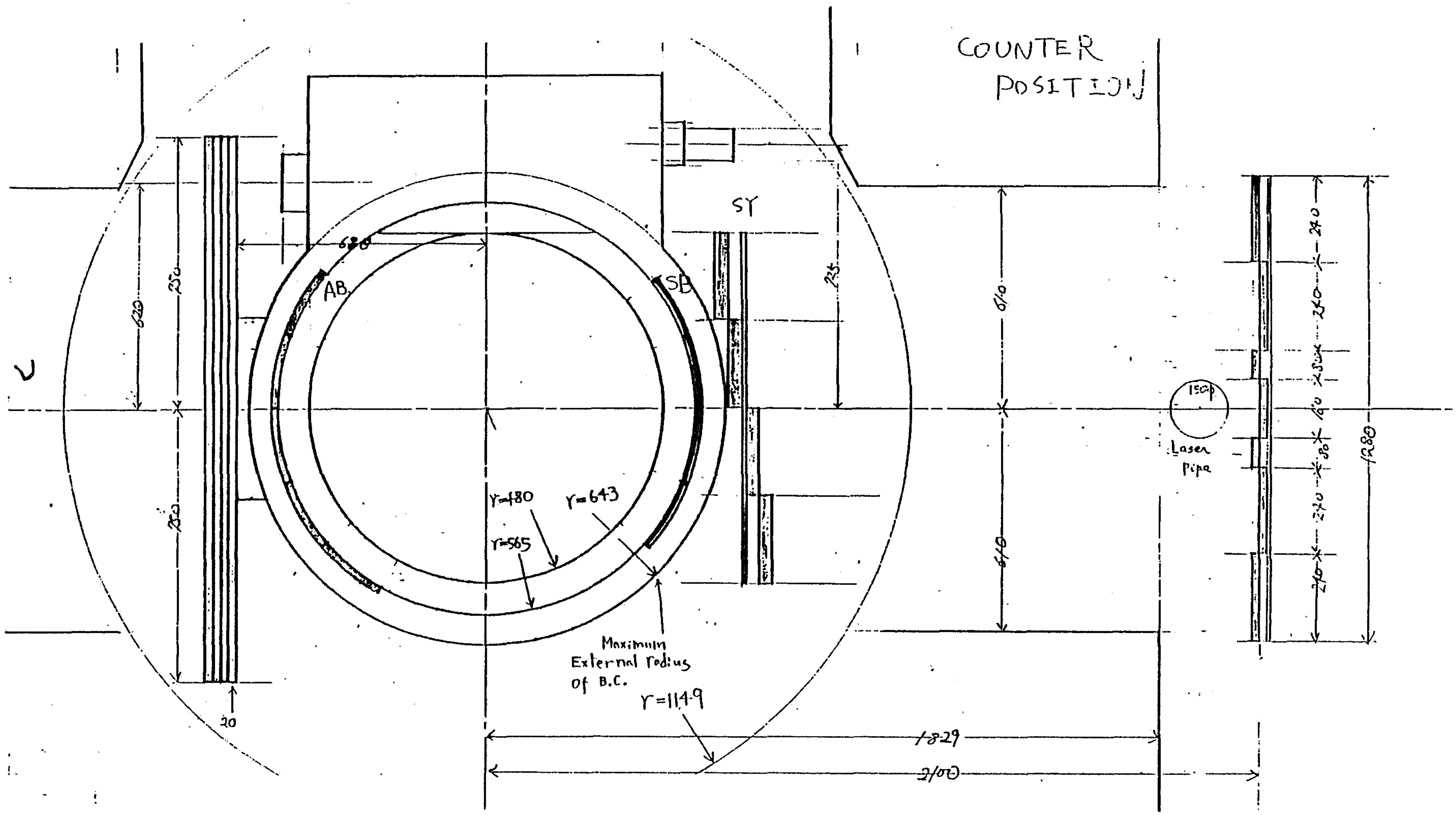

COUNTER
POSITION
SY
AB
SB
630
250
620
225
610
240
1280
150φ
Laser
Pipe
r=480
r=643
r=565
Maximum
External radius
of B.C.
r=1149
20
1829
2100

TOROID MAGNET

(mfc : Tohoku Metal Co.)

$\int B\,dl$ 18 kgauss × 2 m.

Wt. 110 tons

- Improves Muon Acceptance

  E-636 90% for ν_μ CC evts

  80% for μ's from ν_τ decay

- Improves Momentum Resolution

  for lower momentum muons

(to be shipped Oct 20, 1986)

DRIFT CHAMBERS

- 8 planes new

  2 Quadruplets Butterfly Geom.

Improvements of Normal Optics

	Old	New
A. Illumination	See Through	Scotchlite • Uniform tracks throughout
• Depth	1.0 m.	1.4 m.
B. Lenses	3 @ f = 55mm	6 @ f = 40 mm • New lenses Designed and Manufactured by NIKON
C. Cameras	Three	Three with 2 pictures each • One triplet for near field second for far field

Improvements of Hologram Optics

	Old	New
A. Laser	YAG 300 mJ. Not uniform	Ruby 10 J. Uniform beam → good resolution
B. Size of Hologram	60 mm diam.	60 × 70 mm.

Resolution : $\Delta = 1.22 \lambda \frac{X}{D}$

C. Holog QUALITY

marginal region   good region

Line freq of interference
angle of interference lines
in emulsion

D. Camera   1 view   2 views

- different angles
- avoids loss due to imperfection of film.

Fig. 17

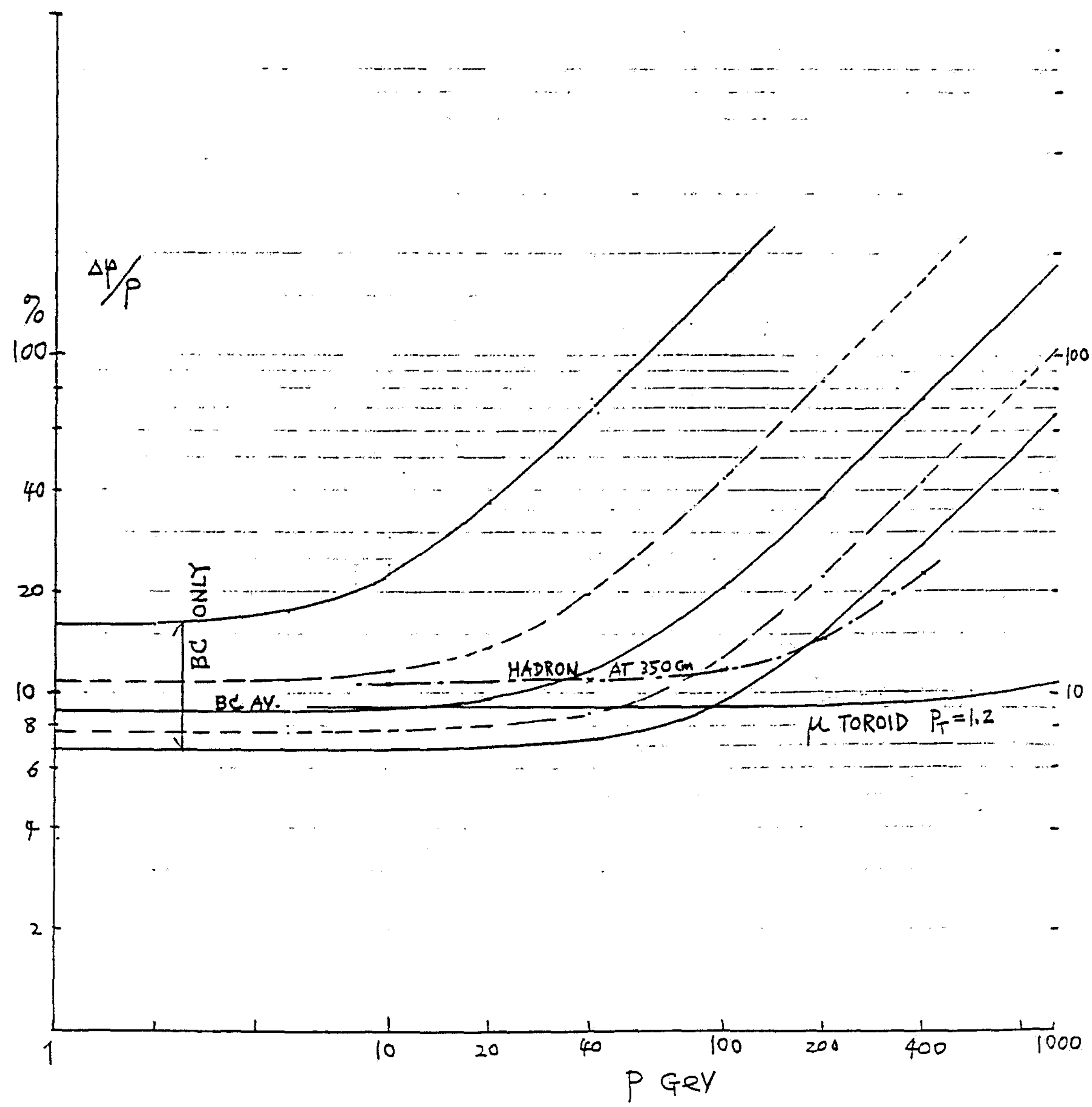

Δp/p
%
100
40
20
10
8
6
4
2
BC ONLY
HADRON AT 350 Gm
BC AV.
μ TOROID P_T=1.2
100
10
1
10
20
40
100
200
400
1000
P GeV

M. Peters
9/22/86

E646 Holography Status Report

1. Laser improvements	Pulse Stretching: Works Simmering	 : In progress
2. Laser beam transport		Works
3. Laser beam monitoring		Designed, parts ordered
4. Dispersing lens/window		Designed, ordered, Partially ground
5. Light baffles		Installed on wall Partially installed in beanie Tested successfully
6. Fiber optic camera		Under discussion

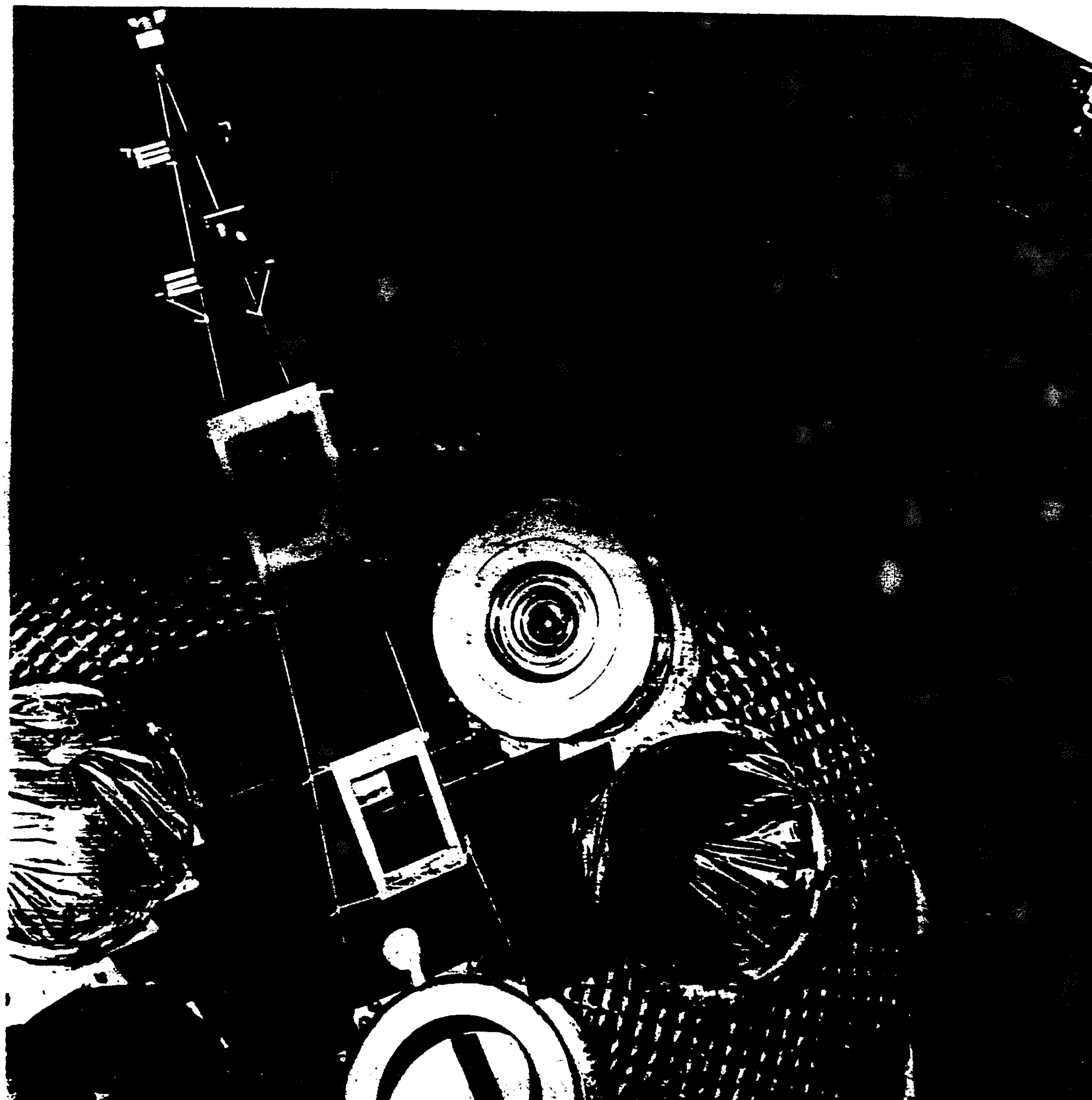

P TAU (GEV)

```
HBOOK     ID =          1                                          DATE  06/08/86              NO =  1

   400          -
   380          I
   360         -I-
   340         I I-
   320         I  I
   300         I  I   -
   280         I  I-- I---
   260         I    I-I  I
   240         I         I-
   220         I          I-
   200         I           I-
   180        -I            I-
   160        I              I--
   140        I                I
   120        I                I--
   100        I                  I
    80        I                  I-
    60        I                   I-
    40        I                    I-
    20       -I                     I--

CHANNELS  10    0         1         2         3         4         5
           1    12345678901234567890123456789[illegible]01234567890

CONTENTS 100     1333322222222222111111
          10    2749426758766218754116532
           1.   05992159070171872374198403

LOW-EDGE 100              1111111111222222222[illegible]44444444
          10     123456789012345678901234567[illegible]123456789
           1.    000000000000000000000000000[illegible]000000000

* ENTRIES =        5000     * ALL CHANNELS = [illegible]       * UNDERFLOW = 0.0000E+00     * OVERFLOW = 0.0000E+00
* BIN WID = 0.1000E+02      * MEAN VALUE   = 0.[illegible]     * R . M . S = 0.5776E+02     * ABNOR CHA= 0.0000E+00
```

τ^+

L TAU (CM)

```
HBOOK      ID =          3                                            DATE  06/08/86              NO =  3

      1160      -
      1120      I
      1080      I
      1040      I
      1000      I
       960      I
       920      I
       880      I
       840      I
       800      I-
       760      II
       720      II
       680      II
       640      II
       600      II
       560      II-
       520      I I
       480      I I
       440      I I-
       400      I  I
       360      I  I-
       320      I   I
       280      I   I-
       240      I    I-
       200      I     I
       160      I     I---
       120      I        I--
        80      I          I------
        40      I                I------------------------- ---- -

CHANNELS  10    0         1         2         3         4         5
           1    12345678901234567890123456789012[illegible]01234567890

CONTENTS1000    1
         100    17543221111
          10    56425714421986644433112121111
          1.    30128387464068521988791519840000[illegible]1312 2113 1

LOW-EDGE  1.              1111111111222222222[illegible]444444444
           0    0123456789012345678901234567890[illegible]90123456789

* ENTRIES =        5000     * ALL CHANNELS = 0.[illegible]     * UNDERFLOW = 0.0000E+00     * OVERFLOW = 0.1200E+02
* BIN WID = 0.1000E+00     * MEAN VALUE   = 0.[illegible]     * R . M . S = 0.6631E+00     * ABNOR CHA= 0.0000E+00
```

τ+

```
P TAU (GEV)

HBOOK      ID =          1                                       DATE  08/08/86               NO =  2

     1120          -
     1080          I
     1040          I
     1000          I-
      960          II
      920          II
      880         -II-
      840         I  I
      800         I  I
      760         I  I-
      720         I   I
      680         I   I
      640         I   I-
      600         I    I
      560         I    I--
      520         I      I
      480         I      I-
      440         I       I-
      400         I        I-
      360         I         I-
      320         I          I-
      280         I           I--
      240         I             I--
      200         I               I-
      160         I                I--
      120         I                  I--
       80         I                    I---
       40         I                       I----------

CHANNELS  10      0         1         2         3         4         5
           1      12345678901234567890123456789012345678901234567890

CONTENTS 1000      1
          100     8098765544332222222111
           10     79843033617296531642986643222 1[illegible]
           1.     749547552454658625518973396411[illegible]

LOW-EDGE  100               1111111111222222222[illegible]4444444444
           10      1234567890123456789012345678[illegible]0123456789
           1.     0000000000000000000000000000[illegible]0000000000

* ENTRIES =        10000     * ALL CHANNELS = 0.[illegible]     * UNDERFLOW = 0.0000E+00     * OVERFLOW = 0.0000E+00
* BIN WID = 0.1000E+02       * MEAN VALUE   = 0.7[illegible]    * R . M . S = 0.6294E+02     * ABNOR CHA= 0.0000E+00
```

τ⁻

L TAU (CM)

```
HBOOK     ID =        3                                        DATE  08/08/86             NO =  4

    3600      -
    3500      I
    3400      I
    3300      I
    3200      I
    3100      I
    3000      I
    2900      I
    2800      I
    2700      I
    2600      I
    2500      I
    2400      I
    2300      I
    2200      I
    2100      I
    2000      I
    1900      I
    1800      I
    1700      I-
    1600      II
    1500      II
    1400      II
    1300      II
    1200      II
    1100      II
    1000      II-
     900      I I
     800      I I-
     700      I  I
     600      I  I-
     500      I   I
     400      I   I--
     300      I     I--
     200      I       I--- -
     100      I          I-I-----------------------------------

CHANNELS  10  0         1         2         3         4         5
           1  12345678901234567890123456789012[illegible]901234567890

CONTENTS1000  31
         100  569753322111 1
          10  96812913285696777443432212111111 1
          1.  7248282276654777407867727849481 3[illegible]74363311513

LOW-EDGE  1.            1111111111222222222[illegible]44444444444
          0   01234567890123456789012345678[illegible]0123456789

* ENTRIES =      10000      * ALL CHANNELS = 0.[illegible]      * UNDERFLOW = 0.0000E+00      * OVERFLOW = 0.1000E+02
* BIN WID = 0.1000E+00      * MEAN VALUE   = 0.4[illegible]     * R . M . S = 0.6090E+00      * ABNOR CHA= 0.0000E+00
```

τ^-

D IMPACT (MICRONS)

HBOOK ID = 5 DATE 06/08/86 NO = 5

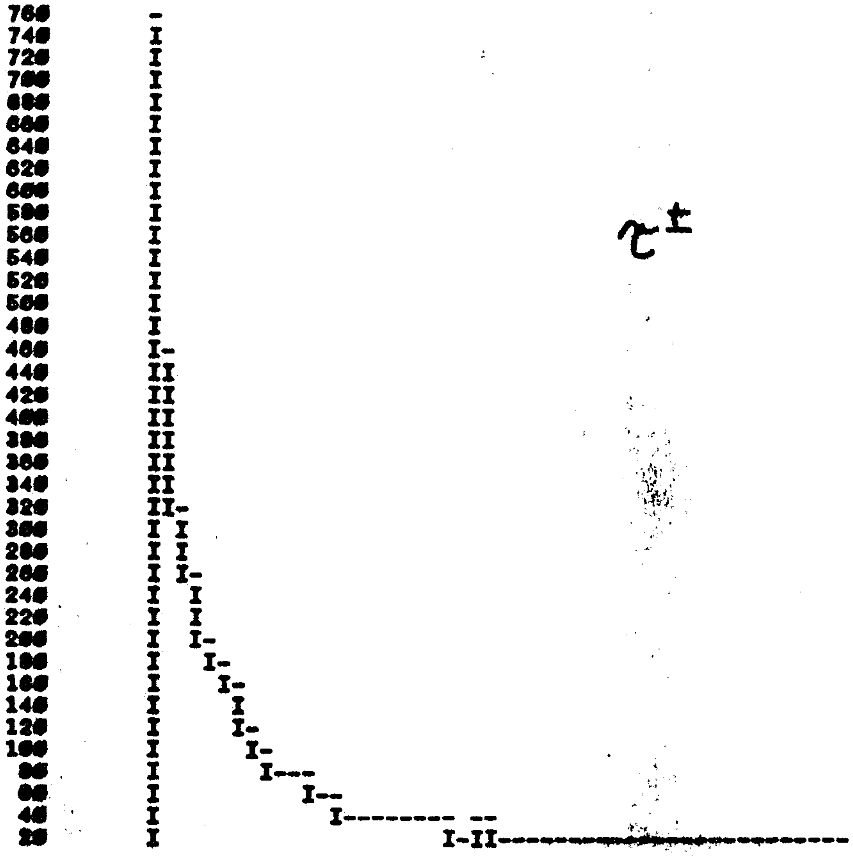


```
CHANNELS  10   0         1         2         3         4         5
           1   12345678901234567890123456789012[illegible]1234567890

CONTENTS 100   74321111
          10   44669751976655333333321221111111
          1.   351675844493541474411523369842[illegible]78402524

LOW-EDGE 100        11111222223333344444555[illegible]99999
          10    24680246802468024680246802[illegible]2468
          1.    000000000000000000000000000[illegible]0000

* ENTRIES =       3405     * ALL CHANNELS = 0.2[illegible]     * UNDERFLOW = 0.0000E+00     * OVERFLOW = 0.6200E+02
* BIN WID = 0.2000E+02     * MEAN VALUE   = 0.14[illegible]    * R . M . S = 0.1852E+03     * ABNOR CHA= 0.0000E+00
```

Minimum Impact Distance

	LEBC	15 Foot BC
D(bub)	20 microns	100 microns
Scan	50	250
Meas	7	35

./ ADD NAME=PICT0004

DISPLAY FILE FOR THE TEKTRONIX 4010

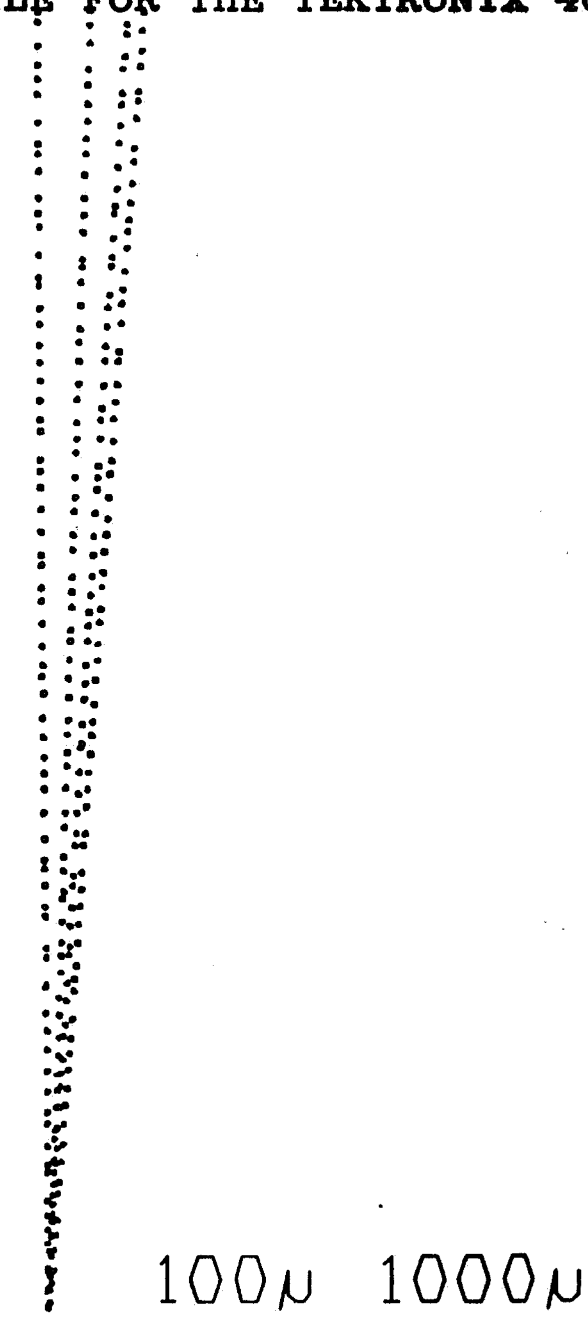

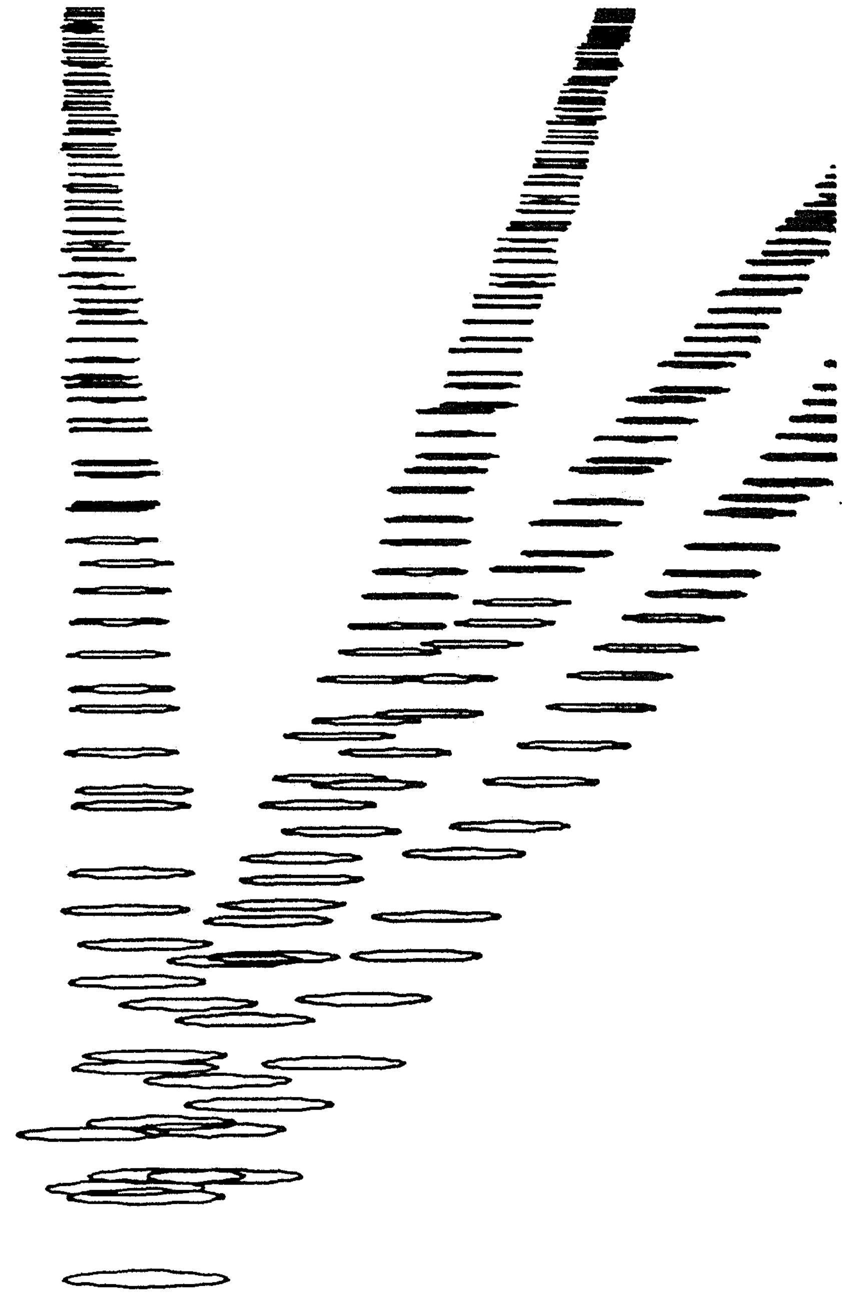

./ ADD NAME=PICT0002

DISPLAY FILE FOR THE TEKTRONIX 4010

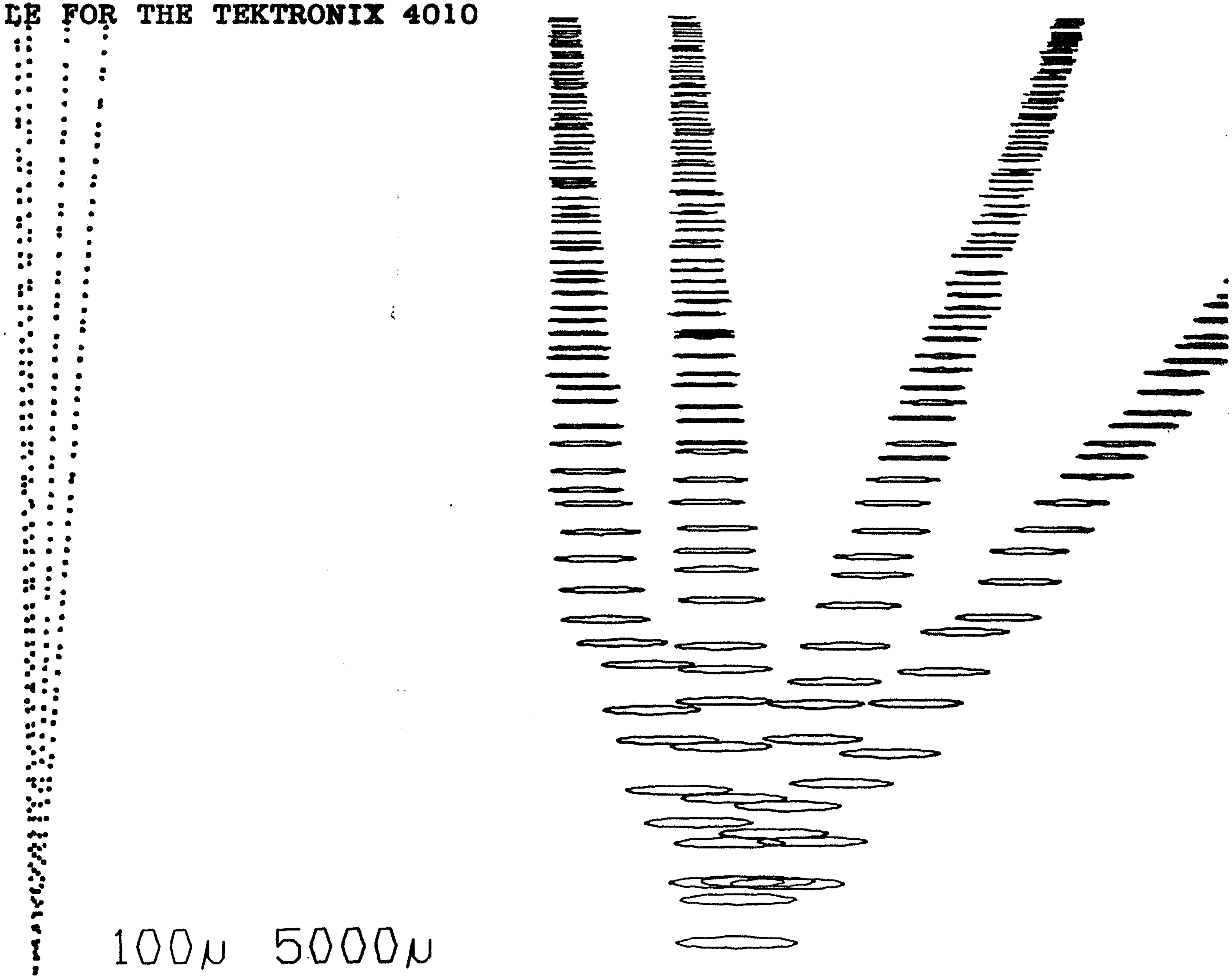

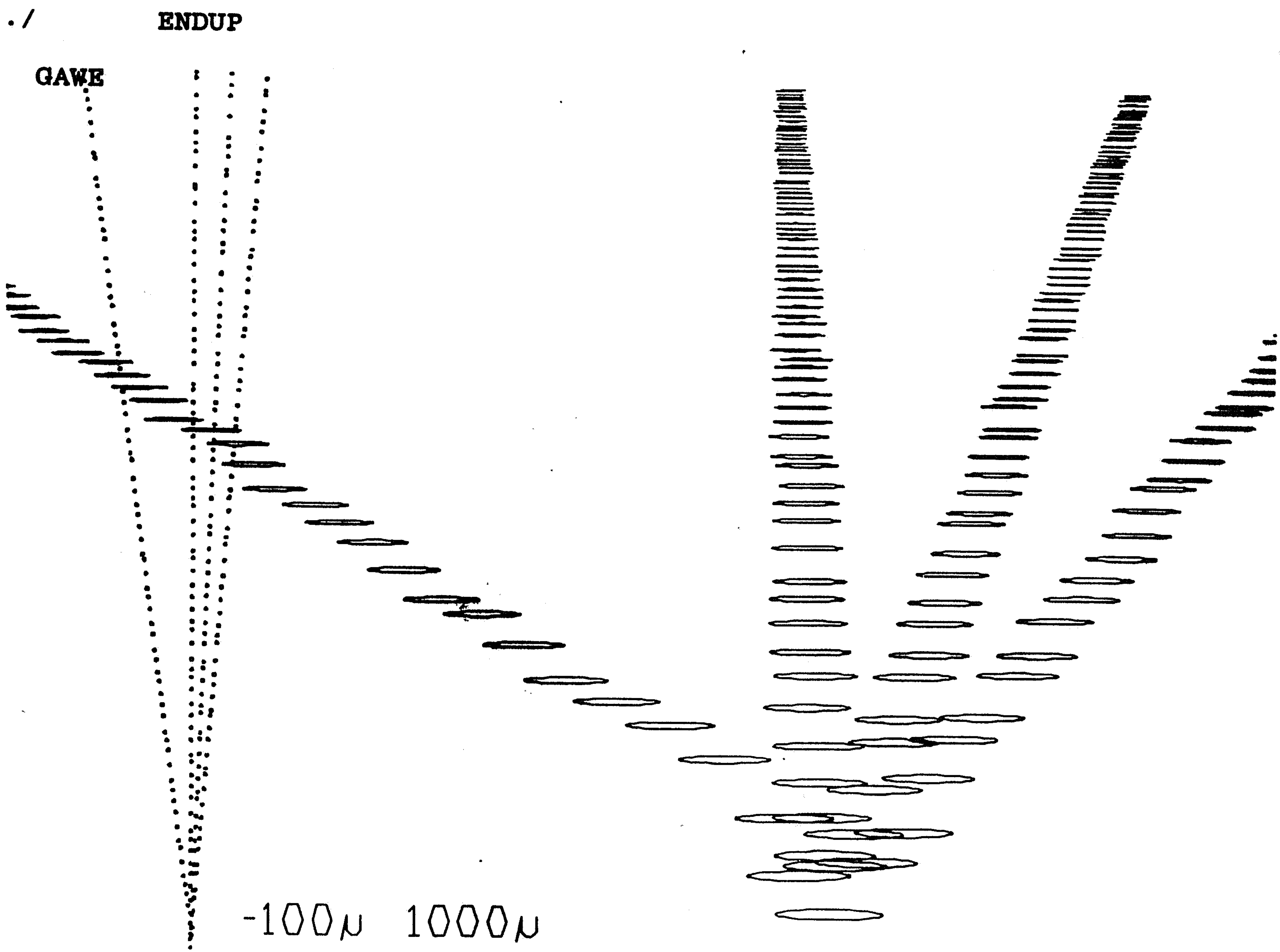

./
ENDUP
GAWE
-100μ 1000μ

./ ADD NAME=PICT0003

DISPLAY FILE FOR THE TEKTRONIX 4010

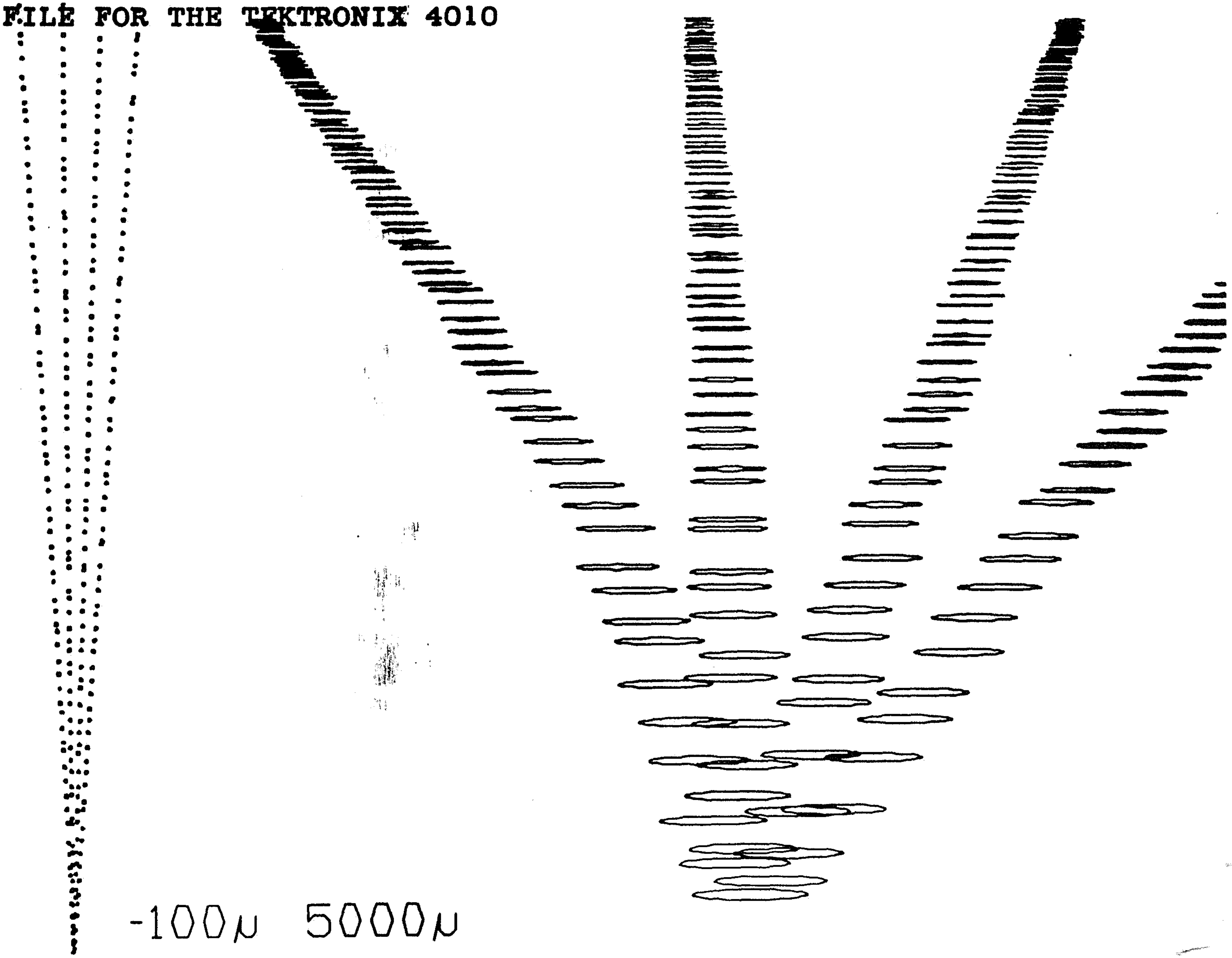

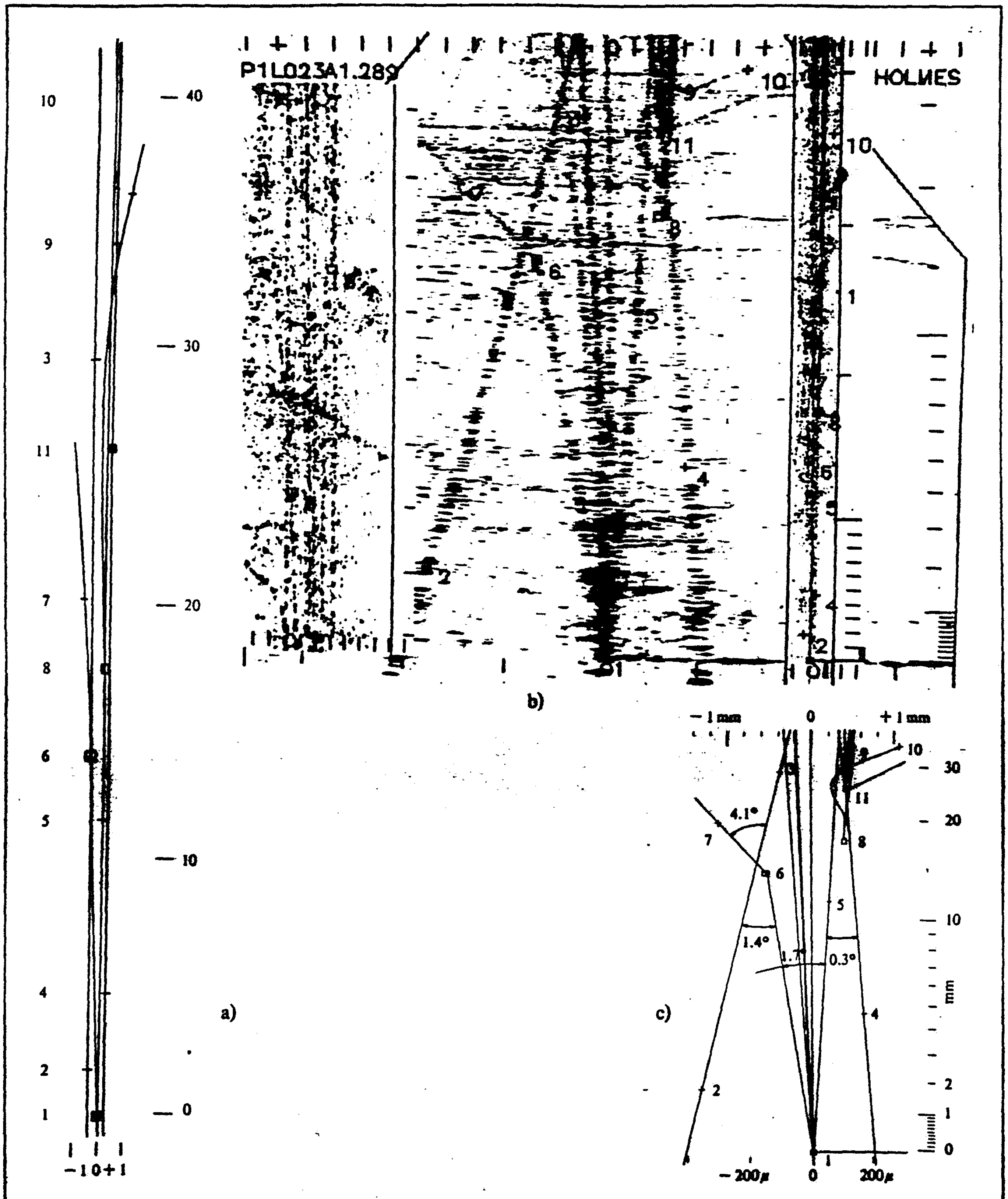
P1L023A1.289
HOLMES
a)
b)
c)
−1 mm
0
+1 mm
4.1°
1.4°
0.3°
−200μ
200μ
mm
−1 0 +1

E646 Tau Detection Efficiency

Tau->l neu ->h neu	100 microns	50 microns
D impact	.29	.45
p tau>10 Gev/c	.95	.95
L tau<2 cm	.96	.96
mu/e det	.95	.95
Combined	.25 *.83=.21	.39 *.83=.32
Tau->3h neu ...		
Visible	.80	.90
P tau>10 Gev/c	.95	.95
L tau<2 cm	.96	.96
Combined	.73 *.17=.12	.82 *.17=.14
Sum	.33	.46

Backgrounds to τ Detection

Decay Mode	Background Event type		Probability
τ->l ν ν	NC	D->l	Prod(NC,D)×BR(D->l)×[1-exp(-l/$\eta c\tau$)]
(35%)	(CC)	D->l	Prod(CC,D)×(1-ϵ)×BR(D->l)×[1-exp(-l/$\eta c\tau$)]
τ->h ν ...	NC	h->h	Mult×[1-exp(-l/L)]×F(1)
(48%)		D->h	Prod(NC,D)×BR(D->h)×[1-exp(-l/$\eta c\tau$)]
	(CC)	h->h	Mult×(1-ϵ)×[1-exp(-l/L)]×F(1)
		D->h	Prod(CC,D)×(1-ϵ)×BR(D->h)×[1-exp(-l/$\eta c\tau$)]
τ->3h ν ...	NC	h->3h	Mult×[1-exp(-l/L)]×F(3)
(17%)		D->3h	Prod(NC,D)×BR(D->3h)×[1-exp(-l/$\eta c\tau$)]
	(CC)	h->3h	Mult×(1-ϵ)×[1-exp(-l/L)]×F(3)
		D->3h	Prod(CC,D)×(1-ϵ)×BR(D->3h)×[1-exp(-l/$\eta c\tau$)]

ϵ=avg eff for electron and muon det	.95
l=length cut	2 cm
L=interaction length	125 cm
$c\tau$=charged D decay len	.028 cm
η=typ charged D p/m	10.7
F(1)=fraction of ints yielding a clean 1 prong	.094
F(3) 3	.047
Prod(CC,D)=fractional chg'd D prod in CC events	.05
Prod(NC,D) NC	.0005
BR(D->l)	.19
BR(D->h)	.63
BR(D->3h)	.15
Mult (chg'd, forward 25 deg, >2 GeV/c)	2.4

E546 Tau Backgrounds

				100 microns			50 microns		
			Events	Eff	Seen		Eff	Seen	
Tau->l neu neu	NC	D->l	.12	.29	.03		.45	.05	
	(CC)	D->l	2.05	.29	.59		.45	.92	
						.63			.97
Tau->h neu	NC	h->h	4.58	1.0	4.58		1.0	4.58	
		D->h	.40	.29	.12		.45	.18	
	(CC)	h->h	.78	1.0	.78		1.0	.78	
		D->h	6.82	.29	1.98		.45	3.07	
						7.46			8.61
Tau->3h neu	NC	h->3h	2.29	1.0	2.29		1.0	2.29	
		D->3h	.09	.80	.07		.90	.08	
	(CC)	h->3h	.39	1.0	.39		1.0	.39	
		D->3h	1.62	.80	1.30		.90	1.46	
						4.05			4.22

Tau Minus Backgrounds

Tau->l neu neu	NC	D->l	.04	.29	.01		.45	.02	
	(CC)	D->l	.68	.29	.20		.45	.31	
						.21			.33
Tau->h neu	NC	h->h	2.29	1.0	2.29		1.0	2.29	
		D->h	.13	.29	.04		.45	.06	
	(CC)	h->h	.39	1.0	.39		1.0	.39	
		D->h	2.27	.29	.66		.45	1.02	
						3.38			3.76
Tau->3h neu	NC	h->3h	1.14	1.0	1.14		1.0	1.14	
		D->3h	.03	.80	.02		.90	.03	
	(CC)	h->3h	.20	1.0	.20		1.0	.20	
		D->3h	.54	.80	.43		.90	.49	
						1.79			1.86

Summary of E646 Tau Detection and Backgrounds

Produced taus	52	208	52	208
D impact (microns)	100	100	50	50
Det eff	.33	.33	.46	.46
Det taus	17	69	24	96
Background	12	24	14	28
S+B	29	93	38	124
Error	5.4	9.6	6.2	11.1
Signif (std dev)	3.1	7.2	3.9	8.6
Error (no sig)	3.5	4.9	3.7	5.3
Upper lim (2 sig)	7.0	9.8	7.4	10.6
F/D lim	.041	.017	.031	.013

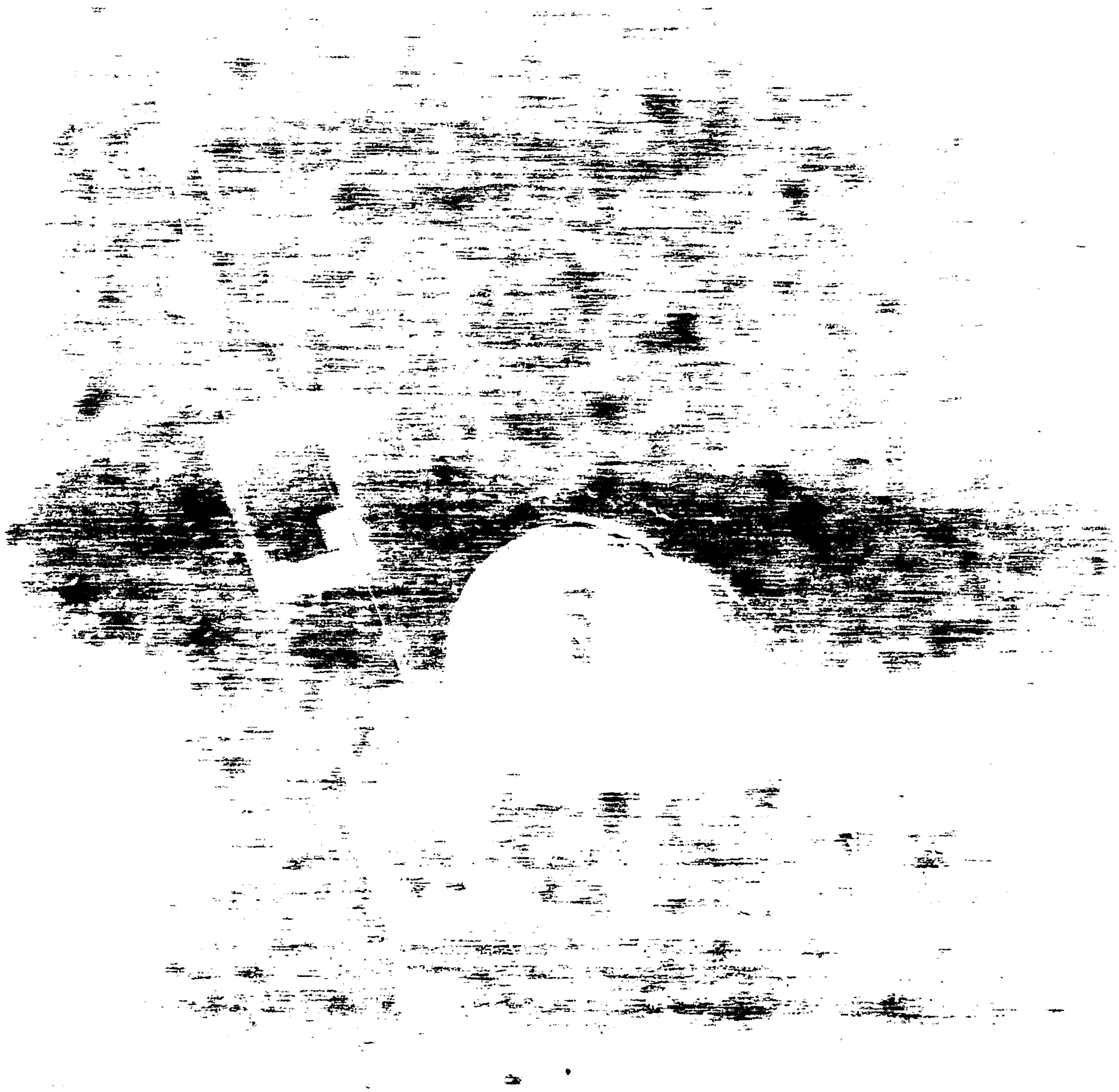

TABLE I
BACKGROUNDS FOR $\tau \to 3$-PRONG EVENTS
(10^{18} protons on target)

OUTGOING LEPTON MOMENTUM ABOVE 4 GeV/c	ν_μ	ν_e	$\bar{\nu}_\mu$	$\bar{\nu}_e$
CC (μ hits both EMI planes)	2.01	-	.73	-
CC (μ hits only inner plane)	.17	-	.07	-
CC (μ misses both planes)	.42	-	.15	-
CC (EMI dead time)	.22	-	.08	-
all CC	2.82	3.87	1.03	1.40
all NC	3.73	2.74	.31	.22
OUTGOING LEPTON MOMENTUM BELOW 4 GeV/c				
CC	1.60	.21	.22	.03
NC	.52	.39	.06	.05
TOTAL CC	4.42	4.08	1.25	1.43
TOTAL NC	4.25	3.13	.37	.27
TOTAL BACKGROUND	8.67	7.21	1.62	1.70

TABLE II
EXPECTED RATES AND UPPER LIMITS

	10^{18} protons	2×10^{18} protons
DETECTED EVENTS	26	51
BACKGROUND	19.2 ± 1.9	38.4 ± 3.8
SIGNAL	6.8 ± 5.4	11.6 ± 8.1
$\sigma(F)/\sigma(D)$	.11 ± .08	.09 ± .06
DETECTED EVENTS (assuming no signal)	19	38
BACKGROUND	19.2 ± 1.9	38.4 ± 3.8
90% C.L. UPPER LIMITS		
SIGNAL	5.3	7.4
$\sigma(F)/\sigma(D)$	.083	.058

Why Run the 15 Foot Bubble Chamber?

1. Why throw away almost 50% of the events?
2. Lower density so less confusion compared with Tohoku Chamber.
3. Greater path length in chamber so better measurements, esp. electrons.
4. Higher identification efficiency for both muons and electrons than Tohoku chamber.
5. Different distance from the dump so answer questions about oscillations, decays, etc.
6. Larger solid angle and more tons for "conventional" events not involving short decays.

Other Physics

'Exotic' particle searchs (Axions, Sparticles, Heavy Leptons, etc.) covered in detail in Apr 86 Beam Dump Workshop

Exciting - but high risk

Consider here instead 'bread + butter' physics sensitivity compared to previous ν beam dump experiments.

PROMPT NEUTRINO EXPERIMENTS

CERN 1977-79 L~900m

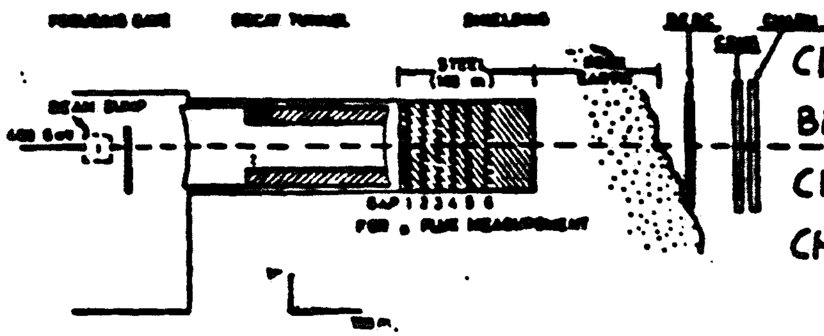

CDHS '77
BEBC '79
CDHS '79
CHARM '79

CERN 1982 L~450m

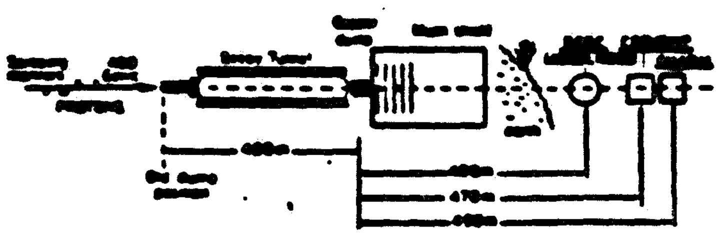

BEBC '82
CDHS '82
CHARM '82

FERMILAB 1981-82 L~60m E613

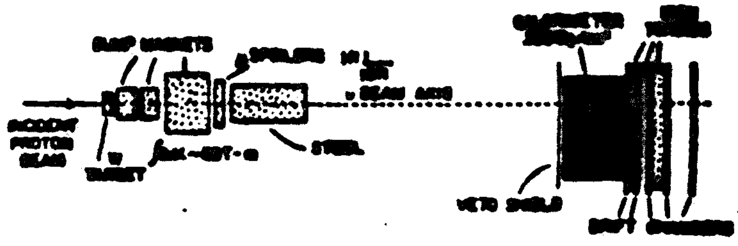

ν_e/ν_μ Flux Ratio for Prompt Neutrino Production

E 613

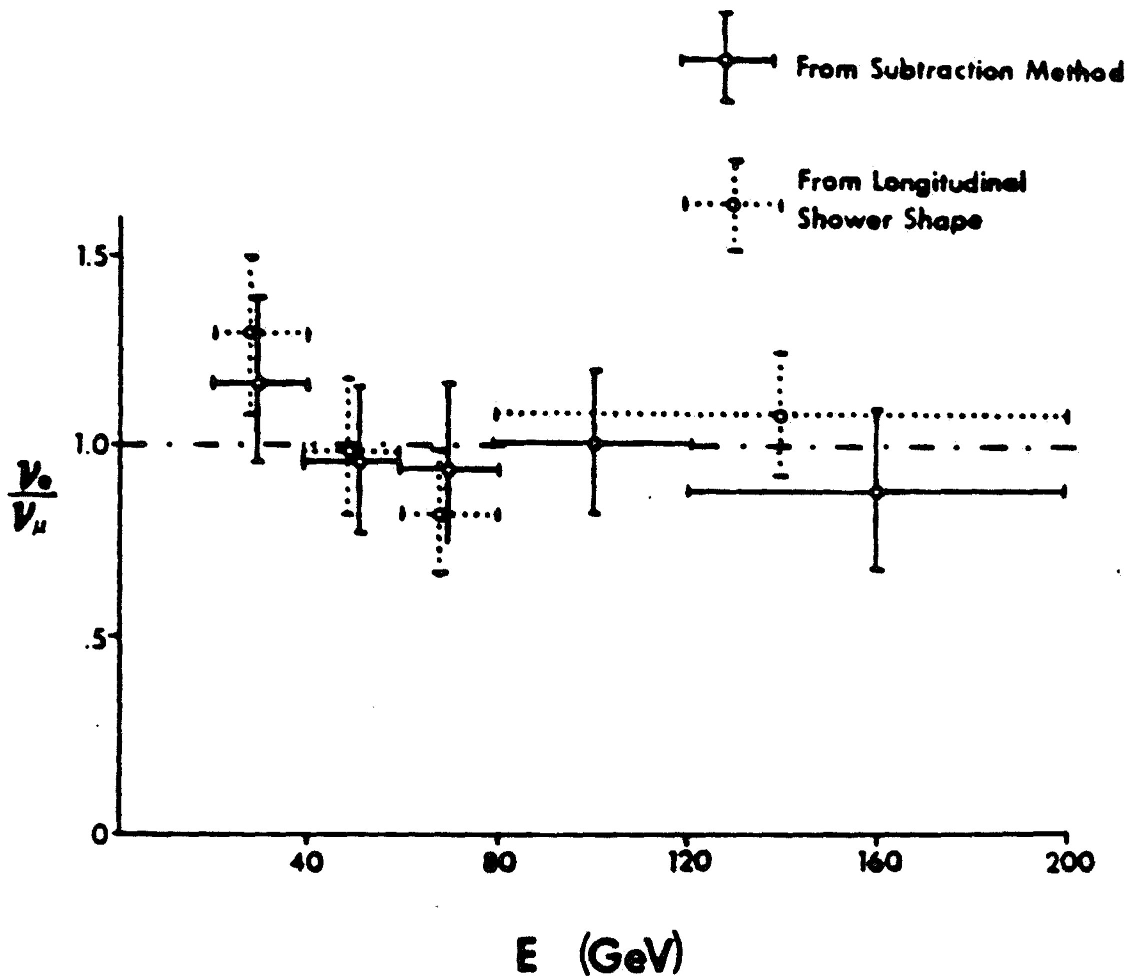

When all data from the CERN and FNAL ν beam dumps are compared major questions remain unresolved for prompt ν_e vs. ν_μ

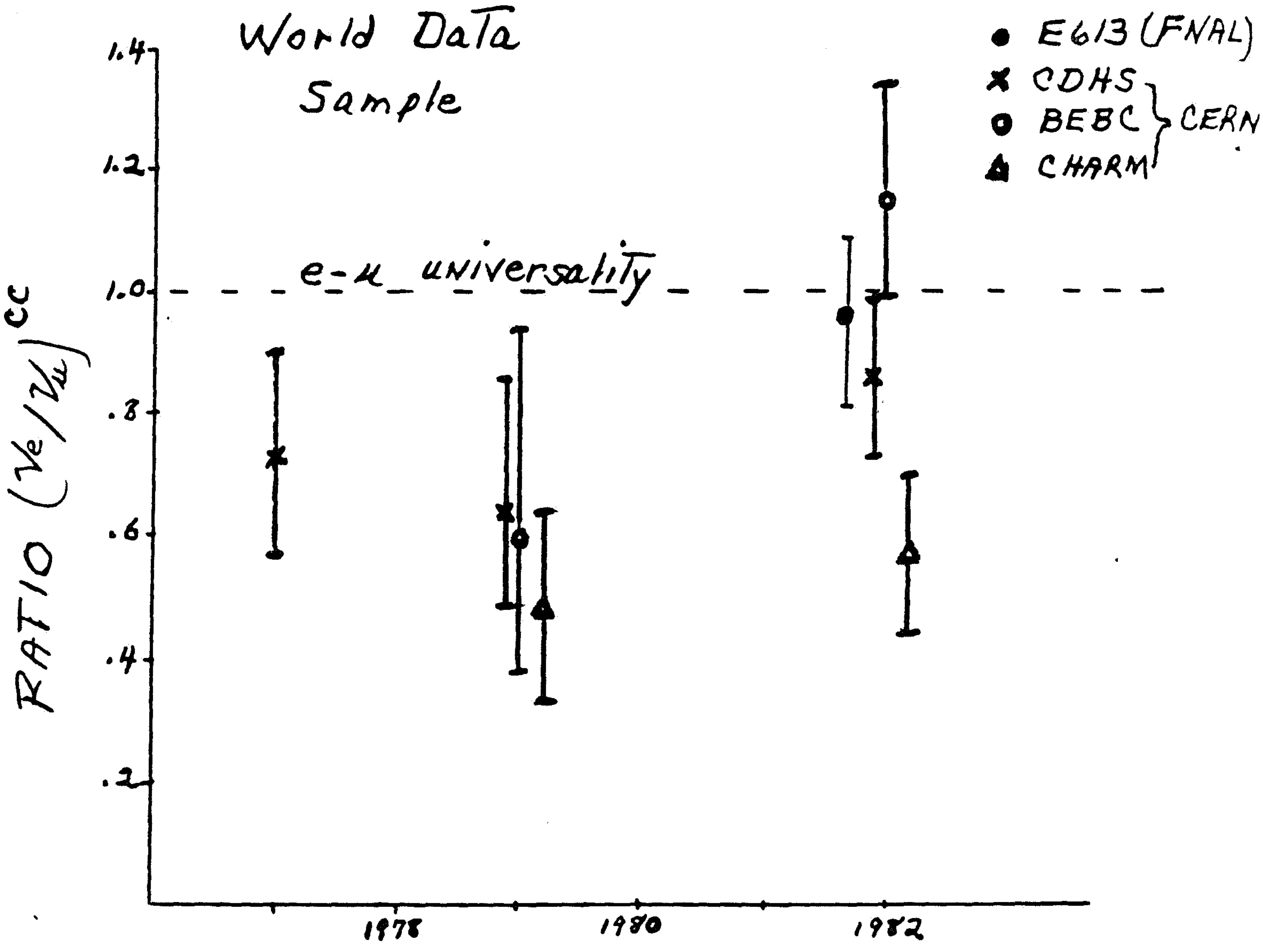

E613 A Dependence
Prompt ν_e

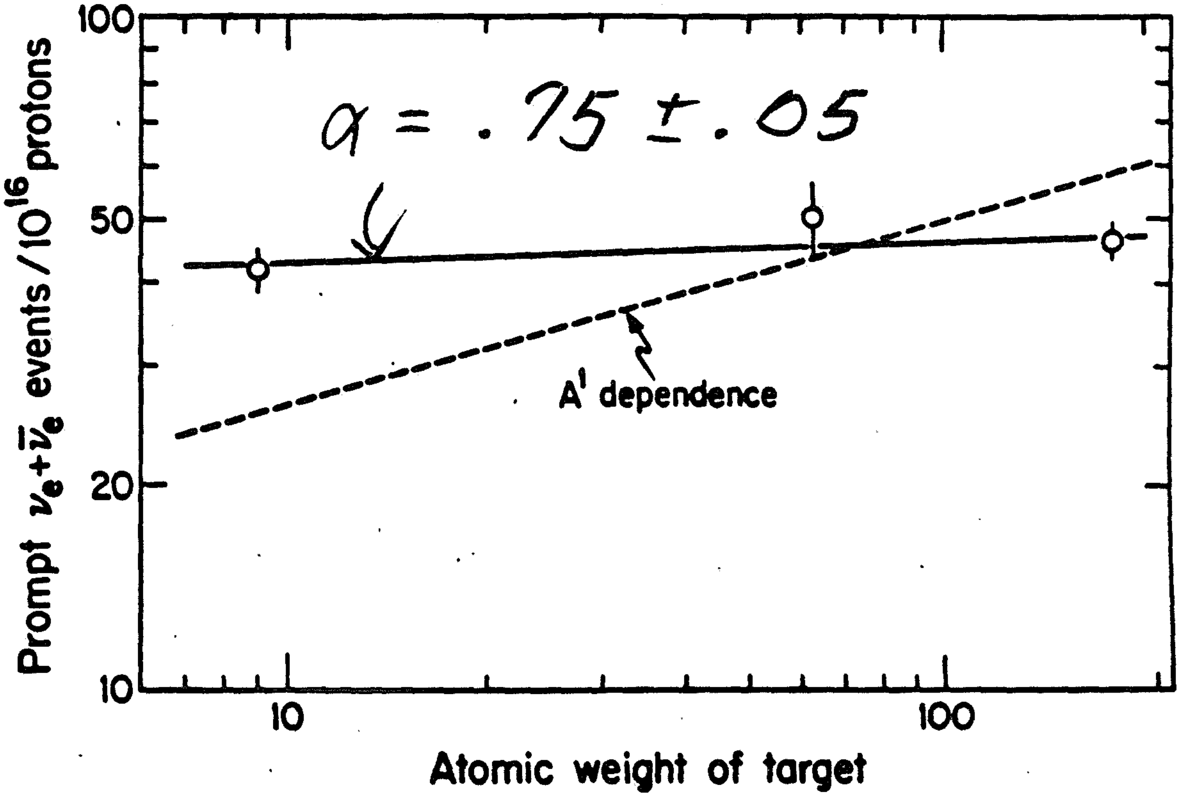

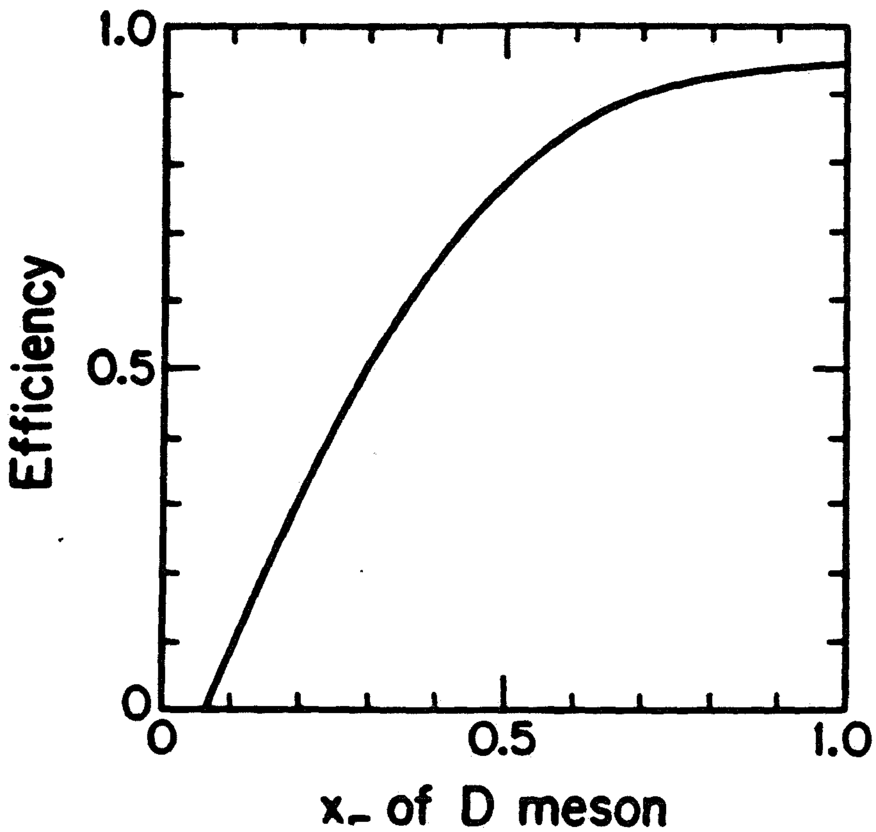

Figure 3

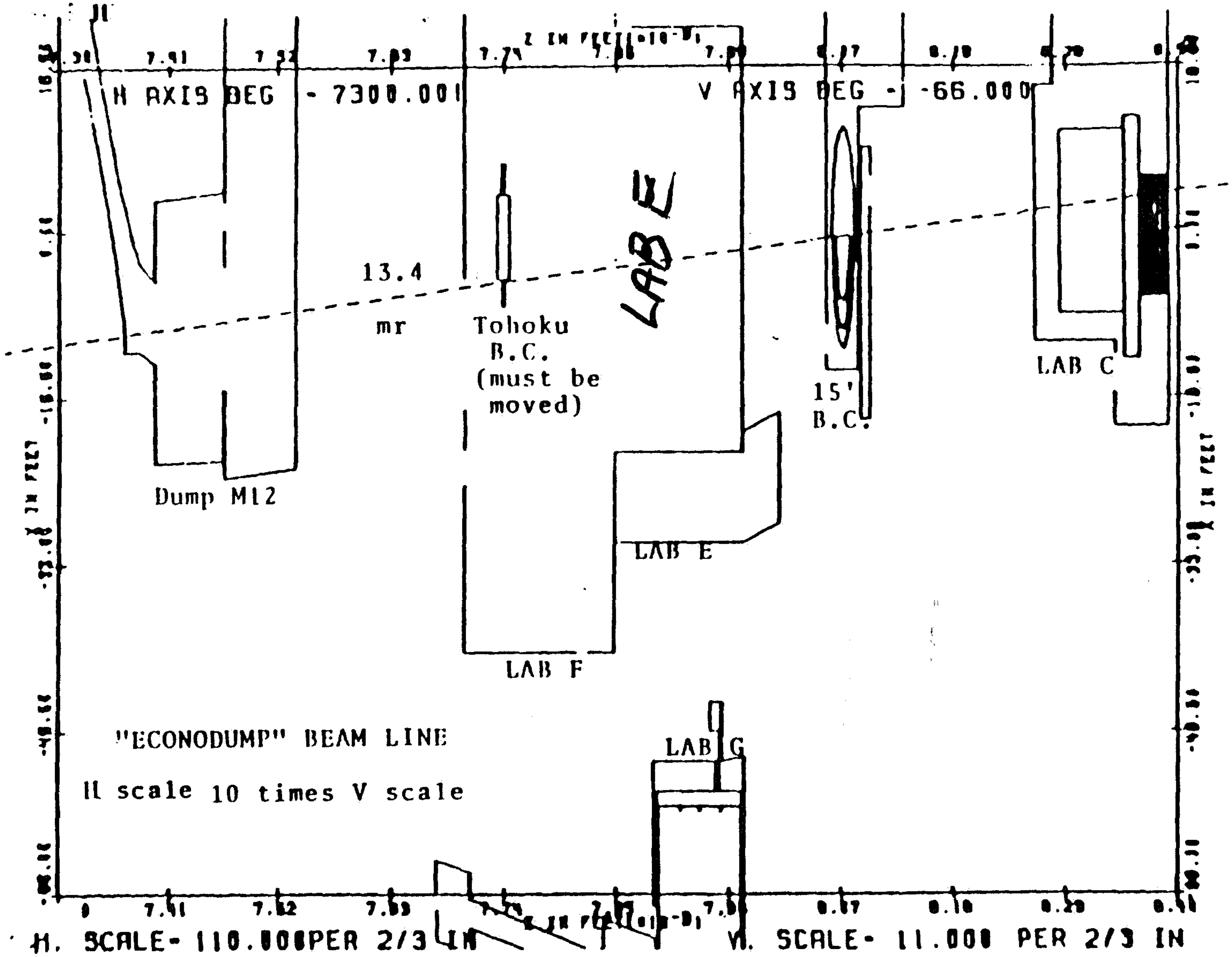
H AXIS DEG - 7300.001
V AXIS DEG - -66.000
13.4
mr
Tohoku
B.C.
(must be
moved)
LAB E
15'
B.C.
LAB C
Dump M12
LAB E
LAB F
"ECONODUMP" BEAM LINE
H scale 10 times V scale
LAB G
H. SCALE- 110.000PER 2/3 IN
V. SCALE- 11.000 PER 2/3 IN

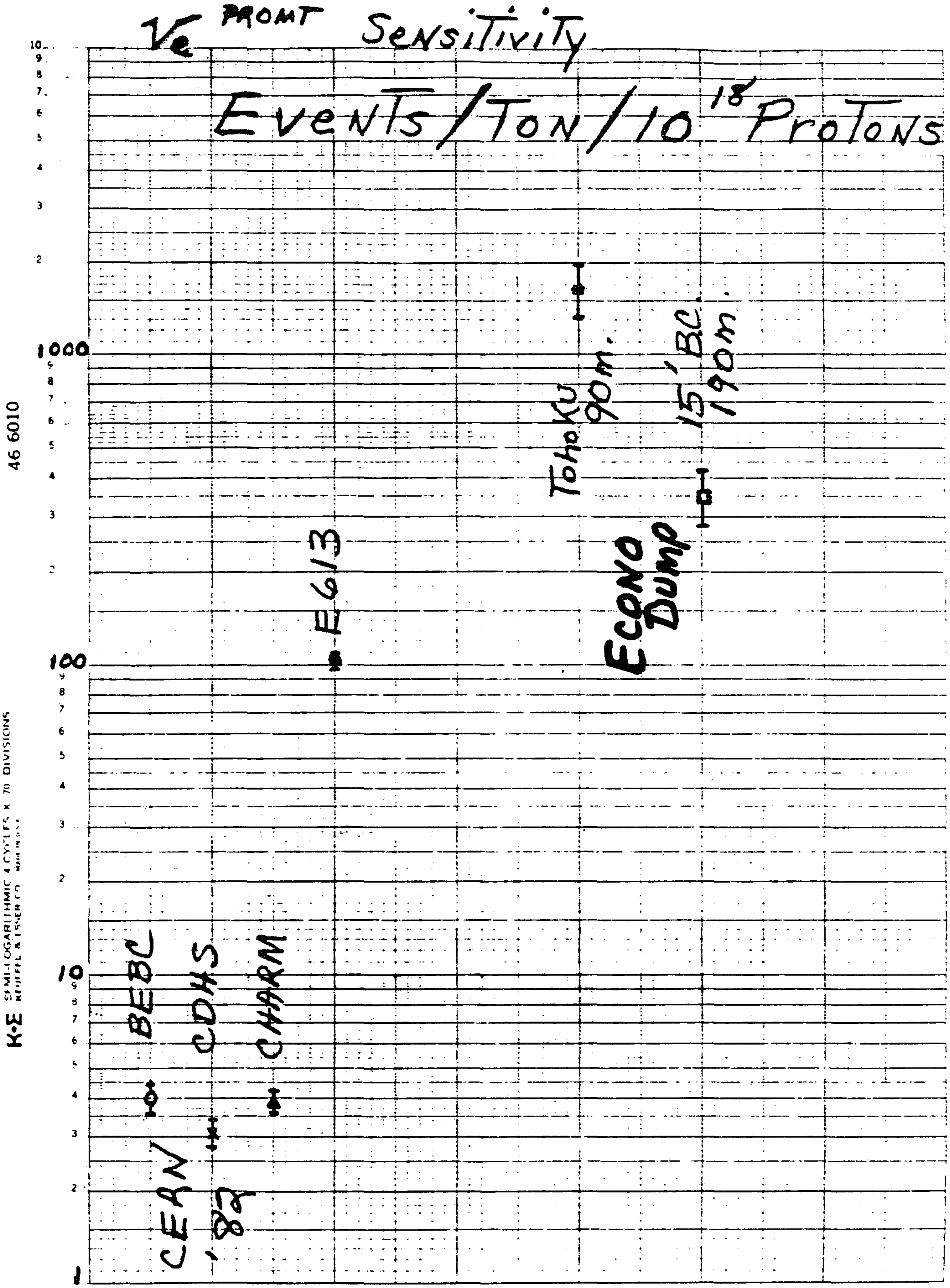
ν_e PROMT SENSITIVITY
Events/Ton/10^{18} Protons
1000
100
10
1
BEBC
CDHS
CHARM
CERN '82
E613
Tohoku 90m.
15' BC. 190m.
ECONO DUMP

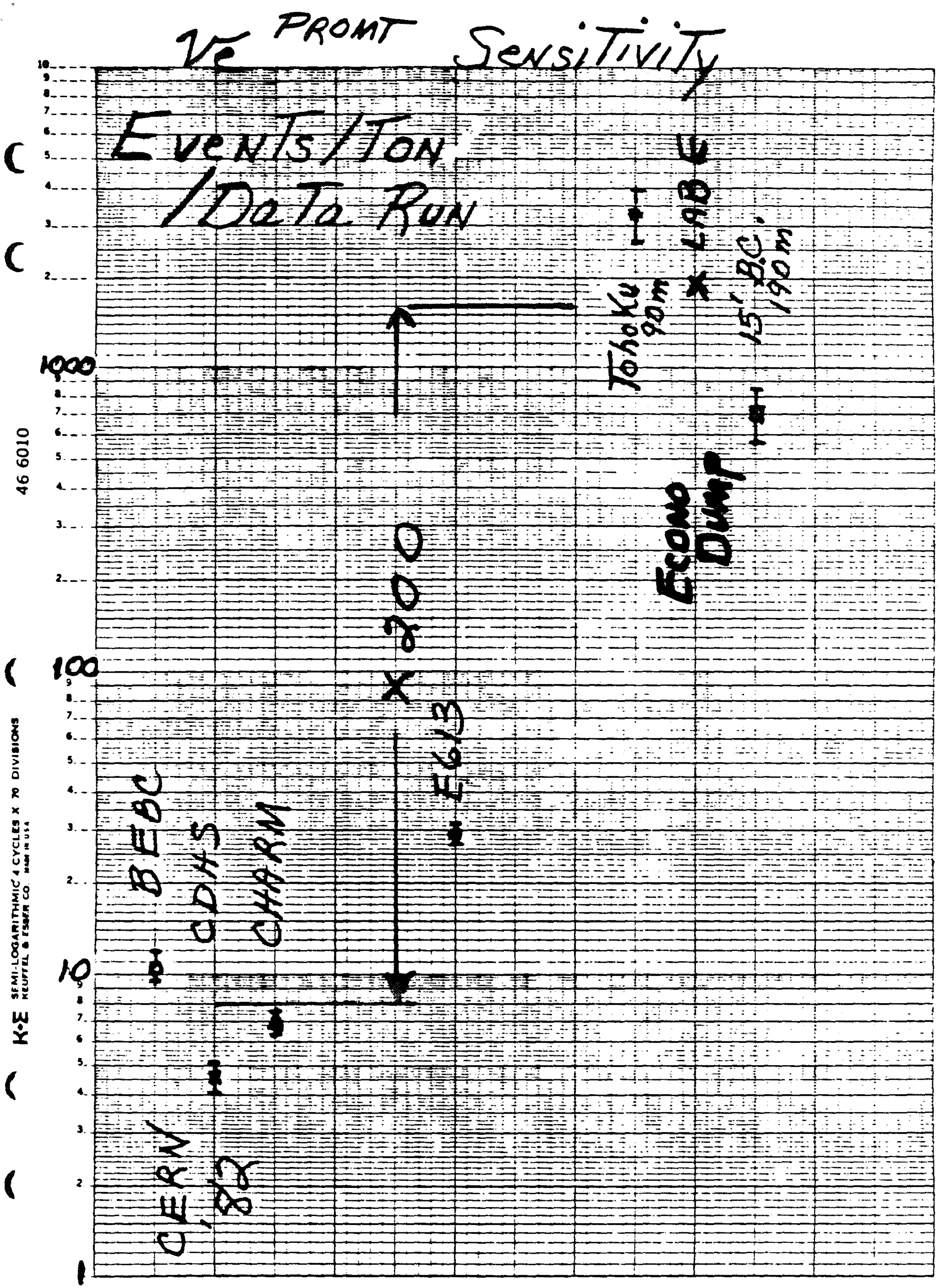
νe PROMT SENSITIVITY
EVENTS/TON /DATA RUN
1000
100
10
1
Tohoku 90m
LAB E
15' B.C. 190m
ECONO DUMP
X 200
E613
BEBC
CDHS
CHARM
CERN '82
46 6010
K+E SEMI-LOGARITHMIC 4 CYCLES X 70 DIVISIONS
KEUFFEL & ESSER CO. MADE IN U.S.A.

Conclusion -

Econodump Sensitivity

ν_e Physics

ν_e / ν_μ universality

A dependence - Charm

•
•
•

Two orders of magnitude greater than best existing ν beam dump results

COST ESTIMATE OVERVIEW

The cost totals associated with the civil construnction and with the technical components planned for the Econodump Facility are listed below:
(Bold print gives for comparison the D.N.L.F. cost totals.)

Description	TOTAL with 15% O & P	TOTAL with Escalation	TOTAL with E.D.I.A.	TOTAL with Contingency
CIVIL CONSTRUCTION				
Beam Pipe, Berm & Enc. NE8	$543,700 **$701,000**	$610,000 **$787,000**	$683,200 **$945,000**	$819,800 **$1,135,000**
Lepton Halls & Service Building NS-5	$1,506,800 **$3,094,000**	$1,692,100 **$3,609,000**	$1,895,100 **$4,330,000**	$2,274,100 **$5,195,000**
H-Piling & Earth Retention	---- **$267,000**	---- **$313,000**	---- **$375,000**	---- **$450,000**
Subtotal	$2,050,500 **$4,062,000**	$2,302,100 **$4,709,000**	$2,578,300 **$5,650,000**	$3,093,900 **$6,780,000**
TECHNICAL COMPONENTS				
Beam Transport System	$455,900 **$1,240,000**	$490,000 **$1,375,000**	$504,800 **$1,650,000**	$605,800 **$1,980,000**
Target System at Lepton Hall	$414,100 **$402,000**	$445,200 **$531,000**	$458,500 **$640,000**	$550,200 **$770,000**
Spoiler Magnets	$1,283,300 **$4,956,000**	$1,379,600 **$5,436,000**	$1,421,000 **$6,520,000**	$1,705,100 **$8,470,000**
Subtotal	$2,153,300 **$6,686,000**	$2,314,800 **$7,342,000**	$2,384,300 **$8,810,000**	$2,861,100 **$11,220,000**
TOTAL FACILITY	$4,203,800 **$10,748,000**	$4,616,900 **$12,051,000**	$4,962,600 **$14,460,000**	$5,955,000 **$18,000,000**

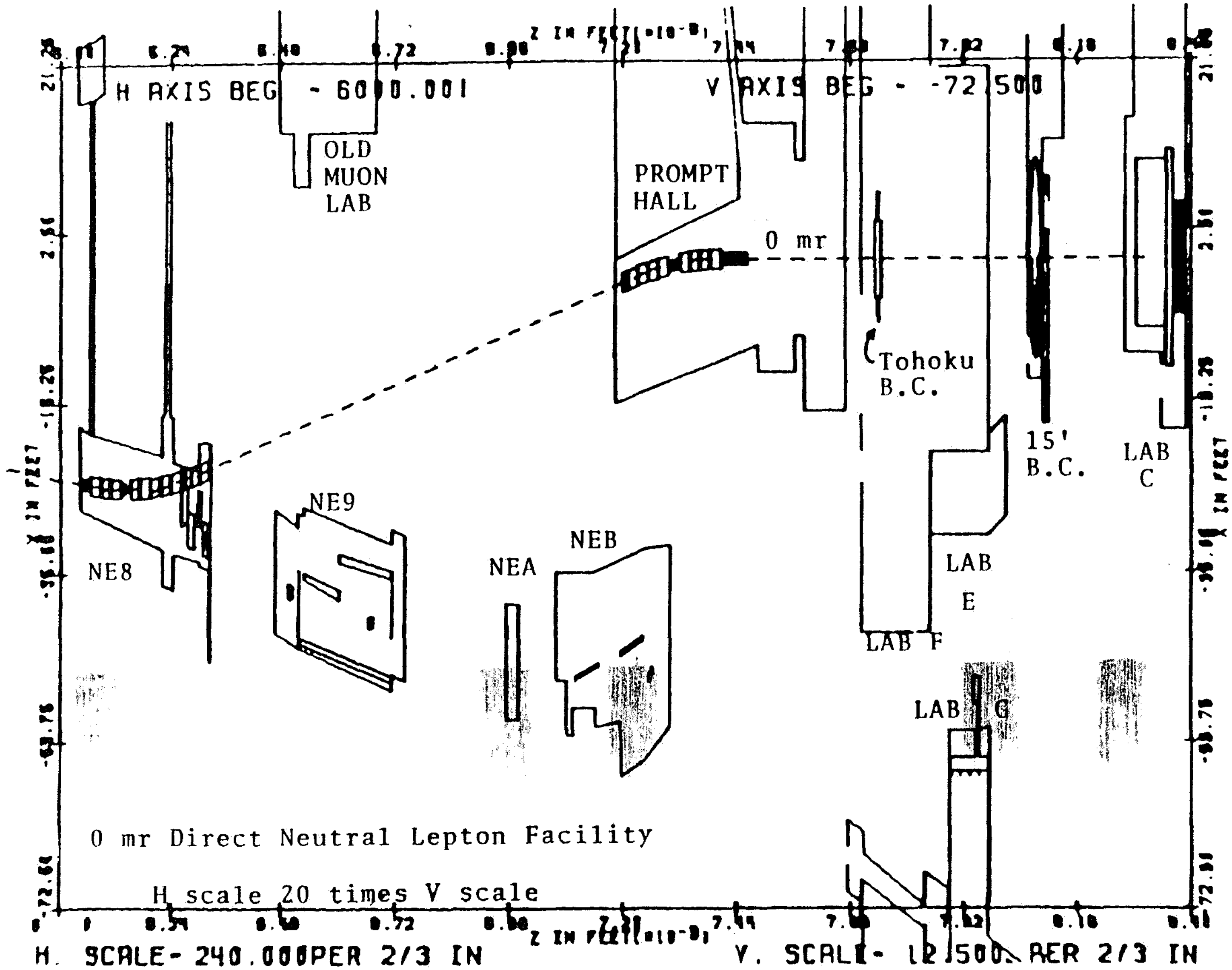
H AXIS BEG - 6000.001
V AXIS BEG - -72.500
OLD
MUON
LAB
PROMPT
HALL
0 mr
Tohoku
B.C.
15'
B.C.
LAB
C
LAB
E
LAB F
LAB G
NE8
NE9
NEA
NEB
0 mr Direct Neutral Lepton Facility
H scale 20 times V scale
H. SCALE- 240.000PER 2/3 IN
V. SCALE- 12.500 PER 2/3 IN

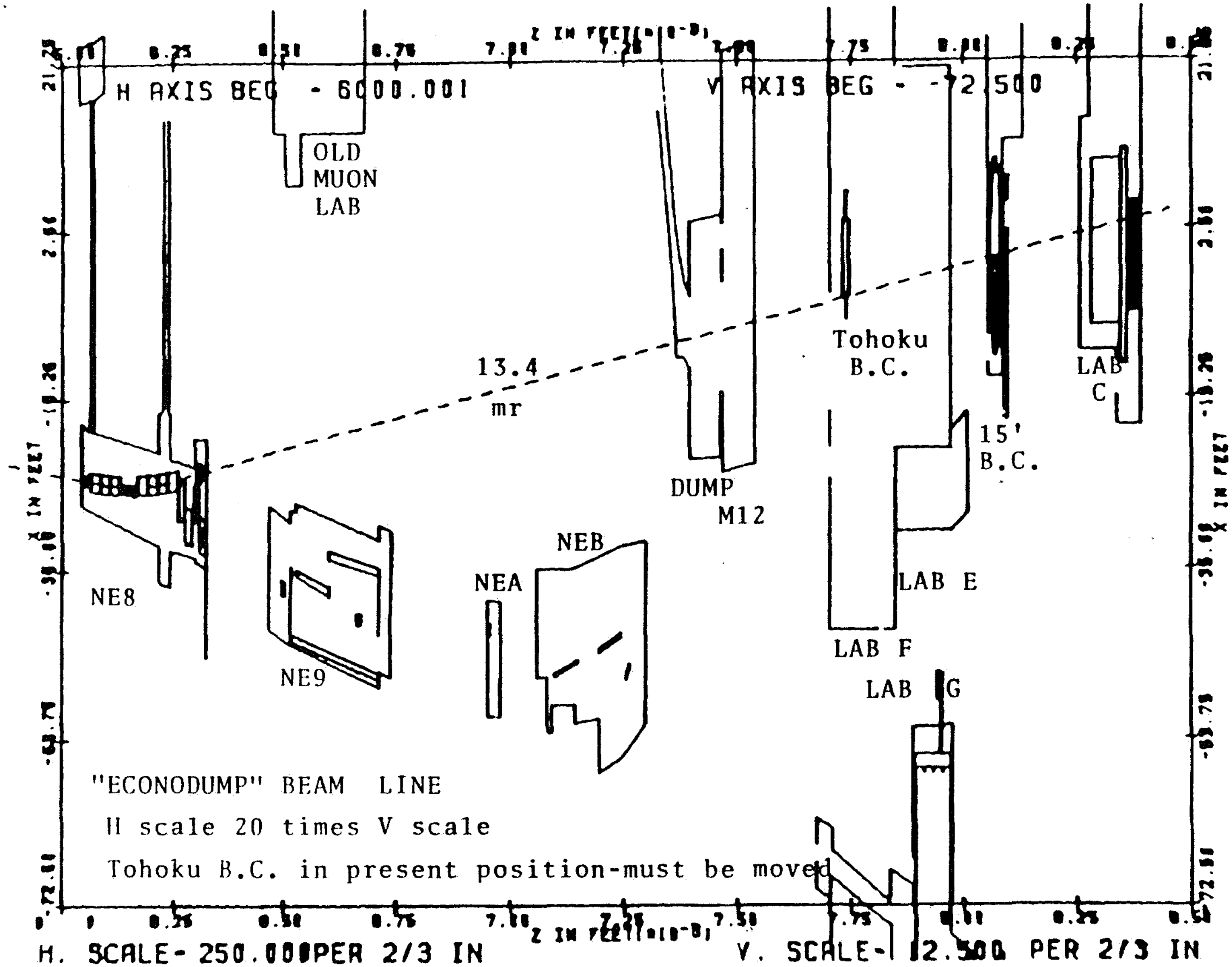

H AXIS BEG - 6000.001
V AXIS BEG - -72.500
OLD
MUON
LAB
Tohoku
B.C.
LAB
C
13.4
mr
15'
B.C.
DUMP
M12
NEB
NEA
NE8
NE9
LAB E
LAB F
LAB G
"ECONODUMP" BEAM LINE
H scale 20 times V scale
Tohoku B.C. in present position-must be moved
X IN FEET
Z IN FEET
H. SCALE- 250.000PER 2/3 IN
V. SCALE- 12.500 PER 2/3 IN

Figure 17

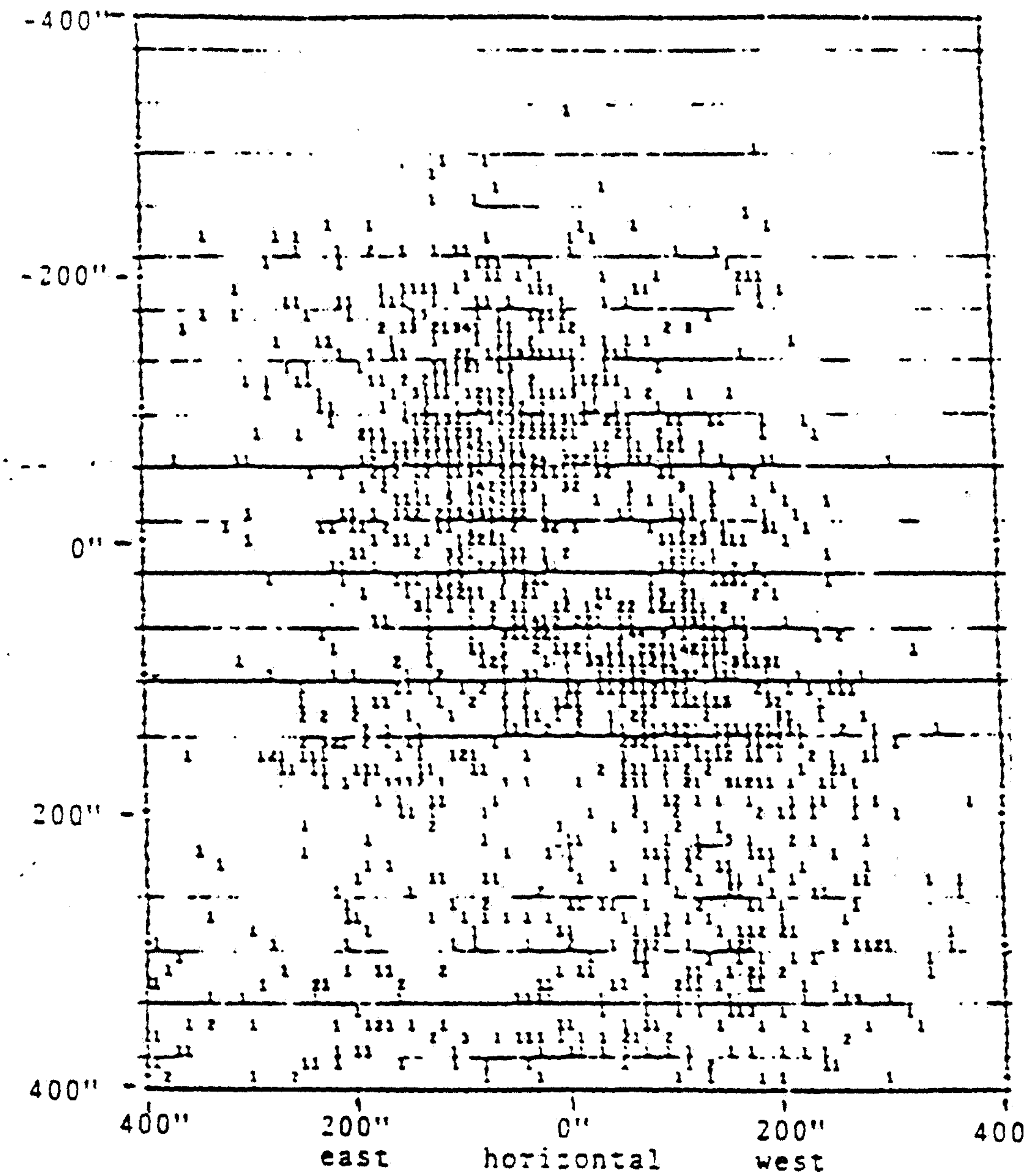

Positive muon sptial distribution in a plane transverse to the beam direction at the location of the tungsten target in Prompt Hall. The muons are procured by the interaction of 2.5 x 10^7 p's at the front of Encl. NE8. (Taken from Figure VI.2 of TM-1155 by C. Baltay et al.)

Figure 16

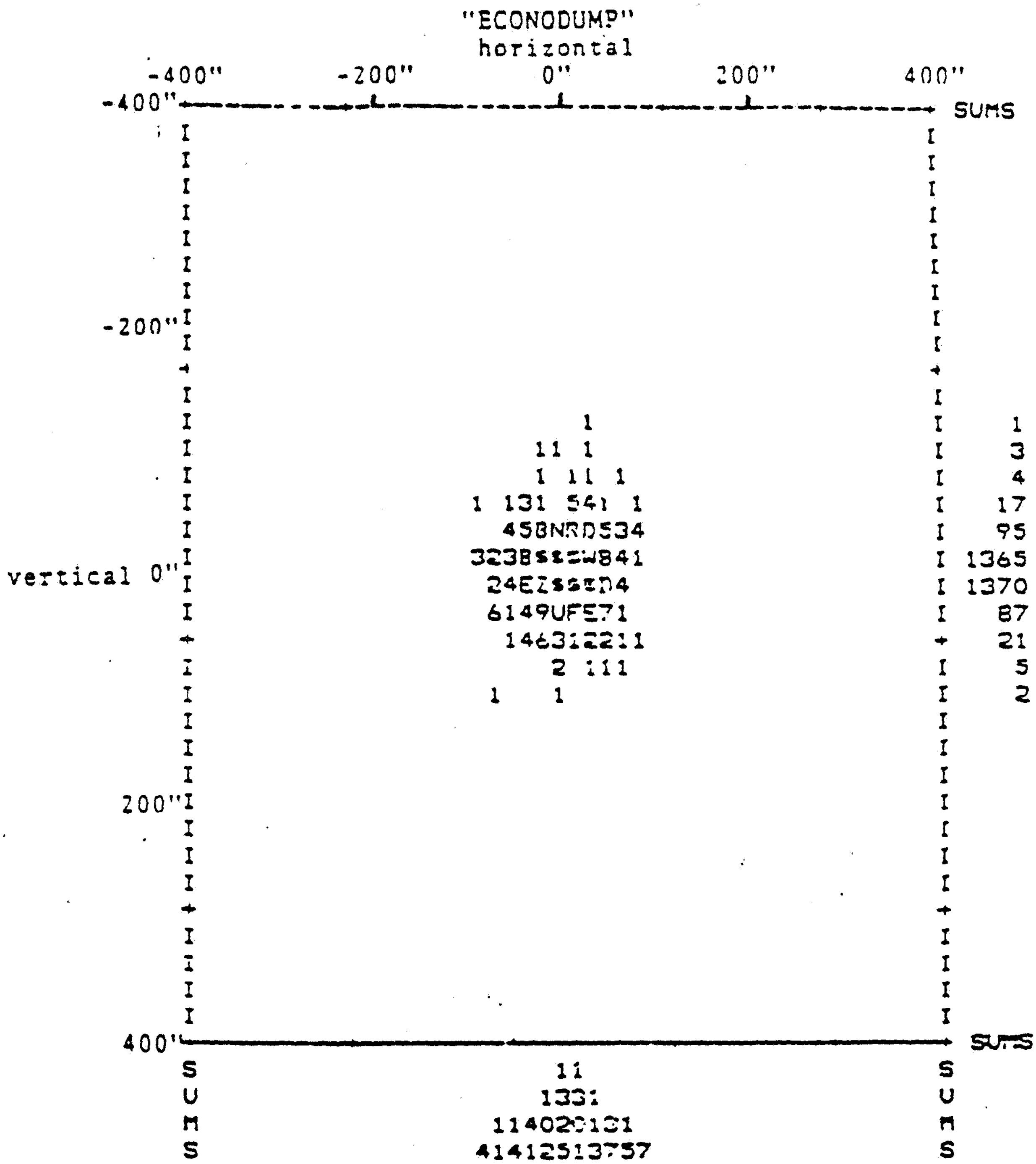

Absorber at 1136' from beam dump. 6" radius pipe buried in berm. 1 entry = 1.928 x 10^6 positive muons. 5 x 10^5 parents at 900 GeV forced to decay at the absorber.

Muon Backgrounds from Target Production

Two of the three computer programs (MIT and Fermilab) used in predicting muon background rates for DNLF have been used extensively in the Econodump design. The programs have been found to give comparable transmission rates for muons through different spoiler configurations, with differences in muon rates at the chambers predominantly due to differences in the two production models used.

The MIT program was the program used predominantly for final stages of the Econodump design.

All background muon sources considered in DNLF were modeled for Econodump. In addition, for muons scattered deep inelastically, subsequent π production and decay was also considered in the Econodump modeling. This process, which was not considered in DNLF, does produce a contribution to the muon flux at the chamber.

The following table gives calculated muon backgrounds from target associated sources:

Projected Muon Rates for the Tohoku Chamber

Based on MIT Production Model and Spoiler Program

	Target, beam dump associated sources;	7 GeV Passive Shield
	Bandpass with Coulomb Scat.	$47\mu/10^{13}$ppp
	Deep Inelastic Scat. (Muon)	9μ
**	Deep Inelastic Scat. ($\pi\to\mu$)	$\approx 20\mu$
	Pair Production (Tridents)	55μ
**	Pole Tip Scat. ($\pi\to\mu$)	$\approx 15\mu$
	TOTAL	$146\mu/10^{13}$protons

** These sources were not considered in DNLF. Results from these processes are preliminary, but are felt to be conservative.

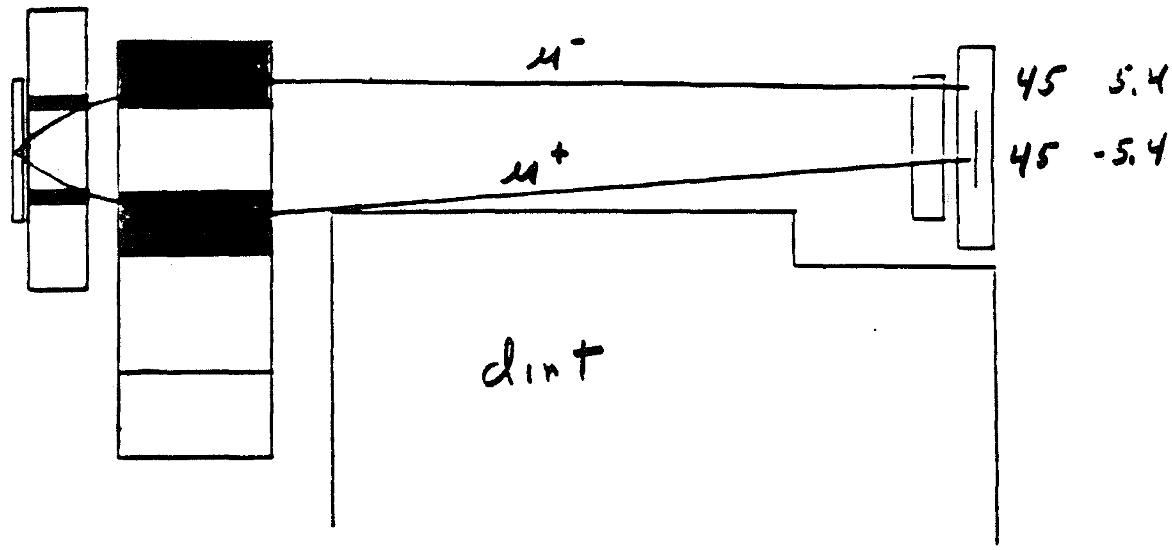
μ-
μ+
45 5.4
45 -5.4
dirt

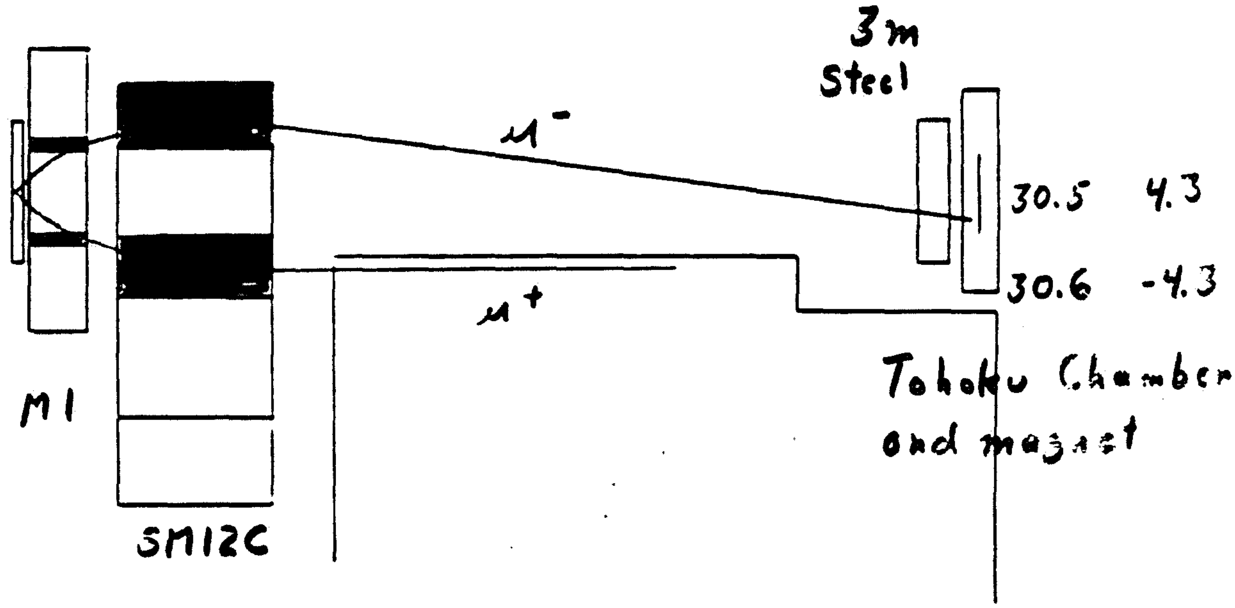
3m
Steel
μ-
μ+
30.5 4.3
30.6 -4.3
Tohoku Chamber
and magnet
M1
SM12C

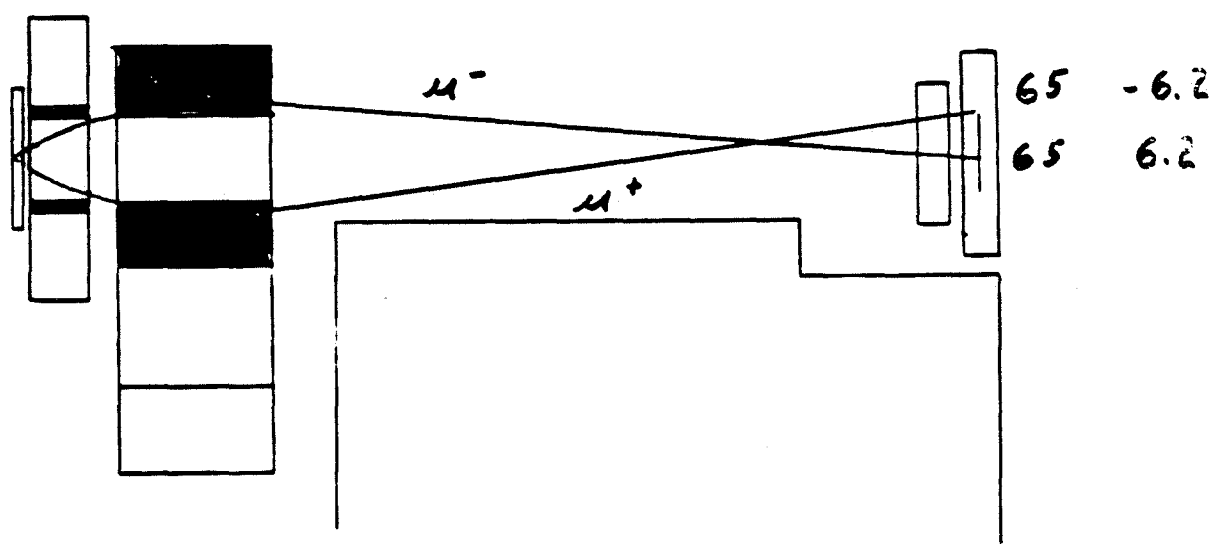
μ-
μ+
65 -6.2
65 6.2

Fig. 7

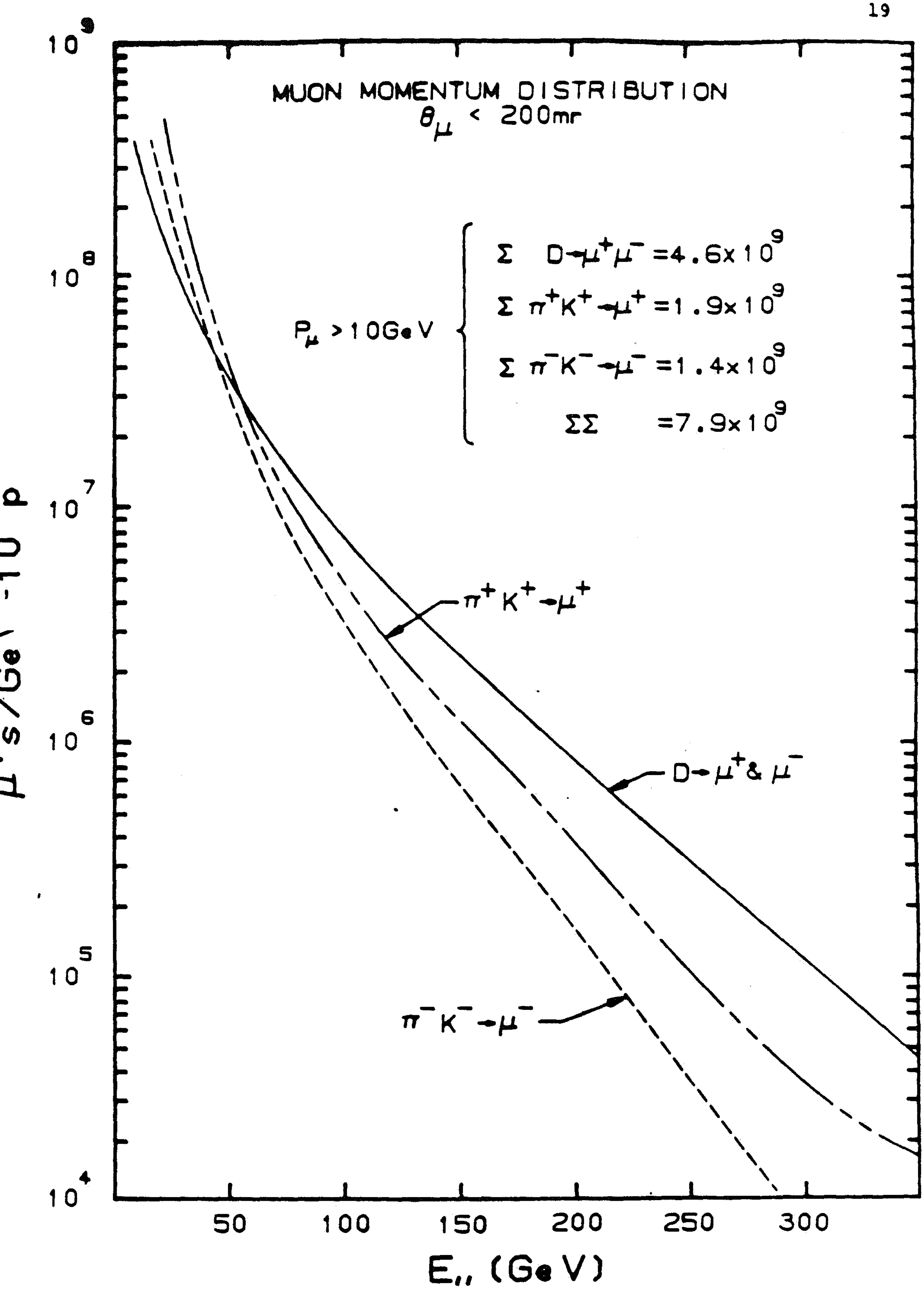

MUON MOMENTUM DISTRIBUTION
θ_μ < 200mr
P_μ > 10GeV
Σ $D \to \mu^+\mu^-$ = 4.6×10^9
Σ $\pi^+K^+ \to \mu^+$ = 1.9×10^9
Σ $\pi^-K^- \to \mu^-$ = 1.4×10^9
$\Sigma\Sigma$ = 7.9×10^9
$\pi^+K^+ \to \mu^+$
$D \to \mu^+ \& \mu^-$
$\pi^-K^- \to \mu^-$
10^9
10^8
10^7
10^6
10^5
10^4
50
100
150
200
250
300
E_{μ} (GeV)

Fig. 8

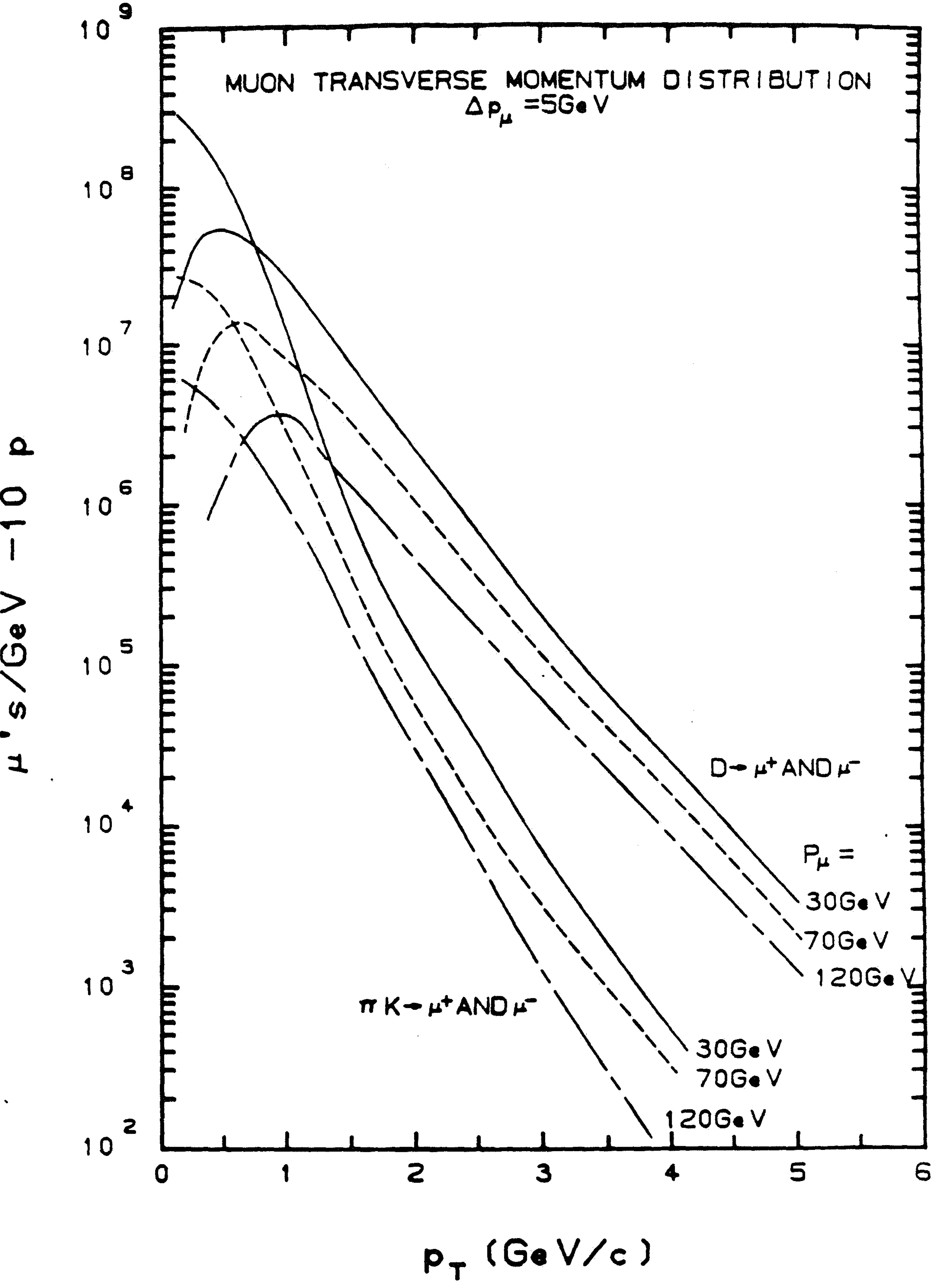
MUON TRANSVERSE MOMENTUM DISTRIBUTION
Δp_μ =5GeV
D→ μ⁺ AND μ⁻
P_μ =
30GeV
70GeV
120GeV
πK→ μ⁺ AND μ⁻
30GeV
70GeV
120GeV
μ's/GeV² - 10¹³ p
p_T (GeV/c)
10⁹
10⁸
10⁷
10⁶
10⁵
10⁴
10³
10²
0
1
2
3
4
5
6

Fig. 9

Direct ℓ/π ×10^-4

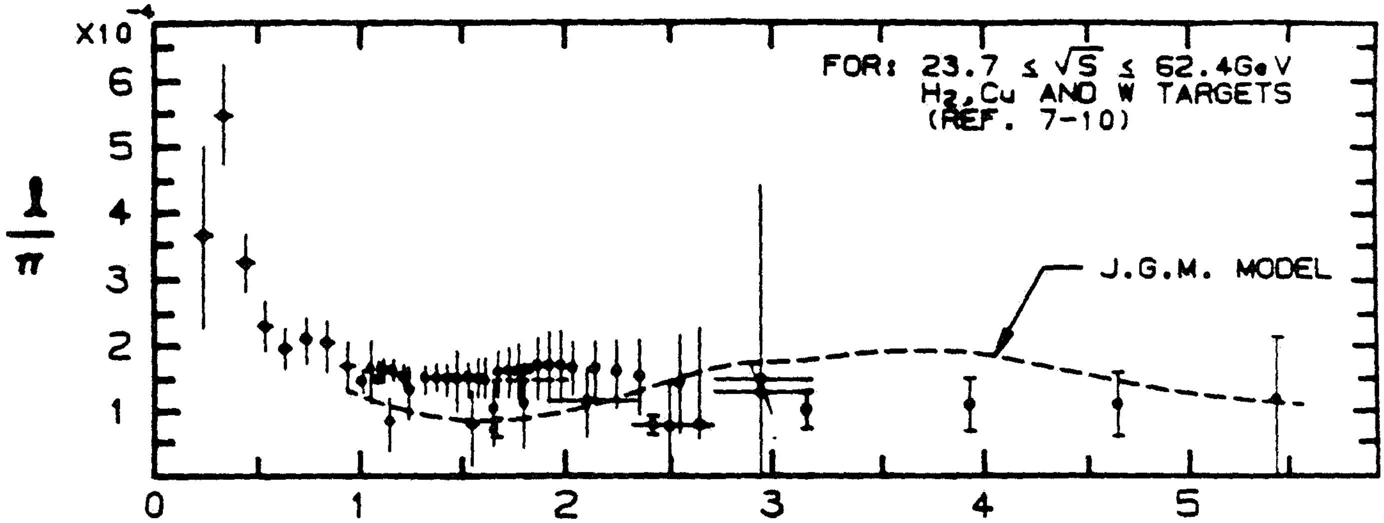

P_T (GeV/c)

the muon flux predictions of Morfin in FN-434.

In the critical kinematic regions for muon background sources the following flux ratios are obtained by comparison between the Morfin/MIT production models.

P_L (GeV)	P_T (GeV)	Morfin/MIT
35 - 40	4.8 - 5.3	3.0
55 - 60	5.3 - 5.8	2.15
75 - 85	0.0 - 2.0	0.67
145-155	0.0 - 2.0	0.33
215-255	0.0 - 2.0	0.31

⇒ $160\mu/10^{13}$

76% from high P_T

If the MIT model results for background muons at the Tohoku Chamber are normalized to the Morfin predictions, the projected background muon flux would become ~$160\mu/10^{13}$ protons with 76% of this background from the Coulomb bandpass.

There are still available several design options which should not increase the Econodump facility cost, which could selectively improve muon rejection in this bandpass region.

During the next Fermilab fixed target run there may be the possibility of measuring the high P_T muon rates in the critical bandpass region-perhaps with the E772 setup.

Econodump vs. DNLF:

Risk factor of design for muon rejection

Will it work?

Beam line - ~ Same

Give up last bend before dump.

⇒ More halo muons, but better rejection by dump

High momentum μs - effective $\int B dl$

Econodump ~ 30% better for Tohoku

~ Same for 15'

Muons at detectors (Target produced

Deep inelastic, pair production

Econodump ~ 30-40 μ/10^{13}p

DNLF ≤ few

High P_T passband

Econodump ~ 120 μ/10^{13}p

DNLF ≲ 1

For Econodump, extensive effort in modeling production spectra/comparison with data.

Fermilab

TM-1415
2961.200

AN "ECONODUMP" DESIGN[1] FOR THE FERMILAB DIRECT NEUTRAL LEPTON FACILITY

S. Childress, C. Brown, G. Koizumi, A. Malensek,
J. G. Morfin, T. Murphy, R. Stefanski, A. Wehman
Fermilab

and

Bin Lu
Virginia PolyTechnic Institute

August 1986

AN "ECONODUMP" DESIGN[1] FOR THE FERMILAB DIRECT NEUTRAL LEPTON FACILITY

S. Childress, C. Brown, G. Koizumi, A. Malensek,
J.G. Morfin, T. Murphy, R. Stefanski, A. Wehmann
Fermilab

Bin Lu
Virginia PolyTechnic Institute

An extensive effort has been directed toward a major redesign of the Fermilab Direct Neutral Lepton Facility (DNLF).[2] The goal has been a very significant cost reduction of the facility, with minimal sacrifice of physics potential. Hence the name "Econodump" applied to the redesign effort.

DESIGN CRITERIA

To achieve the stated design goal, the following criteria have served as guidelines:

Use of existing components where feasible

A major cost in DNLF was the very large spoiler magnet system, designed and to have been constructed especially for DNLF. Utilization of existing magnet components, if feasible, could allow for a much less expensive facility.

Additionally, the proposed DNLF pretarget primary beam enclosure with extensive dipole and quadrupole components was a significant expense for which alternatives might be feasible.

A limit on background muon flux at each bubble chamber of no more than 300μ's/10^{13} protons

The DNLF spoiler magnet design was predicted to give fewer than 10 muons/10^{13} protons.[3,4] Each chamber however is believed to be capable of resolving events without significant efficiency loss with 50 to 100 muons traversing the liquid during expansion. Due to significant uncertainties in modeling muon production and transmission through the active spoiler magnet shield, the DNLF design was very conservative in this regard. This degree of design safety achieved in DNLF was a major factor in the spoiler magnet size and hence cost.

1E13 900 GeV Protons/TeV Cycle in 3-5 Beam Pings

Tevatron accelerator capabilities indicate a probable practical limit on available protons for the neutrino program of about 1E13 protons/TeV machine cycle. This can readily be provided in a sequence of beam pings during the ≥20 second ramp flattop, with spacing of the pings determined by bubble chamber deadtimes.

The Tohoku chamber can accept a repetition rate of five seconds (5 pings) while the present viable rate for the 15 foot chamber is 10 seconds (3 pings). Hence the design limit of 300 muons/10^{13} protons.

900 GeV is probably a practical energy limit for high intensity Tevatron fast spill resonant extraction for the foreseeable future.

Quantitative understanding of muon production in relevant kinematic regions

An Econodump design with predicted muon rates through the active shield at levels comparable to chamber capabilities loses much of the safety factor present in the DNLF design. We have attempted to compensate by achieving more quantitative understanding of muon production in the kinematic regions which contribute the majority of background muons.

The three computer programs developed to predict background muon rates for DNLF (Columbia, Fermilab, and MIT) agreed very well in calculating transmission efficiencies through a given spoiler magnet configuration; but differed by as much as two orders of magnitude in production spectra used.

Minimal design physics compromise, along with more quantitative event rate projections

A maximum target-detector distance for the Tohoku bubble chamber has been chosen to be 90 meters. The 15 foot chamber would then be at 190 meters. Target to chamber distances in DNLF were approximately 60m. and 160m. respectively.

The necessary $\int Bdl$ and hence expense of the active shield is a strong function of the target-chamber distance.

Event rates are also of course dependent on this distance. This dependence is however much less than that expected from a $1/R^2$ scaling, due to the already significant fall off of event rate with production angle, over the detector fiducial volumes, at target distances considered.

Event rate projections have also been updated for the two bubble chambers, based on data not available when DNLF was initially proposed (Fermilab Beam Dump Experiment 613).

Initial Econodump design orientation toward Tau neutrino search with the Tohoku chamber

Comprehensive background calculations have been accomplished for the Tohoku bubble chamber at a target distance of 90 meters. It is expected that backgrounds for the 15' chamber at 190m. will be comparable. However, at this stage, only a few rates have been modeled for the large chamber. Projected event rates have been determined for both chambers.

ECONODUMP DESIGN

Beam Line

A major cost element for the DNLF primary beam transport was the pretarget enclosure containing 17 dipoles and quadrupoles, which provided the following functions:

A) Line up of the proton beam for zero degree targeting on the NO line, on which the existing neutrino detectors are centered.

B) Provide a large angle bend as near upstream of the target as feasible. This enabled significant reduction of muon and neutrino backgrounds aimed at the detectors from upstream sources: scraping of beam tails and beam-gas interactions.

C) Defocusing of the high intensity proton beam before targeting, to lessen peak energy density deposition in the target. This is especially important for very high Z targets, such as tungsten.

D) Enable different targeting angles (0 to 40mr) for measurements over a large angular region.

For the Econodump design, the primary proton beam is aimed directly at the 15 foot bubble chamber from Enclosure NE8, as shown in Figure 1. The DNLF design is shown for contrast in Figure 2.

In the Econodump, the Tohoku chamber would be shifted laterally in Lab F (a simple task) to again centrally intersect the targeted primary beamline. This line would intersect the Lab C detector off center, as seen in Figure 1 and, in finer detail, in Figure 3. As an initial design parameter the proton beam could be centrally targeted for any of the neutrino detectors. Once selected however, this beam trajectory would not be variable.

The larger bend angle required at Enclosure NE8 with the DNLF design necessitated new civil construction and several additional dipoles in the downstream part of the enclosure.

The Econodump targeting configuration requires only a lateral position shift of 7 existing dipoles in NE8 along with the addition of two new elements, as is shown in Figure 4A and 4B. Econodump (NL) beam operation is compatible with slow spill beam to the NEast line. Conversion back to NT/NH beam operation would involve repositioning the seven dipoles.

Defocusing of the primary beam before targeting is greatly simplified with the Econodump design. For DNLF the beam size had to be carefully controlled during transport through the pretarget dipoles, to avoid beam scraping. Then defocusing had to be accomplished with very little distance before the target, requiring a significant number of quadrupoles.

The Econodump has no limiting apertures after NE8, and due to the long lever arm, beam size at the target can be readily controlled with one quadrupole at the downstream of NE8.

Horizontal and vertical beam envelopes as a function of distance along the beamline are shown for Econodump and DNLF in Figures 5 and 6. Upstream of NE8 the beam transports are identical, along existing beamlines.

Downstream of NE8 the Econodump and DNLF both required installation of stainless steel berm pipe through the neutrino berm, to the Target Hall. For the Econodump only one pipe is needed, however, as the DNLF variable targeting angle has been deleted.

Elimination of the 40mr targeting option should involve no compromise for the Tau neutrino search, due to projected flux limitations at large angles.

The greatest potential compromise with the Econodump primary beam design is the long decay path of ~ 1200 feet from NE8 to the target, aimed directly at the bubble chambers. This produces concern of large muon and conventional neutrino backgrounds.

Monte Carlo studies indicate, however, that requirements for reduction of beam halo and beamline vacuum are no more severe than for the DNLF design. Results of these studies are presented in a later section.

Target Hall

The Econodump target hall design is similar to that of DNLF, but with several changes which reduce cost without adverse effect on targeting function:

The hall is shortened considerably in length.

A reduction in the earth berm neutron shield over the target has been effected.

DNLF design had a safety factor of 10^5 for this shield.

Support pilings under the hall can be removed due to reduced loading.

The target design for Econodump is a 1.2 meter Cu target, as in DNLF. Space provision for targets of different atomic weight and effective density has been retained.

Figure 7 shows plan and elevation views of the target and spoiler magnet halls for Econodump. For comparison, in Figure 8 are shown the same views for DNLF.

Spoiler Magnets and Hall

For the DNLF design, the spoiler magnets forming the active muon shield represented a very significant fraction of the project cost. With the Econodump, major changes are made in this active shield. The following table shows a comparison of DNLF with the Econodump spoiler magnet system.

Comparison of 216: M1 and SM12-C

To DNLF Proposal Magnets

	M1 177" long	M1 216" long	M2	M3	M4	M5	SM12-C (34" pole)	
Iron weight	540	659	780	1050	1830	1950	1356	tons
Conductor Weight	7.2	8.4	10.4	21.1	32.2	37.2	85*	tons
DC Power	10.7	12.6	15.4	958	1443	1622	1605	KW

*Aluminum Coil

	5 M1(177") $+\Sigma$ Mi i=2	M1(216") +SM12-C	
Iron Weight	6150	2015	tons
Conductor Weight	108	8.4+85*	tons
PC Power	4049	1620	KW

*Aluminum Coil

The five DNLF spoiler magnets, M1-M5, are replaced by only two magnets for the Econodump; a 216" long M1 and the 567" SM12 magnet previously used in E605, reconfigured as a C-magnet.

For DNLF the $\int Bdl$ was 54 Tesla-meters, while with the Econodump design $\int Bdl = 42.2$ Tesla-meters. The total iron weight in the Econodump magnetic shield is 2015 tons, compared with 6150 tons for DNLF.

New magnet steel purchase for Econodump is restricted to 659 tons for the lengthened M1 magnet. While M1 is to be built from new materials, the SM12-C magnet requires very little beyond existing materials. The A1 coil is reused intact in the C-magnet configuration.

A detailed comparison of specifications for the two Econodump magnets is as follows:

	M1 (216")	SM12-C	
NI_T	54000	940800	Amp-Turns
N_T	72	196	Turns
I	750	4800	A
Conductor	1.288 x 1.288 x 0.618 inches	2.42 * 2.42 x 0.55 inches	
A_{Metal}	1.36	5.62	$Inches^2$
J_{Metal}	551	854	A/in^2
Inductance	1.28	1.0 (approx)	H
Resistance / Length	6.95$\mu\Omega$/ft @ 150^0 F	2.7$\mu\Omega$/ft @ 120^0 F	
Conductor Length	3195	25755	FT
Resistance	.0223	.070	Ω
$\tau = L/R$	57.35	14.5	s
DC Voltage	16.71	336	V
DC Power	12.6	1605	KW
Weight of Conductor	8.4	85	Tons
Steel Weight	659	1356	Tons
Stainless Steel Weight	6.7	-	Tons

Figure 9 shows a cross-section schematic of the M1 magnet (similar to DNLF except in length). Figure 10 shows a corresponding schematic for SM12-C.

The Econodump spoiler hall is scaled down by approximately a factor of two from DNLF, as is shown in Figures 7 and 8. Corresponding civil construction cost savings are achieved. Due to reduced earth loading, support pilings are no longer needed for the Econodump spoiler magnets.

The new NS5 service building is significantly smaller in both building size and technical support systems required, as power and LCW requirements are reduced considerably for the Econodump design.

A passive iron shield before the Tohoku chamber ranges out muons of momentum up to 7 GeV in the Econodump configuration, comparable to the passive shield in DNLF.

ECONODUMP FUNCTION

Neutrino Event Rates

The Econodump Target-Tohoku Chamber distance of 90m is predicted by J. G. Morfin[5] to lower the tau neutrino event rate by 37% from that predicted for the DNLF configuration. Morfin's study on neutrino and muon rates from a high density beam dump was carried out in parallel with the Econodump design effort.

Figure 20 shows projected $\nu\tau$ interaction rates in the Tohoku Chamber for different dump-detector distances, with 1 TeV protons incident. The parameterization of the Monte Carlo predictions is valid for distances of 20m - 100m. Error bars are the same as in FN434.

Most striking is the relative flatness of the event rate versus distance over the region considered (when compared to the fall-off of a $1/R^2$ scaling). As previously noted, this is due to the significant decrease of event rate with production angle over the detector fiducial volume.

Projected ν_τ interaction rates/10^{18} protons at 900 GeV are 40 events with a chamber distance of 90m and 64 events for the DNLF design. These rates assume Bourquin-Gaillard σ scaling.

The calculations are normalized to the measured E613 beam dump direct neutrino event rates at 400 GeV using high density targets. Although an A dependence was measured in this experiment, it is not critical for the ν_τ rate predictions, as the predictions are based on heavy target data extrapolated to the same.

Major uncertainties in the rate predictions are the $\sigma(F)/\sigma(D)$ ratio, assumed to be 0.1 and the S dependence from 400-900 GeV.

There is some trade off possible between ν_τ event rates and design conservation in increased distance of the Tohoku Chamber from the intense flux, high momentum muon lobes above and below the chamber.

At Econodump target distances of 90m and 190m for the Tohoku and 15 foot bubble chambers respectively, the relative magnetic kick given to high momentum μ's compared to DNLF (taking the shift in bend center of the spoiler magnets into account) is:

Tohoku Chamber - 1.30

15' Chamber - 0.96

Hence the Econodump design is somewhat more conservative than DNLF was for the Tohoku Chamber with regard to this potentially serious background source.

It does not appear feasible to lessen the Econodump $\int Bdl$, as a further cost saving measure, to the distance scaled value of 35 Tesla meters, due to the rapid increase of other muon background sources.

A shortening of the Target-Tohoku Chamber distance from 90m to 75m would increase the ν_τ interaction rate by ~20%.

Muon Backgrounds from Target Production

Two of the three computer programs (MIT and Fermilab) used in predicting muon background rates for DNLF have been used extensively in the Econodump design. The programs have been found to give comparable transmission rates for muons through different spoiler configurations, with differences in muon rates at the chambers predominantly due to differences in the two production models used.

The MIT program was the program used predominantly for final stages of the Econodump design.

All background muon sources considered in DNLF were modeled for Econodump. In addition, for muons scattered deep inelastically, subsequent π production and decay was also considered in the Econodump modeling. This process, which was not considered in DNLF, does produce a contribution to the muon flux at the chamber.

The following table gives calculated muon backgrounds from target associated sources:

Projected Muon Rates for the Tohoku Chamber
Based on MIT Production Model and Spoiler Program

Target, beam dump associated sources;		7 GeV Passive Shield
	Bandpass with Coulomb Scat.	$47\mu/10^{13}$ppp
	Deep Inelastic Scat. (Muon)	9μ
**	Deep Inelastic Scat. ($\pi \to \mu$)	$\approx 20\mu$
	Pair Production (Tridents)	55μ
**	Pole Tip Scat. ($\pi \to \mu$)	$\approx 15\mu$
	TOTAL	$146\mu/10^{13}$protons

** These sources were not considered in DNLF. Results from these processes are preliminary, but are felt to be conservative.

Background muons reaching the Tohoku Chamber are predominantly produced in two separate kinematic regions: low energy and high P_T and medium energy and low P_T.

The contribution labeled bandpass with Coulomb scattering comes predominantly from muons with production energy between 30-80 GeV and P_T 4-6 GeV.

This source gave very little background for the DNLF design, due primarily to much larger vertical good field regions for the DNLF magnets. This was, however, a very expensive solution.

Soft field edges extending beyond the coil of the SM12-C magnet are a significant contributing factor to this background source. Figure 11 shows a cross-section view of the SM12-C magnetic field distribution, and Figure 12 illustrates the field distribution versus vertical position. The soft field edges to the pole region are quite apparent. Figure 13 shows a typical ray trace for this background source.

The second important kinematic region contributing to muon backgrounds is for muon production momenta of 75-225 GeV and P_T of 0-2 GeV. The backgrounds due to deep inelastic scattering and pair production (tridents) are predominantly from this region.

Figure 14 illustrates negative muon ray trajectories for muon momenta between 100 and 800 GeV. Interactions of these muons with the dirt, some of which scatter deep inelastically, is a contributing source of background muons at the Tohoku chamber. To further reduce this background source an inexpensive solution may be a trench between the downstream of the SM12 spoiler hall and the passive shield in front of the bubble chamber.

In Figure 15 is shown a positive muon interacting in the SM12-C pole, with resultant muon pair production, and the negative muon being swept back toward the chamber. As in DNLF the solution to controlling this background source is an air gap for the downstream spoiler magnet region. Optimization for the Econodump geometry indicates the need for an air gap over the full SM12-C length. To optimize $\int$ Bdl the pole gap is tapered, ranging from 3" at the upstream to 12" at the downstream of SM12-C.

The optimal pole gap width and length and subsequent soft field edges, for SM12-C involves a trade off between the Coulomb bandpass and pair production backgrounds. Parameters were adjusted to produce roughly comparable backgrounds from each source (based on the MIT program).

Muon Backgrounds from Upstream Sources

Extensive Monte Carlo studies have modeled the effects of beam halo for the Econodump design. Of particular concern is the long decay space (~1200 feet) aimed directly at the bubble chambers at zero degrees. A crucial design feature is the dirt berm surrounding the beam transport pipe (12" diameter for most of its length). This dirt provides ranging for most beam halo muons in the crucial spoiler magnet bandpass momenta region of 30-80 GeV. High P_T is not required for the bandpass if the muon enters the spoiler magnet system significantly off axis. The berm pipe then provides a collimated halo muon distribution centered around the proton beam center. In this region bandpass rejection of the spoiler system is improved by orders of magnitude.

Figure 16 shows a Monte Carlo output (program HALO) of muon spatial distribution generated by an interaction source in Enclosure NE8 for the Econodump design. Figure 17 shows a corresponding distribution for a similar interaction source with the DNLF geometry. In each case the figures have the same coordinate scales. There is an arbitrary event normalization between the two plots, but the difference in muon spatial distributions at the target is striking.

For the beam cleanliness levels projected as necessary in DNLF, $< 1 \times 10^{-7}$ of beam in halo at NE8 and 10^{-5} torr vacuum levels in the pipe downstream of NE8, we obtain a projection of $< 10\mu/10^{13}$ protons at the Tohoku Chamber for the

Econodump design. By contrast, were the dirt berm not present between NE8 and the target, the projected number becomes $1200\mu/10^{13}$ protons.

Non-prompt neutrino backgrounds from upstream interactions and decays are negligible compared with target sources for the beam halo level projected.

Muon Production Model Comparison with Data

As the Econodump design does not allow for a large safety factor in muon background rates, it becomes imperative to achieve better quantitative understanding of muon production in the critical kinematic regions.

Figure 18 and 19 show a comparison of the MIT and Fermilab μ^+ production formulas with data of Bodek et al. at 350 GeV. Comparisons are made both of P_μ and P_T distributions. A similar comparison was made in TM1155R[4] with high P_T data of Cronin et al. at 300 GeV. In all cases the MIT production model predicts rates significantly above the data. A comparison of the MIT model with preliminary E605[6] muon data at 800 GeV indicates that in the region of comparison - high P_μ and low P_T - the muon flux predictions are higher than the data by ~ a factor of 10.

There is concern however, due to the manner in which S dependence is incorporated, that this model does not present conservative flux numbers for high P_T and primary momentum significantly above 400 GeV. This is augmented by the muon flux predictions of Morfin in FN-434.

In the critical kinematic regions for muon background sources the following flux ratios are obtained by comparison between the Morfin/MIT production models.

P_L (GeV)	P_T (GeV)	Morfin/MIT
35 - 40	4.8 - 5.3	3.0
55 - 60	5.3 - 5.8	2.15
75 - 85	0.0 - 2.0	0.67
145-155	0.0 - 2.0	0.33
215-255	0.0 - 2.0	0.31

If the MIT model results for background muons at the Tohoku Chamber are normalized to the Morfin predictions, the projected background muon flux would become $\tilde{}160\mu/10^{13}$ protons with 76% of this background from the Coulomb bandpass.

There are still available several design options which should not increase the Econodump facility cost, which could selectively improve muon rejection in this bandpass region.

During the next Fermilab fixed target run there may be the possibility of measuring the high P_T muon rates in the critical bandpass region-perhaps with the E772 setup.

Econodump Facility Costs

The following table shows the results of a comprehensive "bottoms up" cost estimate for the Econodump facility. A factor of three reduction in facility costs is projected when compared to DNLF, with minimal reduction in physics potential.

COST ESTIMATE OVERVIEW

The cost totals associated with the civil construnction and with the technical components planned for the Econodump Facility are listed below:
(Bold print gives for comparison the D.N.L.F. cost totals.)

Description	TOTAL with 15% O & P	TOTAL with Escalation	TOTAL with E.D.I.A.	TOTAL with Contingency
CIVIL CONSTRUCTION				
Beam Pipe, Berm & Enc. NE8	$543,700 **$701,000**	$610,000 **$787,000**	$683,200 **$945,000**	$819,800 **$1,135,000**
Lepton Halls & Service Building NS-5	$1,506,800 **$3,094,000**	$1,692,100 **$3,609,000**	$1,895,100 **$4,330,000**	$2,274,100 **$5,195,000**
H-Piling & Earth Retention	---- **$267,000**	---- **$313,000**	---- **$375,000**	---- **$450,000**
Subtotal	$2,050,500 **$4,062,000**	$2,302,100 **$4,709,000**	$2,578,300 **$5,650,000**	$3,093,900 **$6,780,000**
TECHNICAL COMPONENTS				
Beam Transport System	$455,900 **$1,248,000**	$490,000 **$1,375,000**	$504,800 **$1,650,000**	$605,800 **$1,980,000**
Target System at Lepton Hall	$414,100 **$482,000**	$445,200 **$531,000**	$458,500 **$640,000**	$550,200 **$770,000**
Spoiler Magnets	$1,283,300 **$4,956,000**	$1,379,600 **$5,436,000**	$1,421,000 **$6,520,000**	$1,705,100 **$8,470,000**
Subtotal	$2,153,300 **$6,686,000**	$2,314,800 **$7,342,000**	$2,384,300 **$8,810,000**	$2,861,100 **$11,220,000**
TOTAL FACILITY	$4,203,800 **$10,748,000**	$4,616,900 **$12,051,000**	$4,962,600 **$14,460,000**	$5,955,000 **$18,000,000**

References

1) Essential contributions to the Econodump design have also been provided by D. Cossairt and L. Koller, of Fermilab, S. Oh of Duke University, and M. Peters of Univesity of Hawaii.

   Engineering design is a result of the efforts of L. Beverly, R. Doyle, R. Fast, C. Federowicz, A. Guthke, C. Kendziora, L. Kula, J. Lindberg, W. Nestander, M. Notarus, T. Pawlak, R. Sanders, and J. Western, all of Fermilab.

2) Fermilab Direct Neutral Lepton Facility Conceptual Design Report, May 1985.

3) C. Baltay et al., The Design of the Magnetized Muon Shield for the Prompt Neutrino Facility, Fermilab TM-1155, October 1982.

4) T. Murphy et al., Magnet Design Study from the Conceptual Design Report for the Direct Neutral Lepton Facility, Fermilab TM-1155R, May 1985.

5) J. G. Morfin, The Intensity and Spectra of Leptons Emerging from a High Density Beam Dump, Fermilab FN-434, July 1986.

6) C. Brown (E605), private communication.

Figure Captions

Fig. 1 Econodump primary beamline from Enclosure NE8 downstream.

Fig. 2 DNLF 0mr primary beamline from Enclosure NE8.

Fig. 3 Econodump primary beam targeting angle with respect to Fermilab neutrino detectors.

Fig. 4 A. Enclosure NE8 in the existing NT/NE configuration.

B. Enclosure NE8 for the Econodump configuration.

Fig. 5 A. Econodump horizontal beam envelope as a function of Z.

B. DNLF horizontal beam envelope as a function of Z.

Fig. 6 A. Econodump vertical beam envelope as a function of Z.

B. DNLF vertical beam envelope as a function of Z.

Fig. 7 Econodump Target and Spoiler Hall

Fig. 8 DNLF Target and Spoiler Hall.

Fig. 9 Cross-section schematic of Econodump M1 spoiler magnet.

Fig. 10 Cross-section schematic of Econodump reconfigured SM12-C spoiler magnet.

Fig. 11 Magnetic field distribution for the SM12-C magnet, as calculated by the program POISSON.

Fig. 12 SM12-C field distribution versus vertical position, along the magnet horizontal center.

Fig. 13 Muon ray trace indicating Coulomb bandpass due to soft field edges.

Fig. 14 Negative muon ray traces for $P_T=0$, $P_\mu=100\text{-}800$ GeV.

Fig. 15 Muon background from pair production.

Fig. 16 Halo muon spatial distribution at the Econodump target for a source at Enclosure NE8.

Fig. 17 Halo muon spatial distribution at the DNLF target for a source also at NE8.

Fig. 18 Comparison of the MIT and Fermilab production formulas with data of Bodek et al. P_μ distribution.

Fig. 19 Comparison with Bodek et al. P_T distribution.

Fig. 20 Projected ν_τ event rate vs. dump-detector distance for Tohoku Chamber, 1000 GeV incident protons.

Figure 1

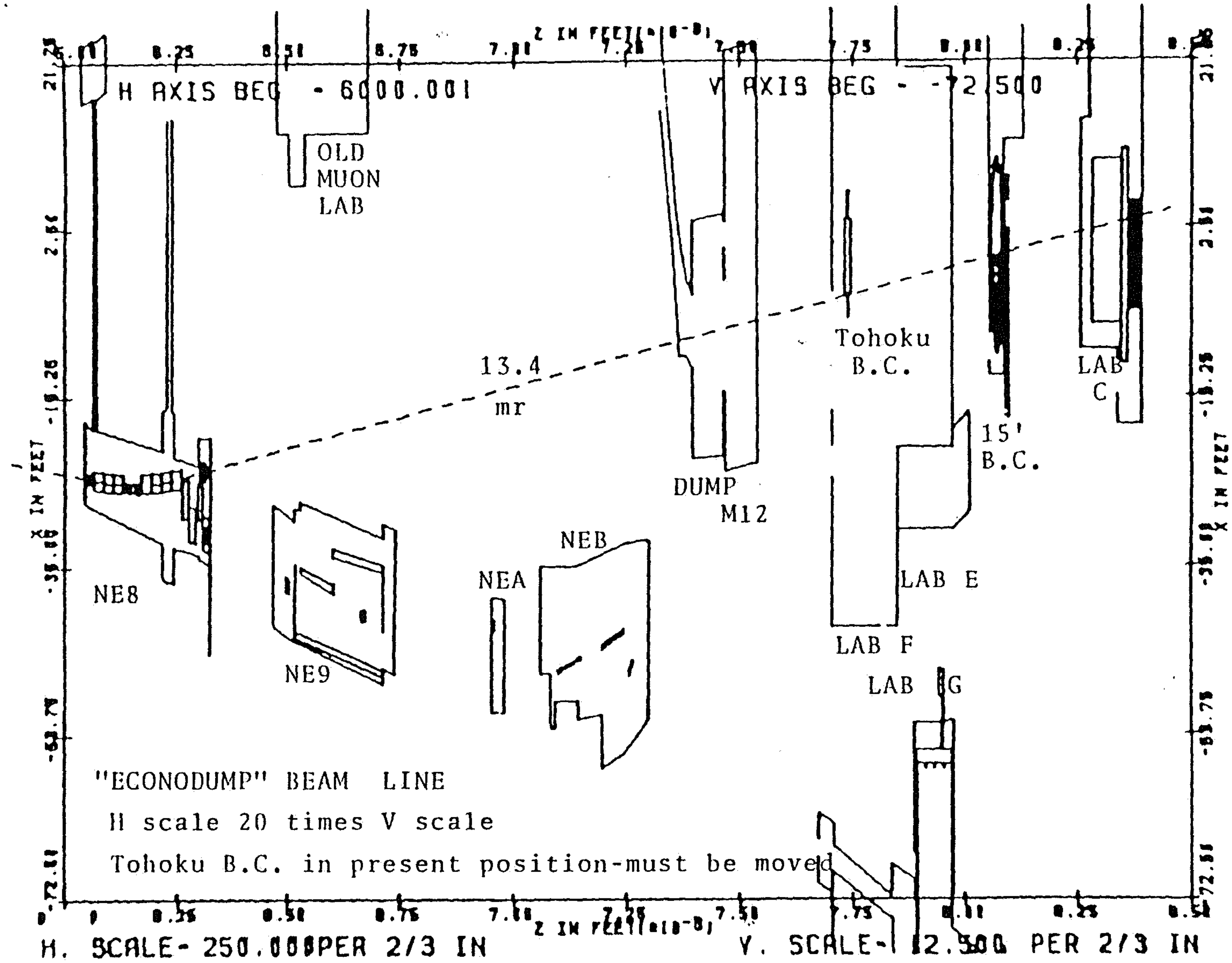

Z IN FEET(x10-0)
H AXIS BEG - 6000.001
V AXIS BEG - -72.500
OLD
MUON
LAB
13.4
mr
DUMP
M12
Tohoku
B.C.
15'
B.C.
LAB
C
LAB E
LAB F
LAB G
NE8
NE9
NEA
NEB
X IN FEET
"ECONODUMP" BEAM LINE
H scale 20 times V scale
Tohoku B.C. in present position-must be moved
H. SCALE- 250.000PER 2/3 IN
V. SCALE- 12.500 PER 2/3 IN

Figure 2

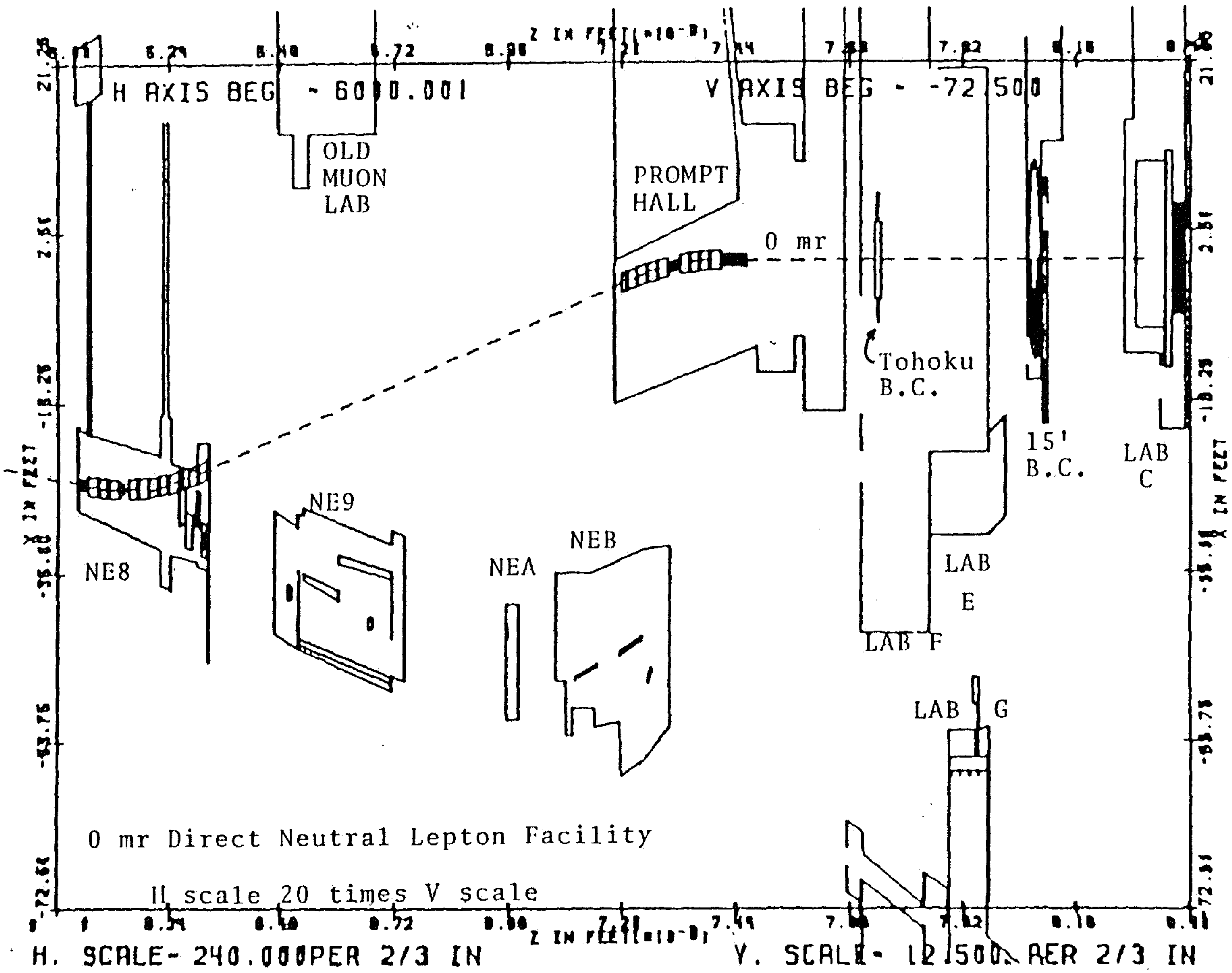

H AXIS BEG - 6000.001
V AXIS BEG - -72.500
Z IN FEET (x10^-3)
X IN FEET
OLD
MUON
LAB
PROMPT
HALL
0 mr
Tohoku
B.C.
15'
B.C.
LAB
C
LAB
E
LAB F
LAB G
NE8
NE9
NEA
NEB
0 mr Direct Neutral Lepton Facility
H scale 20 times V scale
H. SCALE- 240.000PER 2/3 IN
V. SCALE- 12.500 PER 2/3 IN

Figure 3

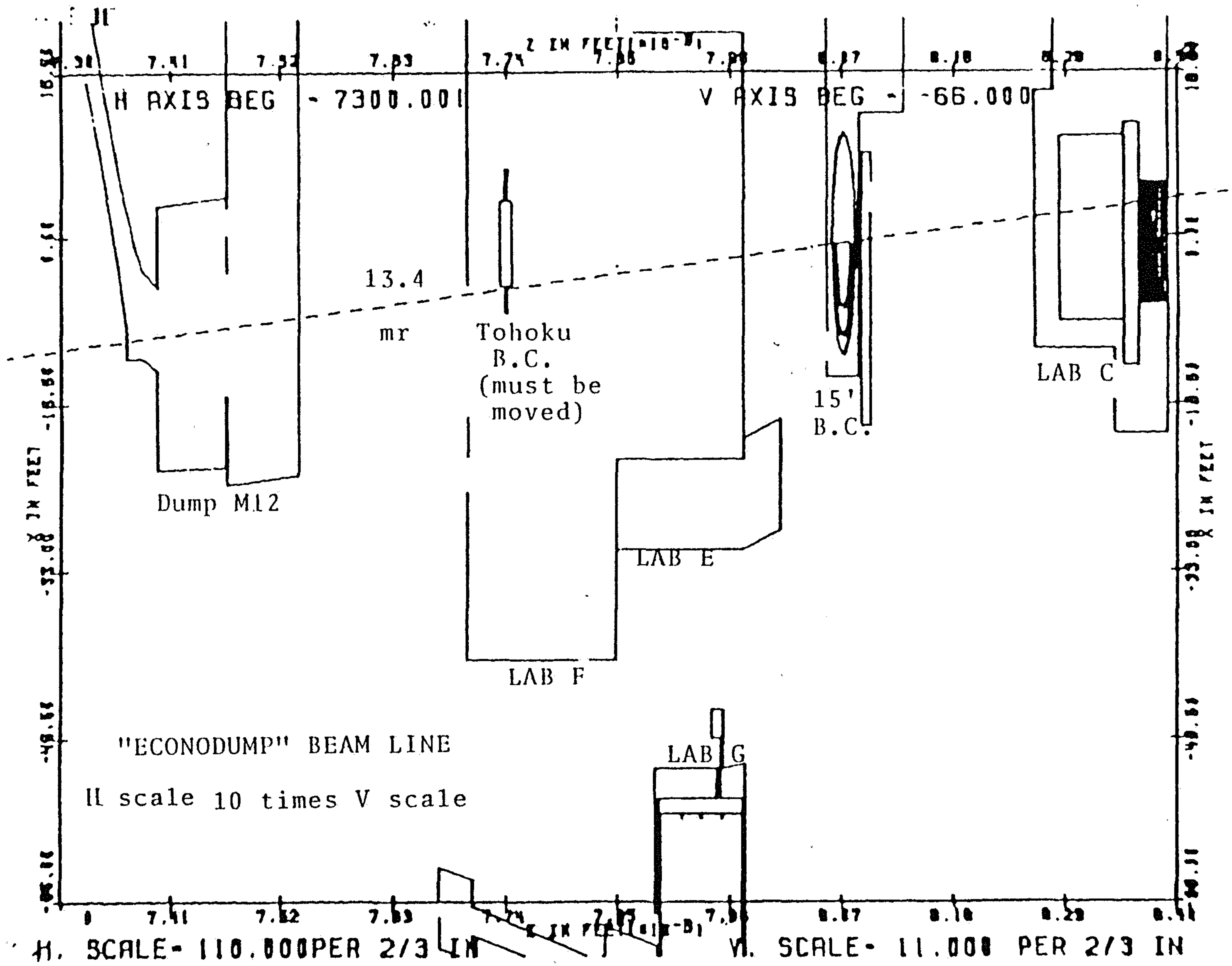
H AXIS BEG - 7300.001
V AXIS BEG - -66.000
13.4
mr
Tohoku
B.C.
(must be
moved)
15'
B.C.
LAB C
Dump M12
LAB E
LAB F
LAB G
"ECONODUMP" BEAM LINE
H scale 10 times V scale
H. SCALE- 110.000PER 2/3 IN
V. SCALE- 11.000 PER 2/3 IN

Figure 4A

Enclosure NE8 configured in the existing NT/NE configuration. Magnets which must be moved transverse to the beam for use in the "Econodump" configuration are shaded. Note that the 7-th 4-2-240 must be rotated.

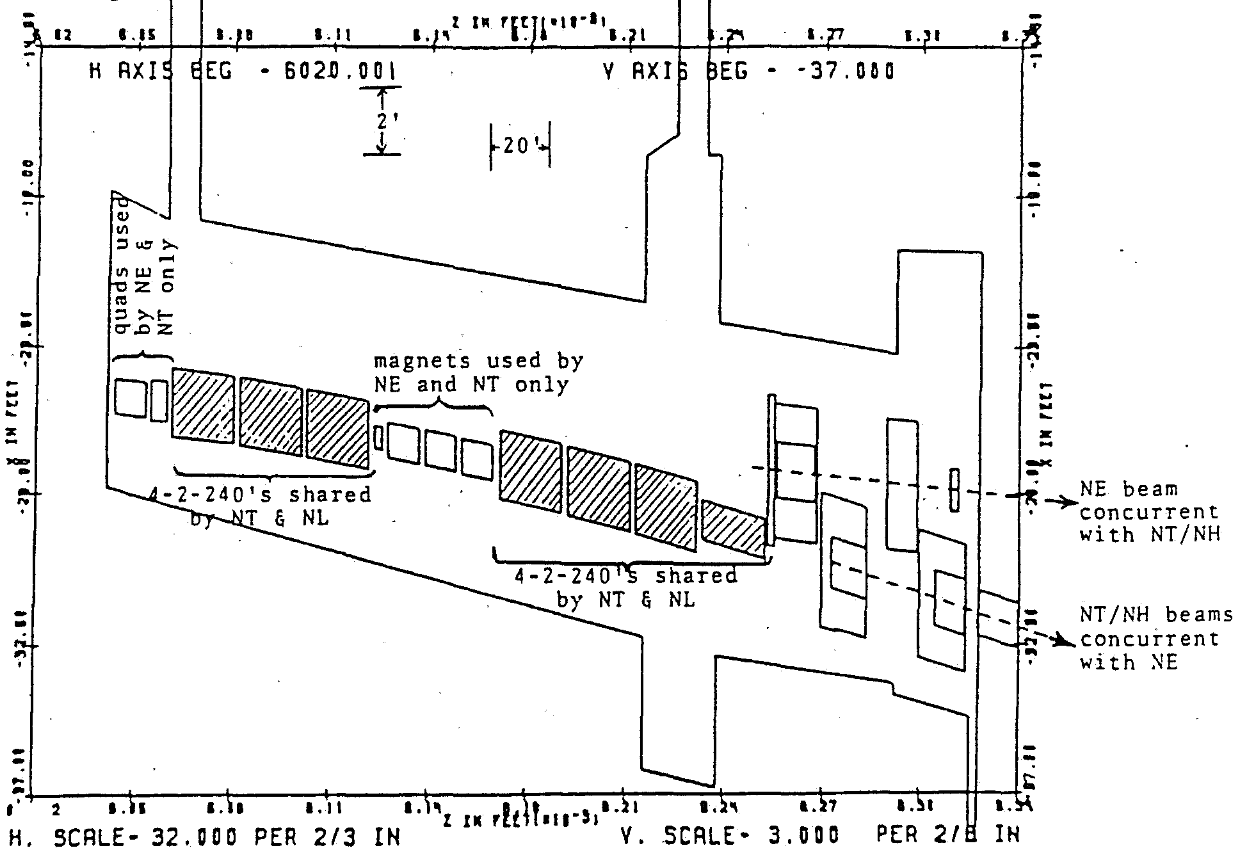

Figure 4B

Enclosure NE8 in the "Econodump" configuration. The magnets used by the "Econodump" beam line are shaded. Distored vertical/horizontal scales.

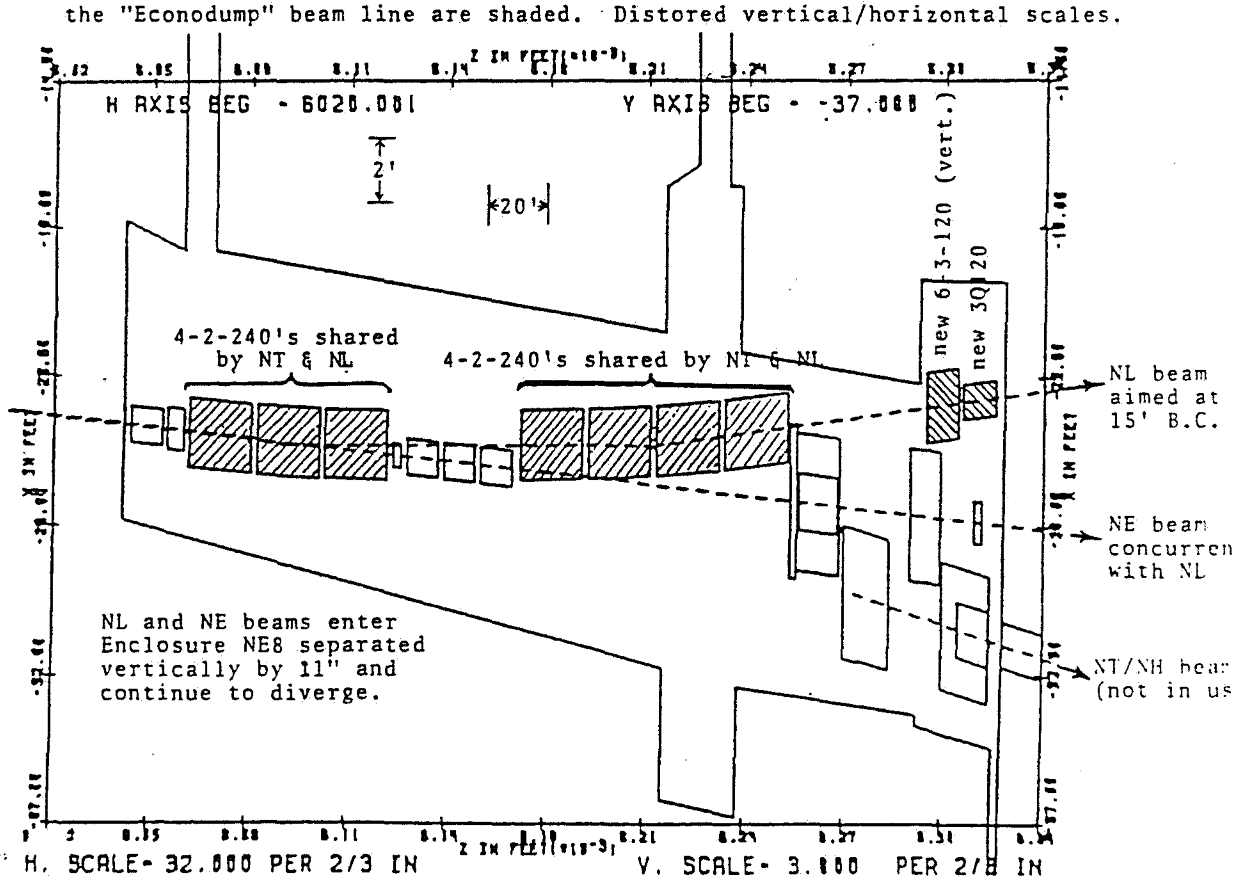

Figure 5A

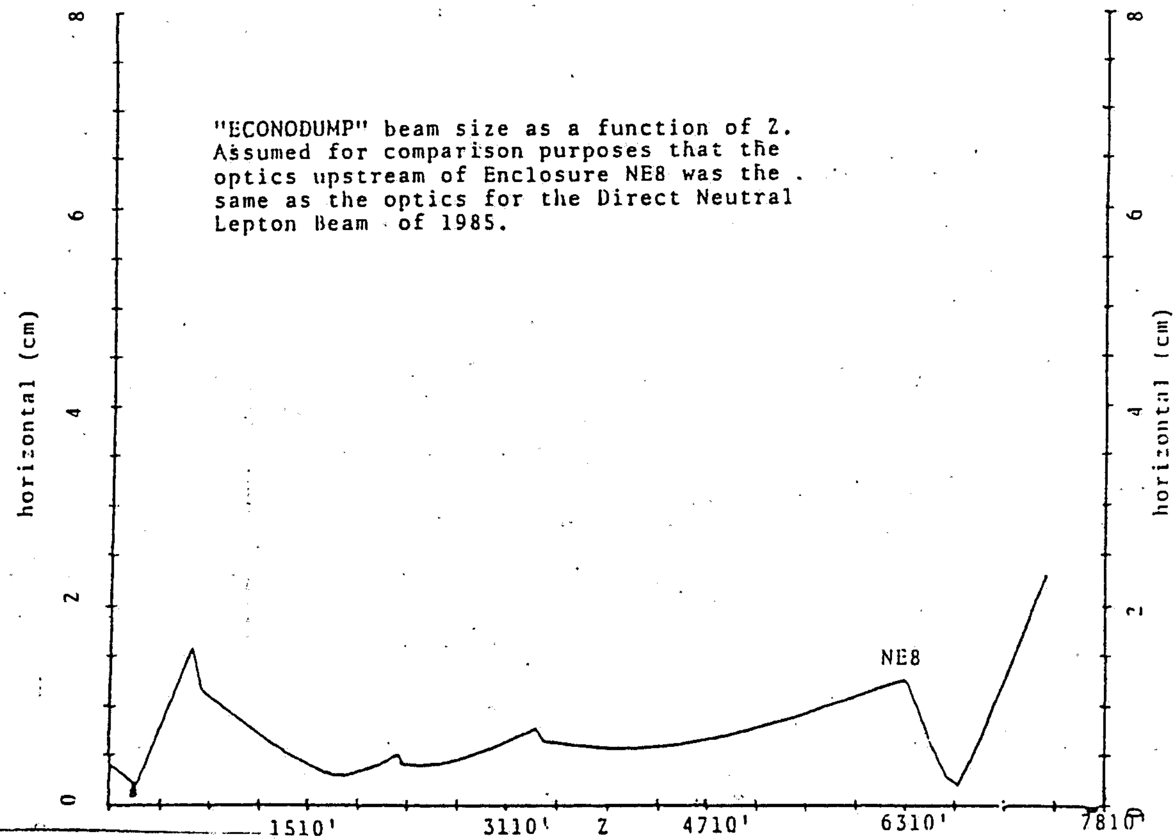

Figure 5B

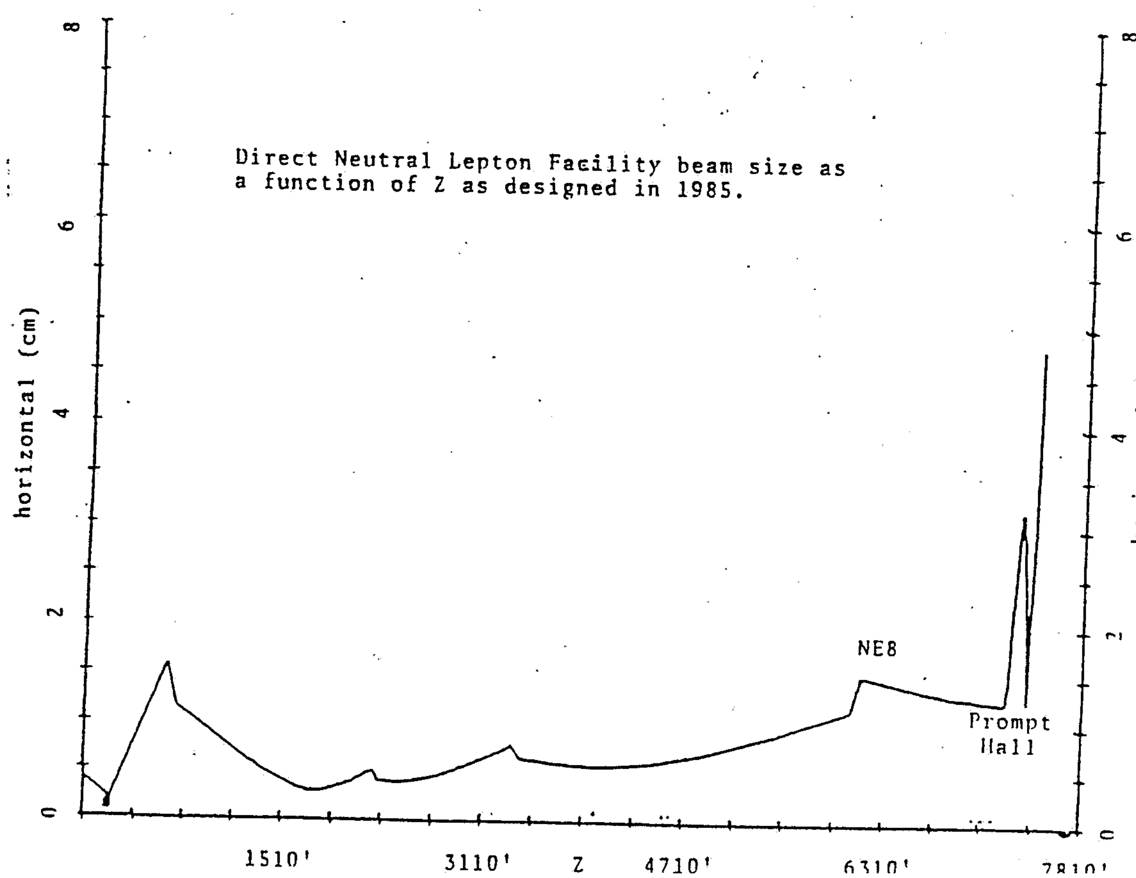

Figure 6A

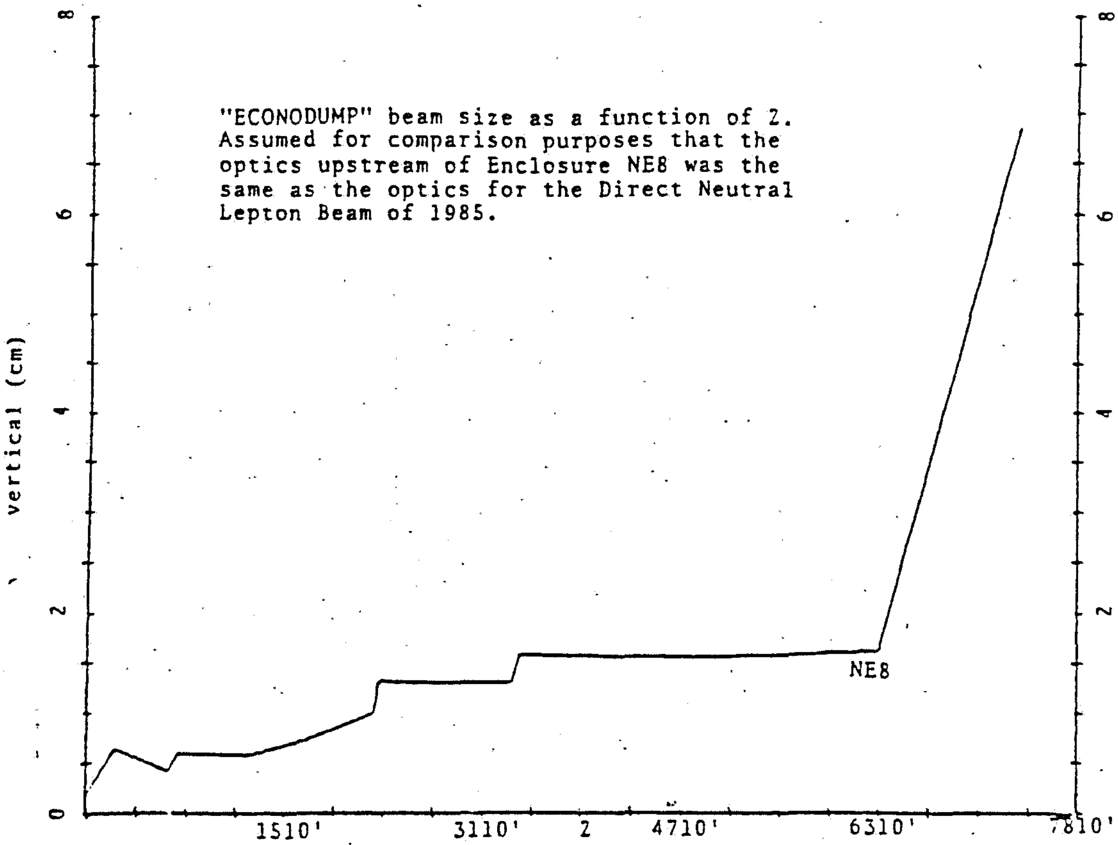

Figure 6B

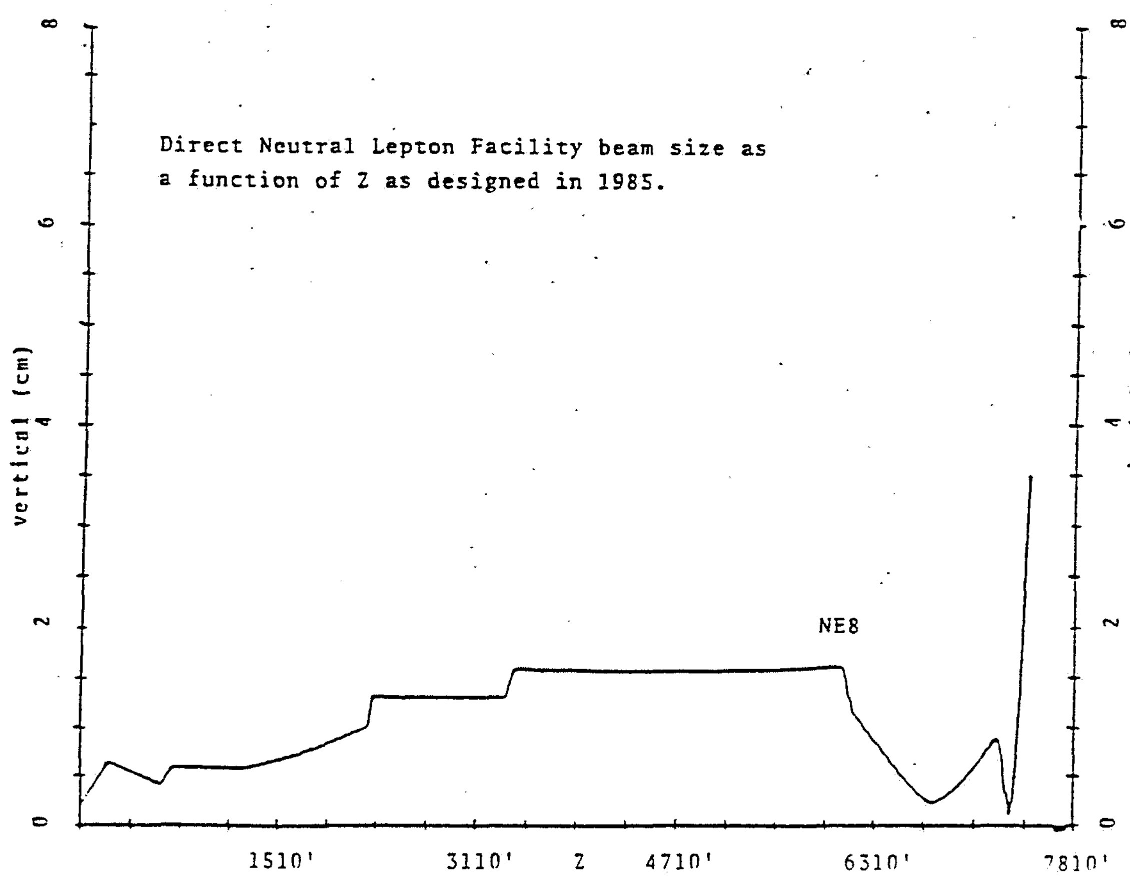

Figure 7

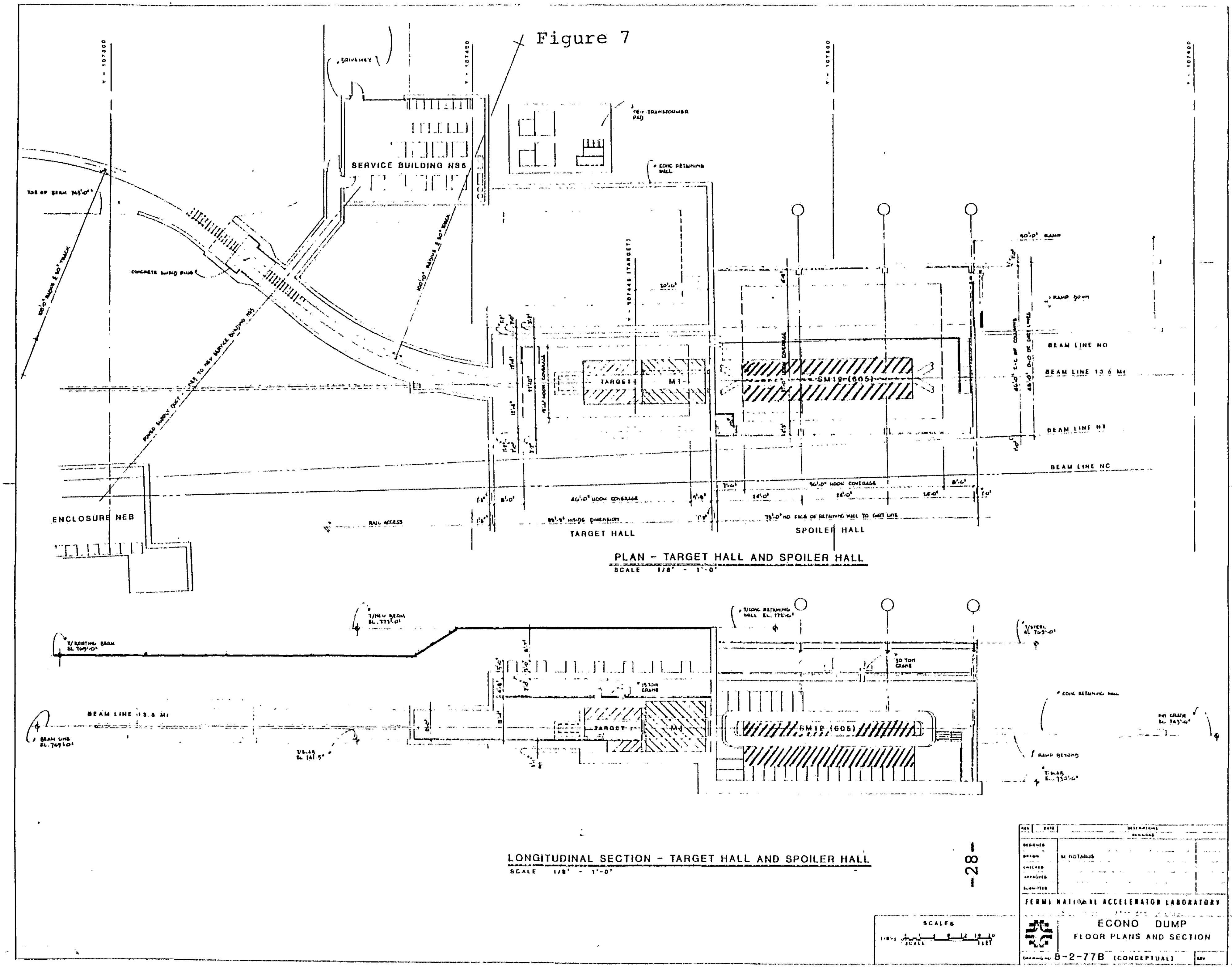
SERVICE BUILDING NS5
ENCLOSURE NEB
BEAM LINE NO
BEAM LINE N1
BEAM LINE NC
TARGET HALL
SPOILER HALL
PLAN - TARGET HALL AND SPOILER HALL
SCALE 1/8" - 1'-0"
LONGITUDINAL SECTION - TARGET HALL AND SPOILER HALL
SCALE 1/8" - 1'-0"
SCALES
FERMI NATIONAL ACCELERATOR LABORATORY
ECONO DUMP
FLOOR PLANS AND SECTION
8-2-77B (CONCEPTUAL)

Figure 8

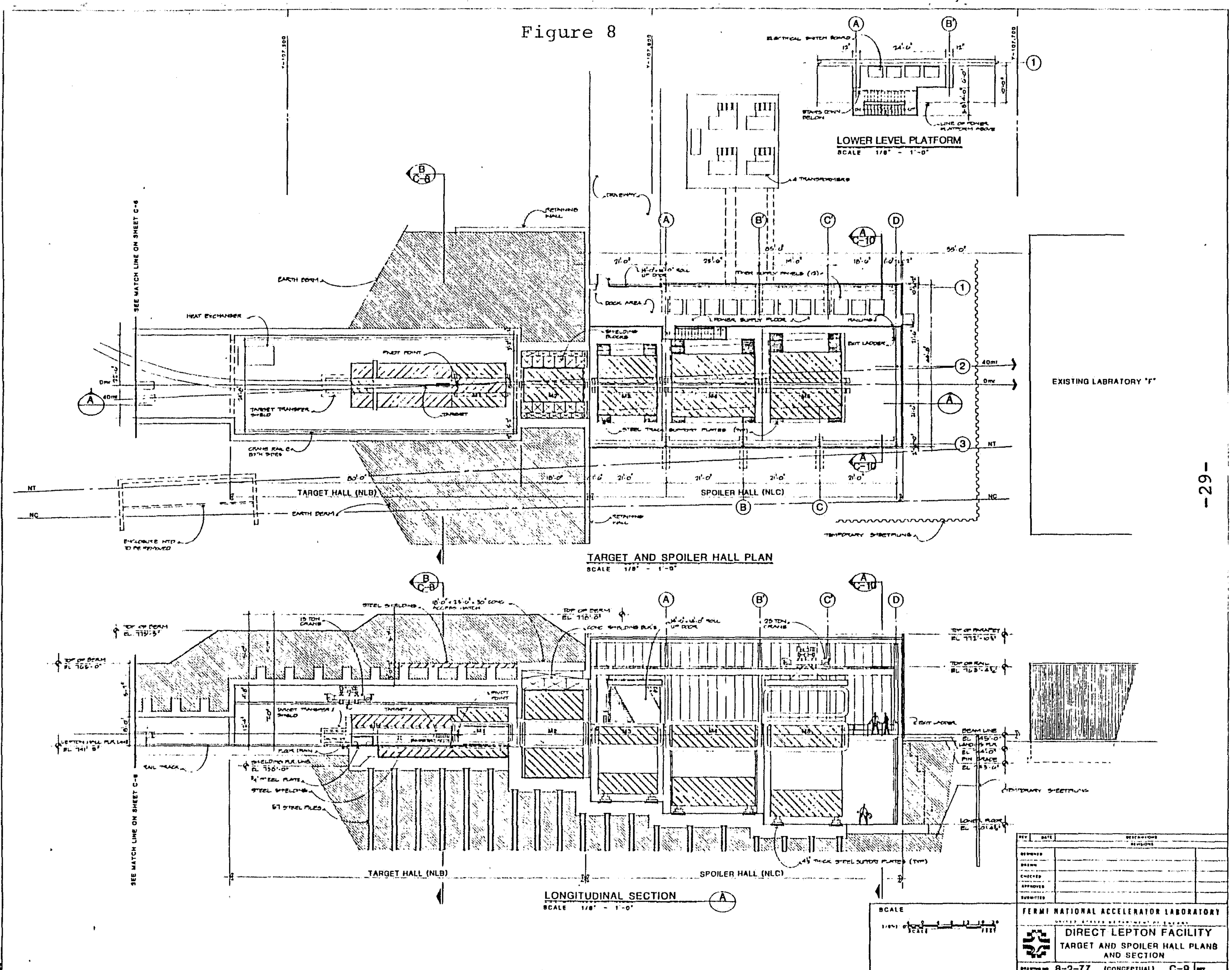
LOWER LEVEL PLATFORM
SCALE 1/8" - 1'-0"
TARGET AND SPOILER HALL PLAN
SCALE 1/8" - 1'-0"
TARGET HALL (NLB)
SPOILER HALL (NLC)
EXISTING LABRATORY "F"
SEE MATCH LINE ON SHEET C-8
LONGITUDINAL SECTION
SCALE 1/8" - 1'-0"
FERMI NATIONAL ACCELERATOR LABORATORY
DIRECT LEPTON FACILITY
TARGET AND SPOILER HALL PLANS AND SECTION
8-2-77
(CONCEPTUAL)
C-9

Figure 9

M1
216" LONG

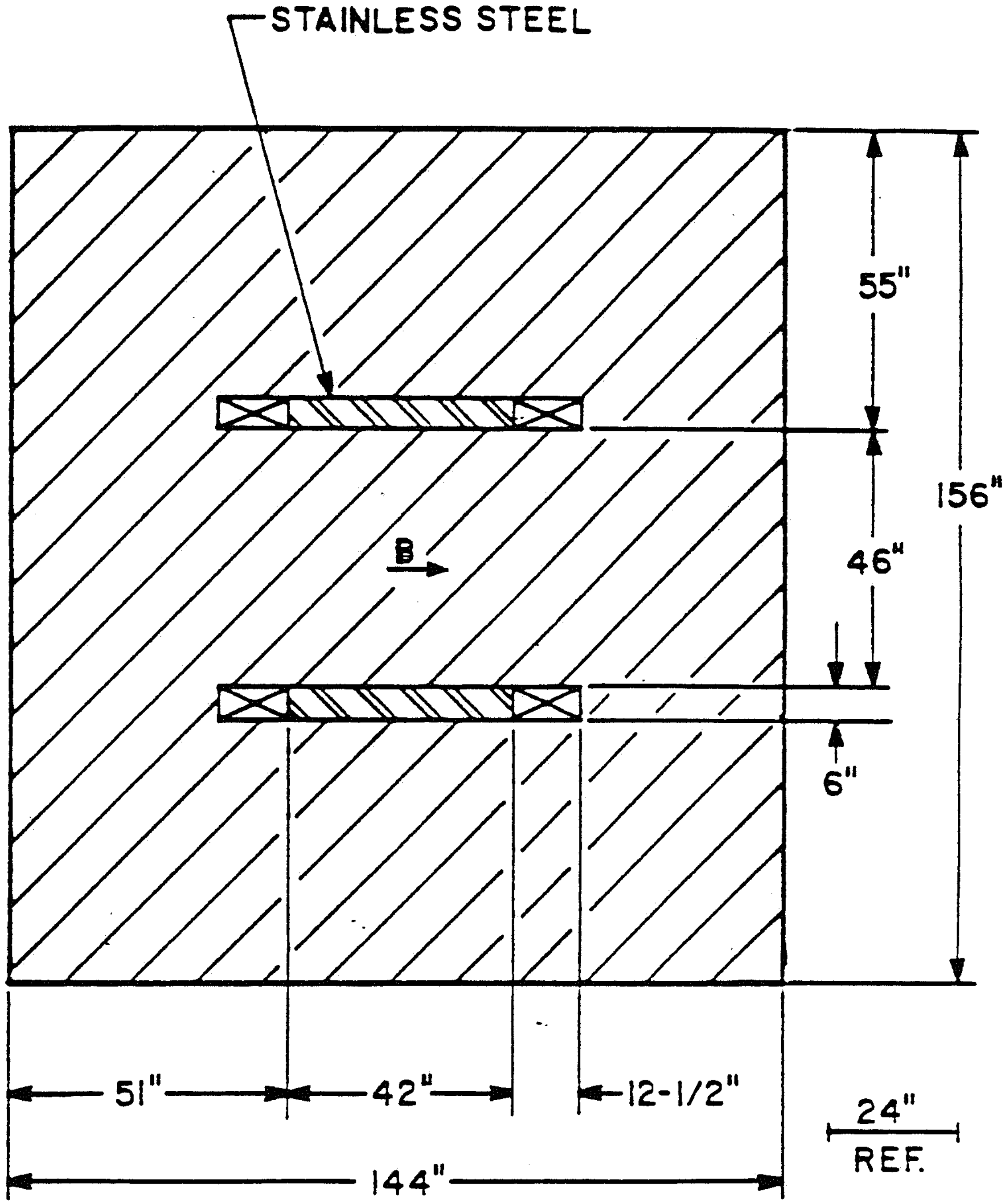

Figure 10. Cross section view of E605 magnet SM12 reconfigured as a C magnet. Dimensions are in inches.

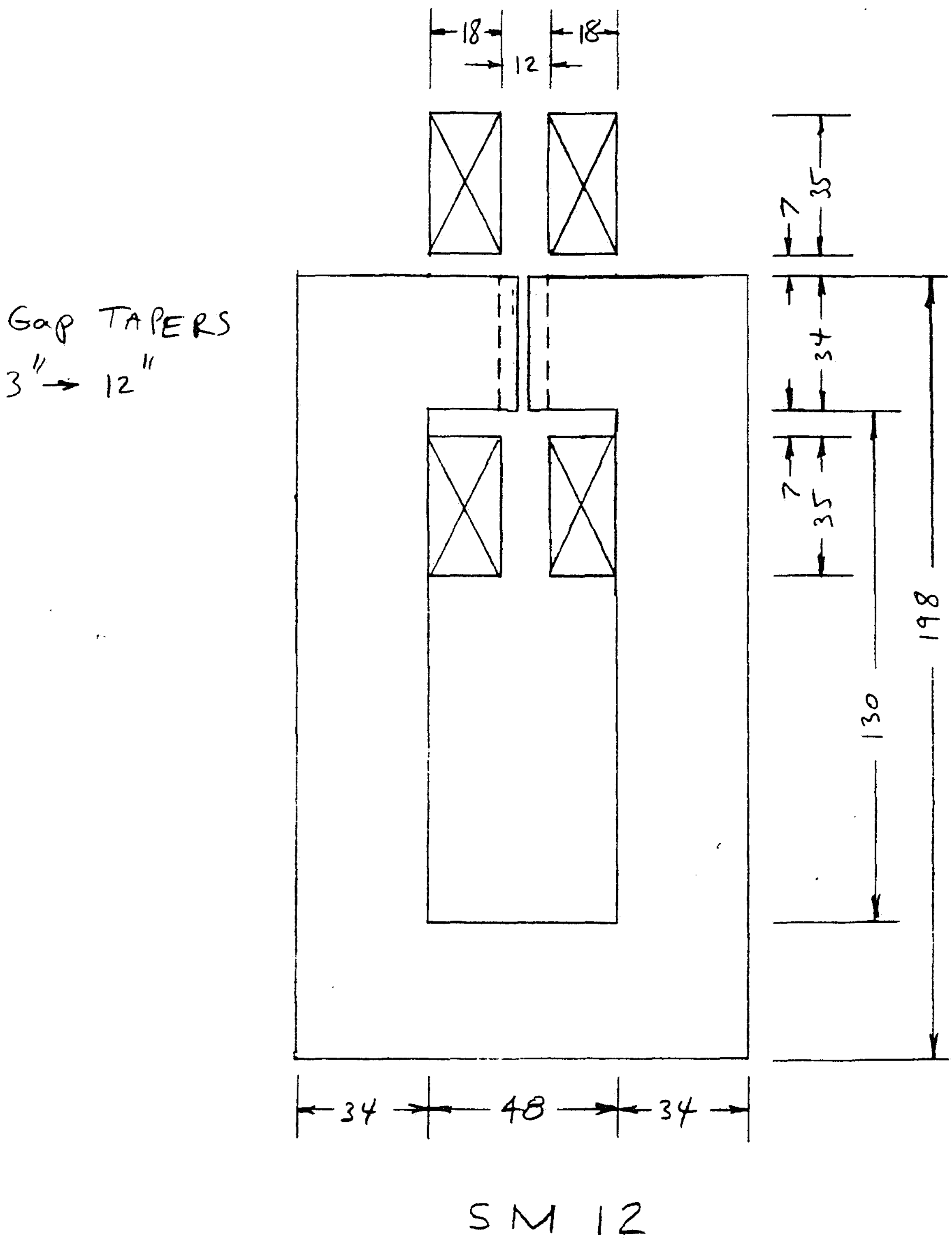

SCALE 1:40

Figure 11

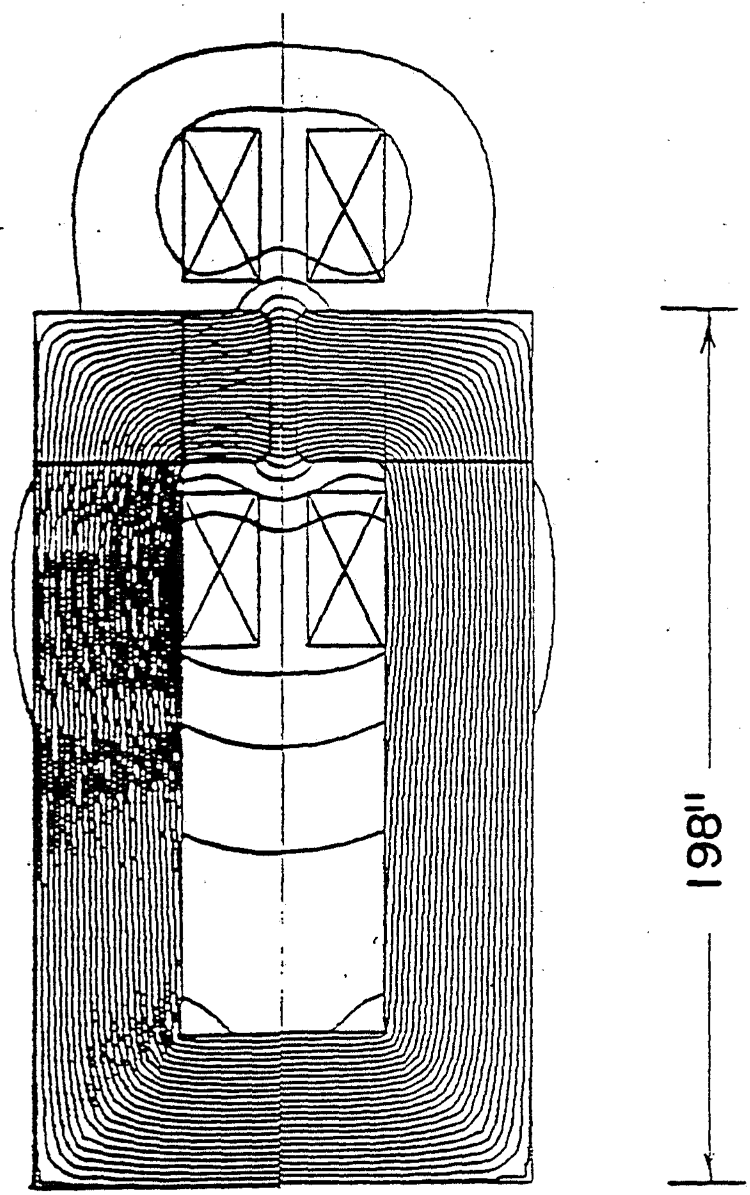

SM12-C

MAGNETIC FIELD

DISTRIBUTION

(7" GAP)

Figure 12

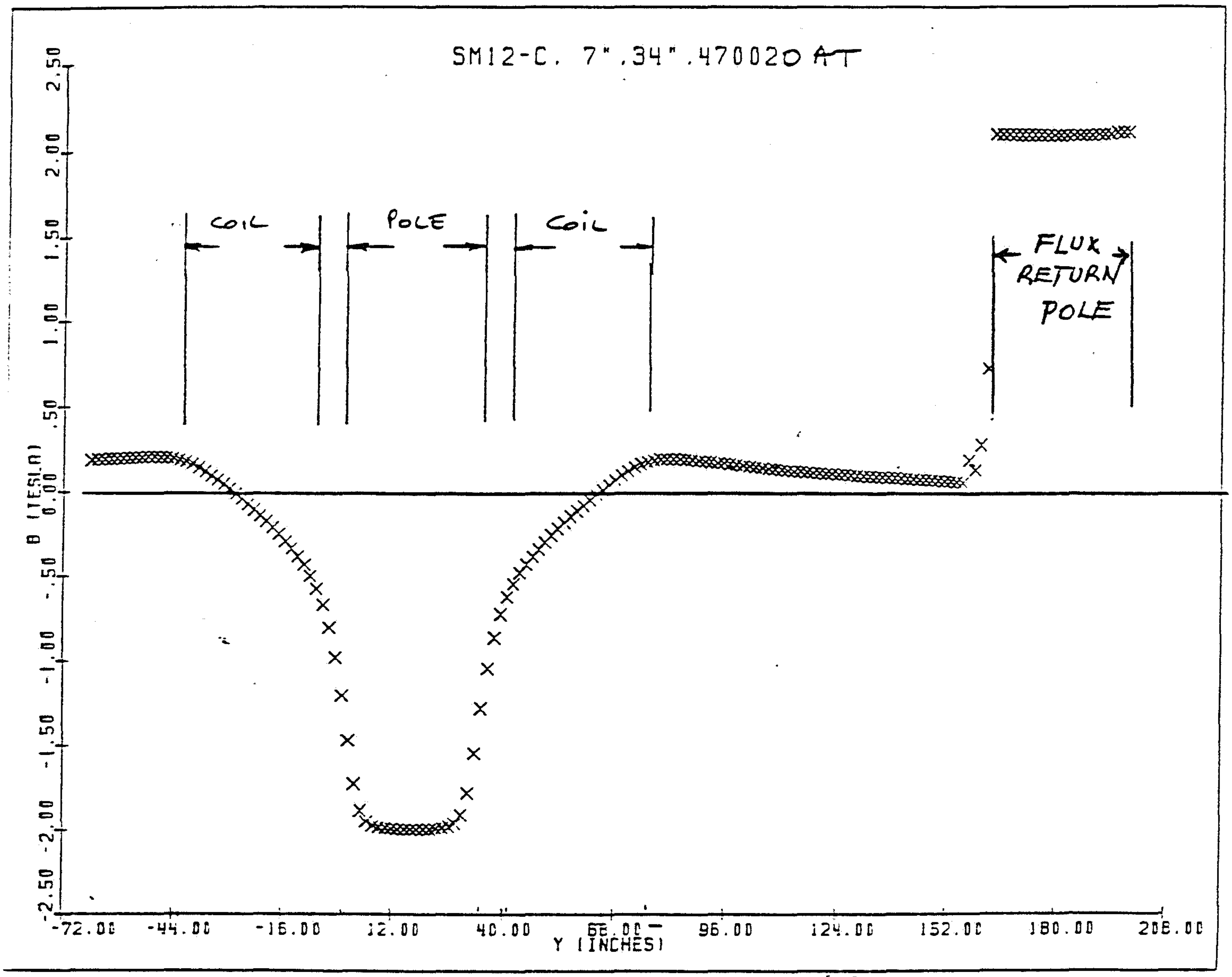

SM12-C. 7".34".470020 AT
COIL
POLE
COIL
FLUX RETURN POLE
B (TESLA)
2.50
2.00
1.50
1.00
.50
0.00
-.50
-1.00
-1.50
-2.00
-2.50
-72.00
-44.00
-16.00
12.00
40.00
68.00
96.00
124.00
152.00
180.00
208.00
Y (INCHES)

Figure 13. Coulomb Bandpass Ray Trace

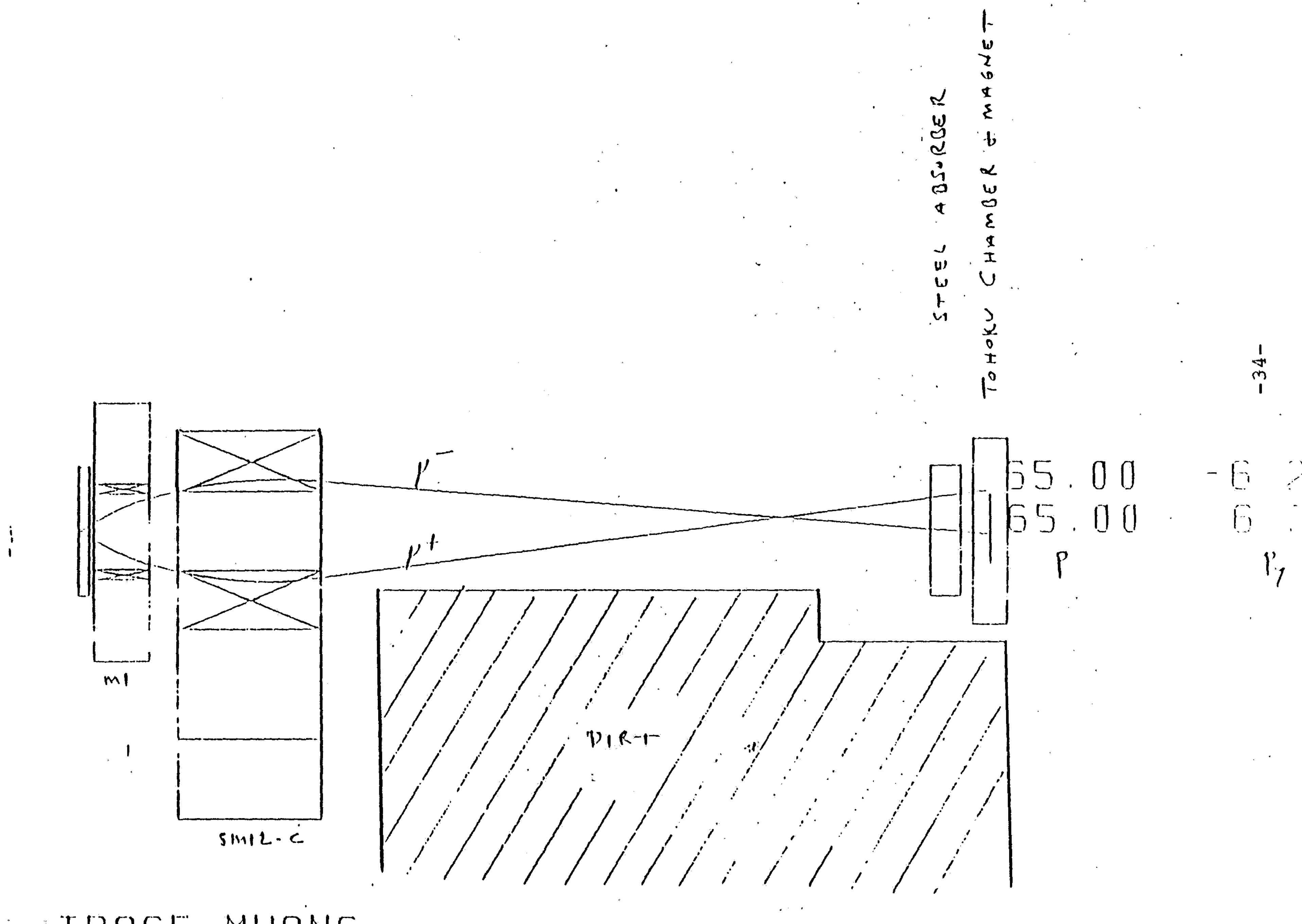

Figure 14

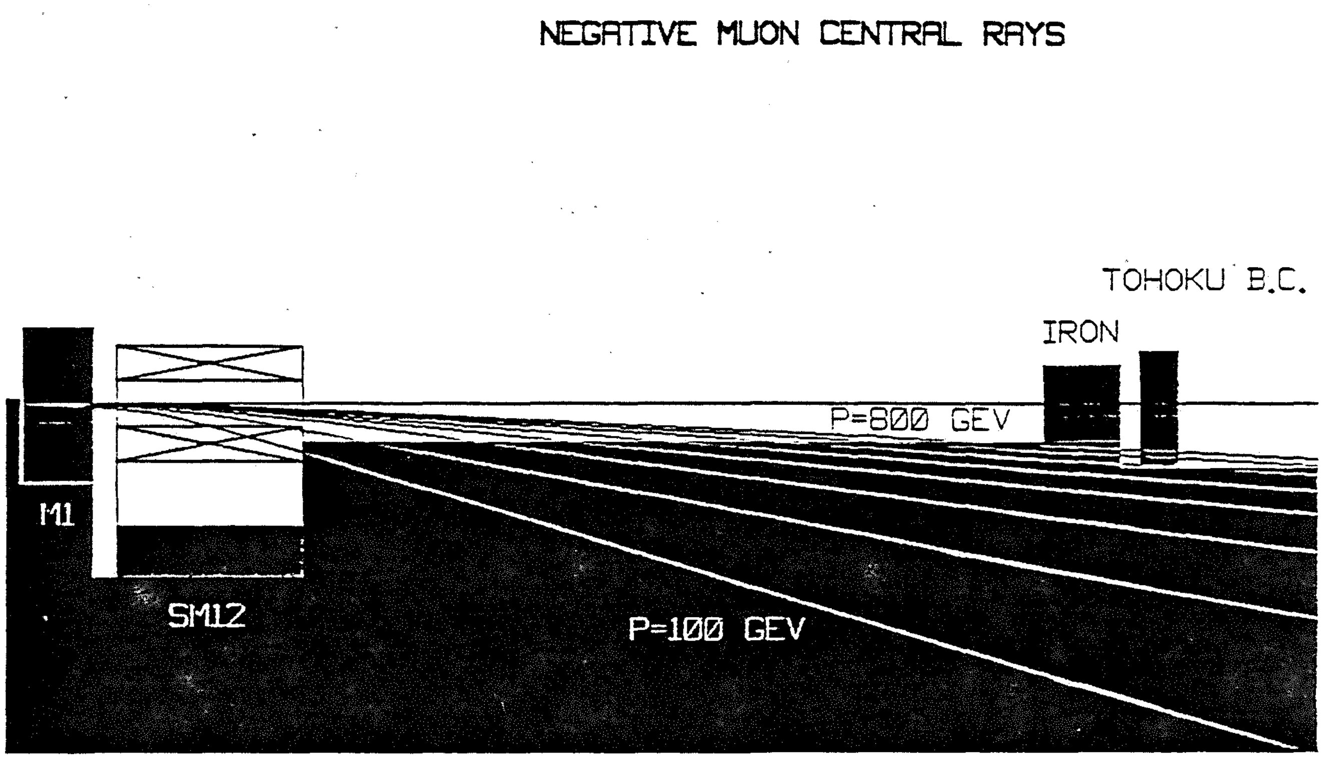
NEGATIVE MUON CENTRAL RAYS
TOHOKU B.C.
IRON
P=800 GEV
M1
SM12
P=100 GEV

Figure 15

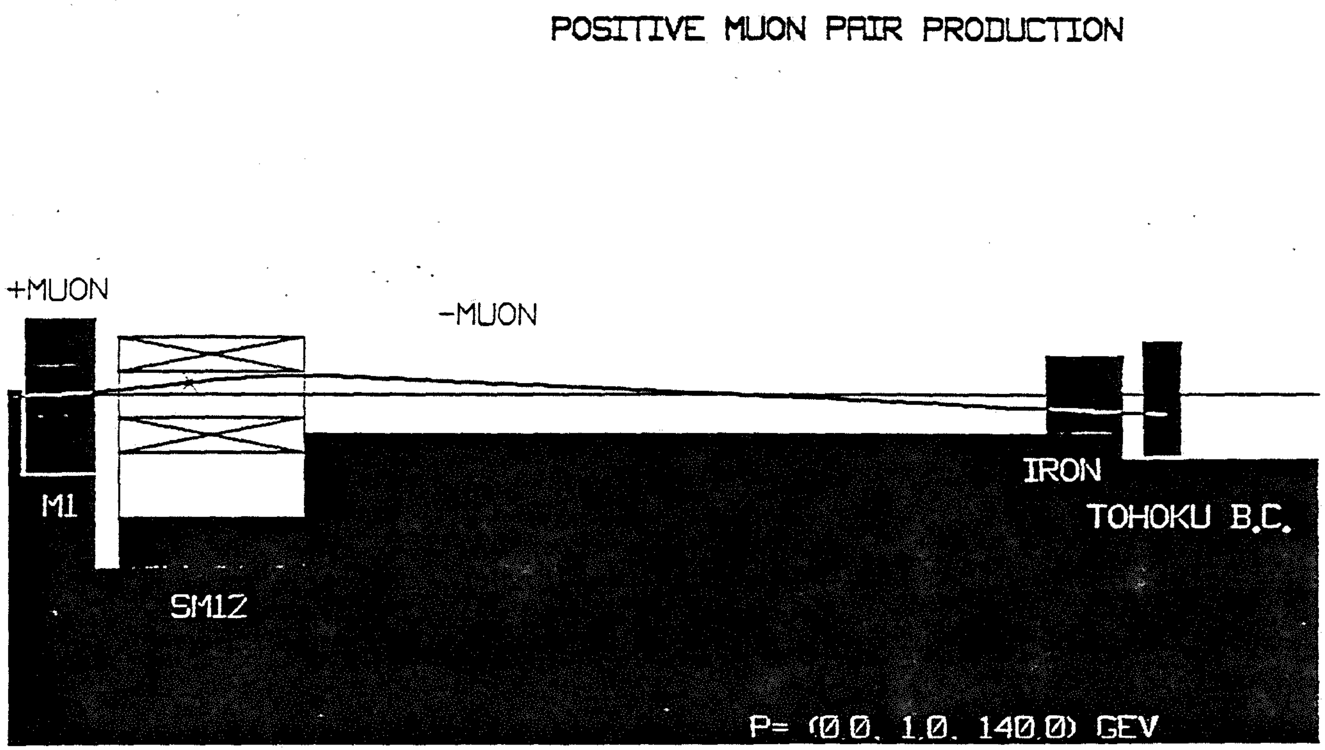
POSITIVE MUON PAIR PRODUCTION
+MUON
-MUON
M1
SM12
IRON
TOHOKU B.C.
P= (0.0, 1.0, 140.0) GEV

Figure 16

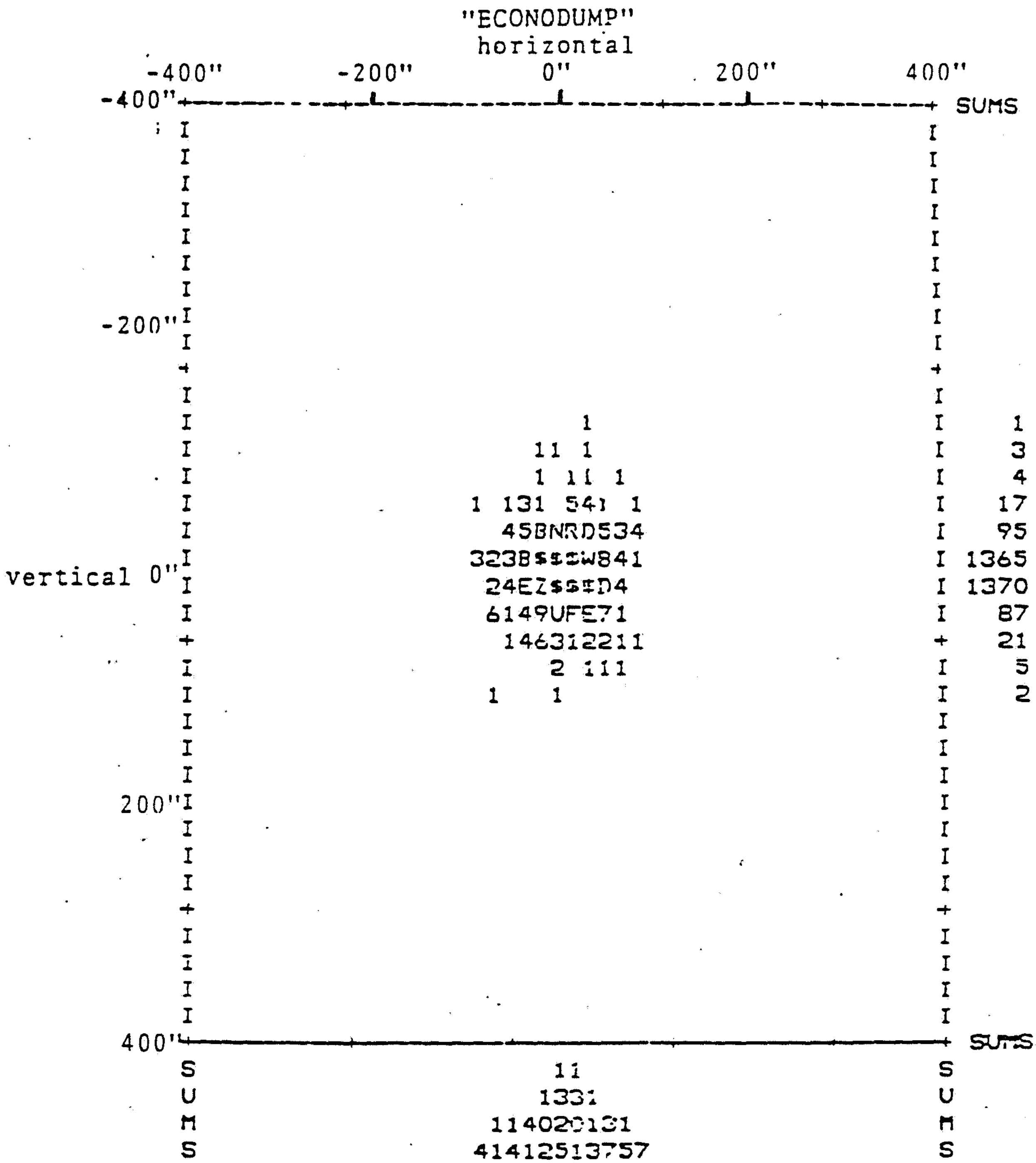

Absorber at 1136' from beam dump. 6" radius pipe buried in berm. 1 entry = 1.928×10^6 positive muons. 5×10^5 parents at 900 GeV forced to decay at the absorber.

Figure 17

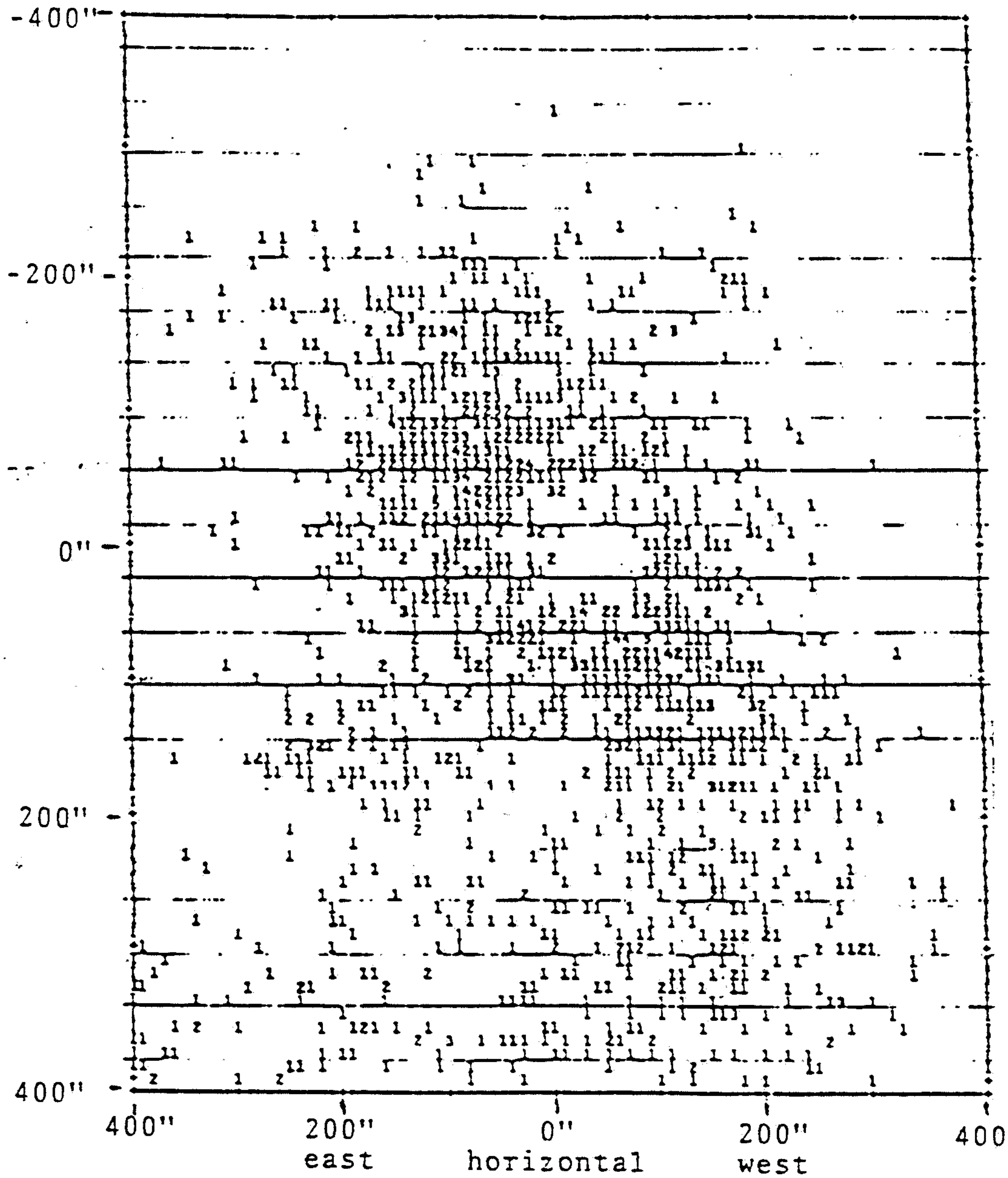

Positive muon sptial distribution in a plane transverse to the beam direction at the location of the tungsten target in Prompt Hall. The muons are procured by the interaction of 2.5 x 10^7 p's at the front of Encl. NE8. (Taken from Figure VI.2 of TM-1155 by C. Baltay et al.)

Figure 18

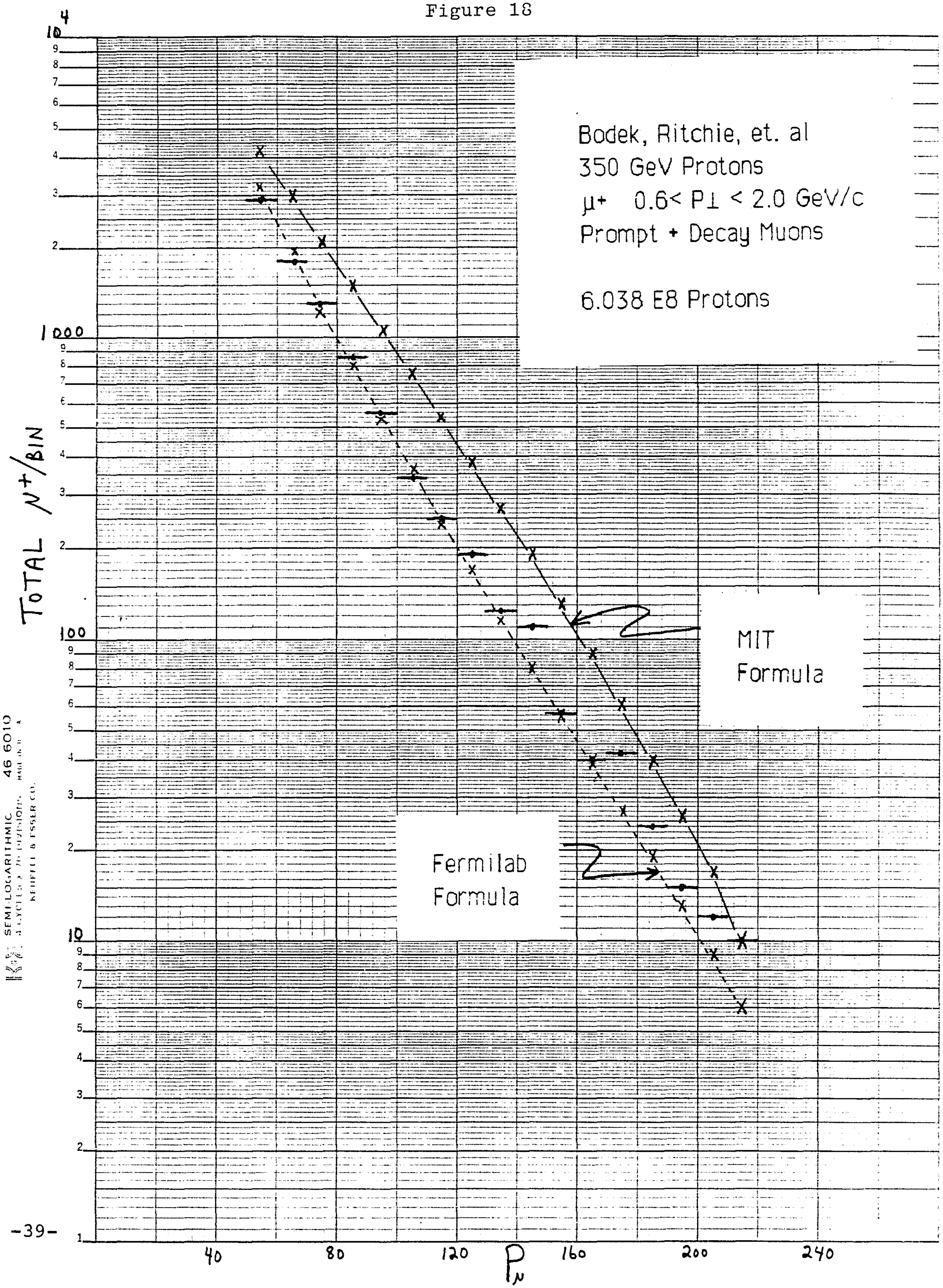

Bodek, Ritchie, et. al
350 GeV Protons
μ+ 0.6< P⊥ < 2.0 GeV/c
Prompt + Decay Muons
6.038 E8 Protons
MIT Formula
Fermilab Formula
TOTAL μ+/BIN
Pμ
40
80
120
160
200
240
10^4
1000
100
10
1
SEMI-LOGARITHMIC 46 6010

Figure 19

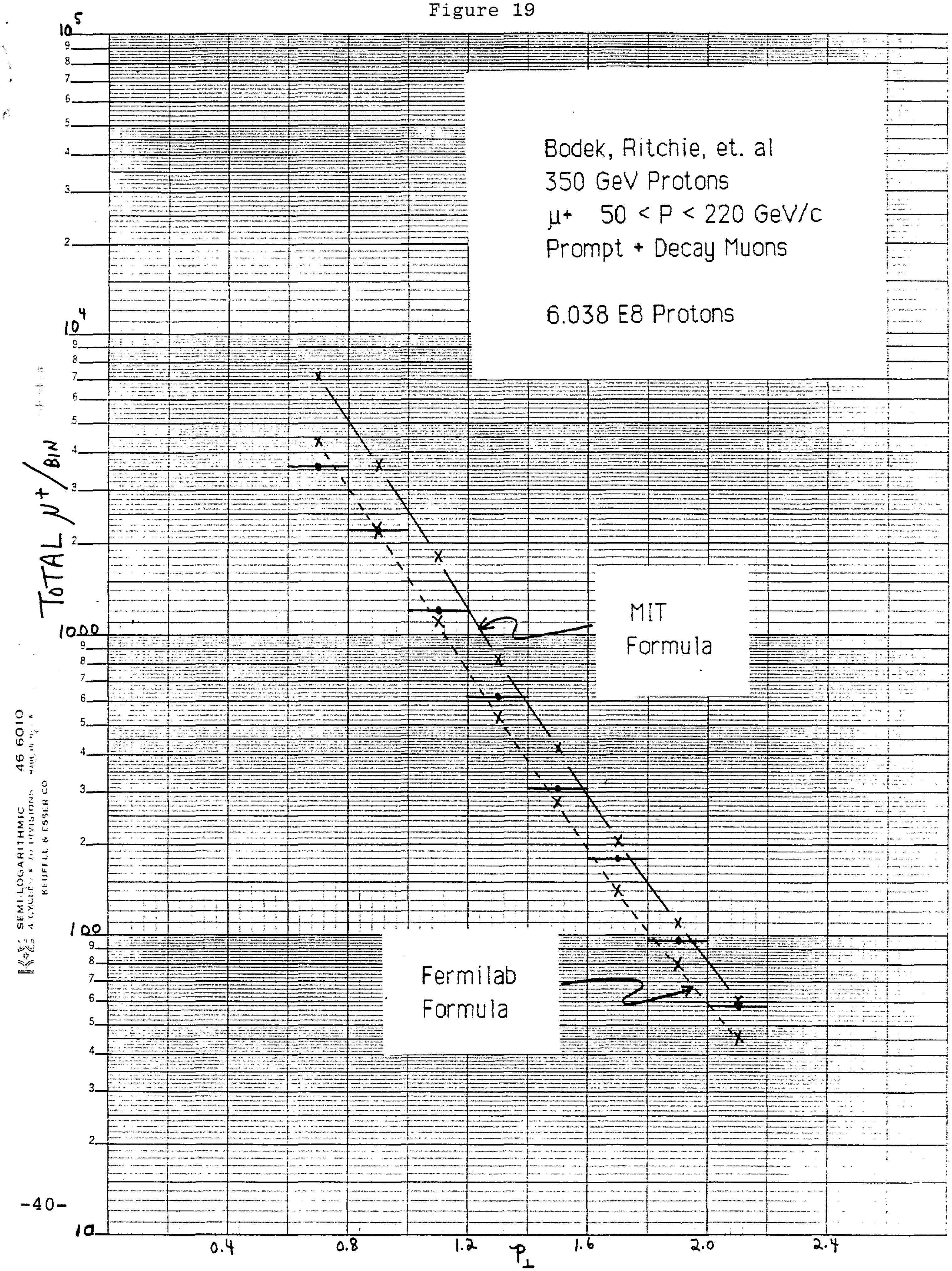
Bodek, Ritchie, et. al
350 GeV Protons
µ+ 50 < P < 220 GeV/c
Prompt + Decay Muons
6.038 E8 Protons
MIT Formula
Fermilab Formula
TOTAL µ+/BIN
P⊥
0.4
0.8
1.2
1.6
2.0
2.4
10^5
10^4
1000
100
10
SEMI-LOGARITHMIC 46 6010
KEUFFEL & ESSER CO.

Figure 20

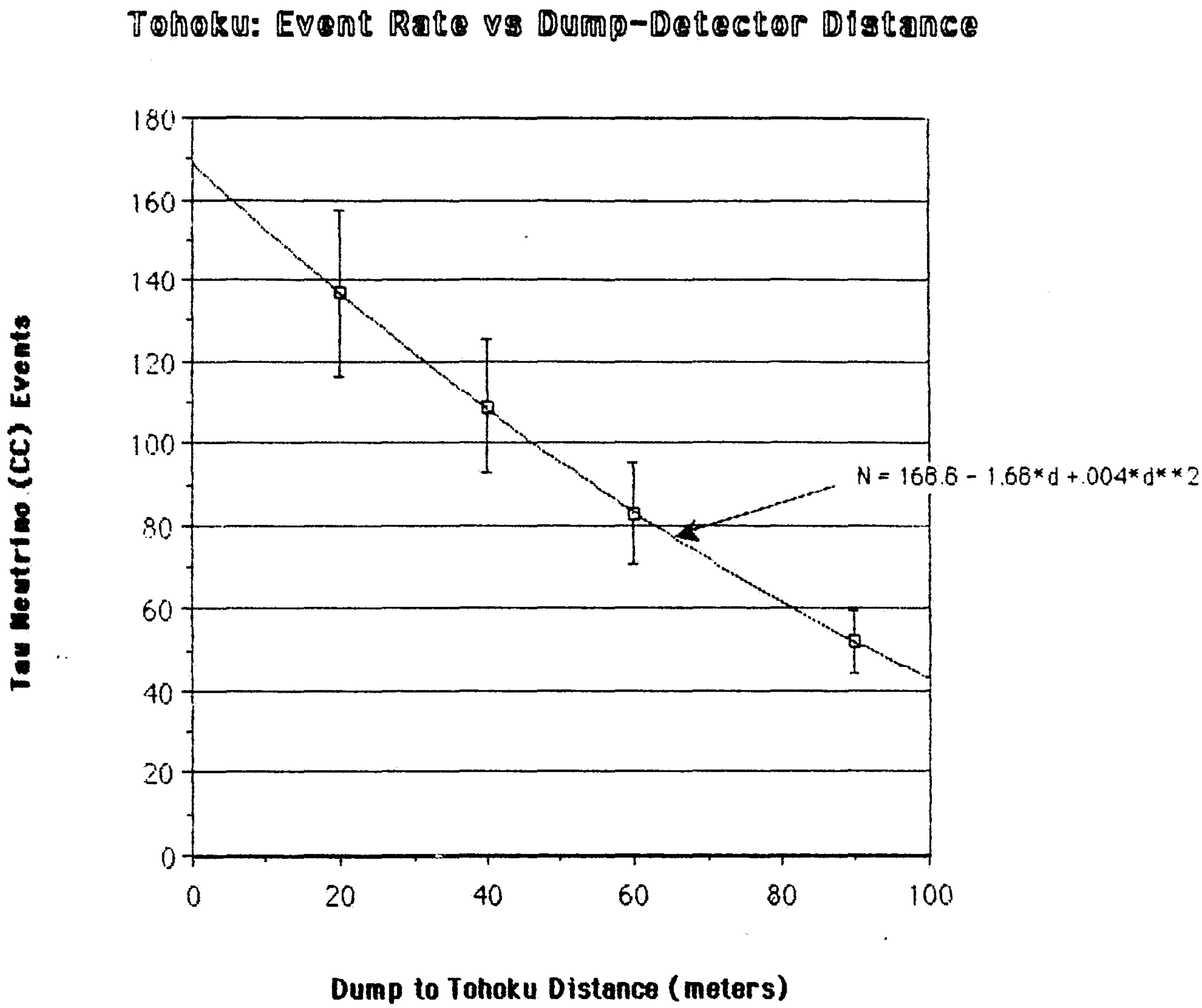
Tohoku: Event Rate vs Dump-Detector Distance
Tau Neutrino (CC) Events
180
160
140
120
100
80
60
40
20
0
0
20
40
60
80
100
N = 168.6 - 1.68*d +.004*d**2
Dump to Tohoku Distance (meters)